IRRIGATION WATER MANAGEMENT USING MULTISPECTRAL VEGETATION INDICES

THESIS

Submitted to
Dr. Panjabrao Deshmukh Krishi Vidyapeeth, Akola
in partial fulfilment of the requirements
for the Degree of

DOCTOR OF PHILOSOPHY
IN
AGRICULTURAL ENGINEERING
(IRRIGATION AND DRAINAGE ENGINEERING)

By
ADAWADKAR MAYUR PRAKASH

DEPARTMENT OF IRRIGATION AND
DRAINAGE ENGINEERING
POST GRADUATE INSTITUTE, AKOLA

DR. PANJABRAO DESHMUKH KRISHI VIDYAPEETH
KRISHINAGAR PO, AKOLA (MS) 444104

Enrolment Number – OO-3197

2023

DECLARATION OF STUDENT

I hereby declare that the experimental work and its interpretation of the thesis entitled '**IRRIGATION WATER MANAGEMENT USING MULTISPECTRAL VEGETATION INDICES'** or part thereof has neither been submitted for any other degree or diploma of any University, nor the data have been derived from thesis/publication of any University or scientific organization. The sources of material used and all assistance received during the course of investigation have been duly acknowledged.

Place : Akola (ADAWADKAR MAYUR PRAKASH)

Date : Enrolment No. OO-3197

CERTIFICATE

This is to certify that thesis entitled **"IRRIGATION WATER MANAGEMENT USING MULTISPECTRAL VEGETATION INDICES"** submitted in partial fulfilment of the requirement for the degree of **'Doctor of Philosophy in Agricultural Engineering (Irrigation and Drainage Engineering)'** of Dr. Panjabrao Deshmukh Krishi Vidyapeeth, Akola is a record of bonafide research work carried out by **Adawadkar Mayur Prakash** under my guidance and supervision.

The subject of thesis has been approved by the Student's Advisory Committee.

Place : Akola Chairman,

Date : Advisory Committee

Countersigned

Associate Dean,
Post Graduate Institute
Dr. Panjabrao Deshmukh Krishi Vidyapeeth, Akola

THESIS APPROVED BY THE STUDENT'S ADVISORY COMMITTEE INCLUDING EXTERNAL EXAMINER (AFTER VIVA-VOCE)

1. Chairman Dr. S. B. Wadatkar _____
2. Member Dr. A. R. Pimpale _____
3. Member Dr. P. B. Rajankar _____
4. Member Dr. I. K. Ramteke _____
5. Member Dr. M. U. Kale _____
6. External Examiner _____

Acknowledgements

It is a great feeling in my life to have completed this research work. This research study would not have been feasible without the support and guidance of numerous persons who contributed and extended their valued aid in the preparation and completion of this study in various ways.

I would like to express my deepest gratitude and heartfelt respect to Dr. S. B. Wadatkar, Dean, Faculty of Agricultural Engineering, Professor and Head, Department of Irrigation and Drainage Engineering, Dr. Panjabrao Deshmukh Krishi Vidyapeeth, Akola and Chairman of my advisory committee, for being the motivating force during the course of this investigation. His scientific excellence, valuable guidance and regular inspiration helped me to a great extent in this scientific endeavor. It is great pleasure and privilege for me to be associated with him.

I have immense pleasure in expressing my whole hearted sense of gratitude to member of my advisory committee Dr. A. R. Pimpale, Associate Professor, Department of Agricultural Engineering, College of Agriculture, Nagpur, for always being there when I needed his support, reviewing my progress constantly, guiding and motivating me through my PhD studies. I express my special thanks to him for his kindness and helpful nature and arranged my stay and food.

Words are insufficient and fall short in expressing my indebtedness to Dr. P. B. Rajankar, Associate Scientist, Maharashtra Remote Sensing Application Centre Nagpur and member of advisory committee, for his valuable, timely guidance and for teaching me all the topics related to GIS and Remote Sensing and continuous encouragement and cooperation.

I shall never forget to express words of thanks to the member of my advisory committee Dr. I. K. Ramteke, Scientific Associate, Maharashtra Remote Sensing Application Centre Nagpur for his constant guidance, keen interest and continuous encouragement during the entire course of investigation.

I also take opportunity to express my humble thanks to Dr. M. U. Kale, Associate Professor, Department of Irrigation and Drainage

Engineering as my member of advisory committee for his timely suggestions and motivation during my research work.

It is my proud privilege to offer sincere and well-devoted thanks to Dr. S. R. Gadakh, Hon. Vice-Chancellor, Dr. PDKV, Akola, Dr. Y. B. Tayade, Associate Dean, Post Graduate Institute, Dr. PDKV, Akola for providing necessary facilities during the research work.

It was impossible to do my research without financial support for that I want to give my deepest thanks to institute members, Mahatma Jyotiba Phule Research and Training Institute (MAHAJYOTI), Nagpur for Mahatma Jyotiba Phule Research Fellowship, Government of Maharashtra for providing me the financial support for my research work.

I am thankful to Dr. M. M. Deshmukh and Dr. A. N. Mankar, Associate Professors and Shri. P. A Gawande, Assistant Professor, Department of IDE, Dr. PDKV, Akola for their timely help during study.

I am thankful to Mr. Rushikesh Talole, Shri. Arun Naiknaware, Shri Avinash Morey, faculty members of Department of Irrigation and Drainage Engineering, Dr. PDKV, Akola for their valuable help and kind cooperation for completion of this research work.

I record cordial thanks to my friends Aniruddha, Aniket, Sudarshan, Ankita, Vaishali, Rupesh, Dipesh, Chetan, Pruthviraj, Tushar, Prashant for their love, moral support and care.

I am very thankful to my spiritual guru's Shri. Tukaram Maharaj Jevurkar and Shri. Dnyaneshwar Maharaj Beldarwadikar for their blessings to complete my research work.

No words of gratitude can equate the tremendous encouragement and love best owed on me by father Shri. Prakash Adawadkar and my mother Sau. Indumati Adawadkar, whose blessing and inspirations encouraged and supported me to achieve this goal of my life. I am very thankful to my beloved wife Priyanka, sister Kavita and brother-in-law Darshan for their kind support, inspiration and enliven my ability to completion of this research work.

I am very thankful to all the authors and researchers, whose articles helped me in organizing my research work in proper manner and utilize proper tools for interpretation of the results. Finally, I am thankful to all who helped me directly or indirectly in completion of this research work.

Place: Akola (Adawadkar Mayur Prakash)

Date : / / 2023 Enrolment No. OO-3197

Table of Contents

A) List of Tables

B) List of Figures

C) List of Plates

D) Abbreviation

Abbreviation	Description
%	Per cent
ºC	Degree centigrade
Agric.	Agriculture
Agril. Eng.	Agricultural Engineering
AOI	Area of Interest
ASAE	American Society of Agricultural Engineering
ASCE	American Society of Civil Engineering
Bull.	Bulletin
Cm	Centimeter
Conf.	Conference
Conser.	Conservation
Div.	Division
Environ.	Environmental
et al.	Et alibi (and other)
etc	Etcetera
ET	Evapotranspiration
ETo	Reference Evapotranspiration
EVI	Enhanced Vegetation Index
FAO	Food and Agriculture Organization
fAPAR	Fraction of Photosynthetically Active Radiation
FASAL	Forecasting Agricultural Outputs using Space, Agrometeorology and Land based observations
Fig.	Figure
GIS	Geographical Information System
Govt.	Government
GT	Ground Truth
Ha	Hectare
hr	Hour
Hydrol.	Hydrology

i.e.	that is
Int.	International
IRS	Indian Remote Sensing Satellite
ISRO	Indian Space Research Organization
J.	Journal
Kc	Crop Coefficients
Kg	Kilogram
Km	Kilometer
LAI	Leaf Area Index
m	Meter
Mha	Million hectare
mm^3	Million cubic meter
MRSAC	Maharashtra Remote Sensing And Application Centre
MSL	Mean Sea Level
MSAVI2	Modified Soil Adjusted Vegetation Index
MXL	Maximum Likelihood
NDVI	Normalized Difference Vegetation Index
NDWI	Normalized Difference Water Index
No.	Number
NRSA	National Remote Sensing Agency
OSM	Open Series Map
PDKV	Panjabrao Deshmukh Krishi Vidyapeeth
PGI	Post Graduate Institute
Plann.	Planning
Proc.	Proceeding
Res.	Research
Rev	Review
Resour.	Resource
RI	Reference Image
RS	Remote Sensing
s	Second

SAVI	Soil Adjusted Vegetation Index
Sci.	Science
SCS	Soil Conservation Service
SEBAL	Surface Energy Balance Algorithm for Land
Soc.	Social
SOI	Survey of India
Symp.	Symposium
USDA	United State Department of Agriculture
VIs	Vegetation Indices

E) THESIS ABSTRACT

a)	**Title of thesis**	:	**Irrigation Water Management using Multispectral Vegetation Indices.**
b)	**Full name of student**	:	**Mayur Prakash Adawadkar**
c)	**Name and address of Major : Advisor**	:	**Dr. S. B. Wadatkar** Dean and Head, Department of Irrigation and Drainage Engineering, Dr. PDKV, Akola – 444104.
d)	**Degree to be awarded**	:	Ph. D. (Agril. Engg.)
e)	**Year of award of degree**	:	2023
f)	**Major subject**	:	Irrigation and Drainage Engineering
g)	**Total number of pages in thesis**	:	168
h)	**Number of words in abstract**	:	804
i)	**Signature of Student**	:	
j)	**Signature, name and address of forwarding authority**	:	

Head,
Department of Irrigation and Drainage Engineering,
Post Graduate Institute, Dr. PDKV., Akola.

ABSTRACT

Irrigation water management is the process of scheduling and managing irrigation water applications in order to meet the crop water requirements without waste of water, soil and plant nutrients. Crop water requirements are commonly evaluated using guidelines provided in FAO-56 bulletin that employ tabular crop coefficients (Kc). These crop coefficients are point-based and crop evapotranspiration (ETc) is highly reliant on crop coefficient curves. The trend of remote sensing-derived multispectral vegetation indices (VIs) is similar to that of crop coefficients (Kc). Therefore, VIs may be used to predict crop coefficients and act as a substitute Kc. The application of VI may provide spatial dimension to Kc

and therefore spatial variability of water requirement can be well recorded. Therefore, the current study entitled “Irrigation Water Management using Multispectral Vegetation Indices” was done with the primary goal of identifying the most appropriate VI that has a close correlation with crop coefficients of *rabi* wheat and onion crops for two consecutive years 2020-21 and 2021-22.

The research was conducted in three districts viz, Dhule, Jalgaon and Nashik situated in North Maharashtra. Multi-date and multi-spectral images from the Sentinel 2A, MIS sensor were used to produce the multi-temporal vegetation indices NDVI, NDWI, SAVI, MSAVI2 and RVI for year 2020-21 and 2021-22. The spectral behavior of the wheat and onion crops showed that the VIs have a pattern similar to that of crop coefficients for both years 2020-21 and 2021-22. By applying hybrid classification using K-means clustering and visual analysis of remote sensing, the agricultural acreages were calculated. For wheat these estimations indicated deviations of 3.66 per cent for year 2020-21 and 8.72 per cent for year 2021-22 from the Department of Agriculture predictions. For onion acreage estimations indicated overall deviation of 9.08 per cent for year 2020-21 and 10.57 per cent for year 2021-22 respectively.

According to age expressed in weeks, the values of the multidate vegetation indices NDVI, NDWI, SAVI, MSAVI2 and RVI were arranged for both years 2020-21 and 2021-22. The MPKV, Rahuri recommended week-wise crop coefficients (Kc) were utilized to create the correlation with VIs. The correlations were developed as prediction models using linear regression analysis. It was discovered that all vegetative indices (VIs) have greater R^2 values for both crops and a good correlation with crop coefficients (Kc) for *rabi* season of 2020-21 and 2021-22. Among all the VIs, NDWI model performed best in the cases of wheat and onion for both years 2020-21 and 2021-22. For wheat, NDWI was found highest R^2 and D values of 0.954 and 0.990 (2020-21), 0.937 and 0.986 (2021-22) and 0.962 and 0.992 (pooled VIs) with lowest values of SE, RMSE and PD of 0.0796, 0.0748 and 3.14 for year 2020-21, 0.0932, 0.0875 and 3.07 for 2021-22 and 0.0725, 0.0681 and 2.71 for pooled VIs respectively. For onion, NDWI was found highest R^2 and D values of 0.909 and 0.979 for year 2020-21,

0.870 and 0.970 for year 2021-22 and 0.920 and 0.982 for pooled VIs with lower values of SE, RMSE and PD of 0.0697, 0.0652, and 0.85 (2020-21), 0.0833, 0.0779 and 1.14 (2021-22) and 0.0652, 0.0610 and 0.81 (pooled VIs) respectively. Therefore, NDWI was found most preferred remote sensing vegetation index for estimation of wheat and onion crop coefficients respectively.

NDWI model was utilized to estimate week-wise crop coefficients. The water requirement of wheat for Dhule was 449.65 mm (2020-21) and 431.62 mm (2021-22). For Jalgaon water requirement was found 440.92 mm for 2020-21 and 398.43 mm for 2021-22. Water requirement for Nashik was found 429.16 mm (2020-21) and 395.97 mm (2021-22) respectively. For the year 2020–21, the total crop evapotranspiration i.e. water requirement for onion in Dhule, Jalgaon, and Nashik was determined to be 486.52 mm, 482.77 mm, and 488.79 mm respectively. Total crop evapotranspiration for Dhule, Jalgaon, and Nashik was determined to be 493.74 mm, 473.91 mm, and 477.29 mm respectively, for the year 2021–2022.

The water demand for wheat and onion per week for each district in 2020-2021 and 2021-2022 was calculated by multiplying crop coverage. The water demand for wheat in the Dhule, Jalgaon, and Nashik districts were 177.60 Mm^3, 266.59 Mm^3, and 230.30 Mm^3 correspondingly during the 2020–21 crop year. For the year 2021-2022, the demands for wheat in Dhule, Jalgaon, and Nashik were calculated to be 170.91 Mm^3, 224.45 Mm^3, and 204.48 Mm^3 respectively. Water demand of *rabi* onion for Dhule, Jalgaon and Nashik for year 2020-21 was estimated as 70.54 Mm^3, 43.80 Mm^3 and 693.23 Mm^3 respectively and for year 2021-22, water demand was found as 128.16 Mm^3, 33.94 Mm^3 and 825.76 Mm^3 respectively.

The findings of this study show the potential of multispectral vegetation indices for predicting spatial crop coefficients, which leads to proper site-specific crop water demand and precision irrigation water management, which may save a significant amount of water with high water use efficiencies.

Keywords: Crop coefficients, Vegetation indices, Remote sensing, GIS, Sentinel 2A.

CHAPTER I

INTRODUCTION

1.1 Background information:

Agriculture is a significant component of our economy, contributing 14% of the GDP and around 11% of exports. India has the greatest gross irrigated area (88 million hectares) and the second-largest agricultural land base (159.7 million hectares) in the world, respectively, after the United States. More notably, over 60% of the population of the nation including several million small farming households depend on agriculture as their major source of income and land continues to be their most valuable asset in terms of securing their way of life. Water used in agriculture is utilized to generate food grains, fresh vegetables and support livestock. Availability of water per capita in India has decreased from 5000 cubic meters (m^3) annually in 1950 to around 2000 m^3 at this time, and it is anticipated that it would decrease to 1500 m^3 by 2025, leaving much less water available for agriculture. Since the nation consumes more than 80% of its surface water for agriculture alone the supply of water for this usage has reached a critical point.

Plants require adequate and timely watering for vegetative growth and development. Under or overwatering can result in low yield, poor quality and inefficient fertilizer usage. Management strategies are the most important way to improve agricultural water use while maintaining optimal yield and production. The key is to put in place management strategies that increase water use efficiency through better irrigation scheduling and crop-specific irrigation management. Per drop more crop approach seeks to increase agricultural productivity per unit of water, which is an essential consideration. Thus, not only conservation but also the precise use of irrigation water to crops has improved plant health, resulting in higher yields and lower costs. Therefore, proper knowledge of the water requirement for each crop is essential for precision agriculture.

Evapotranspiration (ET) includes water evaporation that transports water directly to the air from soil, canopies and water bodies and transpiration that transports water from the soil through leaves and bodies of vegetation and then into the air. Evapotranspiration is a combination of evaporation and transpiration that is studied to better understand agricultural water requirements and irrigation scheduling. ET is major consumer of water in agriculture for irrigation and varies with space and time along with the biological and meteorological factors that drive it. Hence, assessing ET in a region offers water managers with a versatile tool for evaluating water usage.

The amount of water necessary to compensate for evapotranspiration loss from a planted area is referred to as crop water requirement. Water requirements vary greatly from crop to crop and also during the growing period of individual crops. The accurate assessment of crop water requirements is an important part of agricultural planning. Water use efficiency, which is primarily determined by crop evapotranspiration (ET_c), may be enhanced on a regional scale by adequate irrigation planning, scheduling and decision making based on expected ET_c, which is dependent on crop coefficient (K_c). Though there are several ways for estimating crop evapotranspiration (ET_c), the FAO Penman-Monteith approach (Allen *et al*., 1998) has been deemed the only standard method. Using meteorological data, this approach estimates location-specific daily reference evapotranspiration (ET_o), which is then multiplied by crop coefficients (K_c) to calculate crop evapotranspiration (ET_c).

$$ET_c = K_c \times ET_o \qquad \text{----------(1)}$$

Crop coefficients are often calculated through field studies employing lysimeters (Jensen, 1968), which are planted with the crop being investigated at monthly intervals to coincide with the main growth stages of the crop. The K_c values indicate the combined impacts of changes in leaf area, plant height, crop features, irrigation technique, crop development rate, crop planting date, canopy cover, canopy resistance, soil and climatic conditions and management strategies. Each crop will have its own set of crop coefficients that will estimate different water usage for various crops at

different stages of growth. In the FAO-24 publication, Doorenbos and Pruitt (1977) provided tabular values of Kc for several crops using lysimeters for the important stages of crop growth.

These K_c values correspond to ideal agronomic conditions and are often limited to three major growing stages i.e. $K_{c\ ini}$, $K_{c\ mid}$ and $K_{c\ end}$. Because crop properties vary during the growing season, K_c for a specific crop varies from the beginning of sowing to the end of harvesting. Furthermore, actual field conditions are typically non-optimal in nature, such as the presence of pests and diseases, water scarcity, water logging, soil salinity, etc resulting in stunted plant growth and low plant density, resulting in evapotranspiration rates falling below ET_c. K_c should be modified in such cases to account for all types of stress and environmental restrictions.

Crop coefficients derived from the literature may give a useful guideline for scheduling irrigation, but they are subject to significant inaccuracy in calculating crop water requirements due to their empirical aspect (Jagtap and Jones, 1989). As a result, crop coefficient values must be adjusted based on local conditions. *Rabi* onion and wheat are key crops cultivated during the *rabi* season in the research region. The Mahatma Phule Krishi Vidyapeeth in Rahuri, Maharashtra, conducted lysimeter tests to determine weekly crop coefficient values for *rabi* onion and wheat and advised that these values be used (Krishi-Darshini, MPKV, 2021).

Precision irrigation is a unique sustainable agriculture strategy that permits the delivery of water and nutrients to the plant at the correct time and location in small calculated dosages to create optimal growing conditions. Precision irrigation management necessitates the determination of ETc under varying climatic and field circumstances. Due to differences in crop variety and growth stage from field to field, crop coefficients also lack spatial variability. Therefore, determining a regional water need for a certain period is challenging since the sowing dates of the same crop may vary within a shorter distance. With current crop coefficient approaches, identifying spatial and temporal changes in water use is quite challenging.

Crop acreage estimates are derived on thorough enumeration by revenue agencies (Giradwari system), sample surveys and personal assessments by local patwaris. In this approach, the patwari must dedicate sufficient time and attention to the giradwari. Because the patwari agency is overwhelmed with several tasks and must deal with a broad geographical jurisdiction, it takes longer and produces incorrect findings. Planners and policymakers must have accurate and timely crop area estimates in order to make crucial choices on procurement, storage, public distribution, export, import and other related concerns for successful and timely agricultural development. Remote sensing and GIS technology may be used to create a new paradigm for acreage estimation and precision irrigation water management.

1.2 Study Importance

The most precise and time-efficient technique to irrigation water management is to use remote sensing to estimate crop water requirements in irrigation orders. The crop coefficient derived by remote sensing responds to actual crop conditions in a field and reflects variability between fields caused by varied crop sowing dates, crop type, soil and field condition. Across the last few decades evapotranspiration (ET) over larger regions has been studied notably utilizing data from remote sensing. The primary advantage of adopting remote sensing is that water consumption by the soil-water-vegetation system may be calculated directly without having to quantify other complex hydrological processes.

Satellite remote sensing addresses some of the drawbacks of time-based K_c curves by providing real-time and/or near real-time spatial data on K_c and ET_c use as impacted by actual cropping patterns. Multispectral vegetation indices (VIs), which are calculated as differences, ratios, or linear combinations of reflected light in the visible (blue, green or red) and near infrared (NIR) bands, have been shown to be strongly connected to a variety of crop development parameters (Moran *et al*., 1995). Many researchers have discovered similarities between the temporal patterns of K_c and VI. As a result, K_c may be modelled in terms of VI and utilized to

estimate crop water requirements. Weekly or biweekly VI extraction can offer more precise K_c, allowing for near real-time irrigation scheduling.

Remote sensing has opened up new avenues in agricultural statistics across the world. Through officially supported programmes, remotely sensed spectrum satellite data has been regularly used for this purpose. Area estimates for important crops such as rice, wheat, sugarcane, onion, sorghum, peanuts and cotton are said to be prepared on a regular basis. The enhanced resolution and multitemporal spectral images of modern remote sensing satellites may be used to improve accuracy even more. This technique may be used in small areas such as panchayats and even at the village level. Remote sensing-based acreage estimate is both time efficient and accurate. Furthermore, remote sensing simplifies an otherwise arduous operation.

Wheat (*Triticum aestivum* L.) is the most important cereal crop after rice in India. It is enriched with many nutrients like carbohydrates, vitamins and proteins. In India, wheat is cultivated in a variety of soil types. Wheat grows well in well-drained loams and clay loams. However, good wheat crops may be grown on sandy loams and black soils. Soils should be reaction-neutral. Wheat cultivation needs a cool climate and moderate rainfall. Wheat can grow effectively in temperature ranges between 16^{o}C to 25^{o}C. For wheat cultivation 450-650 mm of water is sufficient.

The onion (*Allium cepa* L.), also known as bulb onion is a vegetable that is widely cultivated. India is second largest producer of onion in the world next to China. Maharashtra is leading state in production of onion in India followed by Madhya Pradesh, Karnataka and Gujrat. Onion can be cultivated in a variety of soil types, including sandy loam, clay loam, silt loam and heavy soils. However, deep, friable loam and alluvial soils with high drainage, moisture holding ability and sufficient organic matter are the ideal soils for effective onion growth. The ideal temperatures for the vegetative phase and bulb development are 13^{o}C to 24^{o}C and 16^{o}C to 25^{o}C, respectively. It needs around 70% relative humidity to develop well. Water required for onion ranges between 600-750 mm. Wheat and onion crops require application of proper amount of irrigation water at proper time

in order to get optimum yields. Therefore, precision application of water is needed.

Taking into account all of the benefits of remotely sensed data in precise irrigation management this study concentrated on integrating the VI-based K_c within the framework of FAO methods for forecasting real-time spatial water use patterns for establishing optimal irrigation schedule. As a result, the experiment was conducted for the *rabi* onion and wheat for three district of Maharashtra state where these *rabi* crops are prominent, because limited work has been tried on this approach thus far.

1.3 Objectives of Study

The study was carried out with following objectives:

1. To develop temporal spectral profile for *rabi* onion and wheat.
2. Identification and estimation of *rabi* onion and wheat acreages using remote sensing.
3. To develop the relationships between vegetation indices and crop coefficients.
4. To utilize the developed relationship for near real time irrigation water management.

1.4 Scope and Limitations

This study will assist us in testing a method for adopting the VI-based K_c inside the framework of FAO 56 approaches for forecasting real-time spatial water consumption patterns to determine the most effective irrigation scheduling. By identifying the crops being studied and calculating the area they occupy, water needs may be met. For crop identification, area calculation and real-time accurate evapotranspiration determination, one can utilize the temporal spectral profile of VI.

In this work, it was attempted to develop/find connections between VIs and crop coefficients for *rabi* onion and wheat crops. VI having closest relation with K_c was identified and VI-K_c relation is developed. This near real-time VI may be used as a substitute for crop coefficients to precisely estimate the need for near real-time irrigation water, providing planners and

stakeholders with a scientific and less strenuous tool. By integrating near real-time VI data from remote sensing satellites with near real-time agro-meteorological data from automatic weather stations, this method is beneficial for constructing expert systems for irrigation scheduling of a vast region.

However, there are certain drawbacks for using such novel technology, such as:

1. Cloud cover frequently limits the use of imagery during the rainy season, when most rainfed crops are grown.
2. Accurate identification is impacted by large field-to-field variations in sowing and harvesting dates, cultural techniques and crop management.
3. In the event of mixed cropping, the type of crop must be correctly identified. It is challenging to do this when the farm plots are smaller than image pixel.
4. Crop evapotranspiration estimates are only valid for the time period covered by the images. These constraints restrict the use of satellite technologies for figuring out the probability distributions and long-term variability of soil moisture stress in rainfed crops.

However, these drawbacks can be resolved by employing high resolution data that has more repeatability, which is simple to do with newly developed remote sensing satellites that include on-board fine resolution sensors.

1.5 Hypothesis

Remote sensing is critical for agricultural water management. FAO-56, crop coefficient (K_c)-based crop evapotranspiration estimation is one of the most widely used irrigation water management methods. However, uncertainties in this method can contribute to crop evapotranspiration estimates that differ significantly from actual crop evapotranspiration at a given site. Remote sensing-derived vegetation indices (VIs) reach their maximum value when the crop reaches full effective green cover, which corresponds to the maximum crop coefficient and follow nearly the same

behavior as crop coefficients throughout the life cycle of crop. Taking into account the similarities between the crop coefficient curve and the temporal pattern of VIs, crop coefficients can be modelled as a function of VIs. These VI models can be tested to determine the best performing vegetation index. This vegetation index can be used to calculate evapotranspiration and water requirements for specific sites. The temporal profile of vegetation indices can also be used to estimate crop acreage and, ultimately, total water demand in the region for a specific crop.

CHAPTER II

REVIEW OF LITERATURE

To address water shortages while increasing water efficiency, efforts must be focused on effective water management based on accurate water requirements. This work employs a crop coefficient technique based on vegetation indices for accurate calculation of spatial crop evapotranspiration and ultimately, agricultural water demand. This chapter reviews and elaborates on previous studies relevant to the study issue within the following headings:

2.1 Evapotranspiration and Crop coefficient

2.2 Concepts and applications of Vegetation Indices (Vis)

2.3 Temporal spectral profile of Crops

2.4 Crop Identification and Acreage estimation using remote sensing.

2.5 Relationships between Vegetation Indices and Crop Coefficients.

2.6 Irrigation Water Management using Remote Sensing Techniques.

2.1 Evapotranspiration and Crop coefficient

Appropriate estimation of crop evapotranspiration is important in assessing the crop water requirement and crop production hence knowledge of evapotranspiration is necessary. The crop coefficient (K_c), which is the ratio of crop evapotranspiration to reference evapotranspiration, is required to determine crop evapotranspiration for irrigation planning in the regional sector.

Thornthwaite (1948) was the first to take into account the need for evapotranspiration. He defined evapotranspiration as the combined process of soil evaporation and plant transpiration. He introduced the term “Potential Evapotranspiration”. Potential evapotranspiration, according to him, is the maximal evapotranspiration from a plant that completely covers the ground surface and has an unrestricted water supply to its roots. He also proposed a temperature-based empirical equation for estimating evapotranspiration.

Penman (1948) proposed a new approach for estimating evapotranspiration based on the energy balance of the surface. This approach, often known as the Penman method, is one of the most widely debated ways of calculating evapotranspiration. When the evapotranspiration calculated by the Penman technique was compared to actual observations, only minor variations were found.

Blaney and Criddle (1950) discovered that the quantity of water consumed by crops throughout their growing season was strongly connected to mean monthly temperatures and daylight hours. He calculated monthly consumptive use as the product of the corresponding month's consumptive use coefficient and consumptive use factor.

Monteith (1965) updated the Penman equation by including the ideas of energy balance and resistance to water vapor flow. He included another surface (vegetation) resistance term. The combination equation is another name for this modified Penman equation. When applied to a plant canopy, this equation treats the entire surface as a single large leaf.

Doorenbos and Pruitt (1977) presented the specifics of determining crop evapotranspiration and crop coefficients using the Penman equation in the paper of FAO-24. Researchers discovered that the approach published in FAO-24 overestimated the reference evapotranspiration and proposed using the Penman-Monteith equation instead of the Penman equation (Allen *et at.* 1994).

Wright (1982) generated crop coefficient curves for several Pacific Northwest Irrigated crops such as alfalfa, potatoes, maize and peas based on the alfalfa reference evapotranspiration.

Allen *et al.* (1989) discovered that the Penman-Monteith technique gave more accurate estimates of evapotranspiration than earlier forms of Penman equation. Researchers commonly utilize the Penman-Monteith equation to assess crop evapotranspiration. For crop evapotranspiration estimate, potential evapotranspiration was used to assess evapotranspiration from a reference crop surface such as short grass or

alfalfa and was multiplied by a factor known as the crop coefficient (Doorenbos and Pruitt, 1977 and Wright, 1982).

Irrigation and Drainage paper FAO 56 (Allen *et al.* 1998) incorporated the improved methodologies for determining reference evapotranspiration. The reference crop in this paper is a hypothetical grass surface growing under good conditions with a height of 0.12 m, a fixed surface resistance of 70 dsm^{-1} and an albedo of 0.23. In addition, two crop coefficients are included in this article: a single crop coefficient for use when the soil surface is dry and a dual crop coefficient (a base crop coefficient plus a soil evaporation factor) for use when the soil surface is moist, as recommended by Wright (1982).

Allen *et al.* (2000) defined the crop coefficient as the ratio of reference evapotranspiration to crop evapotranspiration. The crop coefficient accounts for the impacts of crop height, surface resistance and albedo differences between the hypothetical reference crop and various field crops. The crop evapotranspiration of three agricultural crops, snap beans (*Pisum sativum* L.) and sugar beets (*Beta vulgaris* L.), grown in ten lysimeters in Kimberly, Idaho, was compared to crop evapotranspiration computed using the FAO-56 technique. They noticed that both strategies generated similar outcomes.

Tyagi *et al.* (2000) determined evapotranspiration and crop coefficients for rice and sunflower with lysimeter at Karnal, India. The estimated values of crop coefficients for rice at four growth stages were 1.15, 1.23, 1.14 and 1.02, respectively and the corresponding values for sunflower are 0.63, 1.09, 1.29 and 0.40. The projected crop coefficient values for sunflower deviate significantly from those proposed by FAO at all phases, however computed values for rice are fairly near to those reported by FAO. Local calibration of crop coefficients is thus critical.

Tyagi *et al.* (2000) evaluated the evapotranspiration and crop coefficient of wheat and sorghum and crop coefficients were compared by FAO-56. Crop coefficient estimates deviate significantly from FAO recommendations for these crops. The calculated K_c values in this study

differed significantly from FAO values in the first and second growth stages of wheat and all phases (until the third stage) of sorghum.

Howell *et al.* (2006) measured evapotranspiration with large precision weighing lysimeters to establish crop coefficients for important irrigated crops in the Texas High Plains. Corn (*Zea mays* L.), wheat (*Triticum aestivum* L.), sorghum (*Sorghum bicolor* L.), soybean (*Glycine max* L.), cotton (*Gossypium hirsutum* L.) and alfalfa were among the crops grown (*Medicago sativa* L.). These crop coefficients, named "Bushland crop coefficients," were employed in evapotranspiration networks in Texas and neighbouring states.

Suleiman *et al.* (2007) discovered that the FAO-56 approach successfully estimated cotton evapotranspiration under deficit irrigation conditions in humid regions.

Reddy *et al.* (2015) calculated crop coefficients for groundnut, paddy, tobacco, sugarcane and castor crops in Tirupati, Nellore, Rajahmundry, Anakapalli and Rajendranagar, Andhra Pradesh using reference crop evapotranspiration (ET_o) estimated from the Penman-Monteith equation and lysimeter measured ET_c. Crop coefficients were calculated and compared to FAO-56 recommendations. Though a similar trend was detected, the mean crop coefficients at different stages of growth were considerably different from those of the FAO-56 curve.

Fathizad *et al.* (2016) estimated actual evapotranspiration by using Remote sensing technique in Chaviz sub-basin of Ilam dam catchment. They used an image from the ETM+ Landsat satellite taken on June 15, 2010. The ENVI 4.7 software was used to extract the necessary data from the image of the ETM+ Landsat satellite. They found that maximum evapotranspiration occurs in gardens (8.9 to 11.71 mm/day), but it cover just a small portion of the basin (10 per cent) and the minimum evapotranspiration occurs in range land use (0 to 2.92 mm/day), which covers a major portion of the basin (63 per cent).

Prajapati *et al.* (2016) evaluated the crop coefficient for biodegradable mulched cotton under a variable irrigation regime at

Junagadh Agricultural University. He developed two sets of K_c curves, a sensor-based K_c curve and generalized K_c values given by FAO that were adjusted for local climate. It gives a significant difference in sensor-based K_c curve and adjusted FAO K_c curve. Overestimation of seasonal ET_c using adjusted FAO K_c values, warning against its use without verification.

MPKV Rahuri (2021) proposed week-wise crop coefficients of wheat and onion for local circumstances based on lysimeter experiments at Mahatma Phule Krishi Vidyapeeth, Rahuri, Maharashtra.

Koc *et al.* (2021) developed crop evapotranspiration and single crop coefficients of maize using a weighing lysimeter in Turkey's Mediterranean region. The biggest disparities between measured K_c and FAO-predicted K_c were detected at the early growth stage of first crop maize and during the end-of-season growing stage of second crop maize. FAO techniques projected K_c values that were 28 and 30 per cent lower than observed K_c values for first and second crop maize, respectively.

Several scientists and researchers have noted that the FAO-56 approach has difficulty in forecasting crop evapotranspiration properly. Allen *et al.* (1999) found that crop evapotranspiration variations may be due to the fact that crop growth circumstances in other research are not indicative of the conditions available for producing the crop coefficients in FAO-56.

2.2 Concepts and Applications of Vegetation Indices (Vis)

Since the first satellite was launched in the early 1970s, many vegetation indices (VIs) have been produced by the linear combination or ratio of distinct spectral bands and are used for vegetation monitoring. Vegetation indices are quantitative assessments of vegetation vigour. They are more sensitive than individual spectral bands at detecting green vegetation. They are valuable for remote sensing image interpretation, detecting land use changes, evaluating vegetative cover density, forestry, crop discrimination and crop prediction. Plant canopy reflectance factors and derived multispectral VIs are gaining popularity in agricultural research as reliable surrogates for traditional agronomic parameters such as leaf

area index (LAI), fraction of green cover, fraction of absorbed photosynthetically active radiation (fAPAR) and so on. Worldwide, multi-date, multi-spectral data in the form of several vegetation indices have been used for crop identification and area calculation.

Jordan (1969) introduced the ratio vegetation index (RVI). It is based on the idea that since leaves absorb more red light than infrared light, the ratio will be higher the more leaves there are in the canopy. He came to the conclusion that the ratio of light at 0.800 mm to that at 0.675 mm on the forest floor may be used to calculate the leaf area index of a forest.

Pearson and Miller (1972) are the inventors of vegetation indices. They developed the first, two ratio-based indices for estimating and monitoring vegetative cover: the "Ratio Vegetation Index" (RVI) and the "Vegetation Index Number" (VIN).

Rouse *et al.* (1973) also proposed the most extensively used Normalized Difference Vegetation Index (NDVI) to enhance the identification of vegetated regions and their state. However, the NDVI measure is saturated in high biomass areas and is prone to a range of perturbing phenomena, including atmospheric effects, cloud, soil and anisotropic effects among others. To address these shortcomings a variety of variants and alternatives to NDVI have been proposed in the scientific literature.

Tucker (1979) developed the Transformed Normalized Difference Vegetation Index (TNDVI) by multiplying NDVI by 0.5 and calculating the square root. It always has positive values and its variance is proportionate to its mean values.

Huete (1988) introduced a Soil Adjusted Vegetation Index (SAVI) to mitigate the influence of soil differences on the NDVI in lower vegetation cover regions by incorporating a correction factor L. The SAVI was discovered to be a crucial step toward the development of a simple "global" model capable of describing dynamic soil-vegetation systems based on remotely sensed data.

Qi *et al.* (1994a) included the Soil Adjusted Vegetation Index (SAVI) into MSAVI2 to overcome some of the limitations of the NDVI when used to locations with a high degree of exposed soil surface. He said that the original soil adjusted vegetation index (SAVI) had the disadvantage of requiring the specification of the soil-brightness correction factor L, which ranged from 0 for very high vegetation cover to 1 for extremely low vegetation cover. For moderate vegetation cover, most studies choose 0.5 for L. SAVI is similar to NDVI when L = 0.

Moran *et al.* (1994) presented a Water Deficit Index (WDI) that took the Soil Adjusted Vegetation Index into account (SAVI). Evapotranspiration rates on mixed surfaces have been estimated using the WDI index. The WDI index achieves a value of 1 when the plant is under extreme stress and 0 when crop evaporation is at its potential rate.

Liu and Huete (1995) created the Enhanced Vegetation Index (EVI) to optimise the vegetation signal with increased sensitivity in high biomass locations by adding both background adjustment and atmospheric resistance principles into the NDVI.

Gitelson *et al.* (1996) proposed a Green Normalized Difference Vegetation Index (GNDVI), in which the green band replaces the red band in the NDVI equation and demonstrated that the green band, in combination with the NIR band, is more closely associated with variability in leaf chlorophyll, nitrogen content and grain yield than the red band.

Gao (1996) developed the Normalized Difference Water Index (NDWI). NDWI has ability to detect the moisture content of plants and soil. This index unlike NDVI is robust to atmospheric impacts.

Yoshioka *et al.* (2000) noted that internal variables like variation in the canopy, leaf optical characteristics and canopy backdrop affect VIs as well as external factors like sensor calibration, sun and view angle, meteorological condition, etc.

Wang *et al.* (2001) suggested the Vegetation Temperature Condition Index (VTCI), in which the surface temperature -NDVI space behaved like a

triangle. This approach has been frequently employed in the Southern Plains of the United States (Wang *et al.*, 2004).

Sandholt *et al.* (2002) introduced the Temperature-Vegetation Dryness Index (TVDI), which is calculated from space LST-NDVI and may be used to predict soil moisture and hence vegetation water stress.

Barnes *et al.* (2003) described that vegetation indices may be utilised as a mapping tool. They employed imagery classification to identify distinct types and densities of vegetation, to differentiate between vegetated and non-vegetated regions and to track seasonal fluctuations in vegetative vigour, abundance and distribution.

Mandal *et al.* (2007) created a sorghum crop yield model based on vegetation indices and water production functions. They observed that a sorghum yield model based on the water production function and MSAVI produced more appropriate results.

Glenn *et al.* (2008) noted that various researchers have demonstrated a strong association between the NDVI and the biophysical properties of plants, such as fractional cover (fc), leaf area index (LAI), chlorophyll content and wet and dry biomass. Additionally, there is a substantial correlation between NDVI and physiological systems that rely on light absorption.

Ahmad (2012a) conducted change detection experiments in Pakistan, districts of Mullan and Faisalabad, using the Enhanced Vegetation Vegetation Index (EVI), Normalized Difference Vegetation Index (NDVI), Transformed Normalized Difference Vegetation Index (TNDVI) and Soil Adjusted Vegetation Index (SAVI).

Ahmad (2012b) compared and tested the sensitivity of vegetation indices to soil background influences. Five vegetation indices, Normalized Difference Vegetation Index (NDVI), Transformed Normalized Difference Vegetation Index (TNDVI), Enhanced Vegetation Index (EVI), Soil Adjusted Vegetation Index and SAVI and Modified Soil Adjusted Vegetation Index -2 (MSAVI2), were quantitatively evaluated over the Cholistan Desert using Landsat ETM+ dataset to find the best vegetation index for use in sparsely

vegetated semi-arid and arid tracks of Pakistan. He came to the conclusion that EVI is the best for optimising the vegetation signal with better sensitivity in high biomass regions by including both background adjustment and atmospheric resistance principles and MSAVI2 in low biomass regions.

Robertson *et al.* (2013) used a four-band radiometer to continuously monitor the reflectance of soybean and maize crops, studying the diurnal and seasonal temporal behaviour of reflectance and arguing that the temporal profile of vegetation indices (NDVI and EVI2) can clearly indicate crop phenology, water stress, early and late sowing, disease and pest attacks. Differences in agricultural planting timing can also be noticed. The VIs has also been utilised to track broad phenological changes as well as crop growth phases like soil/residue.

Singh *et al.* (2013) investigated diverse NDVI profiles of 10 classes of cotton in Sirsa district of Haryana and discovered that these classes showed variable growth, indicating different cotton planting dates in the research region, from May 1st fortnight to June 1st fortnight. However, the growth pattern was comparable, with the exception of vegetative growth. The NDVI readings also showed that the peak occurred 112 days after June 1st, mean at September 21st.

Ozcan *et al.* (2014) suggested that MSAVI has been employed in different rangeland studies, where it has frequently been linked to field data on plant cover, biomass and leaf area index and as an input layer for mapping land cover or vegetation classes. They suggested that MSAVI may be used to assess biomass, desertification and plant water deficits.

Zolfagharnejad *et al.* (2017) used remote sensing to determine the vegetation index-derived crop coefficient of wheat (*Triticum aestivum*). They investigated and calculated the monthly K_c of winter wheat (*Triticum aestivum* L.) in four basins in Golestan province, Iran, using five vegetation indices (VIs): Normalized Difference Vegetation Index (NDVI), Difference Vegetation Index (DVI), Soil Adjusted Vegetation Index (SAVI), Infrared Percentage Vegetation Index (IPVI) and Ratio Vegetation Index (RVI). Monthly K_c of wheat was estimated using Landsat-8 images classified by

crop growth stage. VIs were estimated using Geographical Information System (GIS) software from infrared and near-infrared bands of Landsat 8 images.

Kadam *et al.* (2019) conducted an experiment on Crop Evapotranspiration and Normalized Difference Vegetation Index relationship for wheat crop at Mahatma Phule Krishi Vidyapeeth, Rahuri. Wheat crop NDVI readings ranged from 0.16 to 0.56 over the crop growth period. The lowest NDVI was recorded during the early and late stages of crop growth, whereas the highest NDVI was seen during the crop development stage, suggesting full crop canopy formation. As a result of the findings, NDVI index is useful for estimating vegetative biomass since low values correlate to low biomass and high values correspond to large biomass.

Pimpale *et al.* (2019) conducted an experiment using a remote sensing technique to provide rapid and reliable estimations of crop coefficients of *rabi* sorghum growing in five districts of Maharashtra. The vegetation index MSAVI2 was discovered to have a somewhat excellent association with the crop coefficient of *rabi* sorghum. They suggested that the multispectral vegetation index MSAVI2 may be utilised as a proxy for *rabi* sorghum crop coefficient.

Prananda *et al.* (2020) used Simple Ratio (SR), Normalized Differenced Vegetation Index (NDVI), Enhanced Vegetation Index (EVI), Green Atmospherically Resistant Vegetation Index (GARI), Wide Dynamic Range Vegetation Index (WDRVI) for Mangrove leaf area index modelling. The results demonstrate that NDVI has the best accuracy, with an R^2 value of 0.83 and an estimation accuracy of 89.10 per cent.

Alvino *et al.* (2020) evaluated vegetation indices to detect variability in irrigated corn crops in Sao Desiderio, Bahia State (Brazil). For this study they collected data using an OLI sensor (Operational Land Imager) embedded to a Landsat-8 satellite platform and assessed five corn growing plots under central pivot irrigation. The vegetation indices NDVI (Normalized Difference Vegetation Index), EVI (Enhanced Vegetation Index), SAVI (Soil Adjusted Vegetation Index), GNDVI (Green Normalized

Difference Vegetation Index), SR (Simple Ratio), NDWI (Normalized Difference Water Index) and MSI (Moisture Stress Index) were evaluated. NDVI, EVI and SAVI produced superior outcomes during corn crop growth, despite the fact that NDVI was less susceptible to large biomass levels and SAVI was subjective in terms of adjustment factor weight. However, MSI and NDWI can be used to supplement information on leaf water content in corn plants. Overall, all indices were discovered to be concordant with one another, with excellent correlations.

Sharma *et al.* (2021) compared different vegetation indices of Noida City using Landsat data. Between 2011 and 2019, they investigated the vegetation condition of the city using five spectral indices: NDBI, GARI, SAVI, GSAVI and NDVI. Six image quality measures, including mean absolute deviation (MAD), correlation coefficient (CC), root mean square error (RMSE), standard deviation (SD), ERGAS and mean absolute percentage error (MAPE), were used to evaluate the applicability of the indices. In comparison to other vegetation indices for urban environments, SAVI is substantially more sensitive to urban greenness, according to the examination of the six quality characteristics.

2.3 Temporal Spectral Profile of Crops

Many investigators across the world researched temporal spectral profiles of different crops using various vegetation indices to achieve varied goals.

Hunsaker *et al.* (2003) found that K_{cb} and NDVI increased in a comparable manner from early crop growth until a maximum K_{cb} was reached in their cotton research in Arizona, USA. Maximum K_{cb} occurred around the period of effective canopy closure, when NDVI was also at its apex. After effective complete cover, NDVI fluctuated within a limited range. Following that, the NDVI fell, suggesting the start of agricultural senescence. Unlike the horizontal trend that happened for NDVI after complete cover, K_{cb} began to decline after the maximum value was reached.

Wardlow *et al.* (2007) classified crop-related LULC in Kansas using time-series MODIS 250 m Enhanced Vegetation Index (EVI) and Normalized Difference Vegetation Index (NDVI) datasets. They examined the spectral profiles of sorghum, alfalfa and winter wheat and discovered that each crop's multitemporal VI signature corresponded to its overall phenological features and that most crop classes were spectrally separable at some time throughout the growth season. Regional intra-class VI signature variations were discovered for several crops across Kansas, reflecting changes in temperature and planting time. The multi-temporal EVI and NDVI data showed comparable seasonal responses for all crops and were significantly connected throughout the growing season. However, variations in EVI and NDVI responses were particularly noticeable during the senescence stage of the growing season.

Mandal *et al.* (2007) investigated the spectral properties of sorghum in Hyderabad. They measured distant cosine receptor reflectance. Six vegetation indices were obtained: SR, NDVI, PVI, GNDI, SAVI and MSAVI. They discovered that all of these vegetation indices rise with crop growth until they reach a maximum value during the booting to anthesis stage of crop development and subsequently decline as the crop approaches senescence. Reflectance in the near infrared area reached the maximum value of the season after the 7^{th} week of sowing, whereas reflectance in the visible section reached the lowest value. Reflectance in the NIR dropped while that in the visible area increased after the first week after seeding due to plant yellowing and withering.

Suifan *et al.* (2007) studied the NDVI trends of vegetable crops in Mafraq, Jordan. Initial findings of a substantial polynomial relationship between NDVI and days after planting (DAP) for several irrigated vegetable crops revealed a significant polynomial relationship with correlation coefficient values greater than 0.90. The visual interpretation of the DAP-NDVI connection revealed that NDVI levels were practically constant during the early stages of most irrigated vegetable crops. This time differed from crop to crop. Similarly, the length of the development stage varied

according to crop type, with some crops seeing a rapid increase in NDVI values while others had a gradual increase over a long period of time.

Zhang *et al.* (2009) investigated the fluctuating tendencies of NDVI, SAVI and SR vegetation indices in Texas for soybean and cotton fields and discovered that these indices peak during maximum growth (July) and thereafter decline down.

Russo *et al.* (2010) investigated the spatial and temporal connection of several indices (NDVI, EVI and WDVI) with crop coefficients known in the literature for various herbaceous and arboreal cultivations present in the research area (Basilicata region, southern Italy). They discovered that the relationship increases throughout the growth season ($R^2 > 0.80$) and falls during the winter ($R^2 < 0.30$). Such behaviour appears to be directly related to the temperature dependence of vegetative indices, which revealed a specular correlation cycle. The investigation for each cultivation revealed that NDVI produced a very strong correlation for all of the tested cultivations, with the highest values for wheat ($R^2 = 0.89$) and vineyards ($R^2 = 0.83$).

Palacios *et al.* (2012) investigated the growth of wheat NDVI using Landsat 5 and Landsat 7 images in 13 plots in Irrigation District 038, Mayo River, Sonora, Mexico, during the 2008 agricultural year. They investigated the trend of NDVI development by plotting days elapsed from the initial image vs NDVI. They discovered that the NDVI of wheat crops ranges between 0.3 and 0.75 during initial growth, is almost constant throughout peak growth and then progressively falls.

Farg *et al.* (2012) conducted research on wheat crops in Egypt's south Nile Delta to estimate crop coefficients (K_c) and crop evapotranspiration (ET_c) using SPOT-4 satellite data linked with meteorological data and the FAO-56 technique. They calculated NDVI and SAVI using three SPOT-4 satellite images reflecting the three phases of crop life cycle. The vegetation indices computed from SPOT-4 satellite images revealed that the mid-season growth stage had greater NDVI and SAVI values than the developing and late-season growth stages. Furthermore, vegetation indices derived from satellite images as well as

crop coefficients measured and forecasted values show the same tendency across growth stages.

Singh *et al.* (2013) discovered seasonal variation in the NDVI and SAVI pattern of cotton in the Haryana district of Sirsa. NDVI and SAVI values were calculated from Landsat TMS images collected during the growth season. They plotted NDVI and SAVI versus the number of days since June 1st. They discovered that the profiles of different cotton classes strongly identified the varied cotton planting dates.

Kamble *et al.* (2013) investigated seasonal NDVI and K_c trends for irrigated and rainfed maize in Nebraska and discovered that irrigated maize has higher NDVI than rainfed maize throughout the growing season. Irrigated maize showed a gradual increase in greenness intensity, with a tendency to decrease at the ending of the season. Crop coefficient (K_c) values were greater at the peak under irrigated conditions than in rainfed conditions.

Parmar *et al.* (2020) worked on wheat crop growth monitoring using Multi-Spectral Vegetation Indices in Bhal Region, Gujarat State. At various development phases, wheat and cotton multi-date spectral indices were produced. The spectral profiles of these two crops (wheat and cotton) have been found to show that the crops are well segregated at various development phases since their crop phenology is highly different. In order to record the change in crop NDVI from sowing to maturation and harvesting, NDVI profiles of the crop have been developed utilising the multi-temporal NDVI values from sowing to maturity.

The majority of the studies given above clearly suggest that the spectral growth profile of VI for a crop characterises the particular crop and represents crop growth dynamics, which may be used for crop identification and crop area coverage in a region. The similarity of the VI and K_c growth patterns also suggests the possibility of the two elements establishing a relationship.

2.4 Crop Identification and Acreage Estimation using Remote Sensing.

Accurate and timely crop area estimation is critical for estimating annual agriculture production in order to develop national budgets and agricultural policy. The use of remote sensing data for crop identification

and discrimination is based on the fact that each crop has a unique spectral signature.

Ayyangar *et al.* (1980) performed an experiment in the agricultural area surrounding Mandya, Karnataka. They employed spectral temporal profiles with red and near infrared bands generated from a modular multispectral scanner at a height of 1000 m above ground level for crop identification and condition evaluation of rice and sugarcane crops. They evaluated and interpreted spectral data derived from ground data. It was able to tell the difference between wet and dry paddy fields. The spectral information in the form of ratios also allowed for the differentiation of rice and sugarcane.

Munshi (1982) used space-borne data and visual mapping for wheat crop in four districts of Punjab in his study.

Dadhwal and Parihar (1985) made the first attempt in the nation to employ satellite data in wheat crop acreage calculation using Landsat MSS data in the Karnal area of Haryana. The study focused on the utilisation of single date data and the supervised Maximum Likelihood (MXL) classification technique.

Rao and Rao (1987) employed LANDSAT MSS data with an 80 m spatial resolution in the form of false colour composites (FCCs) to identify the rice crop with an accuracy of 90 to 94 per cent from cropping patterns with more than 50 per cent of cropped area under rice. Cropping patterns with less than 50 per cent of cropped land under rice and the remainder under different crops were detected with a 75 per cent accuracy.

Guruge (1996) used aerial photographs and RS images to track the development of sugarcane in the Buttala region of Monaragala district, Sri Lanka, from 1983 to 1994. For four years, sugarcane areas were calculated using digital photographs (1983, 1988, 1992 and 1994).

Kimothi *et al*. (1997) applied IRS-1A and 1B, LISS-I and LISS-II data to detect and map apple and almond crops in the Shimla area of Himachal Pradesh. The overall identification accuracy was 87 per cent with a 90 per cent confidence interval.

Tsiligirides (1998) assessed acreage, productivity and wheat yield for the Hellenic regions of Macedonia and Thrace in Greece using area frame of square segments methods and Landsat TM images.

Narciso and Schmidt (1999) studied the use of satellite images for detecting and identifying sugarcane as well as delivering timely and acceptable accuracy information on sugarcane producing areas. The approach was tested in the Eston area using an April 22, 1996 Landsat Thematic Mapper image. To test the accuracy of the identification processes, digital maps of farms and a database of real sugarcane area were employed.

Sawasawa (2003) noted that remotely sensed data (RS) can give consistently high quality spatial and temporal information regarding crop type, crop area and crop evapotranspiration.

Pandit *et al.* (2006) used digital image processing of multidate, multi-sensor high resolution satellite data for identification of sugarcane and onion crops. They used the multi-date data of IRS P6 (RESOURCESAT) sensors like AWiFS, LISS-III and LISS-IV as well as multispectral data of IKONOS with suitable digital imaging processing techniques to identify Sugarcane and Onion of Niphad Tahsil, Nasik District, Maharashtra. They found better accuracy using high resolution LISS-IV and

IKONOS data for sugarcane and onion classification.

Dua *et al.* (2007) estimated potato acreage in prominent potato growing areas in India's Indo-Gangetic region using IRS P6 AWiFS data. They employed a two-stage unsupervised classification method based on the ISODATA clustering concept. Their findings revealed that data collected during the near-peak vegetative stage is optimal for potato crop categorization. However, they suggested that the use of multi-date data and improved classification algorithms should be investigated in order to account for early and late seeded crops, as well as the marginal/fragmented crop condition.

Pakhale *et al.* (2010) determined the area under wheat cultivation in the Karnal district of Haryana, India, using Landsat ETM+ images and

applying Artificial Neural Network. The confusion matrix was generated using ground truth samples. The accuracy of a classification result was determined by comparing it to ground truth data. The cropping season's classification accuracy was determined to be 96.80 per cent, with a Kappa value of 0.9418. The classified image revealed that the area under wheat crop was 127340 hectares.

Mukherjee *et al.* (2010) compared wheat acreage estimated by LISS III and AWiFS sensors data of Indian remote sensing satellite at Rupnager district of Punjab, India. They used supervised Maximum Likelihood classification and district boundary mask approaches for crop acreage estimates. They concluded that LISS-III data estimates district wheat acreage better (RD = -1.5 per cent) than AWiFS (Advanced Wide Field Sensor) data (RD = 9.41 per cent).

Goswami *et al.* (2012) used remote sensing and GIS for wheat crop acreage estimation of Indore District, Madhya Pradesh, India. For acreage estimation, he employed single date, cloud-free ResourceSat IRS P-6 LISS- III digital data that coincided with the flowering period of the wheat crop. ERDAS IMAGINE 9.1 image analysis software and Arc GIS 9.2 software were used for data processing and analysis**.** He discovered that employing remote sensing and GIS technology to estimate district-level wheat acreage differed from the (Land record Commissioner) LRC by +19.

Jha *et al.* (2013) performed an experiment on Wheat acreage estimation by using remote sensing in *Tarai* region of Uttarakhand. For the investigation, two types of data were used: LANDSAT satellite data from the Haldwani area on March 22, 2010 and ground truth data. For image processing and data analysis, ENVI-4.8 (Environment for Visualizing Images-4.8) software was utilised. Supervised classification was used to identify the wheat crop. They found that the total area under wheat was 1484.55 hectares.

Siyal *et al.* (2014) estimated wheat acreage by using LANDSAT 8 images which was obtained from United States Geological Survey portal (GLOVIS) and classified with maximum likelihood algorithm using ArcGIS 10.1. From classified image they revealed that in Hyderabad district wheat

covered 10,210 hectares (9.74 per cent of total area) against 15000 hectares (14.3 per cent of total area) reported by Crop Reporting System (CRS), Sindh which is 30 per cent less than that reported by CRS.

Pimpale *et al.* (2015) compared remote sensing-based wheat acreage estimation and crop statistics given by Department of Agriculture, Government of Maharashtra. The study was conducted in five districts situated in central part of Maharashtra *i.e*., Pune, Solapur, Ahmednagar, Beed and Osmanabad. Multi-date, multispectral satellite images of IRS-P6, AWiFS (Advanced Wide Field Sensor) Sensor was used for the study. Ground Truth Data were collected from 82 sites of wheat and other crops in the study area. ERDAS Imagine and ArcGIS software was used for image processing. They discovered that the wheat acreage estimated by this method for the research region is 189481 ha, which deviates by 9.78 per cent from the reference data published by the Government of Maharashtra.

Ahmed and Sajjad (2015) estimated crop acreage of Boro paddy using Remote sensing and GIS technique in Nagaon district of Assam, India. They used NDVI, RVI and supervised classification to examine the variation of these models in acreage estimation. They utilised the topographical sheet from the Survey of India to extract the district area mask and the statistical data from the Assam Agricultural Department to determine the percentage of deviation. This study found that supervised classification was a more accurate model than NDVI and RVI. The relative deviation of projected paddy acreage from surveyed data in the NDVI and RVI models was negative, -3.65 and -9.06 per cent, respectively. The variance in supervised classification was +1.06 per cent.

Goswami *et al.* (2016) distinguished LISS-III and AWiFS sensor data for wheat acreage estimation. The acreage estimated using LISS-III sensor data was 9841000 ha, whereas the acreage estimated using AWiFS sensor data was 10570000 ha. When compared to AWiFS estimations, LISS - III results suggest -6.89 per cent underestimate. When the acreage estimates from both sensors (LISS-III and AWiFS) are compared to the actual acreage data (9720000 ha), it is clear that higher spatial resolution

(LISS-III) sensor satellite data are more accurate than low spatial resolution (AWiFS) sensor data.

Csillik and Belgiu (2017) presented their findings on cropland mapping utilising Sentinel-2 time-series data and objects as spatial analysis units. The Time-Weighted Dynamic Time Warping (TWDTW) approach was used to classify image objects for cropland mapping and monitoring in the south-eastern section of Romania. The cropland mapping approach that was deployed produced an overall accuracy of 93.43 per cent and a kappa index of 92 per cent.

Aich *et al.* (2017) assessed wheat acreage of Jalandhar district in Punjab by using Single date, no clouds LISS-III computerised information in sync with wheat flowering phase. For data preparation and research, ERDAS IMAGINE 9.1 image processing software and Arc GIS 9.2 software were used. The NDVI images were layered. Area covered by wheat was found 137444 ha. It was found some overestimate due to some other crop reflectance like potato.

Torbick *et al.* (2017) mapped rice crops across Myanmar using Sentinel-1A broad interferometric imagery. Using a random forest technique, they combined and categorised land use land cover maps from Sentinel-1, Landsat-8 OLI and PALSAR-2. An automated technique used to map rice paddy characteristics refined the farmland class by extrapolating various rice crop stages indices from the dense Sentinel-1 time data. According to their evaluation, the rice region harvested was 6652111 hectares with overall accuracy (R^2=0.78) based on state census data.

Chai *et al.* (2018) used high spatial resolution Sentinel-1 multi temporal imagery to discover rice-based cropping patterns in the bulk of rice-growing areas in the Philippines, collecting 30 dual-polarizing pictures across two provenances (Nueva Ecija and Tarlac). When compared to the decision tree classifier approach, the rule-based classifier achieves an overall accuracy of 83 per cent in delineating rice cropping patterns.

Bhatt and Nain (2018) investigated the feasibility of utilising Sentinel-1A data from the European Space Agency to measure rice acreage in Udham Singh Nagar, a key rice producing area in Uttarakhand state. The accurate Land use land cover map created by the SAR dataset categorised with a Support Vector Machine (SVM) algorithm supplied in ENVI-5.1 indicates that Udham Singh Nagar covers rice area (108095 ha) with an overall classification precision of 92.88 per cent and a Kappa coefficient of 0.89.

Desai *et al.* (2018) assessed paddy crop acreage in Shorapur taluk of Yadgir district, Karnataka, India, by choosing 20 ground truth locations and utilising LISS-III data of RESOURCESAT-1 and Landsat-8. In order to analyse the data, ERDAS IMAGINE 2014 and Arc GIS 9.0 software were used. During the investigation, the state of the rice crop was assessed using several proximate sensors such as an NDVI metre, a SPAD metre, an infrared gun and a canopy analyser. The supervised classification with maximum likelihood technique was used to estimate acreage. In Shorapur taluk, the estimated area under paddy crop was 19,398 hectares. When acreage estimates based on remote sensing data and GIS were compared to acreage estimates supplied by the Department of Agriculture, the relative divergence was +17.00 per cent.

Mohite *et al.* (2018) conducted rice area mapping in four districts of Andhra Pradesh: Krishan, Guntur, West Godavari and East Godavari during the kharif season of 2017. They employed Sentinel-1 (SAR sensor) multi-date images with a frequency of 12 days and a spatial resolution of 10 metres. Initially, their model was created utilising two images accessible in mid-June 2017, then a different model was created by adding one succeeding image till the end of August 2017. The agriculture, non-agriculture and aquaculture layers have been masked off, which are sourced from ESA's worldwide land cover. Overall categorization precision ranged from 78.11 to 87.00 per cent.

Paul and Kumar (2019) compared Landsat-8 and Sentinel-2A datasets for *Rabi* crop classifications. For crop classification, two experiments are utilised: I) surface reflectance of spectral bands and II)

NDIs and VIs, combined with surface reflectance of spectral bands, are used as features in the SVM classifier. In both studies, the Sentinel-2A dataset performance was better than Landsat-8 dataset in crop classification accuracy. Using Landsat-8 and Sentinel-2A datasets, they discovered that the average overall accuracy for crop classification was 80.96 and 88.16 per cent, respectively.

Qadir *et al.* (2019) conducted an experiment on crop acreage and yield estimation by using Remote sensing and GIS techniques in the Bulandshahr district, Uttar Pradesh, India for the year of 2000 and 2014. The Landsat 5TM images of 8th October 2000 and 21st September 2014 were downloaded from USGS website. The study included four methodologies. First, supervised classification was used to create maps of land use and land cover (LULC). Second, crop yield is estimated using the normalised difference vegetation index (NDVI). Third, the correlation coefficient approach was used to calculate NDVI accuracy. Fourth, the difference vegetation index (DVI) was used to identify crops. ERDAS Imagine 9.3 was used for supervised classification. Through supervised classification, five land use land cover classes were found, including built-up land, open land, crop land, natural vegetation and water bodies, with an accuracy of 97.9 and 99.5 per cent for the years 2000 and 2014, respectively. They discovered that the maximum NDVI values in 2000 and 2014 were 0.4141 and 0.4166, respectively, while the minimum were -0.4127 and -0.4166.

Kumari *et al.* (2019) estimated soyabean acreage using Temporal microwave and Optical remote sensing data for Nizamabad district of Telangana. They used temporal Sentinel-1B SAR and Sentinel-2A/2B optical data to identify the soybean crop from other competing kharif season crops. Data from multi-temporal VH backscatter intensity and the Normalised Difference Vegetation Index (NDVI) were utilised to define the backscatter and greenness behaviour of the soybean crop, as well as to frame the rules for soybean crop identification. The findings showed that the total accuracy and Kappa coefficient reached were 80.7 and 0.71 per cent, respectively. The soybean crops in study area were classified with

user's accuracy of 82.2 per cent and producer's accuracy of 81.4 per cent. They found slight over-estimation of soyabean crop (64.8 lakh ha) when compared to crop statistics of Telangana Government (57.5 lakh ha).

Sun *et al.* (2019) performed crop classification using machine-learning methods Support Vector Machines (SVM), Artificial Neural Networks (ANN) and Random Forest (RF) on a combination of spectral bands, derived textural measures and vegetation indices from Sentinel-1 SAR, Sentinel-2 optical and Landsat-8 optical datasets. They discovered that when using a single remote sensing data set to categorise crops, Sentinel-2 had the greatest overall accuracy (0.91) and Kappa coefficient (0.89). The combination of Sentinel-1, Sentinel-2 and Landsat-8 data resulted in the highest overall accuracy (0.93) and Kappa coefficient (0.91). In terms of identity classification, the RF approach performed the best.

Gandharum *et al.* (2020) studied on Remote sensing vs the area sampling frame method for estimating paddy acreage in Indramayu regency, West Java province, Indonesia. To determine rice development phases (RGS), they compared Area Sampling Frame (ASF) and remote sensing Synthetic Aperture Radar (SAR) approaches. The SAR-based technique utilised a combination of k-means clustering, hierarchical cluster analysis (HCA), a visual interpretation and a support vector machine (SVM) classifier on time-series of Vertical Horizontal (VH) polarisation of Sentinel-1A data. SAR approach produced more accurate findings, with an overall image classification accuracy of 81.89 per cent and a kappa coefficient of 0.73. The comparative result was rather small, accounting for 4,094.89 hectares greater than the ASF figures (3.5 per cent difference)

Dimitrov *et al.* (2021) used Sentinel-1 and Sentinel-2 data for crop type mapping in Bulgaria. In their study, 14 crop type classes were mapped over Bulgaria utilising three bi-monthly composite image mosaics created in the Google Earth Engine (GEE) cloud computing platform for 2019. When both Sentinel-1 and Sentinel-2 mosaics were utilised, the total accuracy was 78 per cent, but the accuracy was somewhat lower when only Sentinel-2 data was used (75 per cent). Cereals, maize, sunflower, winter rapeseed and rice had the highest accuracy - more than 80 per cent for

both users and producers. However, accuracy was low for classifications such as "Vegetables," "Technical crops," "Forage crops," "Fallow," etc.

Rawat *et al.* (2021) evaluated wheat acreage using remote sensing and GIS in Jabalpur (M.P., India). They used a single-date Imagery from Sentinel-2 to classify crops and performed Unsupervised Classification. For the identification, Sentinel-2's Near Infrared, Red, Green and Blue spectral bands were layered. The findings indicate that 83.07 per cent of the land is planted with wheat, 14.64 per cent is planted with grains and pulses and 2.28 per cent is planted with other crops. The categorization utilising Sentinel-2 images has an overall accuracy rate of 85.71 per cent and an overall Kappa Statistics of 0.819 per cent, respectively. Estimated area under wheat was found 205048 ha using remote sensing technique and it was over-estimated by 6.10 per cent as reported by Ministry of Agriculture and farmer welfare (193246 ha).

Subbarao *et al.* (2021) discovered that multi-temporal Sentinel-1 SAR data with an RF classifier may correctly estimate acreage. The study calculated the *rabi* rice acreage in Maharashtra's Bhandara district to be 1760 km^2 with an overall accuracy of 91 per cent and a Kappa coefficient value of 0.80.

Hudait and Patel (2022) used multi-spectral NDVI acquired from Sentinel-2 images and two ML algorithms, KNN and RF, to identify the primary summer crop acreage in West Bengal's Purba Medinipur area. Though both approaches produced overall accuracy of greater than 90 per cent, the Random Forest (RF) method had a higher overall accuracy of 97.22 per cent at a Kappa index value of 96.08 per cent. The approach was discovered to be capable of extracting both bigger and smaller fields successfully.

2.5 Relationships Between Vegetation Indices and Crop Coefficients

Many of the drawbacks of the traditional crop coefficient can be overcome using remote sensing techniques. VIs estimated as differences, ratios or linear combinations of reflected light in the visible (blue, green and red) and near infrared (NIR) spectra have been shown to be strongly

connected to crop coefficients. Several research have been conducted to investigate the capability of multispectral vegetation indices (VIs) to measure vegetation growth and so estimate K_c. Several writers have reported on K_c-VIs connections and uses of this approach.

Jackson *et al.* (1980) advocated using multispectral VIs as near real-time crop coefficient surrogates. They noticed a resemblance between the seasonal trend of a wheat VI and the wheat crop coefficient.

Bausch and Neale (1987) demonstrated the consistency of a seasonal NDVI curve and a basal crop coefficient curve for maize using a hand-held radiometer that recorded radiance in three bands identical to Landsat TM bands 3, 4 and 5. They determined that crop coefficients obtained from NDVI are real-time crop coefficients. They also discovered that at a LAI of 3.2, the NDVI attained its asymptote.

Leprieur (1989) found that the NDVI saturates at a LAI of 3, When using data from an aerial visible/infrared imaging spectrometer to analyse mixed vegetation locations. Analysing the correlations between LAI, ET, NDVI and crop coefficients reveals a largely linear trend up until a LAI of 3. Beyond this threshold, increases in LAI have very little impact on the three parameters that are connected to it. This relationship suggests that the NDVI will offer information directly related to ET provided it is adjusted to vegetation appropriately.

Bausch (1993) noted that soil background impact might alter NDVI-based crop coefficients and hence advocated using SAVI. He employed the soil adjusted vegetation index (SAVI) to represent the K_{cr} in the reflectance-based crop coefficient for maize. As a result, soil background effects were reduced, eliminating the need for extra calibration for varied soils.

Choudhury *et al.* (1994) discovered a statistically significant correlation between the transpiration coefficient and LAI, as well as between the transpiration coefficient and vegetation indices such as SAVI and NDVI for an unstressed wheat crop. Their findings also revealed that

predicted evapotranspiration values based on vegetation indices coincided with lysimeter data.

Ahmed and Neale (1997) estimated the daily integrated crop water requirements in an irrigation region with a mixed cropping pattern using high resolution aerial multispectral inputs using a reflectance-based crop coefficient approach.

Ray and Dadhwal (2001) calculated crop coefficients by developing a linear relationship between monthly averaged SAVI and crop coefficients. The remote sensing data was gathered from the IRS-IC satellite's wide-field sensor. The regression equation was used to calculate crop coefficient values for each pixel.

Hunsaker *et al.* (2003) created regression models to predict the seasonal distribution of K_{cb} with NDVI in a full-season cotton cultivar produced in the southwestern United States. An initial testing of the model revealed that the NDVI-based K_{cb} generated ET_c estimates that closely matched those obtained for another cotton cultivar cultivated under conditions different from those under which the model was generated. They found that the NDVI-based K_{cb} functions may be easily included within the FAO-56 dual crop coefficient methods, allowing for the use of remotely sensed data in real-time cotton irrigation scheduling. They also discovered that cotton K_{cb} and NDVI had comparable evolutions between planting and full cover, but K_{cb} began to fall shortly after reaching full cover, whilst NDVI stayed practically constant. As a result, they created two distinct relationships: a linear regression equation for the pre-full-cover stage and a bi-parameter equation for the post-full-cover stage.

Hunsaker *et al.* (2005) used NDVI to create wheat basal crop coefficients and showed that measured and calculated ET agreed. They proposed using remotely sensed vegetation indicators like NDVI to calculate a real-time crop coefficient for irrigation scheduling.

Neale *et al.* (2005) used radiometer-derived reflectance measurement to establish SAVI-based crop coefficients for beans and potatoes produced in southern Idaho. They proposed that high resolution

aerial photographs be utilised to capture in-field variability in crop growth and that crop coefficients be employed for irrigation scheduling.

Tasumi *et al.* (2005) created an equation for the Idaho study region by using ordinary least squares (OLS) to observed K_c and NDVI data, as follows: $K_c = 1.1875*NDVI + 0.05$

Duchemin *et al.* (2006) discovered that for winter wheat cultivated in Central Morocco, the relationship between the basal crop coefficient and NDVI determined using a hand-held radiometer was linear.

Er-Raki *et al.* (2007) examined three approaches for calculating the crop coefficient for winter wheat grown under different irrigation regimes in Central Morocco and compared crop evapotranspiration to actual evapotranspiration measured using the eddy covariance method. The results demonstrated that the FAO- 56 approach was incapable of correctly estimating crop evapotranspiration. As a consequence, the FAO-56 crop coefficients were locally calibrated and found to produce satisfactory results. They also proposed that basal crop coefficients might be calculated using NDVI since NDVI produced from ground reflectance measurements and basal crop coefficients exhibited similar seasonal trends.

Calera and Gonzalez (2007) developed a linear relationship of K_c with NDVI for wheat as, $K_c = 1.15*NDVI + 0.17$ in Spain.

Suifan *et al.* (2007) investigated correlations between FAO-Kc and NDVI from the ASTER satellite for all irrigated vegetable crops and discovered that the relationship between K_c and NDVI is linear with a high correlation coefficient (above 0.94) for all vegetable crops.

Rafn *et al.* (2008) examined previously produced NDVI relationships to estimate ET in Idaho and Colorado in the essentially distinct scenario of Eastern Idaho, concluding that these equations can be efficiently utilised for eastern Idaho even for different years in which they were developed.

Gontia and Tiwari (2010) estimated actual crop evapotranspiration of wheat crop cultivated in Tarafeni South irrigation command of West Bengal State in India using remote sensing and GIS methods. They calculated the NDVI and SAVI indices using four images from the IRS P6 satellite's wide

field sensor (WiFS) taken during the winter season. They discovered a correlation between vegetation indices and wheat crop coefficients (K_c) for the corresponding months. The relationships were based on FAO crop coefficients and wheat crop coefficients proposed by Bandopadhyay and Malik (1993). They discovered that the vegetation indicators had a strong association with FAO crop coefficients as,

$K_{cFAO} = 2.7109\ (NDVI) + 0.424$ and $K_{cFAO} = 1.5141\ (SAVI) + 0.4077$

It has a high coefficient of determination (R^2) of 0.799 and 0.897, respectively and it was reported that SAVI is superior than NDVI in expressing wheat spectral crop coefficients.

Er-Raki *et al.* (2010) said that vegetation index approaches substitute crop coefficients with VI that represents the crop's actual growth phase at the time of measurement. Crop coefficients based on VI have been produced for individual and mixed crops in numerous agricultural locations for many years. Several correlations between K_c and VIs have been identified in this context. However, there is no consensus on the nature and scope of these interactions. He noted that whereas some researches have shown these associations to be linear, others have discovered non-linear ones. As a result, developing a distinct relationship between crop coefficient and spectral vegetation indicators is a current field of research.

Rahimian *et al.* (2011) calculated the winter wheat crop coefficient for the Azadegan region, Iran, using MODIS-derived vegetation indices. They tested DVI, IPVI, MSAVI, MSAVI2, PVI, RVI, SA VI, WDVI and NDVI vegetation indices for their correlation with wheat crop coefficients documented in FAO-56 and formed polynomial models, discovering that SAVI, MSAVI (modified version of SAVI) and PVI are the best vegetation indices for estimation of crop coefficients in the studied site, with high correlation coefficients and low RMSE and MAE values. Because the Red and NIR regions of the spectrum are the primary formative elements of these indices, another simple equation for estimating wheat K_c for the examined region was developed. They provided a simple equation for estimating the winter wheat coefficient instead of the recommended FAO

K_c based on NIR and R band reflectance as most VIs are based on these values.

$K_c = 16*NIR – 21*RED +0.5$ ($R^2adj = 0.93$, RMSE = 0.11, MAE = 0.09).

They said that further assessment and development for various agro-climatological circumstances, as well as other remote sensing platforms, are required before the proposed equation may be generalised.

Farg *et al.* (2012) completed research on wheat crop in Egypt's south Nile Delta to estimate crop coefficient (K_c) and crop evapotranspiration (ET_c) using SPOT-4 satellite data combined with meteorological data and the FAO-56 technique. The FAO Penman-Monteith equation was used to determine reference evapotranspiration (ET_o) and the tabulated single crop coefficient values were corrected to real values. The vegetation indices (NDVI and SAVI) were driven by geometrically and radiometrically corrected SPOT-4 images. The research revealed that NDVI, SAVI, K_c and expected K_c all followed the same pattern throughout the development phases. The crop coefficient (K_c) prediction equations for the different growth phases using vegetation indices were developed using multi linear regression analysis. Their results indicated a high R^2 for the projected values of crop coefficient for developing, mid-season and late-season growth stages as 0.82, 0.90 and 0.97, respectively, with low RMSE values of 0.0091, 0.0014 and 0.0007, indicating that assessment of crop coefficient and water requirements using remote sensing data is fundamentally significant.

Singh *et al.* (2013) conducted cotton crop research in the Haryana district of Sirsa. K_{cb} value was estimated using spectral indexes such as SAVI (Soil Adjusted Vegetation Index) and Fractional Vegetation Cover (Fe). Landsat TM5 images with high spatial resolution were utilised to construct spectral profiles of NDVI, SAVI and Fe for various crop cover. Using empirical models, the crop coefficient was calculated from SAVI data. They discovered that remote sensing-based K_{cb} follow the same seasonal variation pattern as crop fraction, SAVI and NDVI.

Kamble *et al.* (2013) studied the ability of directly determining crop coefficients of irrigated and rainfed crops using moderate resolution satellite data (MODIS) and crop coefficients (K_c) estimated from flux data recorded for different crops and cropping strategies using AmeriFiux towers.

They used temperature and latent heat data from AmriFiux sites to estimate reference evapotranspiration using the Hargreaves and Samani (1985) equation (ET_o). Maize, sorghum, alfalfa, soybean, wheat and cotton were the most important crops farmed in this region. They reported the results for irrigated, rainfed and combination agriculture production systems individually using the 2007 dataset as:

Irrigated Agriculture,	$K_c = 1 .3558NDVI - 0.0744$	$R^2=0.8123$
Rainfed Agriculture,	$K_c = 1.4819\ NDVI - 0.2236$	$R^2=0\ .8101$
Combined relationship,	$K_c = 1.4571(NDVI) - 0.1725$	$R^2=0.8259$

These findings were validated at a completely different site using the Bowen - Ratio energy balance system, which discovered a linear regression relationship between measured and predicted K_c with $R^2= 0.91$ and 0.90 for 2006 and 2007, respectively, indicating an accuracy of prediction of K_c of nearly 90 per cent. They determined that NDVI is an indication of vegetative cover density and plant vitality. As a result, it is not surprising that it captures the majority of the variance in K_c when there is no water stress scenario.

Lei and Yang (2014) conducted a study in China for integrating crop coefficients of these crops with remotely sensed vegetative indicators for winter wheat and summer maize. For this investigation, they examined frequently used MODIS satellite VIs, such as NDVI, EVI, $NDWI_{1640}$, $NDWI_{2130}$ and MSAVI and discovered that NDVI and $NDWI_{1640}$ provided the best fit for wheat and maize respectively, while EVI and MSAVI were less accurate for the linear formulation.

Ozcan *et al.* (2014) conducted a study to obtain wheat crop coefficients from vegetation indices NDVI and MSAVI extracted from SPOT 5 satellite images in the Hilvan and Akcakale districts of Turkey and

discovered that the MSAVI values had a comparatively higher linear correlation with K_c values (R^2 = 0.89) for both selected districts with different soil types. The following relationships were discovered:

Hilvan District:

K_c = 1.2819*NDVI + 0.3047 R^2= 0.792

K_c = 1.228*MSAVI + 0.1893 R^2= 0.891

Akcakale District:

K_c = 2.0217*NDVI + 0.3023 R^2= 0.781

K_c = 1.4611*MSAVI + 0.3017 R^2= 0.888

It may be concluded from the relationships between vegetation indices (VIs) and crop coefficients (K_c) mentioned in this section that vegetation indices follow the pattern of crop coefficients and depict dynamic growth of crops. Crop coefficients can be modelled using VIs.

Pimpale *et al.* (2014) used multi temporal satellite data from the IRS-P6 AWiFS sensor to calculate the normalised difference vegetation index (NDVI) for the relevant dates of the chickpea growing season (2011 and 2012). They used a regression model to investigate the relationship between NDVI and crop coefficients (K_c) in the chickpea crop. The regression (correlation) equations so developed and found superior was:

Penman–Monteith method

K_{cPM}= 3.094 NDVI - 0.354 R^2 = 0.874

They concluded that K_c and NDVI had a strong linear correlation, with an R^2 value of 0.874 and a low root mean square error. The results show that this method may be a highly valuable tool for estimating spatial evapotranspiration on a wide scale using the estimated crop coefficient.

Spiliotopoulos *et al.* (2019) investigated particular correlations between crop coefficients and vegetative indices (VI) estimated in the water-limited environment of Lake Karla Watershed, Thessaly, in central Greece. For each crop, NDVI, SAVI and EVI were measured independently. The derived equations had a very high R^2 value (>0.86) for

explaining those correlations. These relationships have been confirmed using independent data.

Rawat and Mishra (2020) compared the spatial crop coefficient (K_c) obtained from the surface energy balance algorithms for land (SEBAL) model to simulated spatial K_c based on the Normalized difference vegetation index (NDVI) and leaf area index (LAI). In terms of geographical K_c, statistical tests revealed that the LAI-K_c model beats the NDVI-Kc model but not the SEBAL-K_c model. According to the data, the LAI-based simulated spatial K_c has a strong coefficient of determination of 0.976 (at 95 per cent) with SEBAL-K_c rather than NDVI-K_c. The relationship of NDVI-K_c and LAI-K_c in study area is expressed by

$K_c = -6.399 \times (NDVI) + 7.4 \times (NDVI) - 0.971$ $R^2 = 0.73$

$K_c = -0.184 \times (LAI) + 1.118 \times (LAI) - 0.443$ $R^2 = 0.95$

Dingre *et al.* (2020) explored the feasibility of linking crop coefficient (K_c) with ground-based normalised difference vegetation index (NDVI) of a sugarcane crop. The findings revealed that the K_c was 16.6 per cent lower than that advised by FAO-56. Sugarcane NDVI at maturity did not decrease from 0.85 even after harvest, unlike other crops, due to the ongoing development of fresh green leaves at the top of the plant. The association between crop K_c and NDVI was studied using 2nd order polynomial regression and the correlation was moderate (r^2=0.75, n=315). By dividing the growth period into the growth phase (r^2=0.98, n=245) and the decline phase (r^2=0.99, n=245), stronger correlations between K_c and NDVI were established.

Mariana *et al.* (2021) investigated the crop coefficient (K_c) estimate as a spectral function of the product of two variables: VIs and the green vegetation cover percentage (fv). Using the OBIA (Object based image analysis) method, multispectral images from experimental maize plots were classed to split pixels into three groups (vegetation, shade and soil). The VIs and fv variables were estimated using just vegetative pixels. K_c based on cumulative growing degree days (CGDD) (K_c-CGDD) was compared to the spectral $K_c$fv:VI models. They demonstrated that three spectral-based

K_c models function well (R^2> 0.80). The model that best suited the K_c values was fv:NDVI R^2 = 0.91 to 0.94), whereas the fv:EVI2 and fv:WDRVI models performed poorly, demonstrating that UAV images with vegetation isolated from soil in high spatial resolution overcome the shortcomings of NDVI index.

Hassan *et al.* (2022) employed basic linear regression analysis on field K_c and LandSAT-8 generated NDVI to build K_c prediction equations for the wheat crop. The linear prediction equation, K_c= 2.0114 NDVI - 0.147, has a high R^2 value of 0.96 and was used to calculate crop evapotranspiration.

2.6 Irrigation Water Management using Remote Sensing Techniques

Water shortage is a serious constraint on irrigated agriculture, particularly in arid and semi-arid regions of the world. Because of global climate change and an imbalance in water supply and demand, it is especially important to enhance crop water usage and it is obtained by using Remote sensing and GIS techniques.

Pakhale *et al.* (2010) calculated the monthly crop water consumption of wheat from 1999 to 2003. They utilised the Hargreaves equation to calculate PET and a locally devised K_c to calculate evapotranspiration. The wheat crop ET_c was calculated using the product of K_c and PET. Crop water demand was calculated by multiplying ET_c by crop area for each month of the season (which was obtained by ANN technique). Crop water requirements ranged from 78.63 to 201.14 mm/month. The highest CWR was recorded in the month of December, while the lowest was recorded in the month of March. They calculated irrigation water requirements based on conveyance and field losses of roughly 35 per cent.

Gontia and Tiwari (2010) estimated the evapotranspiration of a wheat crop cultivated in the Tarafeni South Main Canal (TSMC) irrigation canal in West Bengal, India, using WiFS sensor data and GIS approaches. NDVI and SAVI-K_c connection was used to find pixel-wise crop coefficients and K_c maps were created. The FAO Penman Monteith technique was used to calculate reference evapotraspiration. The real crop

evapotranspiration of wheat crop was approximated spatially using K_c maps and the reference evapotranspiration for irrigation command region. The attribute tables were created to calculate the number of pixels and the area underneath them in maps for each set of ET_c values. By multiplying the area by ET_c, the monthly crop water need was calculated. Wheat crop water demand was relatively precise and regionally dispersed using crop coefficients based on soil adjusted vegetation index (SAVI) data.

Farg *et al.* (2012) used an integrated FAO-56 technique and remote sensing data to determine wheat crop actual evapotranspiration in Egypt's south Nile delta. They calculated monthly wheat crop evapotranspiration (ETa) using the FAO Penman Monteith equation and wheat crop coefficients (K_c) derived from a multilinear regression equation based on NDVI and SAVI. They discovered that water requirements were greater throughout the vegetative and mid-season stages, with a decreasing tendency toward maturity.

Palacios *et al.* (2012) investigated the evolution of wheat NDVI acquired from Landsat 5 and Landsat 7 images in 13 plots during the 2008 agricultural year in Irrigation District 038, Mayo River, Sonora, Mexico. They calculated the normalised difference vegetation index (NDVI) per plot average. The basal crop coefficient (K_c) was calculated using NDVI and a linear relationship. This K_c was then multiplied by the total amount of reference evapotranspiration measured at a representative meteorological station throughout the time of impact of each image. Crop evapotranspiration was calculated using reference evapotranspiration data and K_c values inferred from NDVI values for 15 Landsat 5 and 7 images spanning the whole wheat growth cycle. A programme was also devised to assist growers in improving their water efficiency.

Kumari *et al.* (2013) investigated the association between crop coefficients (K_c) and vegetation indicators derived from AWiFs data and discovered K_c for rice and wheat. Crop coefficient maps were created for each month of the rice-wheat crop season by applying a regression equation to the image in ERDAS Imagine. The FAO-56, Penman Monteith technique was used to estimate monthly reference crop evapotranspiration

(ET_o). ET_o was blended with geographically dispersed K_c maps from several months of the wheat crop season to produce crop evapotranspiration (ET_c) maps for each month. Crop water demand (CWR) was calculated for each month of the crop growing season by multiplying K_c values for rice and wheat crops by potential evapotranspiration.

Ozcan *et al.* (2014) determined ET_c values using K_c based on MSAVI values and ET_o values acquired using the FAO Penman-Monteith method in their wheat crop experiment in the Hilvan and Akcakale areas of Turkey. Crop water demand was calculated using the product of the average ET_c value and the related area. They discovered that water demands for farmed wheat fields varied depending on soil type and land use capability class.

Pimpale *et al.* (2015) estimated water requirement of wheat using multispectral vegetation indices for five wheat-growing districts in central Maharashtra. They used IRS-P6, AWiFS sensor images to construct RVI, NDVI, TNDVI, SAVI and MSAVI2 multi temporal vegetation indices. The NDVI-K_c model has the greatest R^2 and D values of 0.895 and 0.980. The crop coefficients (K_c) calculated using this NDVI-K_c model and reference evapotranspiration (ET_o) calculated using the Penman-Monteith equation were used to calculate wheat crop evapotranspiration (ET_c), which represents the water needs of wheat and found varying from 378.34 mm to 439.10 mm in the study area.

Singh *et al.* (2016) conducted cotton crop research in the Haryana district of Sirsa. The empirical equation was utilised to determine the K_{cb} value using a spectral index such as SAVI (Soil Adjusted Vegetation Index). Landsat TM5 images with high spatial resolution were used. Reference crop ET_o was calculated using the Blaney-Criddle Method and meteorological data from an observatory. To estimate crop evapotranspiration (ET_c), crop coefficients determined from remote sensing data were combined with ET_o measurements. Seasonal agricultural water requirements were calculated by aggregating monthly water requirements from June to November.

Arshad *et al*. (2018) calculated the real-time spatially distributed crop coefficient (K_c) and water demand of a wheat crop cultivated in Faisalabad District of Pakistan. K_c maps were created using MODIS 13Q1 satellite imagery and reference evapotranspiration (ET_o) was calculated using the CROPWAT model, which computes ET_o using the FAO-24 modified Blaney-Criddle technique with several variables. It was discovered that the average ET_c value for wheat grew significantly from December to February, from 0.59 to 1.16 mm/days, subsequently decreasing to 1.05 mm/days in March. Wheat crop water requirements ranged from 265 mm to 665 mm, with an average of 465 mm.

Kivrak *et al.* (2019) quantified water uses by Onion crop in the Mesilla Valley, New Mexico by using plant phenology and Landsat-8 satellite data. Thirteen Landsat-8 satellite images of clear sky days were acquired from www.earthexplorer.usgs.gov and processed using ENVI software for the 2014-2015 and 2015-2016 growth seasons. The Valley's Normalized Difference Vegetation Index (NDVI), albedo and land surface temperature (LST) were then estimated using Landsat-8 data. The ET of the Valley was computed using REEM utilising these factors and ground-measured climatic data. During the growing season, REEM estimated a maximum ET of 973 mm in 2015 and 975 mm in 2016. These readings contrasted favourably to FAO-56 crop coefficient-based ET forecasts of 894 and 955 mm during the same years (2015 and 2016).

Mishra *et al.* (2022) evaluated Irrigation performance using Remote Sensing techniques in the Naryanpur command area, India. Actual and potential evapotranspiration were calculated using meteorological datasets for the same time period. Potential Evapotranspiration was calculated using the surface Energy Balance technique. Actual evapotranspiration was calculated by multiplying the crop water stress index and crop coefficient by potential evapotranspiration. The actual evapotranspiration for both Kharif and *Rabi* crops ranged from 700 mm to 1550 mm.

CHAPTER III

MATERIAL AND METHODS

The current research has been conducted at the Department of Irrigation and Drainage Engineering, Dr. Panjabrao Deshmukh Krishi Vidyapeeth, Akola and Maharashtra Remote Sensing Application Centre (MRSAC), Nagpur. The location of the research region, the database, the materials and the methodologies adopted for the research are all covered in this chapter. The substantial information collected and used for the current study includes meteorological data, remote sensing satellite data, GIS and supplementary data, GPS data, information about different types of crops phenology, sowing / transplanting information and crop evapotranspiration.

3.1 Study Area

Study area comprises of wheat and onion growing three districts of Maharashtra state *viz*. Dhule, Jalgaon and Nashik. (Fig. 1) The study has been carried out for the *rabi* season of 2020-21 and 2021-22 respectively. The study area situated between 73° 78' 98" to 75° 52' 77" E longitude and 19° 99' 75" to 21° 03' 96" N latitude covering an area of 34542 km^2. Average annual rainfall of the study area is between 600-1000 mm. Major soil type of these region is black cotton soil (Regur Soil). Average maximum and minimum temperature of study area is about 41^oC and 18^oC, respectively. There is high temperature in Dhule and Jalgaon districts upto 45^oC in summer.

Due to their dominance during the *rabi* season, wheat and onion are the crops chosen for this study. The other *rabi* crops grown in the region include sorghum, chickpea, pigeon pea, maize and groundnut. There are also fruit crops including pomegranate, grapes, bananas, papaya and custard apple. Biannual cash crop like sugarcane also seen in the field during *rabi* season. Wheat and onion are cultivated using reliable irrigation sources. The main irrigation sources are canals, river and wells.

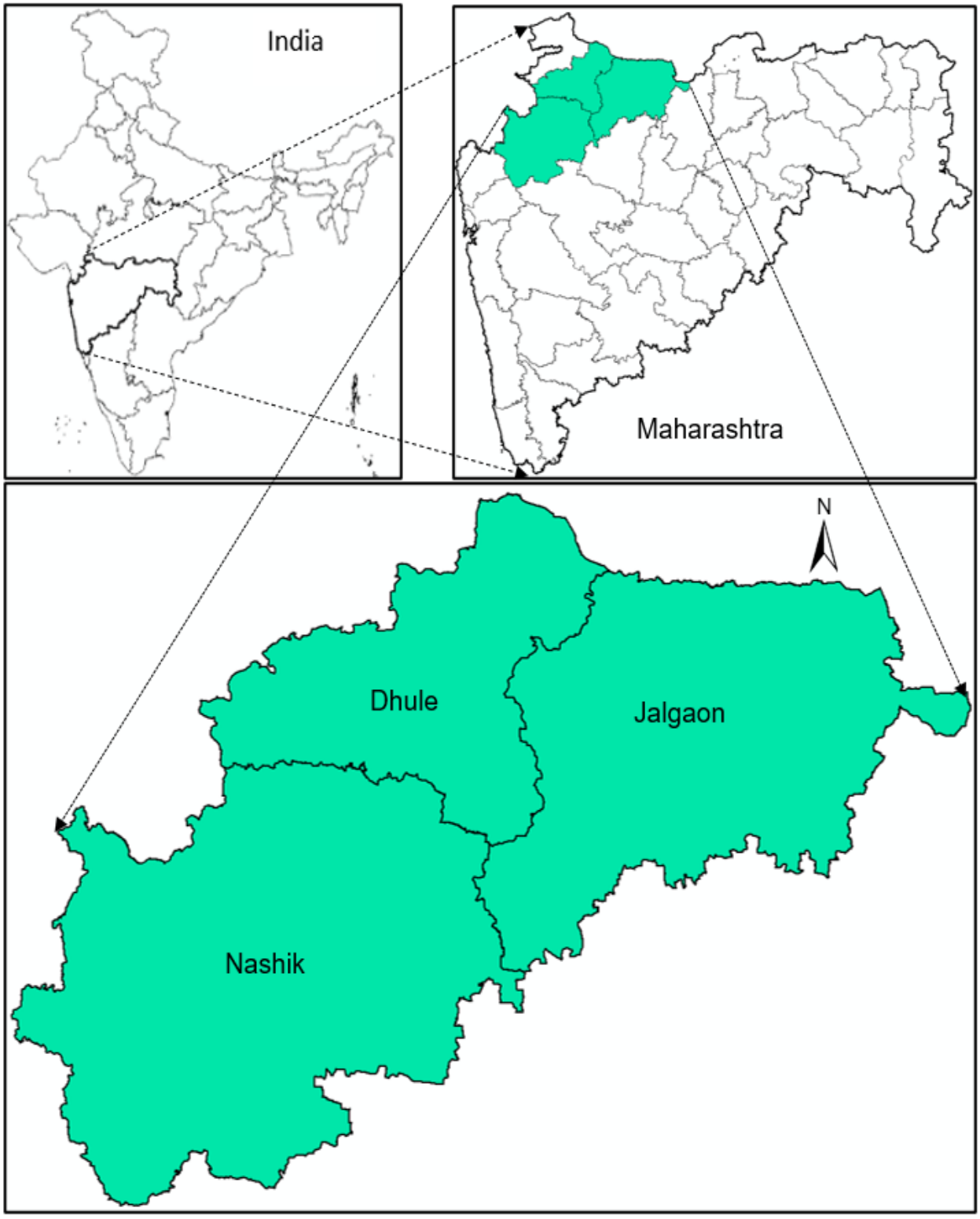

Fig 1. Location of Study Area

3.2 Remote Sensing Data:

The multi-spectral, Multi date satellite data of Sentinel 2A with Multi-spectral Instrument sensor (MIS) covering *rabi* season for the year 2020-21 and 2021-22 were used for the study. Sentinel data includes 13 bands of spectral responses with spatial resolutions of 10 m, 20 m and 60 m, ranging from visible to short wave infrared (SWIR). For this study five bands are used *viz.,* band-2 is Blue (0.443 µm), band-3 is Green (0.560 µm), band-4 is Red (0.665 µm), band-8 is Infra-red (NIR) (0.842 µm) and band-11 is Shortwave Infra-Red (SWIR) (1.610 µm). Blue, Green, Red and Infra-Red bands have 10 m resolution and Shortwave Infra-Red band has 20 m resolution. Sentinel has a swath path of 294 km and revisiting period 5 days. The projection and datum of the data products are Lambert Conformal Conic and WGS 84 UTM respectively. The data is freely available for download at the Sentinel Scientific Data Hub website (https://scihub.copernicus.eu/dhus/#/home).

Satellite images were downloaded for a period of five months from December 2020 to April 2021 and December 2021 to April 2022 with Date of Pass are listed in Table 1 and Table 2. Satellite images corresponding to two dates were obtained for each month. Proper care is taken to select satellite images with lesser cloud cover and with an almost uniform time gap between the consecutive ones. As Band-11 (SWIR) has 20 m resolution, it is necessary to convert into 10 m resolution and this is obtained by resampling process in ERDAS Imagine Software. These five bands were downloaded and raw images were obtained by stacking the layers. These stacked images undergo Mosaic process and then subset and clip process to prepare single false colour composite (FCC) image.

Thus, 10 subset images each, corresponding to study area were prepared, for year 2020-21 and 2021-22 using the data preparation module of ERDAS Imagine software and are shown in Plate 1 and Plate 2. The ERDAS Imagine version 20 and ArcGIS version 10.2 software were used for all remote sensing and GIS analysis.

Table 1. Multi-date Sentinel 2A data used for study (2020-21)

Sr no.	Satellite	Sensor	Date of pass
1.	Sentinel	MSI	15-12-2020
2.	Sentinel	MSI	25-12-2020
3.	Sentinel	MSI	19-01-2021
4.	Sentinel	MSI	29-01-2021
5.	Sentinel	MSI	13-02-2021
6.	Sentinel	MSI	28-02-2021
7.	Sentinel	MSI	15-03-2021
8.	Sentinel	MSI	25-03-2021
9.	Sentinel	MSI	09-04-2021
10.	Sentinel	MSI	19-04-2021

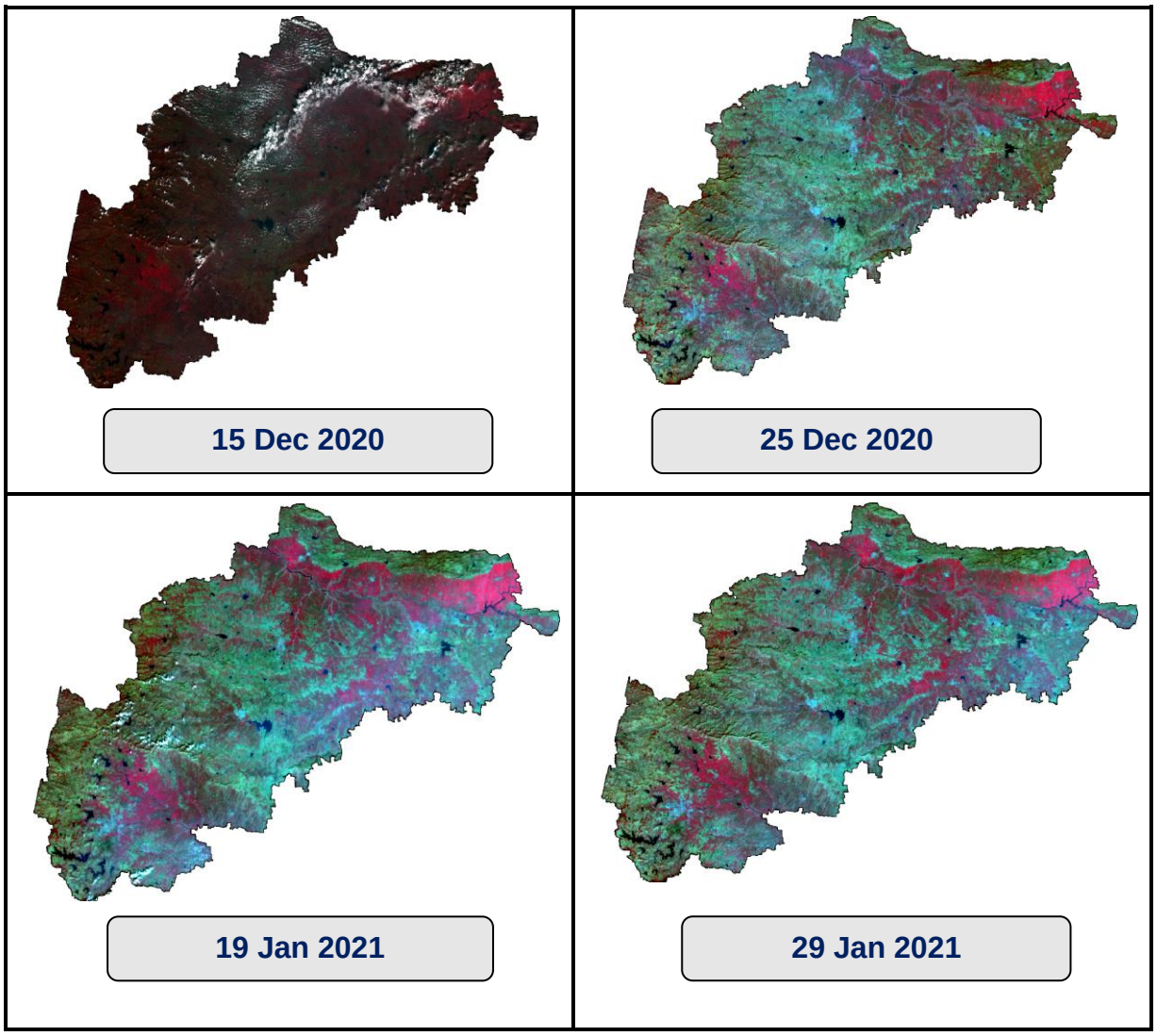

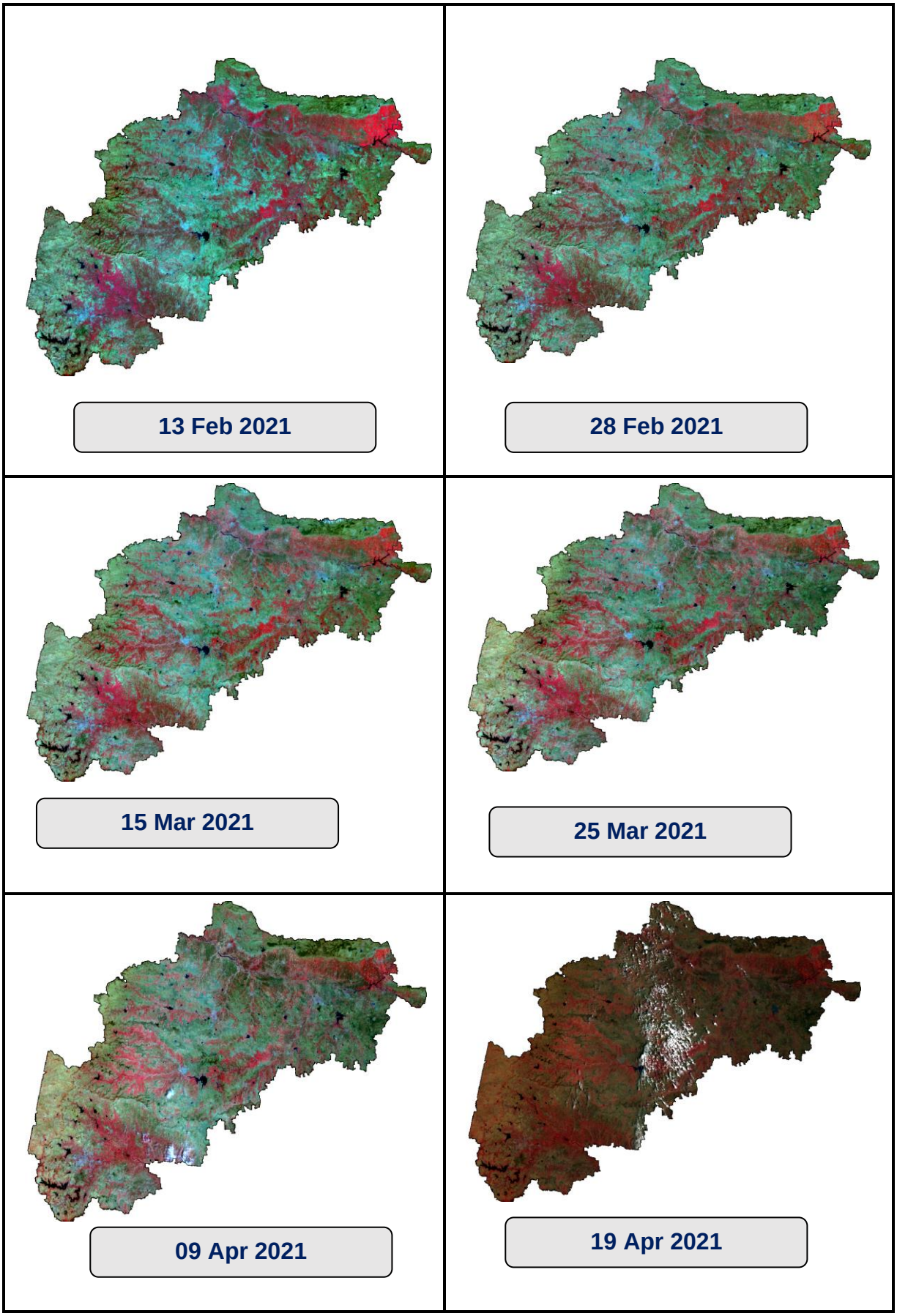

Plate 1. Subset Images of Study area (2020-21)

Table 2. Multi-date Sentinel 2A data used for study (2021-22)

Sr no.	Satellite	Sensor	Date of pass
1.	Sentinel	MSI	10-12-2021
2.	Sentinel	MSI	25-12-2021
3.	Sentinel	MSI	19-01-2022
4.	Sentinel	MSI	29-01-2022
5.	Sentinel	MSI	18-02-2022
6.	Sentinel	MSI	28-02-2022
7.	Sentinel	MSI	15-03-2022
8.	Sentinel	MSI	30-03-2022
9.	Sentinel	MSI	09-04-2022
10.	Sentinel	MSI	19-04-2022

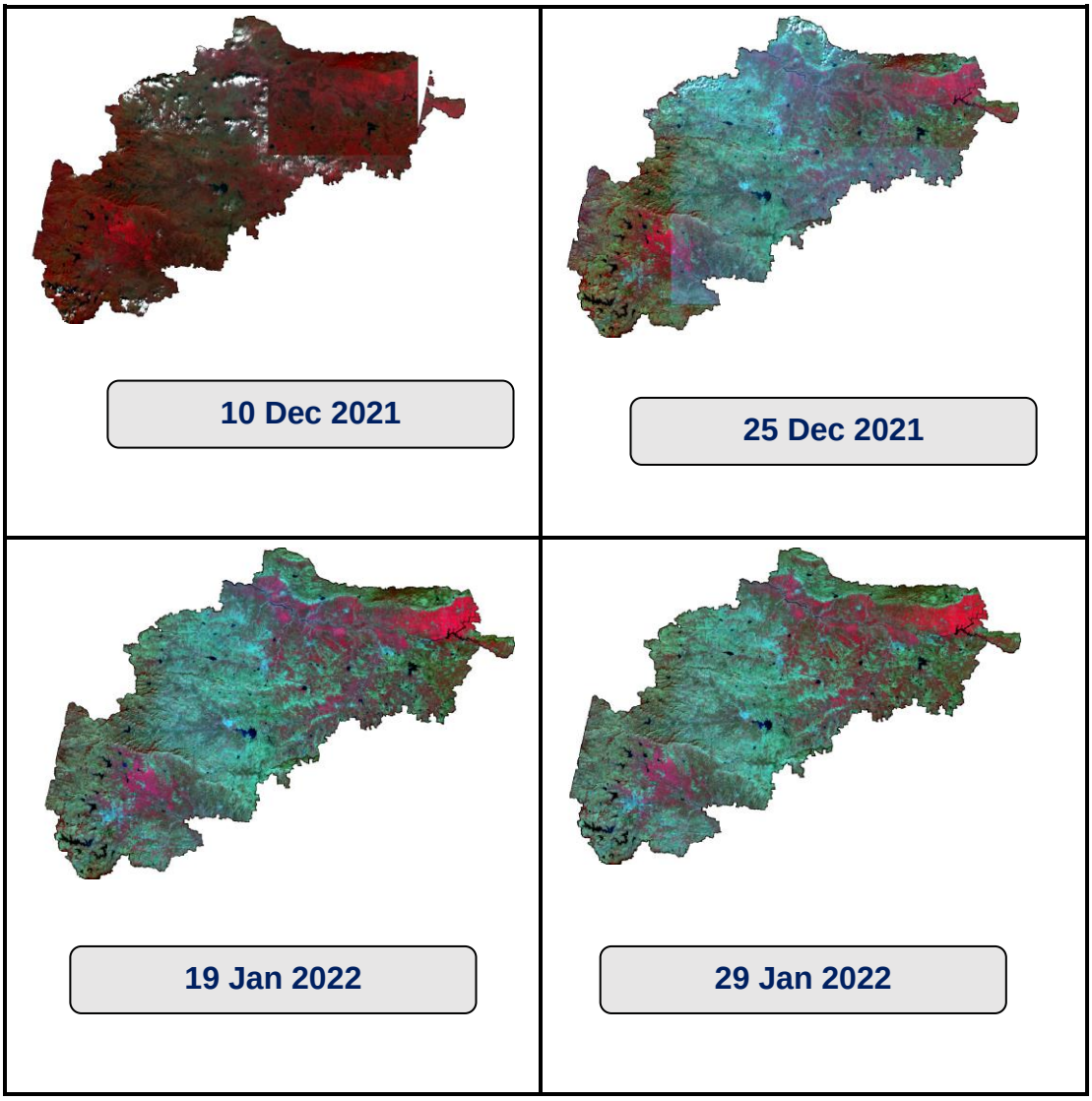

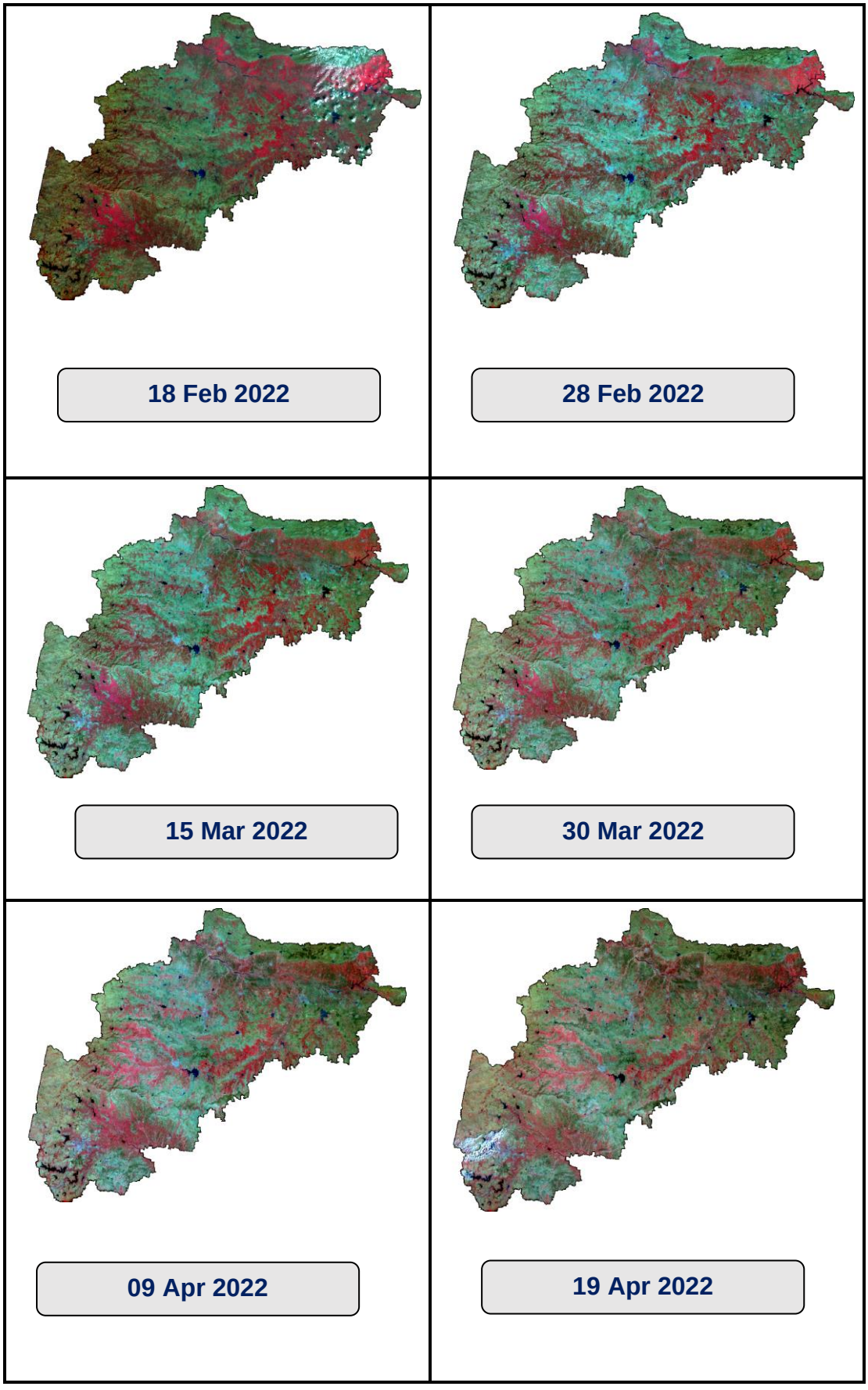

Plate 2. Subset Images of Study area (2021-22)

3.3 Supplementary Data

The Survey of India toposheets were used to digitise the administrative borders of the districts that were the subject of the study. The non-crop mask (NCM) of the research region was created using the water bodies, urban sprawl, forests, wastelands and other non-crop elements offered by MRSAC, Nagpur. In the research region, a vector layer was also produced to show basic elements like roads (national highways, express highways, district roads, etc.), rail lines, dams, canals and so on.

The district-wise crop data released by the Department of Agriculture, Government of Maharashtra, on the website www.krishi maharashtra.gov.in (Crop statistics, 2020-21 and 2021-22) related to study area was used as a guide for interpreting the outcomes of acreage estimation.

3.4 Weather Data

The required weekly meteorological data for the selected stations, namely Dhule, Jalgaon and Nashik (maximum air temperature, minimum air temperature, mean air temperature, mean relative humidity, wind speed, solar radiation was gathered from the website of NASA. (https://power.larc.nasa.gov)

3.5 Digital Analysis

The GIS and image processing software ArcGIS 10.2 and ERDAS Imagine 20 were used to conduct the digital analysis. The flowchart shows the approach used for digital analysis (Fig.2).

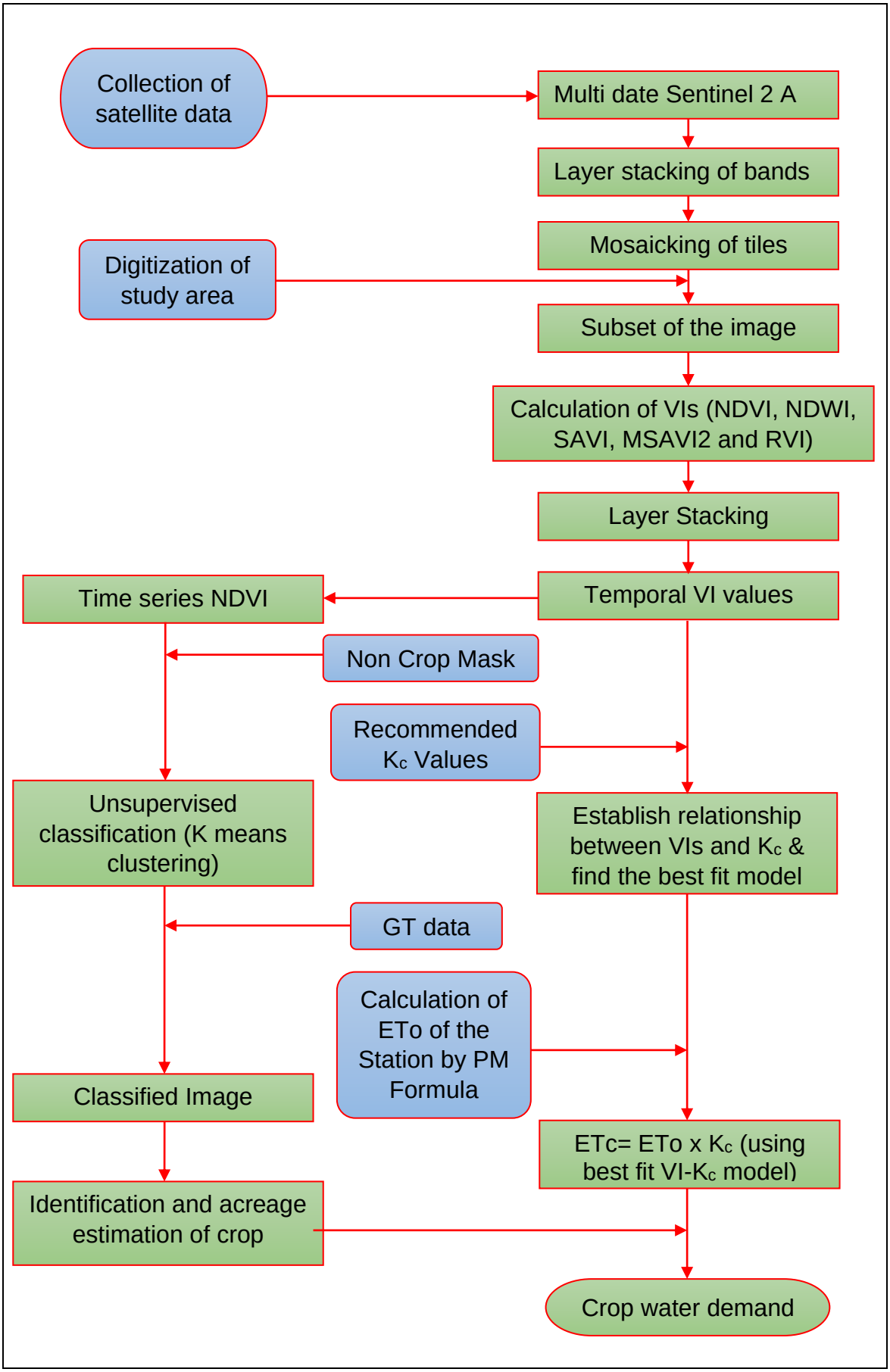

Fig 2. Flowchart for the digital analysis

3.6 Ground Truth (GT) Data Collection

The timing of the satellite data capture was synchronised using ground truth data that was gathered. During the field visit, specific data such as GPS position coordinates of the crop, crop area, sowing / transplanting time, crop development stage, ground cover percentage, other intercrops, crop infestation, soil type, moisture condition, crop calendar, number of irrigations applied, farmer details etc. were gathered. This section explains the process used to get the data from the ground truth sites.

3.6.1 GT planning

The planned ground truth survey's placements for the points, stations and regions were based on:

1. Work experience from the previous year.
2. Spots that are conveniently accessible by road.
3. The dominant crop regions under research.
4. The locations of the crops under investigation were located in satellite images from the previous growing season.

To prepare the GT plan, the following layers were used:

a. A corrected image from the previous year
b. Crop locations from the previous year
c. A road map of the research area.
d. Toposheet layer as a point of reference
e. Websites likes Google Maps and Google Earth

On the base map, locations with a chance of receiving standing onion or wheat crops were noted. To reduce field commuting, printouts of the potential visitation regions were taken to the field.

3.6.2 Equipment used for ground truth survey work

1. Hand held GPS (shown in Fig. 3)
2. Mobile with Android operating system with good quality camera (shown in Fig. 4)
3. Ground Truth Proforma Sheet (shown in Fig. 5)

Fig 3. Hand Held GPS device

Fig 4. Android Mobile with 48-megapixel camera

Ground Truth Sheet

		Date:	**Site ID:**
Sr No.	**Name of observed variable / Item**		**Value/Details of item**
1.	Location	Village	
		Taluka	
		District	
2.	GPS readings (At the middle of Field)	Latitude	
		Longitude	
		Elevation	
3.	Type of crop / LULC		
4.	Date of Sowing / Harvesting, approximate		
5.	Growth Stage		
6.	Size (L x W) in meters, approximate		
7.	Plant Height (cm)		
8.	Visual Soil Exposure, Soil Moisture Condition		
9.	Method of Irrigation / Number of Irrigations		
10.	Farmer Details		

Take photos of

1.Full view of main crop (from side) 2. Selected plants to get growth stage of crop

3. Field view showing surrounding situation 4. Other side of Road

Free hand field sketch (Mark north arrow, site, roads and surrounding details)

Fig 5. Proforma sheet used for recording field observations

3.6.3 Ground truth work

For *rabi* season of 2020-21, The ground truth (field visit) has been done between 24th January 2021 to 30th January 2021 in the research area. Information of 54 sites was collected. For *rabi* season of 2021-22, The ground truth has been done during 31st Jan 2022 to 09th Feb 2022. Data collected from 56 sites of wheat and onion by adopting following procedure,

1. The representative locations for the crops under research were found while navigating the fields in the study region. At the centre of the field, GPS measurements were taken.

2. The stage of the crops under investigation was carefully watched and the spread of the crop as well as adjacent crops and distinguishing characteristics were documented.

3. Based on the farmer's availability in the field, information on the date of sowing / transplanting, the type of crop, the likely date of harvest, the weather, etc., was gathered by interviewing the farmer and recorded into the proforma of the GT Sheet.

4. At each place, Android mobile with 48-megapixel camera was used to capture photos that showed:

a) Overall view of crop.

b) Vegetative development of crop.

c) The border of the nearby field.

d) The crop's stage and the level of soil moisture.

f) Signs on the neighbouring road with distance and directions.

The digital photograph also automatically included the position of station (latitude and longitude).

5. A rough sketch was made on the GT proforma sheet, indicating the position and direction of the road as well as all of the nearby landmarks. On the sketch made on the GT sheet, the position of the point of observation was clearly indicated.

6. Each GT site was properly catalogued and the serial numbers of the photographs were also recorded. The observed sites were assigned sequential IDs in the form of 1, 2, 3 and so on. The approximate (rough) polygons were also created indicating the locations of the crops of interest and the nearby crops.

7. The GT sheet itself was used to record any particular findings or information on the crops that were the subject of the study in that area. for instance, poor crop quality in a specific region, late seeding, etc.

The details of the GT stations and major crops with their co-ordinates are given in Table 3 and Table 4 for year 2020-21 and 2021-22 respectively.

Table 3. Geographical locations and crops of the Ground Truth sites 2020-21

Sr. No	Location of station	Latitude (N)	Longitude (E)	Major crops
1	Gartad	20° 50' 45.61"	74° 47' 46.77"	Maize, Wheat
2	Velhane	20° 46' 43.22"	74° 54' 41.17"	Maize, Wheat
3	Dholi	20° 46' 53.71"	74° 59' 43.56"	Maize, Wheat
4	Deogaon	20° 47' 24.54"	75° 5' 59.91"	Wheat, Gram
5	Mukati	20° 52' 24.73"	74° 55' 32.66"	Wheat, Gram
6	Savkheda	20° 53' 43.69"	75° 14' 0.97"	Wheat
7	Palasdal	20° 54' 30.92"	75° 18' 28.03"	Wheat, Gram
8	Vikharan	20° 57' 25.10"	75° 21' 36.82"	Wheat, Onion
9	Pimpalkotha	20° 59' 2.85"	75° 22' 18.03"	Maize, Wheat
10	Eklagne	21° 0' 46.82"	75° 24' 38.90"	Wheat
11	Khedi Bk.	21° 0' 22.48"	75° 35' 24.62"	Wheat, Sorghum
12	Nashirabad	21° 0' 8.29"	75° 37' 40.57"	Wheat, Sorghum
13	Bhusawal	21° 2' 46.23"	75° 45' 29.90"	Wheat, Sorghum
14	Chinchpura	21° 0' 57.50"	75° 22' 46.83"	Maize, Wheat
15	Nishane	21° 4' 9.48"	75° 14' 54.23"	Maize, Wheat
16	Tawase	21° 10' 20.44"	75° 16' 17.57"	Papaya, Banana, Sugarcane, Wheat
17	Borkund	20° 44' 51.21"	74° 49' 8.67"	Wheat, Maize,Groundnut
18	Gavhane	21° 13' 28.51"	74° 49' 59.09"	Wheat, Sorghum
19	Dabhashi	21° 15' 54.31"	74° 50' 51.58"	Wheat, Sorghum
20	Savalade	21° 17' 38.89"	74° 51' 26.77"	Sugarcane, Wheat
21	Untawad	21° 18' 47.34"	74° 51' 42.15"	Sugarcane, Wheat
22	Shirpur	21° 19' 52.77"	74° 52' 18.23"	Wheat, Banana
23	Gorane	21° 9' 53.65"	74° 49' 5.02"	Wheat

24	Devbhane	21° 02’ 02.9’’	74° 47’ 5.76’’	Wheat
25	War-Kundane	20° 54' 8.16"	74° 40' 23.12"	Wheat, Maize
26	Ner	20° 56' 43.00"	74° 29' 47.80"	Wheat, Onion
27	Khadak Malegaon	20° 11' 55.37"	74° 11' 1.36"	Wheat, Onion
28	Lonwadi	20° 9' 53.83"	74° 2' 1.58"	Wheat, Grapes
29	Tamaswadi	20° 46' 18.84"	75° 3' 0.03"	Onion, Wheat
30	Vikharan	20° 57' 24.71"	75° 21' 36.99"	Onion
31	Vikharan	20° 56' 46.03"	75° 21' 51.25"	Onion, Wheat
32	Akkalpada	20° 56' 29.20"	74° 27' 43.30"	Onion
33.	Ner	20° 55' 39.11"	74° 29' 17.01"	Wheat, Onion
34.	Purmepada	20° 43' 49.70"	74° 42' 4.99"	Onion, Wheat
35.	Chikhal Ohol	20° 36' 32.30"	74° 37' 11.35"	Onion, Wheat
36.	Wake	20° 29' 20.69"	74° 26' 7.27"	Onion, Wheat
37.	Chandwad	20° 18' 26.68"	74° 13' 33.19"	Onion, Wheat
38.	Bhoyegaon	20° 14' 58.77"	74° 10' 33.96"	Onion
39.	Khadak Malegaon	20° 11' 35.80"	74° 10' 58.20"	Onion, Wheat
40.	Sarole kh	20° 9' 58.02"	74° 8' 34.47"	Onion, Grapes
41.	Sakore	20° 26' 55.28"	73° 59' 13.54"	Onion, Grapes
42.	Kalwan kh	20° 29' 30.72"	74° 2' 34.11"	Onion, Grapes
43.	Niwane	20° 28' 35.25"	74° 4' 21.97"	Onion
44.	Matane	20° 27' 48.62"	74° 8' 26.96"	Onion
45.	Malwadi	20° 28' 41.88"	74° 11' 20.61"	Onion
46.	Thengoda	20° 31' 48.71"	74° 11' 39.78"	Onion
47.	Satana	20° 34' 11.65"	74° 11' 39.41"	Onion
48.	Chaugaon	20° 37' 34.91"	74° 14' 10.91"	Onion, Pomegranate
49.	Khirmane	20° 42' 44.74"	74° 17' 40.56"	Onion, Pomegranate
50.	Nampur	20º 44’ 33.5’’	74º 18’ 56.4’’	Onion
51.	Shewadi	20° 59' 4.34"	74° 22' 56.02"	Onion, Wheat
52.	New Tamaswadi	20° 59' 5.94"	74° 23' 58.49"	Onion, Wheat
53.	New Bhadane	20° 56' 48.15"	74° 29' 5.55"	Onion, Wheat
54.	Morane	20° 55' 23.52"	74° 34' 23.22"	Onion, Wheat

Table 4. Geographical locations and crops of the Ground Truth sites 2021-22

Sr. No	Location of station	Latitude (N)	Longitude (E)	Major crops
1.	Borkund	20° 45' 10.89"	74° 48' 40.71"	Maize, Wheat, Onion
2.	Borkund	20° 43' 48.61	74° 51' 17.83"	Maize, Wheat, Onion
3.	Shirud	20° 45' 3.52"	74° 54' 4.85"	Maize, Wheat
4.	Bole	20° 47' 24.00"	75° 1' 34.81"	Maize, Wheat
5.	Songir	21° 3' 18.83"	74° 47' 4.57"	Wheat, Onion
6.	Sawalde	21° 17' 41.58"	74° 51' 27.39"	Wheat, Gram
7.	Untawad	21° 18' 1.92"	74° 51' 34.57"	Wheat, Gram
8.	Shirpur	21° 19' 54.84"	74° 52' 11.93"	Wheat, Banana
9.	Nagaon	20° 57' 18.77"	74° 46' 49.58"	Wheat, Onion
10.	Devergaon	20° 12' 31.05"	74° 10' 37.75"	Wheat, Onion
11.	Lonwadi	20° 9' 49.35"	74° 1' 48.15"	Wheat, Grapes
12.	Dhule	20^0 54’ 22.5’’	74^0 47’ 57.7’’	Wheat, Maize
13.	Navalnagar	20° 56' 5.50"	74° 53' 30.66"	Wheat
14.	Tawase	21° 9' 24.64"	75° 16' 5.50"	Wheat, Banana
15.	Nandri	21° 6' 36.62"	75° 10' 55.13"	Wheat, Maize
16.	Nishane	21° 3' 52.23"	75° 15' 2.91"	Wheat
17.	Pimpale BK`	21° 2' 17.85"	75° 15' 16.45"	Wheat
18.	Koradi	21° 0' 31.41"	75° 18' 39.07"	Wheat, Cotton
19.	Pimpri	21° 1' 11.92"	75° 20' 43.40"	Wheat, Gram
20.	Chinchpura	21° 1' 2.30"	75° 22' 32.06	Wheat, Maize
21.	Paladhi	21° 0' 46.20"	75° 28' 2.16"	Wheat
22.	Nashirabad	21° 0' 1.13"	75° 38' 48.98"	Wheat, Gram
23.	Nashirabad Toll	21° 1' 4.36"	75° 41' 6.96"	Wheat, Sugarcane
24.	Khedi	21° 0' 22.64"	75° 35' 24.62"	Wheat, Gram

25.	Pimpri Er	20° 59' 18.42"	75° 23' 19.05"	Wheat
26.	Palaskhede	20° 55' 5.79"	75° 18' 49.85"	Wheat
27.	Sarve	20° 53' 28.57"	75° 12' 19.78"	Wheat, Gram
28.	Vichkheda	20° 51' 51.54"	75° 4' 11.44"	Wheat,
29.	Borkund	20° 44' 50.02"	74° 48' 40.68"	Onion, Wheat
30.	Sawalde	21° 17' 9.33"	74° 51' 3.38"	Wheat, Gram
31.	Deobhane	21° 0' 30.73"	74° 47' 4.68"	Wheat, Onion
32.	Purmepada	20° 43' 50.84"	74° 42' 4.57"	Onion
33.	Devarpade	20° 37' 44.40"	74° 38' 44.20"	Onion
34.	Chandanpuri	20° 31' 55.25"	74° 30' 24.62"	Onion, Wheat
35.	Wake	20° 29' 22.02"	74° 26' 8.00"	Onion
36.	Chinchve	20° 23' 34.86"	74° 20' 1.87"	Onion
37.	Chandwad	20° 18' 32.87"	74° 13' 33.18"	Onion
38.	Palsur	20° 17' 4.51"	74° 12' 21.16"	Onion
39.	Bhoyegaon	20° 14' 17.69"	74° 10' 29.71"	Onion
40.	Khadak Malegaon	20° 11' 30.03"	74° 10' 51.29"	Onion, Wheat
41.	Ranwad	20° 10' 26.56"	74° 6' 52.84"	Onion
42.	Pimpalgaon Bt	20° 9' 55.64"	74° 0' 33.95"	Onion, Grapes
43.	Tisgaon	20° 17' 12.28"	73° 56' 14.51"	Onion, Grapes
44.	Nanduri	20° 26' 9.89"	73° 56' 33.13"	Onion
45.	Sakore pada	20° 26’ 50.4’’	73^0 58’ 37.0’’	Onion
46.	Manur	20° 28' 42.76"	74° 0' 42.93"	Onion
47.	Kalwan bk	20° 29' 30.83"	74° 2' 34.09"	Onion
48.	Niwane	20° 28' 58.55"	74° 3' 42.24"	Onion
49.	Matane	20° 27' 48.03"	74° 8' 26.50"	Onion
50.	Malwali	20° 28' 41.89"	74° 11' 20.67"	Onion
51.	Sawaki phata	20° 32' 14.80"	74° 11' 36.06"	Onion
52.	Satana	20° 36' 26.78"	74° 12' 57.05"	Onion
53.	Manglur	21° 1' 9.39"	75° 1' 20.74	Onion, Wheat
54.	Nishane	21° 4' 59.69"	75° 14' 30.24"	Onion, Wheat
55.	Vikharan	20° 57’ 4.32’’	75° 21’ 14.96’’	Onion, Wheat
56.	Kasvivihir	20° 52' 37.06"	74° 54' 43.77"	Onion, Wheat

3.6.4 Processing of GT Data

The digital processing of the GT data obtained during fieldwork went as follows:

1. GT survey sheets and sketches were scanned and saved in a specific folder in .jpeg format. Fig 6. depicts an example of a GT proforma sheet with recorded data and a field drawing.
2. The photographs captured during the GT survey were categorised using GT location points like 1, 2, 3, ..., 56. Plates 3 (a, b and c) and 4 (a and b) show a few GT images taken during field observations of *rabi* onion, wheat and other crops during *rabi* season of year 2020-21 and 2021-22 respectively.
3. Preparation of shape file of GT points (Point vector layer): The shape/vector file indicating locations of GT sites was prepared for year 2020-21 and 2021-22 with appropriate annotations and appropriate attribute information were attached (Fig 7. and Fig 8.) The related photographs were also linked with the corresponding sites. ArcMap supports identification of all the information. All the information related to a GT site can be extracted just by clicking the GT site location on the point vector layer.

By using the above process, 54 GT points of year 2020-21 and 56 GT points of 2021-22 were digitally captured and given names in the shape file.

Ground Truth Sheet

		Date: 26/01/2021	Site ID: 17
Sr No.	**Name of observed variable / Item**		**Value/Details of item**
1.	Location	Village	Ratanpura
		Taluka	Dhule
		District	Dhule
2.	GPS readings (At the middle of Field)	Latitude	20°44'51.21"
		Longitude	74°49'8.67"
		Elevation	353
3.	Type of crop / LULC		Wheat / Groundnut / Gram
4.	Date of Sowing / Harvesting, approximate		3rd week of Nov.
5.	Growth Stage		
6.	Size (L x W) in meters, approximate		1 ha
7.	Plant Height (cm)		30-45 cm
8.	Visual Soil Exposure, Soil Moisture Condition		Irrigated
9.	Method of Irrigation / Number of Irrigations		Border + 6 irrigation.
10.	Farmer Details		Mrs. Indumati Prakash Mali

Take photos of No. of photos taken = (7)

✓1. Full view of main crop (from side) ~~2.~~ Selected plants to get growth stage of crop

✓3. Field view showing surrounding situation ~~4.~~ Other side of Road

Free hand field sketch (Mark ~~north arrow~~, site, roads and surrounding details)

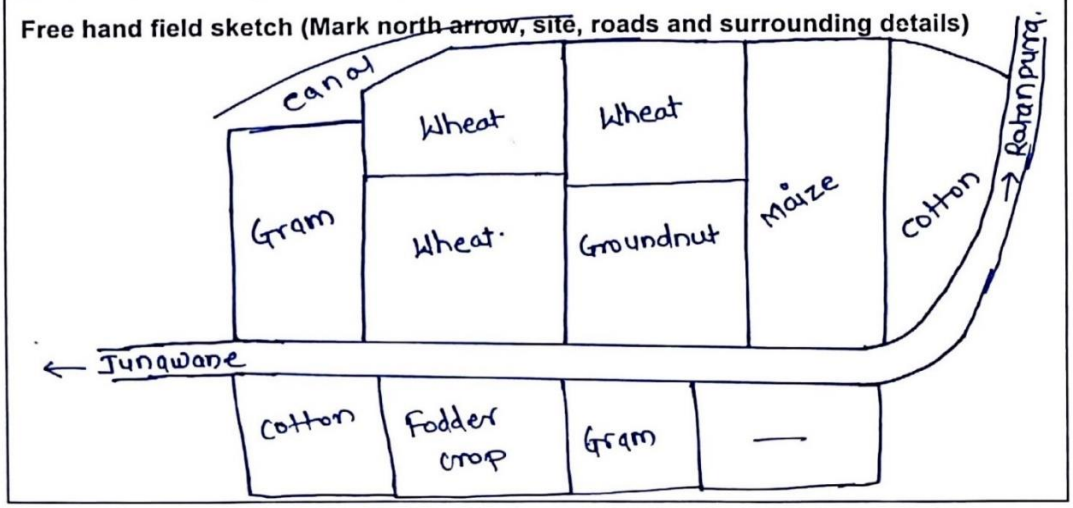

Fig 6. Sample of Ground truth proforma sheet

Plate 3 (a). Observations of wheat and onion crop during GT

Plate 3 (b). Observations of wheat and onion crop during GT

Plate 3 (c). Observations of wheat and onion crop during GT






Plate 4 (a). Observations of other crop during GT

Plate 4 (b). Observations of other crop during GT

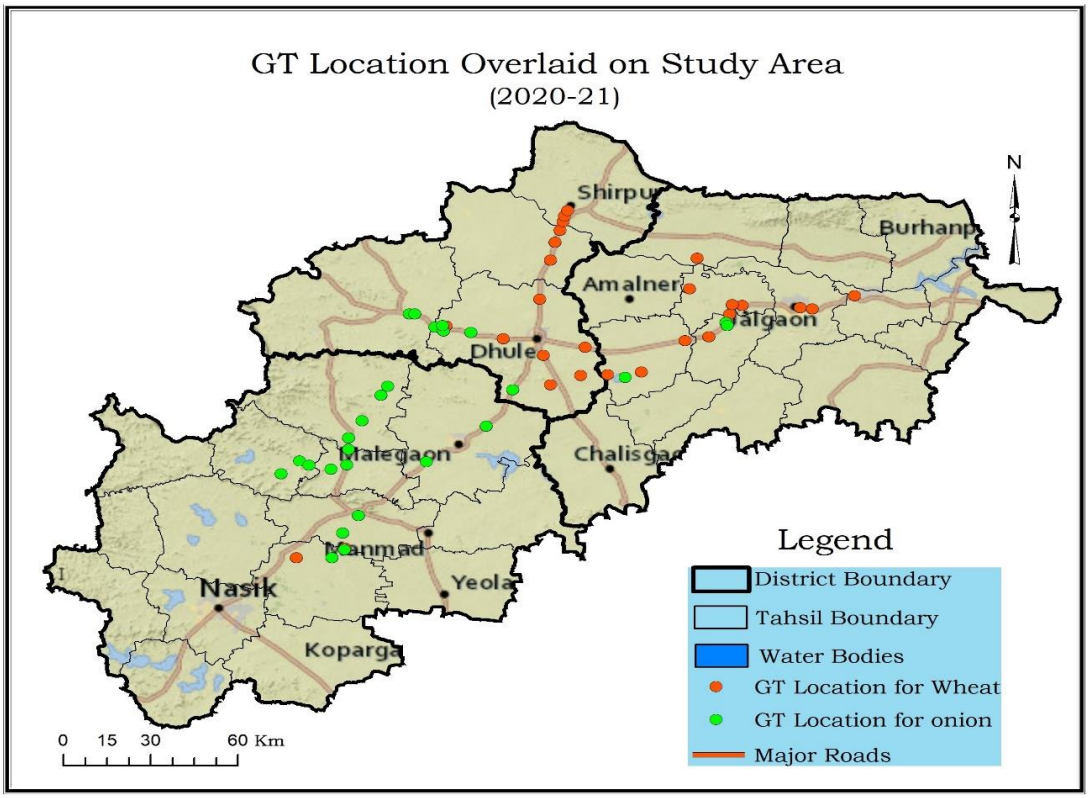

Fig 7. Point vector map of study area showing ground truth stations for 2020-21

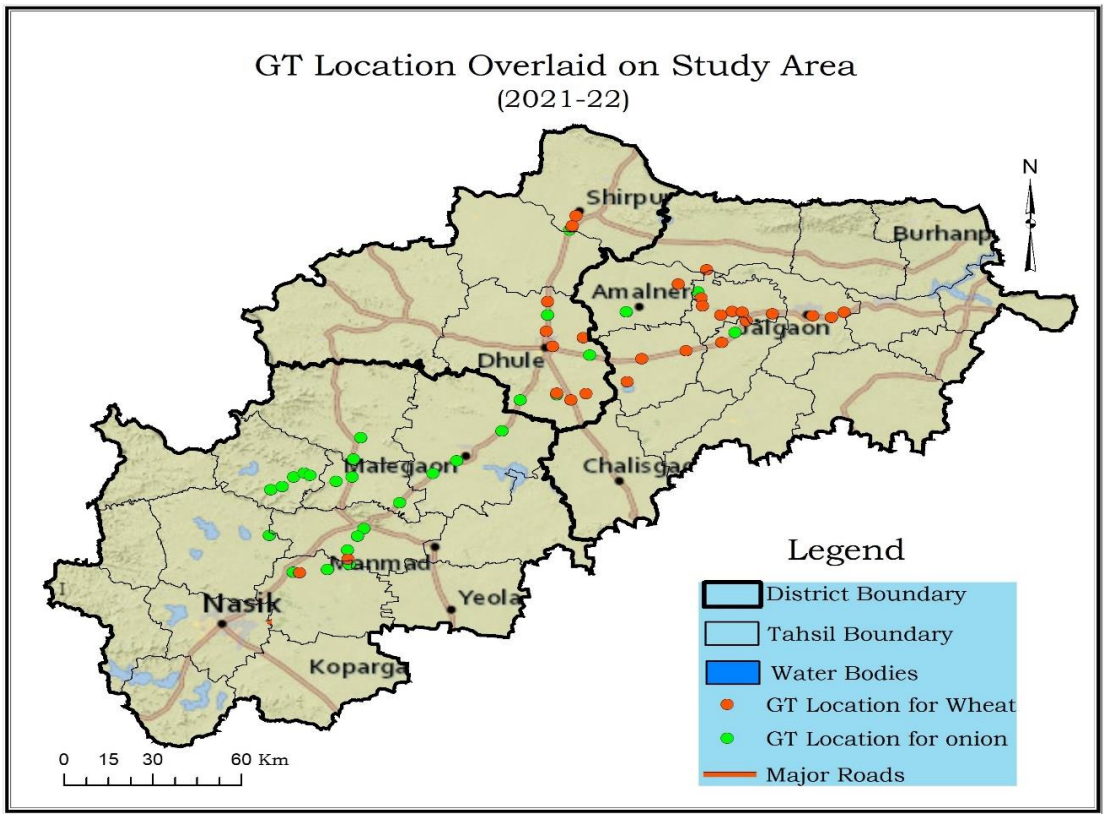

Fig 8. Point vector map of study area showing ground truth stations 2021-22

3.7 Determination of Age of Wheat Crop

The wheat crop fields were visited on the field visits. The criteria for choosing the field were entirely random, however having a farmer in the field was an advantage. By speaking with the farmers, information on the planting date, the variety and the anticipated harvesting date was gathered. The age of the wheat crop was established by visual observations in the absence of a farmer in the field or in the absence of crop age data. In this instance, the Feekes scale of wheat growth, which is depicted in Fig 9., was used to determine the crop age indirectly. This criterion was somewhat modified to fit local situations shown in Table 5.

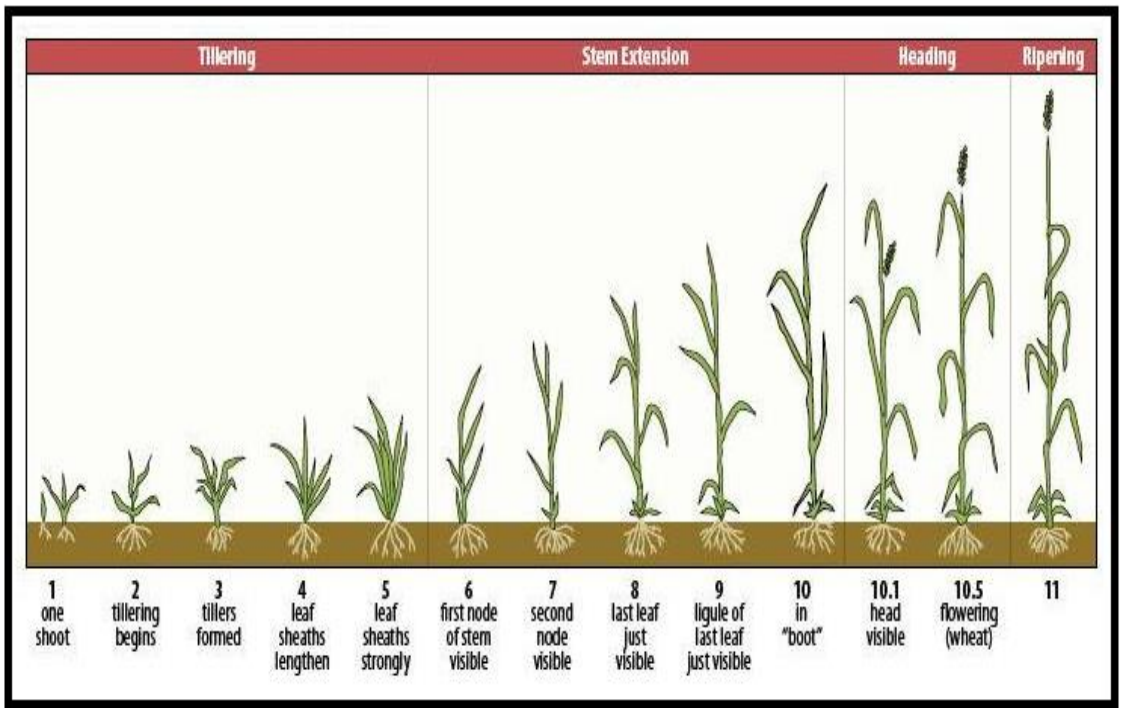

***Source:** Herbek J and Lee C (July 2009)

Fig 9. Feekes scale of wheat development

Table 5. Modification of wheat crop stage detection criterion as per local conditions

Stage No.	Identifying Characteristics	Growth Stage	Days after Sowing	Week	Approx. Weeks
1.	First leaf through coleoptile	Germination	0-10	2	0-2
2.	1-9 leaves unfolded and main shoot	Seedling growth	11-20	3	2-3
3.	Main shoot and 1-9 tillers	Tillering	21-30	4	3-4
4.	1-6 detectable nodes	Stem elongation	31-40	6	4-6
5.	Flag leaf visible, boot swollen and first visible awns	Booting	41-50	7	6-7
6.	First spikelet of head visible to head completely emerged	Head emergence	51-60	9	7-9
7.	Complete flowering process	Pollination	61-70	10	9-10
8.	Kernel (caryopsis) watery ripe to late milk	Milk development	71-80	12	10-12
9.	Early dough to soft dough	Dough development	81-90	13	12-13
10.	Kernel hard (hard to split by thumbnail) to Kernel loosening in day time and overripe	Ripening	91-100	17	14-17

(This information was collected through personal communications with experts in the region)

3.8 Determination of Age of Onion Crop

Rabi Onion field were visited during GT data collection. Field selection is totally random, since availability of farmer in the field become advantageous. Information such as transplanting date, variety, harvesting time, area of field, etc. were collected by discussing with the farmer. In the absence of farmer, date of transplanting, crop age, growth stage, etc. were determined by visual observations. In such situation indirect method of determining the crop age was followed by referring to the criteria suggested by www.sgmnutrition.com and then this criteria was modified as per the local conditions shown in Table 6.

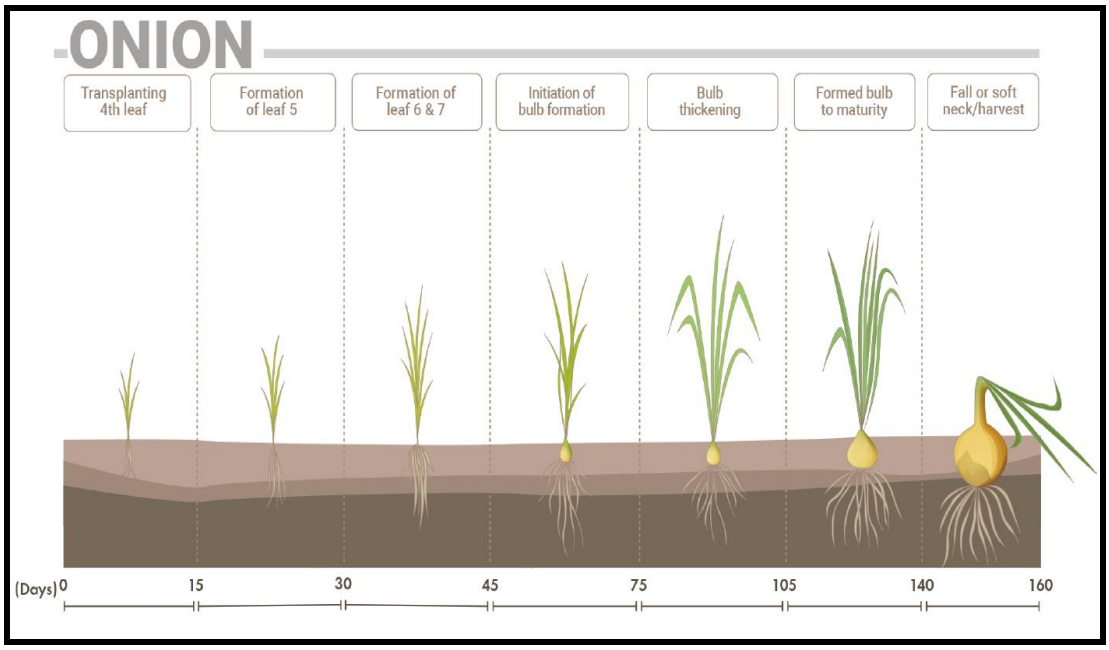

Source (www.sqmnutrition.com)

Fig 10. Phenology of Onion crop

Table 6. Modification of onion crop stage detection criterion as per local conditions

Stage No.	Identifying Characteristics	Growth Stage	Days after Transplanting	Week	Approx. Weeks
1.	4th leaf	Transplanting	0-15	2	0-2
2.	5th true leaf visible	Leek stage	16-30	4	2-4
3.	Formation of 6-7 leaves	Leaf elongation	31-45	6	4-6
4.	Visible 7-8 leaves with bulb initiation	Bulb initiation	45-75	10	6-10
5.	Bulb diameter increases 4 to 7.5 mm	Bulb Thickening	75-105	14	10-14
6.	bulb enlargement complete (>7.5 mm), greater than 50% cropped to dry down	Bulb Maturation / Fall of neck	105-150	16	16 and more

(This information was collected through personal communications with experts in the region)

3.9 Reference Image Date

3.9.1 Determination of reference image (RI) date

For *rabi* season of 2020-21, The ground truth was conducted between 24th to 30th Jan 2021. The images of 19 January 2021 and 29 January 2021 were nearest to the dates of GT. Because there is a shorter time lag between the date of pass 29 January and the field visits, the image of this date was used as a standard or reference image (RI).

Similarly, for *rabi* season of 2021-22, The ground truth was conducted between 31 Jan to 09 Feb 22. The exact date of the field visit and any date of satellite overpass did not coincide. The images of 29 Jan 2022 and 18 Feb 2022 were closest to dates of GT. But there is a shorter time lag between the date of pass 29 Jan 2022 and field visit, the image of this date was considered as reference image.

3.9.2Determination of actual age of crops on RI date

The following criteria were used to determine the exact age of crops (both wheat and onion) in weeks on the reference image date.

1. For *rabi* season of 2020-21

a) For GT taken between 24-26 January 2021:

The crop age in weeks on the GT date is determined using information obtained from the farmer or using the criteria described in sections 3.7 (wheat) and 3.8 (onion). To get age on RI date (29 January 2021) one week is added.

Thus,

Age of crop on reference image date = Age on GT date + 1 Week.

b) For GT taken between 27-30 January 2021:

On the GT date, the crop age in weeks is determined using information provided from the farmer or the criteria given in sections 3.7 (wheat) and 3.8. (onion). Because of the very short time lag, the age in weeks on the RI date, i. e. 29 January 2021, is assumed to be the same.

Age of crop on reference image date = Age on GT date.

2. For *rabi* season of 2021-22

a) For GT taken between 31 Jan to 1 Feb 2022:

The crop age in weeks as of the GT date is calculated using information provided from the farmer or the criteria given in sections 3.7 (wheat) and 3.8 (onion). Because of the very short time lag, the age in weeks on the RI date, i.e. 29 January 22, is assumed to be the same.

Age of crop on reference image date = Age on GT date.

b) For GT taken on 3 Feb 2022:

On the GT date, the crop age in weeks is established using information provided from the farmer or the parameters given in sections 3.7 (wheat) and 3.8. (onion). To get age on RI date (29 January 2022) one week is subtracted.

Thus,

Age of crop on reference image date = Age on GT date - 1 Week.

c) For GT taken on 9 Feb 2022:

The crop age in weeks on the GT date is determined using information obtained from the farmer or using the criteria described in sections 3.7 (wheat) and 3.8 (onion). To get age on RI date (29 January 2022) two weeks are subtracted.

Thus,

Age of crop on reference image date = Age on GT date - 2 Week.

3.9.3 Criteria for week-wise distribution of data values

After determining the age of crop on the reference image date (29 Jan 2021 and 29 Jan 2022), the criterion (trial and error) was developed for determining the age of crop on other image dates, as shown in Table 7 and Table 8.

Table 7. Criterion adopted for week wise distribution of data values for 2020-21

Sr. No.	Image Date	Interval Between Succeeding images (Days)	Interval (Weeks)	Cumulative interval from RI date	Interval (Approx. weeks rounded)	Determined Age in weeks
1.	15 Dec 2020	10	1.4	6.3	1	GT-6
2.	25 Dec 2020	25	3.5	4.9	4	GT-5
3.	19 Jan 2021	10	1.4	1.4	1	GT-1
4.	29 Jan 2021	RI date. Decide age in weeks on this date from the actual age on GT date				
5.	13 Feb 2021	15	2.1	2.1	2	GT+2
6.	28 Feb 2021	15	2.1	4.2	2	GT+4
7.	15 Mar 2021	15	2.1	6.3	2	GT+6
8	25 Mar 2021	10	1.4	7.7	1	GT+7
9	09 Apr 2021	15	2.1	9.8	2	GT+9
10	19 Apr 2021	10	1.4	11.2	1	GT+10

Table 8. Criterion adopted for week wise distribution of data values for 2021-22

Sr. No.	Image Date	Interval Between Succeeding images (Days)	Interval (Weeks)	Cumulative interval from RI date	Interval (Approx. weeks rounded)	Determined Age in weeks
1.	10 Dec 2021	15	2.1	7.0	2	GT-7
2.	25 Dec 2021	25	3.5	4.9	4	GT-5
3.	19 Jan 2022	10	1.4	1.4	1	GT-1
4.	29 Jan 2022	RI date. Decide age in weeks on this date from the actual age on GT date				
5.	18 Feb 2022	20	2.8	2.8	3	GT+3
6.	28 Feb 2022	10	1.4	4.2	1	GT+4
7.	15 Mar 2022	15	2.1	6.3	2	GT+6
8	30 Mar 2022	15	2.1	8.4	2	GT+8
9	09 Apr 2022	9	1.2	9.6	1	GT+9
10	19 Apr 2022	10	1.4	11.0	1	GT+10

3.10 Multispectral Vegetation Indices (VIs)

Images from remote sensing satellites are based on the surface's reflection of solar energy. The type of surface affects its reflectance in different ways. The spectral bands impacting on the surface also affect it. In order to determine the characteristics of a surface, measuring the reflectance of a particular spectral band from that surface is insufficient. By using an index, which is a combination of reflectance data from two or more spectral bands, this issue can be resolved. The indices produced by mixing mostly red (RED) and near infrared (NIR) bands are known as spectral vegetation indices and they serve as indicators of how green a surface is. These might just be referred to as vegetation indices (VIs). Utilizing the distinctive spectral signature of green vegetation in comparison to the spectral signatures of other earth components is the justification for vegetation indices. The visible Red and near-infrared (NIR) spectral reflectance pattern of green leaves is unique. The visible Red light spectrum is strongly absorbed by a few pigments found in plant leaves. The near-infrared light (NIR) wavelengths that are undetectable to human vision are substantially reflected by the leaves themselves. The reflectance in the blue and red areas are incredibly low, whereas, the green region has a slightly greater bump. Therefore, to human sight, the leaves seem green.

As a result, several vegetation indexes have been developed by various researchers, mostly employing Red and NIR band data. By ratioing, differencing, ratioing differences and creating linear combinations of spectral band data, the VIs may be determined. Numerous scientists have developed various vegetation indexes that are particularly important under particular vegetation situations. All the vegetation indicators are strongly connected to leaf area index and vegetation cover. To create typical growth conditions in a location for a specific time of year, VI values can be averaged across time. Further study can then characterise the health of the vegetation in that location in comparison to the normal. VIs can identify where vegetation is thriving and where it is stressed throughout time, as well as changes in vegetation caused by human activity.

In order to investigate the relationship between important vegetation indices and crop coefficients, such as the Normalized Difference Vegetation Index (NDVI), Normalized Difference Water Index (NDWI), Soil Adjusted Vegetation Index (SAVI), Modified Soil Adjusted Vegetation Index (MSAVI2) and Ratio Vegetation Index (RVI) an attempt has been made to incorporate these indices in this study.

3.10.1 Normalized Difference Vegetation Index (NDVI)

NDVI was created for the first time by Rouse *et al.* (1974). It is a ratio that is determined by dividing the total of the reflectance in the infrared (NIR) and red (RED) colour bands for each pixel in the image by the difference between the reflectance in the near-infrared (NIR) and red (RED) colour bands.

$$NDVI = \frac{NIR + RED}{NIR - RED}$$

where,

NIR = wavelength in Near infra-red range

RED = wavelength in red range

The range of the NDVI is -1.0 to +1.0. Rocks and bare soils have positive but lower NDVI values near 0. Due to the strong NIR and low RED reflectance seen in vegetated regions, data from these locations show positive NDVI values. The NDVI value rises to about 1.0 as the quantity of green vegetation increases within a pixel. On the other hand, water, clouds and snow reflect more light in the red band than they do in the NIR range. As a result, these materials have low NDVIs. Deep water is indicated by NDVI values that are negative and close to -1.0. Rock, sand and snow are represented by values between (-0.1 and 0.1). Low positive values correspond to grassland and shrubs (approximately 0.2 to 0.4). High values represent temperate and tropical rainforests (values approaching 1). The usual range is from -0.1 to 0.6. (for a not very green area to very green area). The most well-known and often used index is NDVI.

3.10.2 Normalized Difference Water Index (NDWI)

Gao (1996) invented NDWI, which measures moisture content in soil and plants and is computed similarly to NDVI as:

$$NDWI = \frac{(NIR - SWIR)}{(NIR + SWIR)}$$

where,

NIR = Wavelength in Near infra-red range

SWIR = Wavelength in Shortwave Infra-Red

Instead of considering the red range in NDVI computation, a short-wave near-infrared (SWIR) wavelength, which is a water absorption band, is used. Because SWIR is unaffected by pigments, NDWI is a more reliable predictor of grain production than NDVI, which is impacted by pigments. During drought situations, when the vegetation is greatly dependent on water stress, NDWI is considered to be superior to NDVI, since the vegetative features are largely dependent on water stress.

The NDWI varies from -1 to +1 depending on the hardwood content and the kind of vegetation and cover. High NDWI measurements are associated with high vegetation water content and vegetation percent cover. Low NDWI values are associated with low vegetation water content and fraction cover. NDWI decreases when there is water stress. As a result, high NDWI levels indicate ample water, whereas low NDWI values suggest water stress.

3.10.3 Soil Adjusted Vegetation Index (SAVI)

Huete (1988) proposes the Soil Adjusted Vegetation Index (SAVI) as follows:

$$SAVI = \frac{(NIR-RED)}{(NIR+RED+L)} x\ (1 + L)$$

where,

NIR - Near Infrared band reflectance.

RED - Red band reflectance.

L - Soil Correction factor and generally taken as 0.5

To reduce the impact of soil brightness and create vegetation isolines that are independent of the soil background, the constant L is added. The range of this component, which ranges from 0 to infinity, is determined by the canopy density. SAVI is equivalent to NDVI at L=0.

According to Huete (1988), depending on the density of the vegetation, there may be two or three appropriate adjustment factors (L) (L=1 for low vegetation, L=0.5 for intermediate vegetation densities and L=0.25 for greater density). In comparison to the NDVI, SAVI has reduced soil wetting-related temporal and geographical variations, making it a superior index for partial canopies (Qi *et al*., 1993). Therefore, SAVI works best for intermediate canopies.

3.10.4 Modified Soil Adjusted Vegetation Index (MSAVI2)

MSAVI2 reduces the effect of bare soil on the Soil Adjusted Vegetation Index (SAVI). The original Soil Adjusted Vegetation Index (SAVI) had the drawback of requiring trial-and-error to specify the soil-brightness correction factor (L) based on the amount of vegetation in the study area. L was generally set to the default value of 0.5.

Qi *et al.* (1994b) proposed MSAVI2, which eliminates the need to find the soil line from a feature-space plot or even explicitly specify the soil brightness correction factor, after mathematical substitutions:

$$MSAVI2 = \frac{\left(2*NIR+1-\sqrt{(2*NIR+1)2}-8*(NIR-RED)\right)}{2}$$

where,

NIR = Reflectance in near-infrared band,

RED = Reflectance in red band.

MSAVI values range from -1 to 1, where -1 to 0.2 indicate bare soil, 0.2 to 0.4 is the seed germination stage, 0.4 to 0.6 is the leaf development stage. When the values go over 0.6, the vegetation is dense enough to cover the soil.

3.10.5 Ratio Vegetation Index (RVI)

The ratio vegetation index (RVI) is simply the ratio of NIR to RED and is calculated using the formula (Jordan,1969):

$$RVI = \frac{NIR}{RED}$$

Where,

NIR = Reflectance in near-infrared band,

RED = Reflectance in red band.

It was the first index to be established and is still in widespread use today. The RVI is near to 1 if the reflectance of the NIR and RED bands are comparable. Bare soil RVI values are often close to 1. The RVI rises as a green vegetation content of pixel increases. The RVI values are not constrained and can rise well over 1. Typically, RVI values over 30 are considered to be quite high. During the period of peak growth, RVI is quite sensitive to changes in the vegetation. It is not extremely sensitive when plant cover is scanty.

3.11 Processing of Satellite Data for Vegetation Indices

For *rabi* season of 2020-21 and 2021-22, Spectral vegetation indices (VIs) such as the Normalized Difference Vegetation Index (NDVI), the Normalized Difference Water Index (NDWI), the Soil Adjusted Vegetation Index (SAVI), the Modified Soil Adjusted Vegetation Index (MSAVI) and Ratio Vegetation Index (RVI) were calculated for multidate subset images of all the 10 dates of pass listed in Table 1 and Table 2. Model Builder or Indices Tool in ERDAS Imagine software was used to generate separate images for each vegetation index. ERDAS Imagine software was also used to create stacks of these images for all of the vegetation indices.

3.12 Generating Spectral Vegetation Indices Profile for Wheat and Onion Crops

In the ERDAS Imagine software, the layer stack images for the various vegetation indices elaborated above, as well as the crop-polygon layer representing the crop areas visited during the ground truth survey, were processed together. The signature editor module was used to obtain the temporal values of the vegetation indices. Maximum, minimum, mean and standard deviation values of each vegetation index were obtained for each crop-polygon of wheat and onion crop. This information was exported to Excel worksheets for further analysis.

The mean values of vegetation indices (VIs), such as NDVI, NDWI, SAVI and MSAVI and RVI were compiled for all pure crop pixels in polygons (wheat and onion) corresponding to the respective image dates.

Each crop-polygon was classified based on the crop's age in weeks as of the reference image date. i.e. 29 January 2021 and 29 January 2022, using the criteria discussed in sections 3.7, 3.8 and 3.9.2. These mean VIs of crop-polygons (wheat and onion) were distributed according to crop age in weeks. i.e. weeks after sowing / transplanting, as discussed in 3.9.3. Each week, the mean values were averaged.

By plotting weeks past sowing / transplanting along the abscissa and corresponding average VI values on the ordinate, the multi-temporal VI trend for all wheat and onion polygons was obtained. The overall trends of wheat and onion multidate VIs were obtained. The spectral VI profiles of wheat and onion crops are represented by the trend of VIs with increasing age.

3.13 Identification and Acreage Estimation of Wheat and Onion Crops

A hybrid technique based on K-means clustering and visual classification was used to classify multi-date remote sensing data. The pixels are grouped into several clusters based on their spectral property similarity using the K-means clustering method of unsupervised classification and then followed by a supervised classification in which spectrally similar classes using visual vector analysis. The procedure is depicted in a flowchart, as shown in Fig. 11 and the details are as follows:

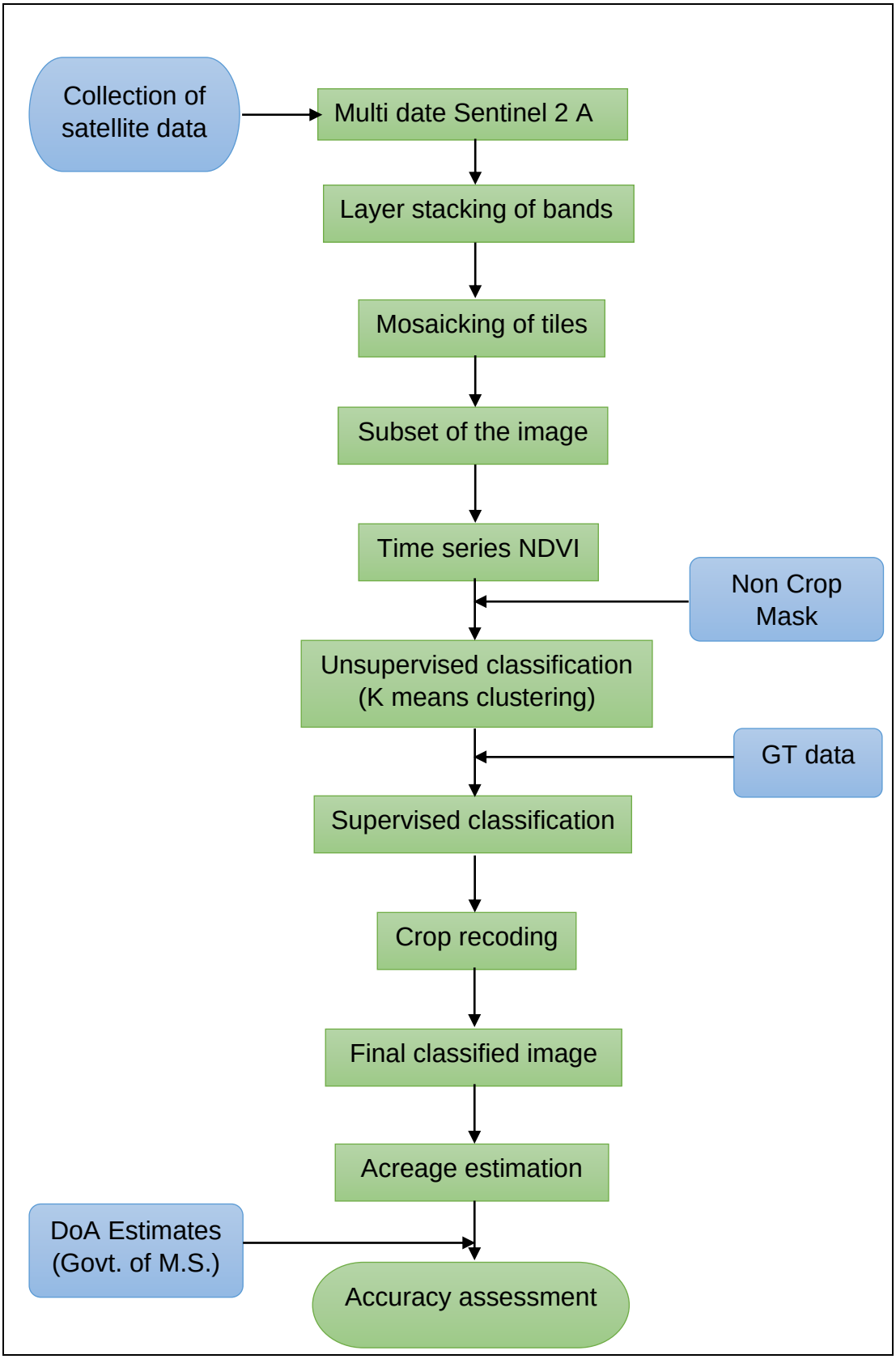

Fig 11. Flowchart for Acreage Estimation

3.13.1 Preparation of Reference Temporal Spectral Profiles (RTSP)

The ground truth study focused on gathering pure wheat and onion crops areas. However, in addition to this crop, signatures were acquired for other co-existing crops such as maize, sorghum and so on. The spatial coordinates of GT locations were put onto the images. In line with the information acquired during field visits, crop-polygons were tagged on the image with an acquisition date close to the date of the field observation. For each satellite image acquisition date, an NDVI image was created, along with a layer stack. Multidate average NDVI values were calculated for the training crop-polygons (training windows). The general signature of the crop is generated by plotting the NDVI values on the various acquisition dates against the optimal crop period, which is December to April. Crop signatures were created in this manner. These signatures offer the reference temporal spectral profile (RTSP) of wheat and onion, which assists in crop identification.

3.13.2 Data load reduction of multi-date RS dataset:

The non-crop mask (NCM) was generated by overlaying the NDVI stack by the dataset that already had information about built-up areas, slopes, forests, wastelands and so on. To reduce the number of data pixels that required to be subjected to K-means clustering, all pixels that belonged to non-agricultural regions were masked out. The NCM image assigned the value 1 to pixels in agricultural regions and 0 to pixels in non-agricultural areas, forests and perennials.

3.13.3 K- means clustering

Unsupervised classification was performed using an NDVI stack dataset that had not been cropped. ERDAS Imagine software was used to execute the K-means clustering approach of unsupervised classification. A total of 100 classes were chosen with a convergence threshold of 0.999 and 30 iterations. The ultimate result of K-means clustering was a classified raster image with 100 classes. In addition, a signature file containing the signatures of all 100 classes was received. The signature file generates the Temporal Spectral Profiles (TSPs) for each class. The available RTSP of the wheat and onion crop as well as the substantial local knowledge of

analyst were then utilised to visually compare each of the 100 TSPs classes.

TSPs from certain clusters were not allocated to the wheat and onion RTSP. These clusters were labelled as "Mix crop." Due to a lack of RTSPs, a few cluster classes in the classified image remained "unclassified." The classification output was saved separately.

3.13.4 Supervised classification:

On the cluster file and multi-date subsets the GT point layer was superimposed. Using accessible RTSPs, visual interpretation was conducted for unclassified pixels and/or pixels that could not be confidently assigned to any crop class. Crop-polygons were assessed and labelled using visual analysis.

3.13.5 Integration of classified images/vector and acreage estimation:

The final classified image was created by combining the findings of supervised and unsupervised classification as well as crop recoding. The Table menu option in the ERDAS Imagine Software may be used to add the area corresponding to each class to the attribute table. The attribute table of the recoded image is used to calculate the area coverage of the wheat and onion crop. Thus, the total acreage of the wheat and onion crop in the research region was calculated for both years 2020-21 and 2021-22 respectively.

3.14 Establishing Relation between Vegetation Indices (VIs) and Crop Coefficients (K_c)

The various vegetative indices (VIs), viz. NDVI, NDWI, SAVI, MSAVI2 and RVI were used to determine their relationship with wheat and onion crop coefficients for both years 2020-21 and 2021-22. In the ERDAS Imagine software viewer, a GT vector file was placed over each VI layer stack. Temporal VI data were acquired one by one for each location and exported to a Microsoft Excel Sheet. These values of each VI were then assigned in the relevant week number based on the age of the crop on the reference image date. The average values of each VI for the wheat and onion crop were then computed for each week.

Crop coefficients given by MPKV Rahuri for wheat and onion (Table 9) were used to determine the relationship between crop coefficients and estimated VIs and therefore to model the VI-K_c correlations. The recommendation of crop coefficients (K_c) was made based on FAO Penman-Monteith method adopted for further investigation.

Table 9. Recommended crop coefficients for wheat and onion

Weeks pass Sowing / Trans	K_c for Wheat	K_c for Onion
1	0.71	0.63
2	0.88	0.69
3	1.03	0.73
4	1.15	0.79
5	1.24	0.85
6	1.31	0.92
7	1.36	1.00
8	1.38	1.08
9	1.36	1.15
10	1.31	1.20
11	1.22	1.23
12	1.1	1.21
13	0.94	1.14
14	0.76	1.01
15	0.57	0.81
16	0.39	0.54
17	0.22	-

Source: (MPKV Krishi Darshani, 2021)

The scattered diagram was generated by plotting the average weekly values of the wheat and onion vegetative indices, including NDVI, NDWI, SAVI, MSAVI2 and RVI against the required weekly crop coefficients (K_c). The trend lines and associated R^2 values were produced. Various orders of linear and polynomial equations were tested. The linear equations, on the

other hand, were more relevant. Each relationship was subjected to a simple linear regression analysis. The relationships between the recommended crop coefficients (K_c) and the vegetative indices (VIs) were then investigated and the best-fit models were identified and evaluated.

The relationship between VIs and K_c is determined using basic linear regression analysis, which may be used to examine a satellite image. The coefficient of determination (R^2), computed from basic regression analysis, determines the degree of fit (R^2=0 indicates no fit and R^2=1 indicates ideal fit). The root-mean-square error is another parameter of how closely the two independent data sets agree (RMSE). The bias and variation from the 1:1 line are also shown in this study. The models were evaluated using R^2 and RMSE, as well as commonly used parameters like as percent deviation (PD) and the Willmott index of agreement (D).

3.15 Calculation of Reference Crop Evapotranspiration (ET_o)

For the definition and calculation of reference evapotranspiration utilising meteorological information like radiation, air temperature, air humidity and wind speed, the FAO Penman-Monteith approach is advised as the only accepted method (Allen *et al.*1998). It was produced for a hypothetical 0.12 m tall, uniform grass that was actively growing and well-watered, with a surface resistance of 70 dsm^{-1} and an albedo of 0.23.

The following is the FAO Penman-Monteith equation (Allen *et al*., 1998):

$$ET_o = \frac{0.408\,\Delta(R_n - G) + \gamma\frac{900}{T+273}u_2(e_s - e_a)}{\Delta + \gamma(1+0.34\,u_2)}$$

Where,

ET_o = Reference Evapotranspiration (mm day^{-1})

Δ = Slope of saturation vapour curve (kPa $^oC^{-1}$)

R_n = Net radiation at the crop surface (MJ m^{-2} day^{-1})

G = Soil heat flux density (MJ m^{-2} day^{-1})

Γ = Psychometric constant (kPa $^oC^{-1}$)

T = Mean air temperature (^oC)

u_2 = Wind speed at 2.0 m height (ms^{-1})

e_a = Actual vapour pressure (kPa)

e_s = Saturation vapour pressure (kPa)

(e_s- e_a) = Saturation vapour pressure deficit (kPa)

This formula was used to determine the weekly reference evapotranspiration (ET_o). According to the procedures outlined in FAO-56, each associated factor in the equation was assessed based on how empirically it connected to the climatological data from the stations.

By entering the factors such as the maximum temperature, minimum temperature, relative humidity and wind speed, Microsoft Excel performed precise ET_o calculations. For the study, the ET_o weekly (average) data were collected.

3.16 Utilization of Developed Relationship for Near Real-Time Irrigation Water Management

The best VI versus K_c correlation was discovered using the above methods. By using the best-performing VI-K_c relation for wheat and onion, respectively, from the estimated VI data, the weekly crop coefficients for the crops were calculated. For all the weeks of the *rabi* season 2020-2021 and 2021-2022, which corresponded to the growing phase of the wheat and onion, the weekly reference evapotranspiration (ET_o) of the chosen stations in the research region was also computed. The weekly ET_o was multiplied by K_c to determine the weekly crop evapotranspiration of wheat and onion in each of the research districts. The crop's total evapotranspiration is calculated as the sum of ET_c for all weeks of the growing season. The area under crop assessed by remote sensing is multiplied by the associated crop evapotranspiration measurements to produce the water demand/water extraction quantity. By adding the water demands of all the study districts, it was possible to determine the overall water requirement for wheat and onion.

CHAPTER IV

RESULT AND DISCUSSION

The present research was conducted to better understand the behavior of multispectral vegetation indices generated from remote sensing satellite images during the growing stage of the wheat and onion crop during *rabi* season of 2020-21 and 2021-22 respectively. Crop identification and acreage calculations were accomplished using GIS and remote sensing methods. The relationships between wheat and onion vegetation indices (VIs) and crop coefficients (K_c) were explored. The best-performing model was chosen after the models showing the relationship between vegetation indices and crop coefficients were developed. This best fit model was used to anticipate weekly and total water requirements of wheat and onion crop during *rabi* season of 2020-21 and 2021-22 respectively. This chapter delves deeper into the important findings.

4.1 Producing Layer Stack Images of Vegetation Indices

The Sentinel 2A satellite data of the study area were acquired for 10 dates each for the year 2020-21 and 2021-22 respectively for *rabi* wheat and onion crop growth season. After resampling the 11^{th} band (20m converted to 10m resolution), layer stack images of bands with all of the required bands were generated for each tile. Layer stack of the same date were merged to form the mosaic. Obtained the subsets of the study area from each mosaic image by using shape file of area of interest. The subset images for both years 2020-21 and 2021-22 is given in section 3.2. These images were processed using the ERDAS Imagine software, which ran models for the five vegetation indices under consideration, namely Normalized Difference Vegetation Index (NDVI), Normalized Difference Water Index (NDWI) and Soil Adjusted Vegetation Index (SAVI), Modified Soil adjusted Vegetation Index (MSAVI2) and Ratio Vegetation Index (RVI) for each of the ten satellite overpass dates for both the years 2020-21 and 2021-22 respectively. Thus total 50 images each for year 2020-21 and 2021-22 of vegetation indices were generated. 10 images of each vegetation index were stacked together in sequencing order of their dates to get final stacked layer image for both years.

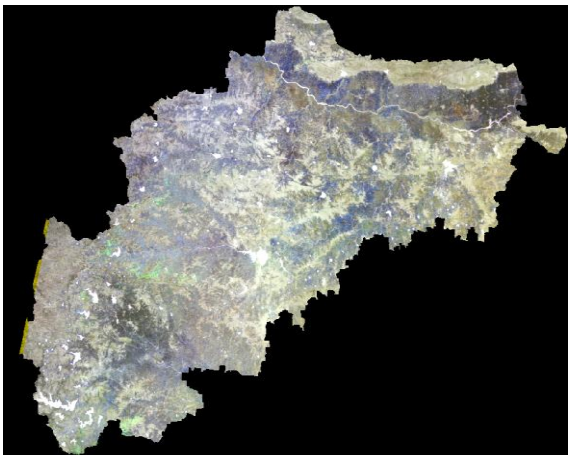

RVI Stack Layer

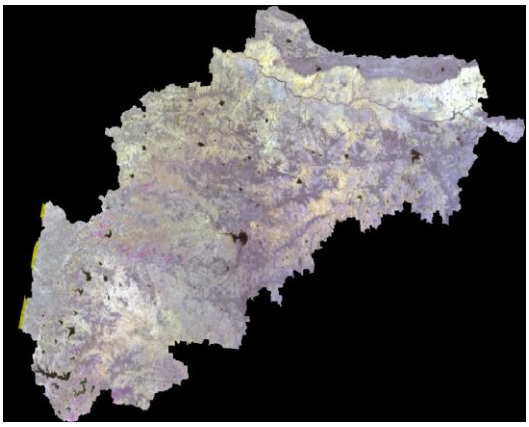

NDVI Stack Layer

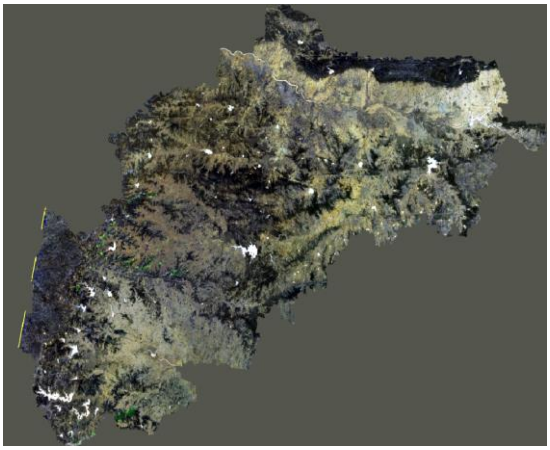

NDWI Stack Layer

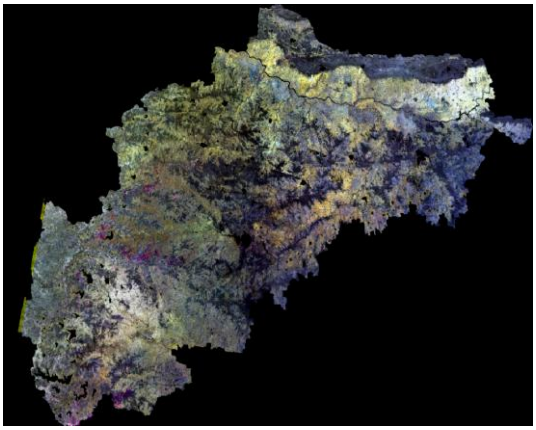

SAVI Stack Layer

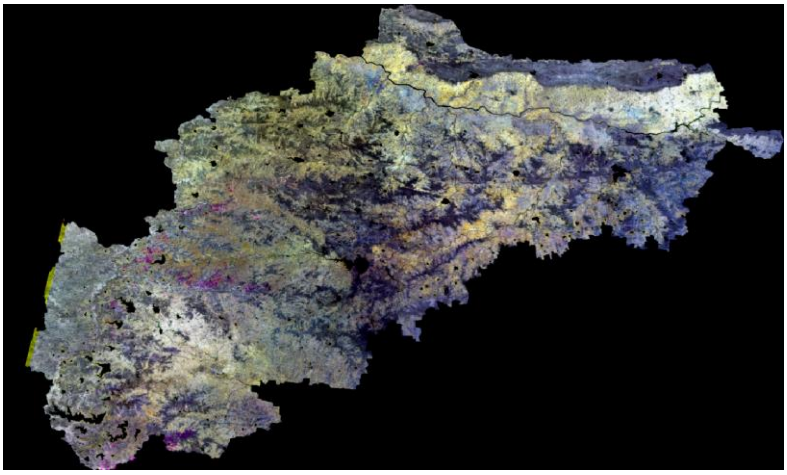

MSAVI2 Stack Layer

Plate 5. VIs stacks 2020-21

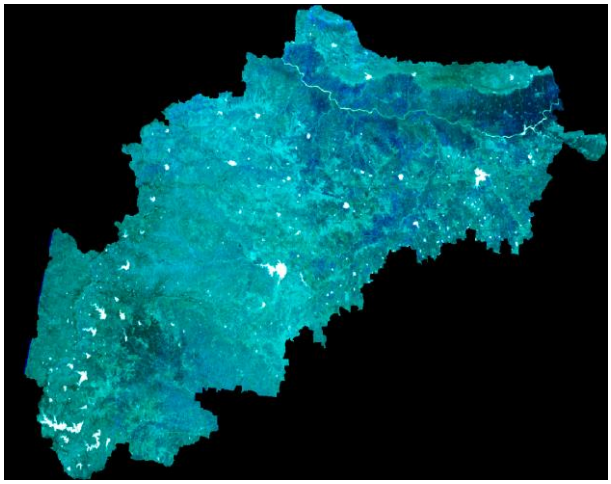

RVI Stack Layer

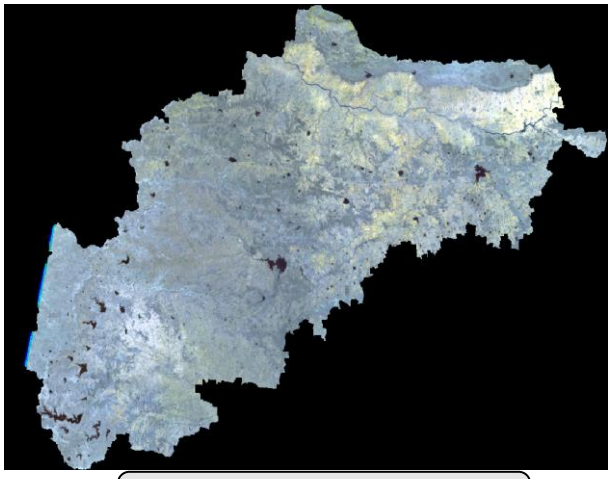

NDVI Stack Layer

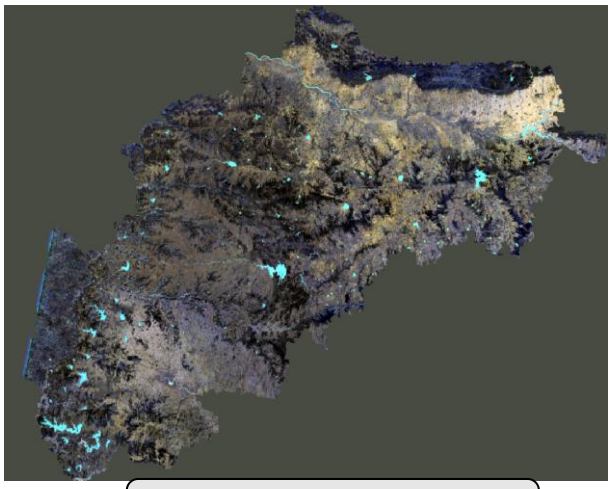

NDWI Stack Layer

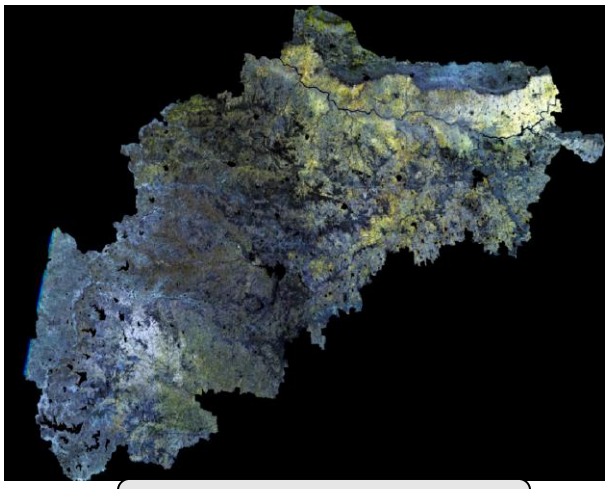

SAVI Stack Layer

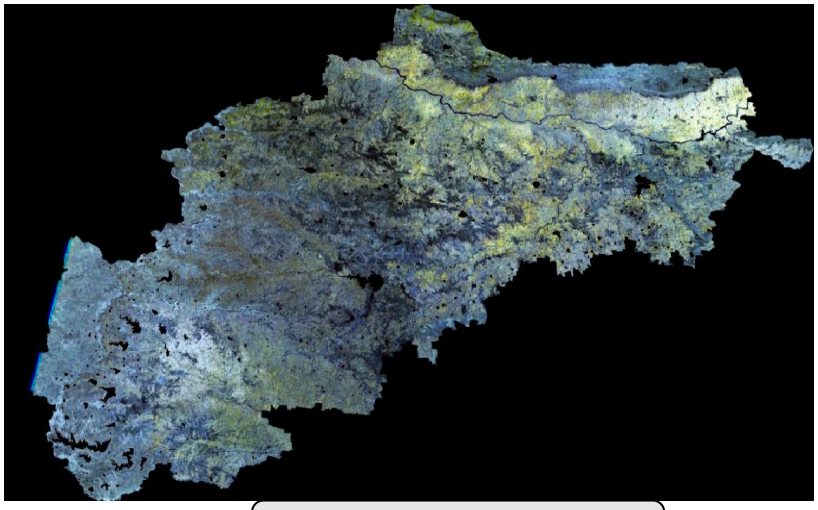

MSAVI2 Stack Layer

Plate 6. VIs stacks 2021-22

The five final stacked images of vegetation indices i.e. NDVI stack, NDWI stack, SAVI stack, MSAVI2 stack and RVI stack were obtained for year 2020-21 and 2021-22 and are shown in Plates 5 and 6 respectively.

4.2 Vegetation Indices Extraction from Pure Crop Pixels

The fields visited during the ground truth survey have been digitized for two years 2020-21 and 2021-22 respectively. By superimposing the GT vector layer on the VI stack layers, the values of the site-specific vegetation indices were determined. During the processing of satellite data, the temporal values of all five vegetation indices for pure crop locations were collected. These site-specific multi-date vegetation indices values were used for further research.

4.3 Spectral Profile of Wheat Crop

For year 2020-21 and 2021-22, The age of the wheat crop was calculated using data collected from farmers during the ground truth survey such as sowing date, variety and estimated harvesting date. For the fields where the farmers couldn't be visited, the criterion used to approximate the age of the wheat crop is explained in section 3.7. The age in weeks of wheat crop of GT polygons on reference image date was obtained as per criteria discussed in section 3.9.2 and age on other dates was determined as given in Table 10 for *rabi* season of 2020-21 and Table11 for 2021-22 respectively. The vegetation index value for the reference image date was thus entered first. The VI values for all other satellite overpass dates were inserted in the appropriate weeks in accordance with the age criteria listed in Table 7. and Table 8. for both the years 2020-21 and 2021-22 respectively. The week-wise distribution of mean NDVI, NDWI, SAVI, MSAVI2 and RVI values for wheat crop polygons of all GT sites for *rabi* season of 2020-21 and 2021-22 are shown in Annexure II. The values of different sites for each week were averaged to obtain a mean VI value corresponding to each week and are shown in Table 12 for 2020-21 and Table 13 for 2021-22 respectively. The pooled VI values are obtained by averaging VIs of both years 2020-21 and 2021-22 and are shown in Table 14. As the condition of the wheat crop varied at each site, the weekly mean VI value served as the representation of the mean of all those crop

conditions corresponding to the same week irrespective of changes in vegetation and soil.

Table 10. Age of wheat crop (weeks) for observed wheat crop on reference image date for *rabi* season of 2020-21

GT ID.	Stage No.	Stage	Age on GT (Weeks)	Age on RI date (Weeks)
1.	8	Milk Development	10	11
2.	8	Milk Development	10	11
3.	8	Milk Development	10	11
4.	8	Milk Development	10	11
5.	8	Milk Development	11	11
6.	6	Head emergence	9	9
7.	8	Milk Development	11	11
8.	8	Milk Development	11	11
9.	8	Milk Development	12	12
10.	8	Milk Development	12	12
11.	7	Pollination	10	10
12.	8	Milk Development	12	12
13.	7	Pollination	10	10
14.	8	Milk Development	12	12
15.	8	Milk Development	12	12
16.	6	Head emergence	9	9
17.	8	Milk Development	11	11
18.	8	Milk Development	12	12
19.	7	Pollination	10	10
20.	7	Pollination	10	10
21.	7	Pollination	10	10
22.	8	Milk Development	11	11
23.	7	Pollination	10	10
24.	8	Milk Development	11	11
25.	8	Milk Development	12	12
26.	8	Milk Development	11	11
27.	6	Head emergence	7	8
28.	6	Head emergence	8	9

Table 11. Age of wheat crop (weeks) for observed wheat crop on reference image date for *rabi* season of 2021-22

GT ID.	Stage No.	Stage	Age on GT (Weeks)	Age on RI date (Weeks)
1.	7	Pollination	10	10
2.	6	Head emergence	8	8
3.	6	Head emergence	9	9
4.	6	Head emergence	9	9
5.	8	Milk Development	12	12
6.	5	Booting	7	7
7.	6	Head emergence	9	9
8.	5	Booting	7	7
9.	6	Head emergence	9	9
10.	8	Milk Development	12	12
11.	6	Head emergence	8	8
12.	8	Milk Development	13	12
13.	8	Milk Development	13	12
14.	8	Milk Development	12	11
15.	6	Head emergence	9	8
16.	8	Milk Development	13	12
17.	8	Milk Development	13	12
18.	5	Booting	8	7
19.	5	Booting	8	7
20.	6	Head emergence	9	8
21.	6	Head emergence	9	8
22.	8	Milk Development	12	11
23.	5	Booting	7	6
24.	5	Booting	8	7
25.	6	Head emergence	9	8
26.	8	Milk Development	12	11
27.	8	Milk Development	12	11
28.	6	Head emergence	9	8

Table 12. Average weekly values of VIs of wheat for *rabi* season of 2020-21

WPS	NDVI	NDWI	SAVI	MSAVI2	RVI
1	0.189	0.117	0.273	0.286	1.244
2	0.239	0.128	0.308	0.316	1.428
3	0.256	0.138	0.369	0.378	1.617
4	0.297	0.195	0.401	0.400	1.983
5	0.327	0.235	0.471	0.495	2.269
6	0.408	0.269	0.576	0.553	3.099
7	0.418	0.294	0.637	0.597	3.327
8	0.440	0.299	0.694	0.634	3.409
9	0.425	0.283	0.654	0.605	3.142
10	0.420	0.285	0.643	0.594	2.869
11	0.406	0.244	0.615	0.573	2.636
12	0.352	0.199	0.524	0.514	2.290
13	0.298	0.106	0.445	0.453	1.902
14	0.250	0.059	0.354	0.385	1.765
15	0.234	-0.001	0.347	0.361	1.650
16	0.201	-0.016	0.266	0.299	1.535
17	0.156	-0.043	0.203	0.237	1.367

Table 13. Average weekly values of VIs of wheat for *rabi* season of 2021-22

WPS	NDVI	NDWI	SAVI	MSAVI2	RVI
1	0.184	0.074	0.276	0.271	1.489
2	0.215	0.098	0.282	0.287	1.674
3	0.256	0.155	0.347	0.351	1.729
4	0.275	0.160	0.369	0.366	1.789
5	0.297	0.178	0.448	0.410	2.076
6	0.411	0.229	0.639	0.579	2.539
7	0.445	0.241	0.680	0.600	2.973
8	0.459	0.247	0.702	0.627	3.267
9	0.444	0.231	0.598	0.572	2.787
10	0.369	0.224	0.553	0.520	2.405
11	0.365	0.219	0.538	0.508	2.386
12	0.301	0.195	0.443	0.448	1.956
13	0.203	0.094	0.298	0.321	1.542
14	0.167	0.069	0.257	0.291	1.379
15	0.161	0.072	0.251	0.284	1.412
16	0.152	0.040	0.220	0.256	1.387
17	0.110	-0.017	0.163	0.183	1.249

Table 14. Pooled values of VIs of wheat

WPS	NDVI	NDWI	SAVI	MSAVI2	RVI
1	0.187	0.095	0.275	0.279	1.367
2	0.227	0.113	0.295	0.302	1.551
3	0.256	0.146	0.358	0.364	1.673
4	0.286	0.178	0.385	0.383	1.886
5	0.312	0.207	0.460	0.453	2.172
6	0.409	0.249	0.607	0.566	2.819
7	0.431	0.267	0.658	0.598	3.150
8	0.449	0.273	0.698	0.631	3.338
9	0.434	0.257	0.626	0.588	2.965
10	0.395	0.255	0.598	0.557	2.637
11	0.386	0.232	0.576	0.541	2.511
12	0.327	0.197	0.484	0.481	2.123
13	0.250	0.100	0.372	0.387	1.722
14	0.208	0.064	0.305	0.338	1.572
15	0.198	0.035	0.299	0.322	1.531
16	0.176	0.012	0.243	0.277	1.461
17	0.133	-0.030	0.183	0.210	1.308

4.3.1 NDVI profile of wheat

The trend of NDVI along the crop growth cycle of wheat is obtained by plotting NDVI values against weeks past sowing for the year 2020-21 and 2021-22 respectively. The solid line drawn through the scattered points represents smoothen data. The NDVI trend of both years is shown in Fig. 12 and Fig. 13. It is observed that it obeys the third order polynomial equation:

For year 2020-21:

$y = 6E\text{-}05x^3 – 0.0057x^2 + 0.0827x + 0.0862$ $R^2 = 0.935$ ----------2

For year 2021-22:

$y = 0.0002x^3 – 0.0102x^2 + 0.1147x + 0.0269$ $R^2 = 0.856$ ----------3

where, y = NDVI and x = weeks past sowing

The early stage of the crop was found to be characterized by lower NDVI values beginning at 0.189 and 0.184 and escalating to a peak value of 0.440 and 0.459 by the eighth week for both years 2020-21 and 2021-22 respectively. The NDVI values for midseason stage from the 6^{th} to the 9^{th}

week are observed to be higher which indicates higher rates of photosynthesis and after that it undergoes a gradual fall till maturity stage that is up to 17th week. The trendline exhibits a uniform rate of change of both increase up to the peak and decrease from the peak.

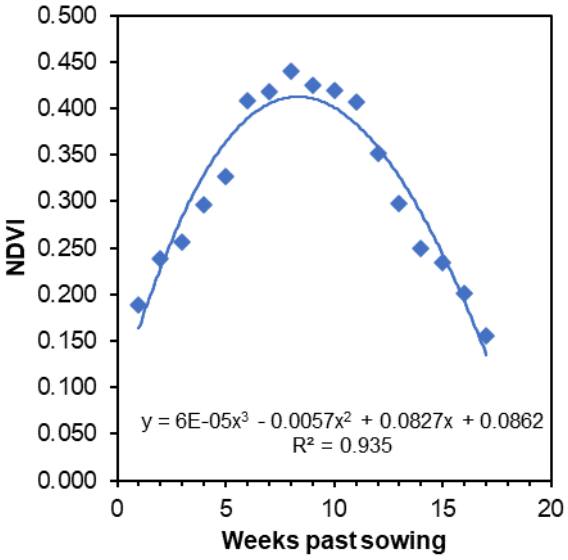

Fig. 12 NDVI profile of wheat for 2020-21

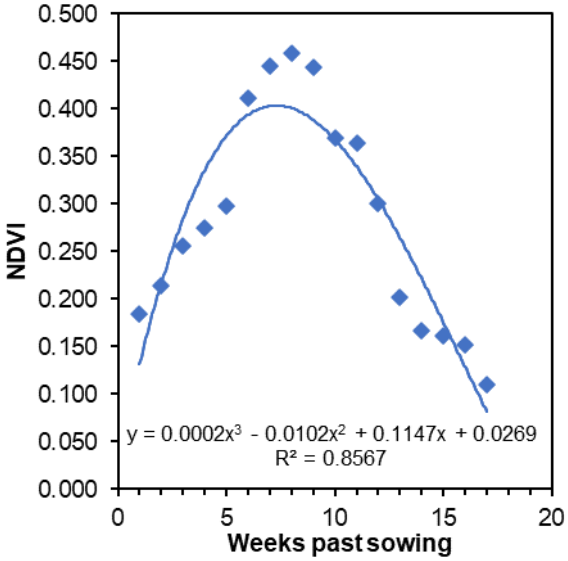

Fig. 13 NDVI profile of wheat for 2021-22

The NDVI values of both years 2020-21 and 2021-22 were pooled. By plotting pooled NDVI versus weeks past sowing, trend is obtained shown in Fig. 14, It follows the third order polynomial equation:

$y = 0.0001x^3 - 0.008x^2 + 0.0987x + 0.0565$ $R^2 = 0.897$ ----------4

where, y = pooled NDVI and x = weeks past sowing

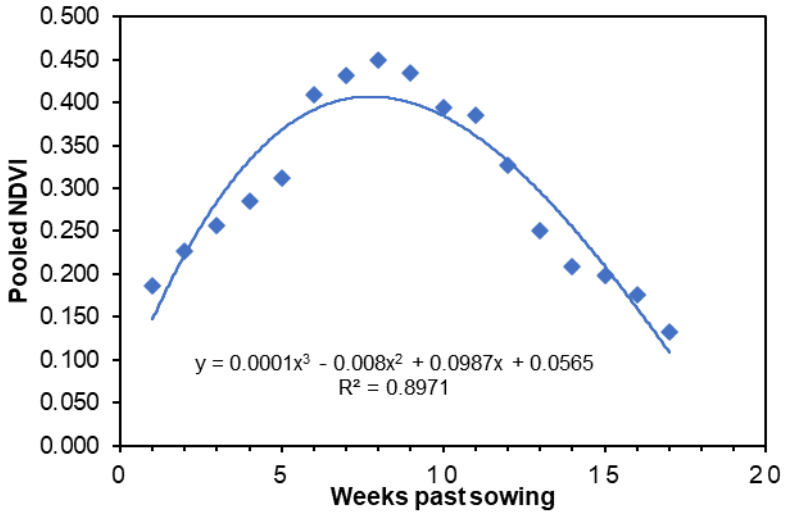

Fig. 14 Pooled NDVI profile for wheat

At initial stage of the wheat crop, lower NDVI values starting at 0.187 and increasing to a peak value of 0.449 at the eighth week. The values of pooled NDVI is higher between 6th to 9th week and then decreases gradually. It is observed that the rate of rising of pooled NDVI up-to peak and falling from peak is uniform. The curve resembles parabola.

When K_c and NDVI were plotted against week past sowing for year 2020-21 (Fig. 15) and 2021-22 (Fig. 16), it is observed that the temporal variations of NDVI is similar to that of the crop coefficients (K_c). For both the years the trend of these two curves looks similar. In 2020-21, NDVI curve crosses K_c curve at 11th week whereas in 2021-22 it crosses at 16th week. During the late season stage the K_c values decrease rapidly whereas the values of NDVI decreases slowly, seen in both years.

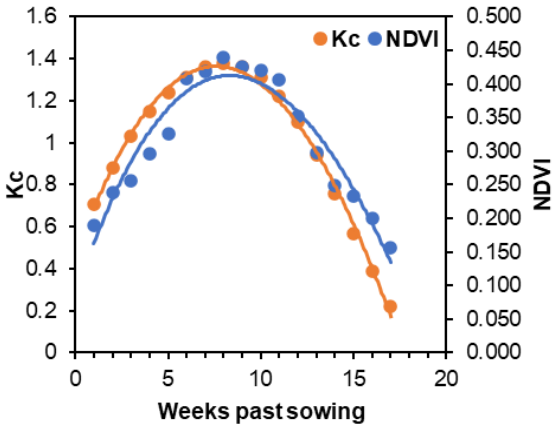

Fig. 15 K_c and NDVI profile of wheat for 2020-21

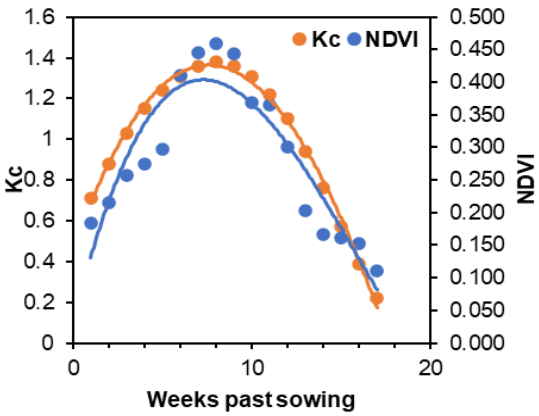

Fig. 16 K_c and NDVI profile of wheat for 2021-22

The pooled NDVI is obtained by averaging the NDVI values of wheat for year 2020-21 and 2021-22. When K_c and pooled NDVI is plotted against weeks past sowing shown in Fig. 17, it is observed that temporal variations of pooled NDVI and crop coefficient (K_c) is indicating similar trend. Pooled NDVI curve crosses K_c curve at 13th week. It is also observed that during the late season stage the Kc values decrease faster whereas the values of NDVI decreases slower. The similarity of these two curves shows that there is possibility of modelling K_c of wheat in terms of pooled NDVI.

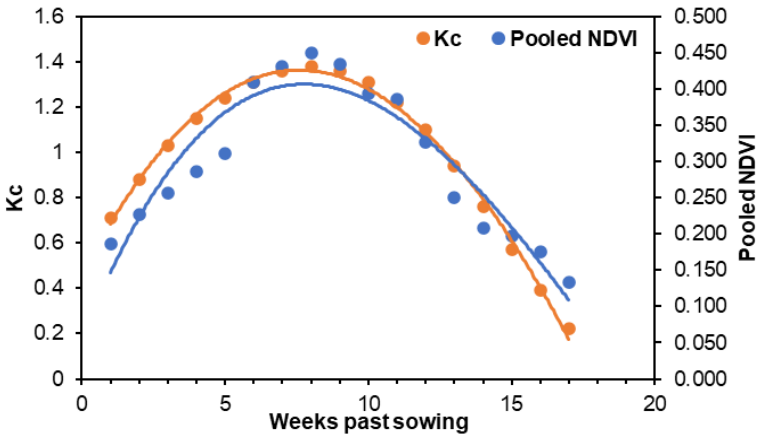

Fig. 17 K_c and pooled NDVI profile of wheat

4.3.2 NDWI profile of wheat

The temporal trend of NDWI is given by the plot between NDWI and weeks past sowing for *rabi* season of 2020-21 (Fig. 18) and 2021-22 (Fig. 19) The NDWI was found to be increasing from 0.117 and 0.074 to 0.299 and 0.247 for the year 2020-21 and 2021-22, respectively up to the eighth week. The values were found higher from 6th to 9th week and after that it decreases up to 17th week in both years. NDWI values of wheat in 2021-22 after 13th week are decreasing faster. The trendline obeys polynomial equation of third order and is given as:

For year 2020-21:

$y = 8E\text{-}05x^3 - 0.0063x^2 + 0.0808x - 0.003$ $R^2 = 0.929$ ----------5

For year 2021-22:

$y = 7E - 05x^3 - 0.0051x^2 + 0.066x - 0.0052$ $R^2 = 0.933$ ----------6

where, y = NDWI and x = weeks past sowing

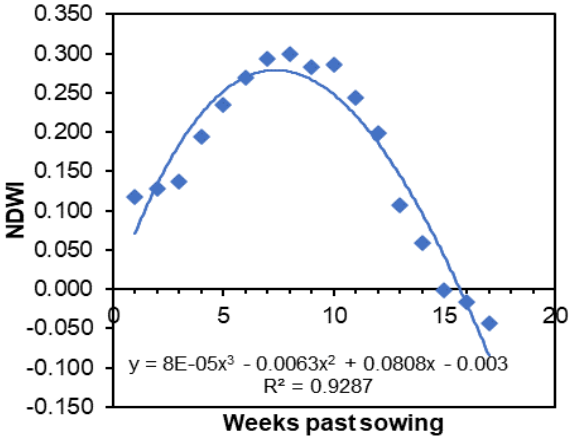

Fig. 18 NDWI profile of wheat for 2020-21

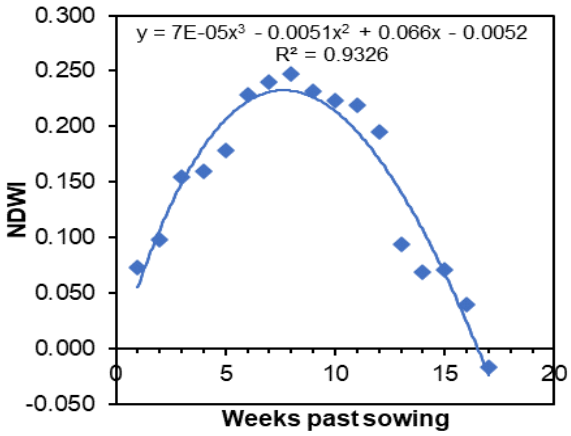

Fig. 19 NDWI profile of wheat for 2021-22

When pooled NDWI is plotted against weeks past sowing (Fig. 20), it is found that lower value of pooled NDWI started from 0.095 at 1st week and increases till 0.273 at 8th week. The values of pooled NDWI are higher in 6th to 9th week and then gradually decreases till 17th week. The trend of this curve follows third order polynomial equation:

$y = 7E\text{-}05x^3 - 0.0057x^2 + 0.0734x - 0.0041$ $R^2 = 0.941$ ----------7

where, y = Pooled NDWI and x = weeks past sowing

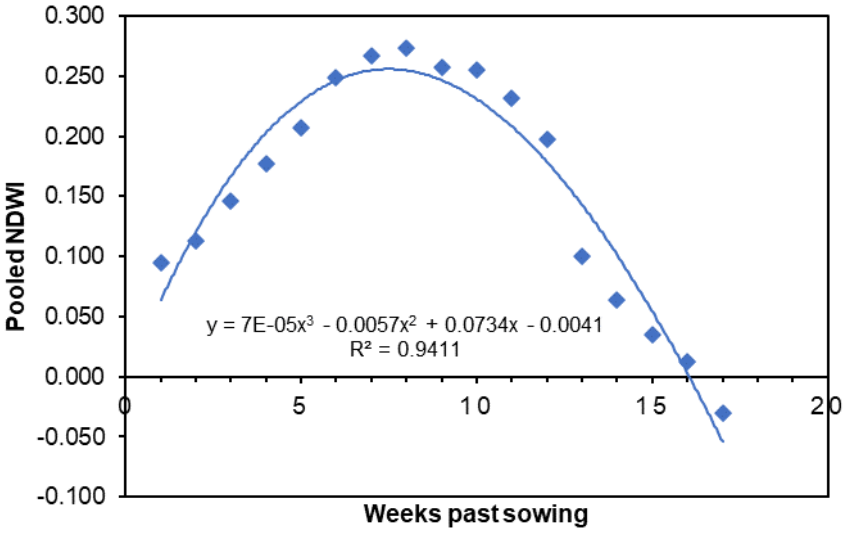

Fig. 20 Pooled NDWI profile for wheat

The temporal trend of NDWI and K_c for both the years 2020-21 and 2021-22 was found to be highly similar to each other as shown in Fig. 21 and Fig. 22. In year 2020-21, NDWI curve overlaps completely to K_c curve. For 2021-22, it is parallel to the K_c curve.

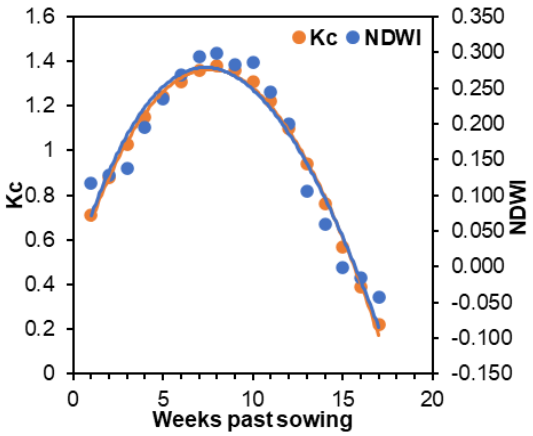

Fig. 21 K_c and NDWI profile of wheat for 2020-21

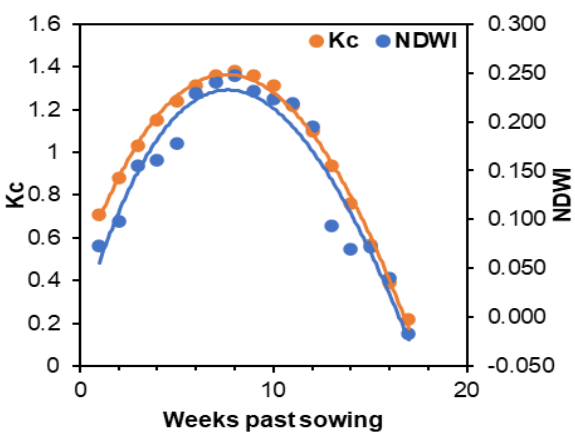

Fig. 22 K_c and NDWI profile of wheat for 2021-22

When K_c and pooled NDWI is plotted against weeks past sowing shown in Fig. 23, it is observed that temporal variations of pooled NDWI and crop coefficient (K_c) is almost similar. Most portion of pooled NDWI curve overlaps K_c curve. K_c and pooled NDWI increases gradually and reaches at peak and after that falling gradually till maturity of wheat crop. Trend of these two curves is similar. The similarity of these two curves shows that there is possibility of modelling K_c of wheat in terms of pooled NDWI.

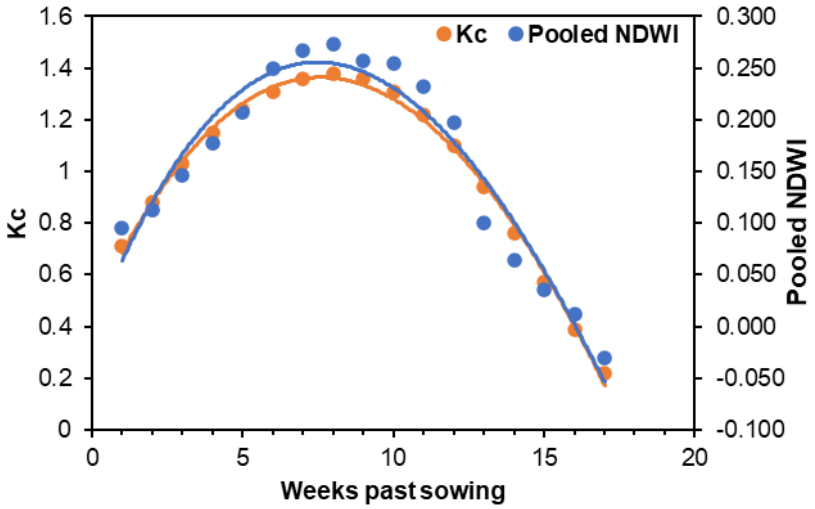

Fig. 23 K_c and pooled NDWI profile of wheat

4.3.3 SAVI profile of wheat

By plotting SAVI values against weeks past sowing as shown in Fig. 24 and Fig. 25 for both the years 2020-21 and 2021-22, the temporal profile of SAVI is obtained. For both years SAVI values are increasing at beginning from 0.273 and 0.276 to 0.694 and 0.702 up to 8th week. For year 2020-21 after peak, SAVI values decreases gradually till 17th week. But in year 2021-22, It is observed that SAVI values decreases faster after peak. It confirms the polynomial equation of third order given as:

For year 2020-21:

$y = 3E\text{-}05x^3 - 0.0075x^2 + 0.1234x + 0.0971$ $R^2 = 0.915$ ----------8

For year 2021-22:

$y = 0.0003x^3 – 0.0156x^2 + 0.1762x + 0.012$ $R^2 = 0.834$ ----------9

where, y = SAVI and x = weeks past sowing

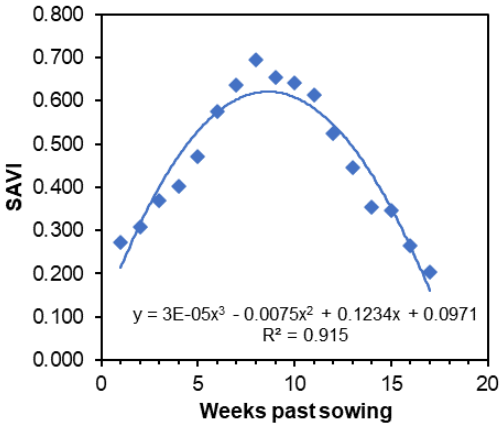

Fig. 24 SAVI profile of wheat for 2020-21

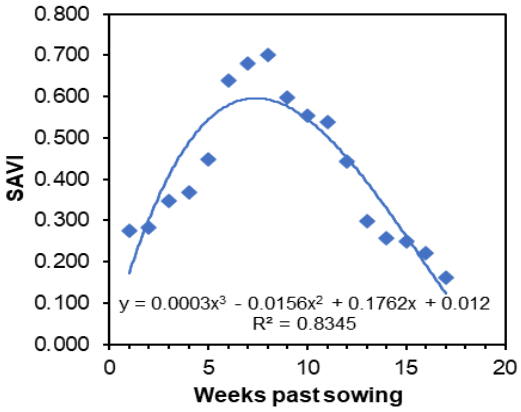

Fig. 25 SAVI profile of wheat for 2021-22

When pooled SAVI and weeks past sowing is plotted together, it is observed that the value of pooled SAVI at beginning is 0.275 (Fig. 26). Peak value of pooled SAVI is obtained in 8th week (0.698) coinciding the period of maximum growth and maximum K_c. After reaching at peak pooled SAVI decreases gradually till maturity of crop (17th week). It obeys the polynomial equation as:

$y = 0.002x^3 - 0.0115x^2 + 0.1498x + 0.0545$ $R^2 = 0.878$ ----------10

where, y = Pooled SAVI and x = weeks past sowing

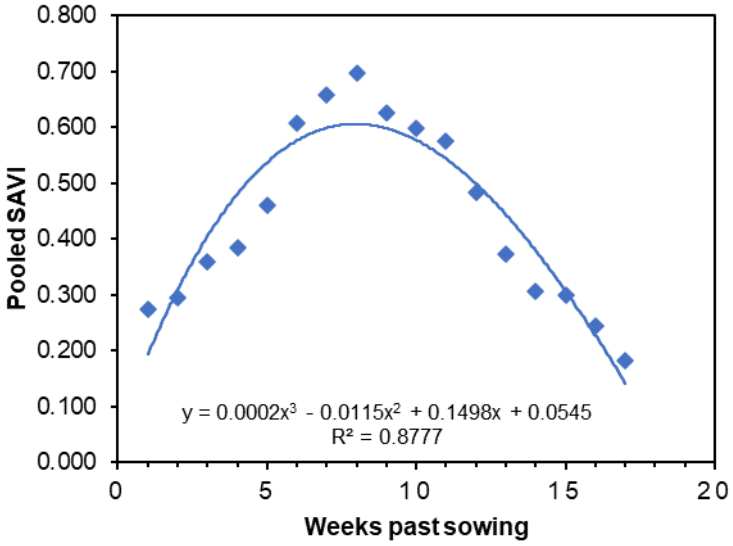

Fig. 26 Pooled SAVI profile for wheat

On comparison of SAVI and K_c for both year 2020-21 and 2021-22 shown in Fig. 27 and Fig. 28, both the trends are found to be almost similar. For both year peak value of SAVI is obtained in 8th week. In 2020-

21, SAVI curve crosses the K_c curve at 12th week whereas in 2021-22 it crosses at 16th week.

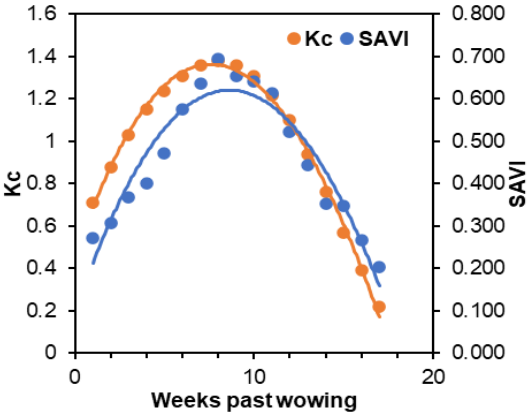

Fig. 27 K_c and SAVI profile of wheat for 2020-21

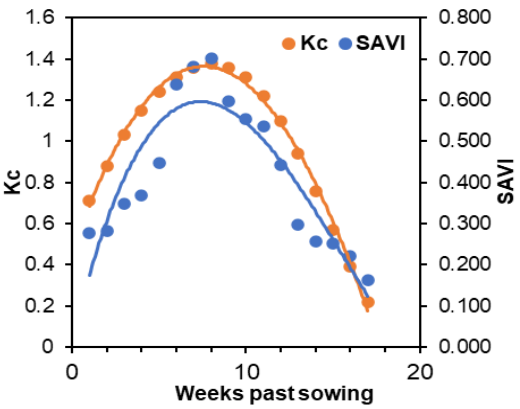

Fig. 28 K_c and SAVI profile of wheat for 2021-22

When pooled SAVI and K_c plotted against the weeks past sowing as shown in Fig. 29, it is seen that it follows the similar trend. Comparison of pooled SAVI and K_c indicates that wheat crop shows increasing SAVI values at initial stages and reach to peak at 8th week as that of crop coefficients. Later that SAVI values gradually decreases as that of crop coefficients. In 2020-21, SAVI curve and K_c curve crosses at 12th week whereas in 2021-22 it crosses at 16th week. The similarity of these two curves shows that there is high possibility of modeling K_c of wheat in terms of pooled SAVI.

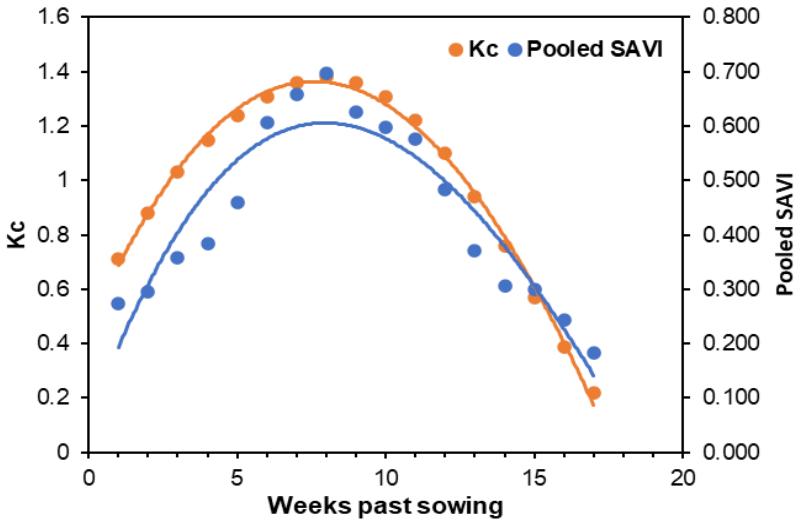

Fig. 29 K_c and pooled SAVI profile of wheat

4.3.4 MSAVI2 profile of wheat

The plot of MSAVI2 against weeks past sowing for *rabi* season of 2020-21 and 2021-22 shows the temporal development of MSAVI2. The pattern of MSAVI2 with growing age of wheat crop is shown by Fig. 30 and Fig. 31. It is found that MSAVI2 increase from 1st to 8th week for both years. It is observed that for year 2020-21 and 2021-22 MSAVI2 started from 0.286 and 0.271 and increases till 0.634 and 0.627 respectively. In year 2020-21, the rate is decreasing gradually whereas in 2021-22 it is little faster. It confirms the polynomial equation of third order as:

For year 2020-21:

$y = 4E - 05x^3 - 0.0067 x^2 + 0.1066x + 0.1402$ $R^2 = 0.946$ ----------11

For year 2021-22:

$y = 0.0002x^3 - 0.011x^2 + 0.1343x + 0.0765$ $R^2 = 0.855$ ----------12

where, y = MSAVI2 and x = weeks past sowing

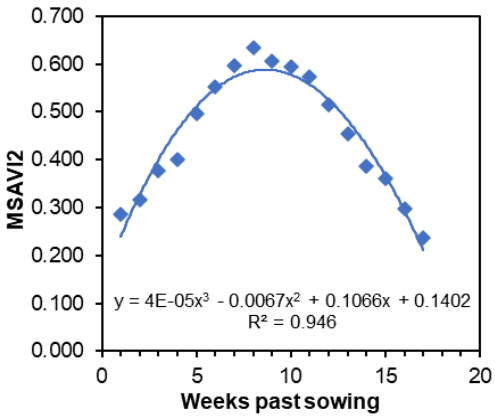

Fig. 30 MSAVI2 profile of wheat for 2020-21

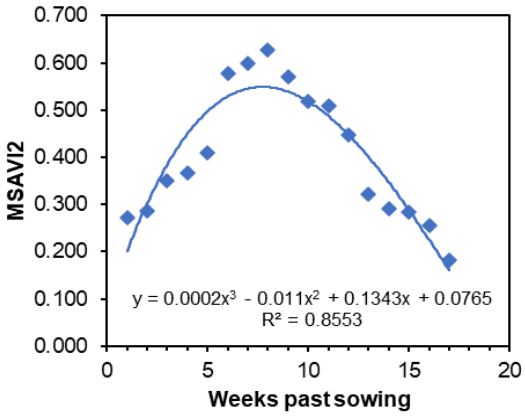

Fig. 31 MSAVI2 profile of wheat for 2021-22

Pooled MSAVI2 versus weeks past sowing are plotted together and shown in Fig. 32 pooled MSAVI2 begins at 0.279 (1st week) and increases to 0.631 (8th week). After reaching at peak, it gradually decreases till 17th week at the time of senescence. It follows polynomial equation of third order:

$y = 0.0001x^3 - 0.0088x^2 + 0.1205x + 0.1084$ $R^2 = 0.907$ ----------13

where, y = Pooled MSAVI2 and x = weeks past sowing

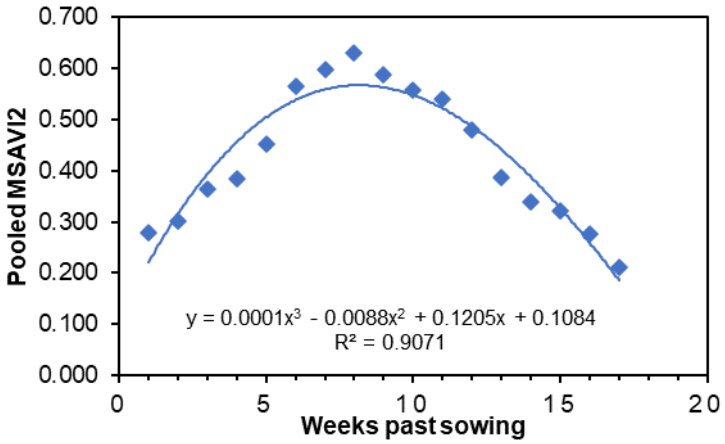

Fig. 32 Pooled MSAVI2 profile for wheat

For year 2020-21 and 2021-22, MSAVI2 and K_c are plotted against week past sowing shown in Fig. 33 and Fig. 34, It is observed that the trend of MSAVI2 resembles to a great extent to the trend of crop coefficient for both years. In year 2020-21, MSAVI2 curve crosses K_c curve at 9th week and that of 2021-22 it crosses at 15th week.

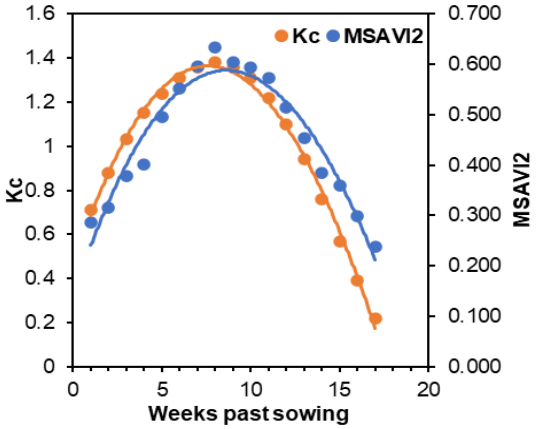

Fig. 33 K_c and MSAVI2 profile of wheat for 2020-21

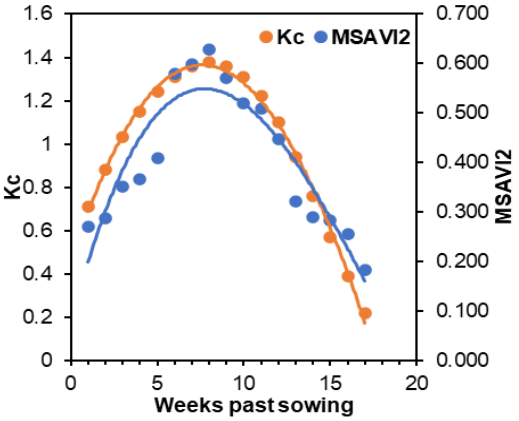

Fig. 34 K_c and MSAVI2 profile of wheat for 2021-22

Comparison of pooled MSAVI2 and K_c (Fig. 35) indicates that wheat crop shows maximum pooled MSAVI2 values at the initial stages and reached to the peak at 8th week as that of K_c. After that pooled MSAVI2 values gradually decreases similar to K_c. Pooled MSAVI2 curve crosses K_c curve at 11th and 12th week.

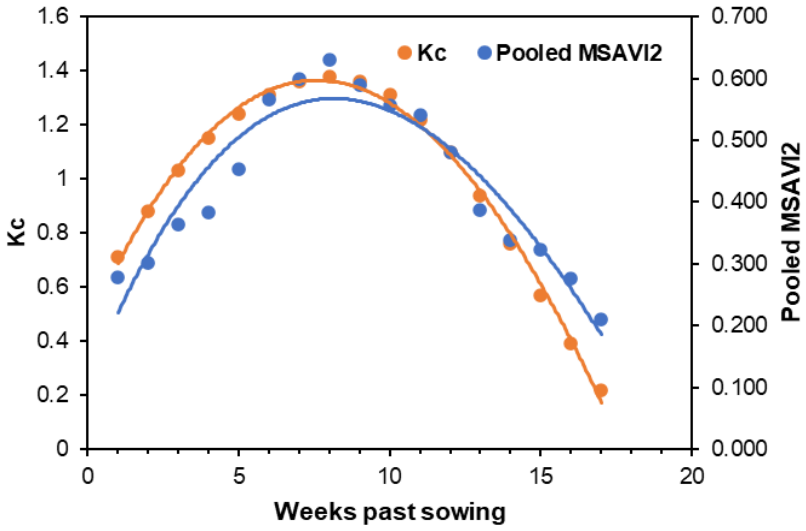

Fig. 35 K_c and pooled MSAVI2 profile of wheat

4.3.5 RVI profile of wheat

The plot of RVI versus weeks past sowing shows the trend during the life cycle of wheat crop for *rabi* season of 2020-21 and 2021-22 shown in Fig. 36 and Fig. 37 The initial values of RVI started from 1.244 and 1.489 and increases up to 3.409 and 3.267 at 8th week. Higher values of RVI are found in between 6th to 8th week and then decreases.

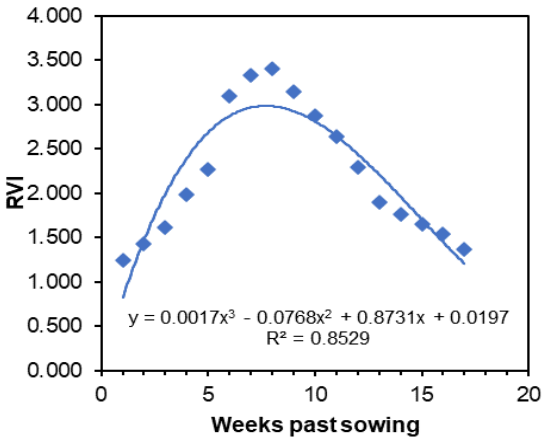

Fig. 36 RVI profile of wheat for 2020-21

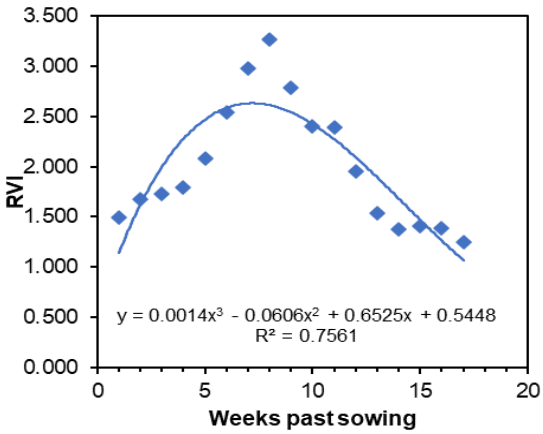

Fig. 37 RVI profile of wheat for 2021-22

It obeys the polynomial equation as:

For year 2020-21,

$y = 0.0017x^3 - 0.0768x^2 + 0.8731x + 0.0197$ $R^2 = 0.853$ ----------14

For year 2021-22,

$y = 0.0014x^3 - 0.0606x^2 + 0.6525x + 0.5448$ $R^2 = 0.756$ ----------15

where, y = RVI and x = weeks past sowing

Pooled RVI plotted against weeks past sowing as shown in Fig. 38 shows that pooled RVI values increasing gradually and reached to peak at 8th week and then gradually decreases till the maturity of wheat crop. It follows third order polynomial equation as:

$y = 0.0016x^3 - 0.0687x^2 + 0.7628x + 0.2822$ $R^2 = 0.814$ ----------16

where, y = pooled RVI and x = weeks past sowing

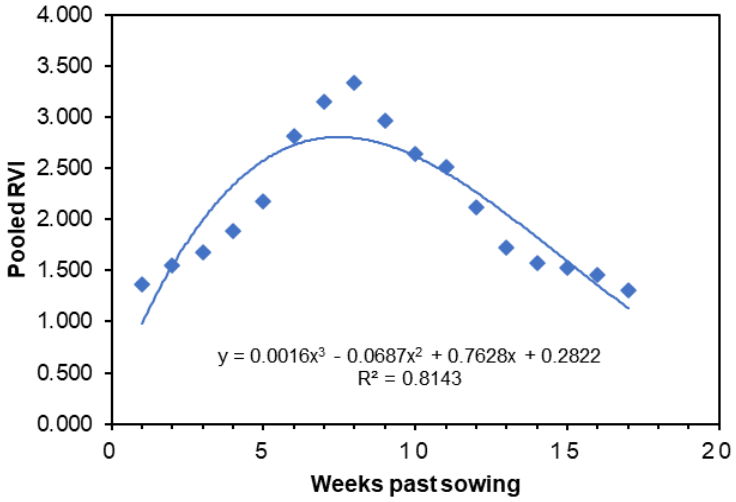

Fig. 38 Pooled RVI profile for wheat

For *rabi* season of 2020-21 and 2021-22, when temporal pattern of RVI and K_c are plotted against weeks past sowing it is noticed that there is similarity in pattern as shown in Fig. 39 and Fig. 40. Peak value of RVI is obtained in 8th week (3.338) and then decreases up to 17th week. In 2020-21 the RVI curve crosses at 14th week whereas in 2021-22 it crosses at 15th week.

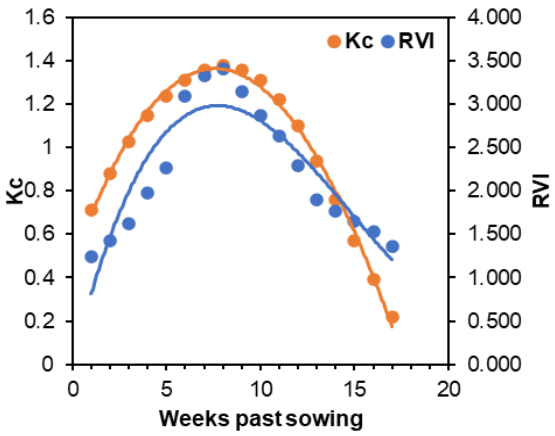

Fig. 39 K_c and RVI profile of wheat for 2020-21

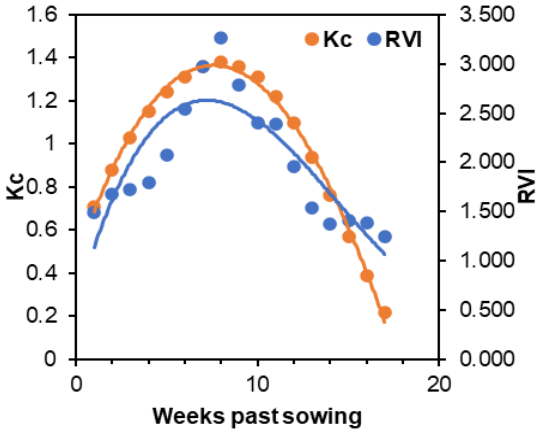

Fig. 40 K_c and RVI profile of wheat for 2021-22

When K_c and pooled RVI plotted against weeks past sowing as shown in Fig. 41 indicates that both the curves follow similar trend. Pooled RVI values are increases from 1st week to 8th week and then decreases till 17th week. Pooled NDVI curve and K_c curve crosses each other at 15th week.

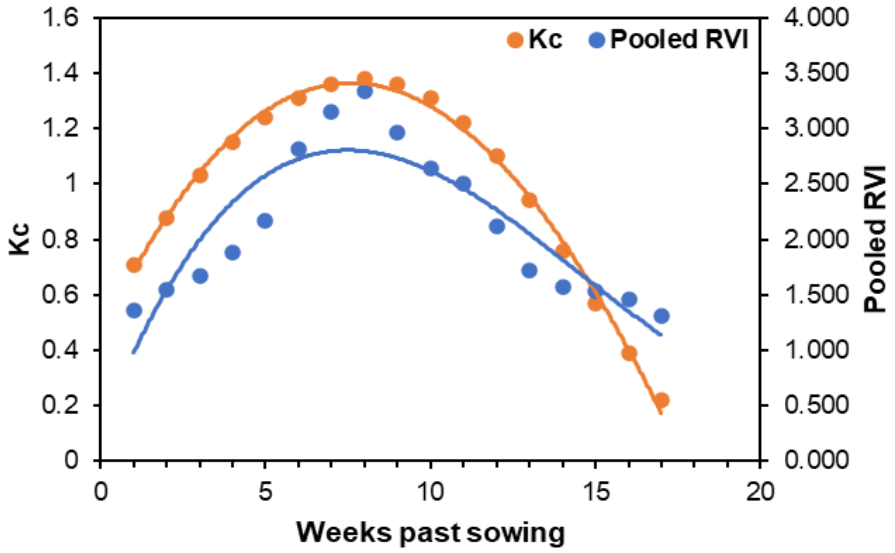

Fig. 41 K_c and pooled RVI profile of wheat

4.3.6 Overall trend of VIs for wheat

Mean weekly values of the vegetation indices of wheat for *rabi* season of 2020-21 and 2021-22 are shown in Table 12 and Table 13 respectively. Also, mean weekly values of pooled VIs of *rabi* wheat are presented in Table14. The VIs profile of both years and their pooled VI profile which are illustrated in 4.3.1 to 4.3.5 indicate that the VIs show lower values during the initial stages of germination and go on increasing through stem elongation stage still 8th week where these indices reach at peak value coinciding with maximum growth at mid-season during booting and head emergence stage and then gradually reduced indicating ripening and senescence up to the end season stage. As photosynthetic activity decreases VI show decreasing trend at later stages. Similar patterns of crop coefficients representing the growth of crops were observed by Mandal *et. al* (2007) for sorghum, Palacios *et al.* (2012) for wheat, Farg *et al.* (2012) for wheat. Kamble *et al.* (2013) for maize and soybeans. Pimpale *et al.* (2014) for cheakpea, Ozcan *et al.* (2014) for wheat, Pimpale *et al.*

(2019) for wheat and sorghum, Dingre *et al.* (2020) for sugarcane and Kosle *et al.* (2021) for wheat.

4.4 Spectral Profile of Onion

The age of *rabi* onion crop visited during the ground truth survey date was noted by getting information from farmers and also using criteria discussed in section 3.7 for the *rabi* season of 2020-21 and 2021-22 respectively. The age in weeks of the onion crop in these polygons on reference image date was obtained as per criteria discussed in 3.9.2 and recorded as given in Table 15 for 2020-21 and Table 16 for 2021-22. Accordingly, the value of vegetation index corresponding to the reference image date was entered first for both years. The VI values on all other dates of satellite overpass were entered in respective weeks as per age criteria given in Table 7 for year 2020-21 and Table 8 for 2021-22. The week-wise distribution of mean NDVI, NDWI, SAVI, MSAVI2 and RVI values for *rabi* onion crop (ground truth) polygons are shown in Annexure III for both years. These mean week-wise VIs averaged for each week past transplanting, indicating general condition of crop are shown in Table 17 for 2020-21 and Table 18 for 2021-22. The pooled weekly VIs was obtained by averaging weekly VIs of 2020-21 and 2021-22, shown in Table 19.

Table 15. Age of onion crop (weeks) for observed onion crop on reference image date for *rabi* season of 2020-21

GT ID.	Stage No.	Stage	Age on GT (Weeks)	Age on RI date (Weeks)
1.	4	Bulb initiation	8	9
2.	5	Bulb Thickening	11	12
3.	5	Bulb Thickening	11	12
4.	4	Bulb initiation	9	10
5.	4	Bulb initiation	6	7
6.	4	Bulb initiation	6	7
7.	3	Leaf elongation	5	6
8.	3	Leaf elongation	5	6
9.	4	Bulb initiation	7	8
10.	3	Leaf elongation	4	5
11.	4	Bulb initiation	6	7
12.	3	Leaf elongation	4	5
13.	4	Bulb initiation	6	7
14.	4	Bulb initiation	6	7
15.	3	Leaf elongation	4	5
16.	3	Leaf elongation	4	5
17.	3	Leaf elongation	4	5
18.	3	Leaf elongation	5	6
19.	3	Leaf elongation	5	6
20.	4	Bulb initiation	6	7
21.	4	Bulb initiation	6	7
22.	3	Leaf elongation	4	5
23.	3	Leaf elongation	4	5
24.	3	Leaf elongation	3	4
25.	3	Leaf elongation	4	5
26.	4	Bulb initiation	6	7

Table 16. Age of onion crop (weeks) for observed onion crop on reference image date for *rabi* season of 2021-22

GT ID.	Stage No.	Stage	Age on GT (Weeks)	Age on RI date (Weeks)
1.	4	Bulb initiation	8	8
2.	3	Leaf elongation	5	5
3.	4	Bulb initiation	7	7
4.	4	Bulb initiation	10	8
5.	3	Leaf elongation	6	4
6.	3	Leaf elongation	6	4
7.	4	Bulb initiation	9	7
8.	4	Bulb initiation	10	8
9.	4	Bulb initiation	9	7
10.	3	Leaf elongation	6	4
11.	3	Leaf elongation	8	6
12.	3	Leaf elongation	6	4
13.	2	Leek stage	5	3
14.	3	Leaf elongation	8	6
15.	3	Leaf elongation	7	5
16.	2	Leek stage	5	3
17.	3	Leaf elongation	8	6
18.	3	Leaf elongation	6	4
19.	3	Leaf elongation	8	6
20.	3	Leaf elongation	8	6
21.	4	Bulb initiation	9	7
22.	4	Bulb initiation	10	8
23.	3	Leaf elongation	7	5
24.	4	Bulb initiation	10	8
25.	4	Bulb initiation	10	8
26.	4	Bulb initiation	12	10
27.	3	Leaf elongation	7	5
28.	3	Leaf elongation	6	4

Table 17. Average weekly values of VIs of onion for *rabi* season of 2020-21

WPS	NDVI	NDWI	SAVI	MSAVI2	RVI
1	0.126	0.017	0.188	0.221	1.291
2	0.161	0.026	0.242	0.271	1.409
3	0.165	0.032	0.247	0.279	1.405
4	0.195	0.039	0.297	0.321	1.539
5	0.231	0.041	0.348	0.364	1.662
6	0.247	0.121	0.370	0.392	1.669
7	0.313	0.149	0.471	0.471	1.960
8	0.320	0.162	0.460	0.466	1.971
9	0.387	0.221	0.580	0.554	2.309
10	0.405	0.227	0.608	0.575	2.440
11	0.398	0.220	0.594	0.556	2.397
12	0.369	0.206	0.549	0.526	2.240
13	0.391	0.229	0.575	0.561	2.303
14	0.332	0.159	0.444	0.487	2.083
15	0.294	0.044	0.305	0.365	1.612
16	0.220	0.033	0.348	0.392	1.839

Table 18. Average weekly values of VIs of onion for *rabi* season of 2021-22

WPS	NDVI	NDWI	SAVI	MSAVI2	RVI
1	0.136	0.011	0.214	0.243	1.413
2	0.162	0.024	0.221	0.254	1.433
3	0.170	0.027	0.237	0.261	1.437
4	0.160	0.047	0.244	0.271	1.475
5	0.189	0.053	0.294	0.324	1.523
6	0.199	0.063	0.298	0.331	1.549
7	0.202	0.076	0.291	0.334	1.526
8	0.208	0.113	0.308	0.337	1.528
9	0.242	0.141	0.362	0.387	1.639
10	0.270	0.157	0.402	0.422	1.712
11	0.252	0.152	0.354	0.379	1.647
12	0.253	0.145	0.398	0.409	1.689
13	0.238	0.124	0.364	0.388	1.659
14	0.235	0.113	0.336	0.384	1.641
15	0.204	0.080	0.293	0.339	1.536
16	0.181	0.048	0.251	0.294	1.494

Table 19. Pooled weekly values of VIs of onion

WPS	NDVI	NDWI	SAVI	MSAVI2	RVI
1	0.131	0.014	0.201	0.232	1.352
2	0.162	0.025	0.232	0.262	1.421
3	0.167	0.029	0.242	0.270	1.421
4	0.178	0.043	0.271	0.296	1.507
5	0.210	0.047	0.321	0.344	1.593
6	0.223	0.092	0.334	0.362	1.609
7	0.258	0.113	0.381	0.403	1.743
8	0.264	0.138	0.384	0.402	1.749
9	0.315	0.181	0.471	0.470	1.974
10	0.337	0.192	0.505	0.498	2.076
11	0.325	0.186	0.474	0.468	2.022
12	0.311	0.175	0.474	0.467	1.964
13	0.315	0.176	0.469	0.474	1.981
14	0.284	0.136	0.390	0.435	1.862
15	0.249	0.062	0.299	0.352	1.574
16	0.200	0.041	0.300	0.343	1.666

4.4.1 NDVI profile of onion

The average NDVI values of onion for *rabi* season of 2020-21 and 2021-22 were plotted against weeks past transplanting to understand the seasonal trend. The trend observed is in the form of 3rd order polynomial and is shown in Fig. 42 for 2020-21 and Fig. 43 for 2021-22 which satisfies the polynomial equation as:

For year 2020-21,

$y = -0.0004x^3 + 0.0073x^2 - 0.0065x + 0.1326 \quad R^2 = 0.977$ ----------17

For year 2021-22,

$y = -0.0002x^3 + 0.0033x^2 - 0.0053x + 0.1495 \quad R^2 = 0.932$ ----------18

where, y = NDVI and x = weeks past transplanting

It is observed that in initial stages (4-5 leaves) the crop shows lower NDVI i.e. 0.126 for year 2020-21 and 0.136 for 2021-22 respectively and goes on increasing till 10th week indicating maximum growth during crop

development stage. Higher NDVI values are observed between 8th to 11th week and then decreasing gradually till physiological maturity of crop i.e. 16th week indicating senescence.

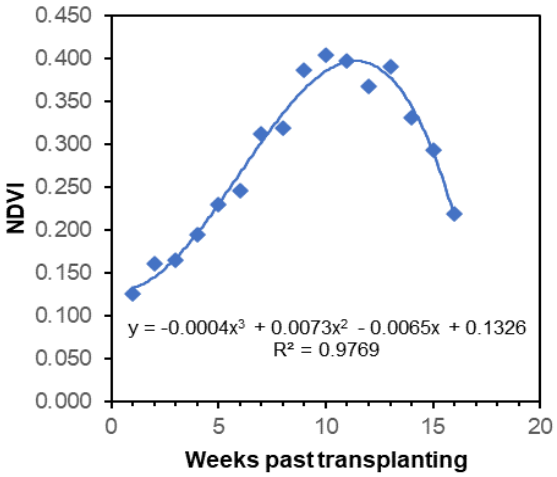

Fig. 42 NDVI profile of onion for 2020-21

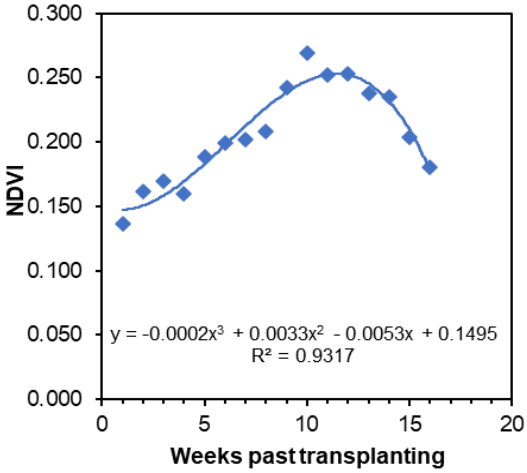

Fig. 43 NDVI profile of onion for 2021-22

Pooled NDVI plotted against weeks past transplanting as shown in Fig. 44 shows that pooled NDVI begins from 0.131 (1st week) and accelerating till 0.337 (10th week). After reaching at peak i.e. 10th week the pooled NDVI values decreases gradually. It follows third order polynomial equation:

$y = -0.0003x^3 + 0.0053x^2 - 0.0059x + 0.141$ $R^2 = 0.977$ ----------19

where, y = pooled NDVI and x = weeks past transplanting

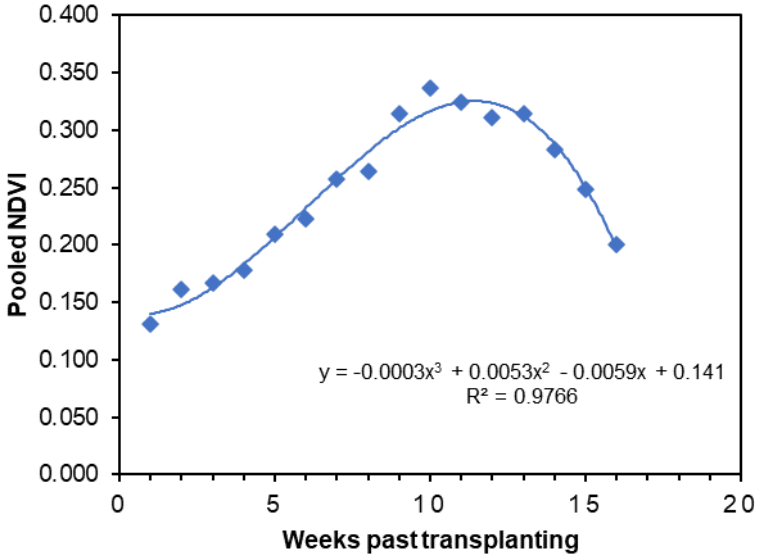

Fig. 44 Pooled NDVI profile for onion

When K_c and NDVI plotted against weeks past transplanting as shown in Fig.45 and Fig. 46 for year 2020-21 and 2021-22, it shows similar trend. For both year NDVI increases gradually till 10th week and then decreases up to 16th week.

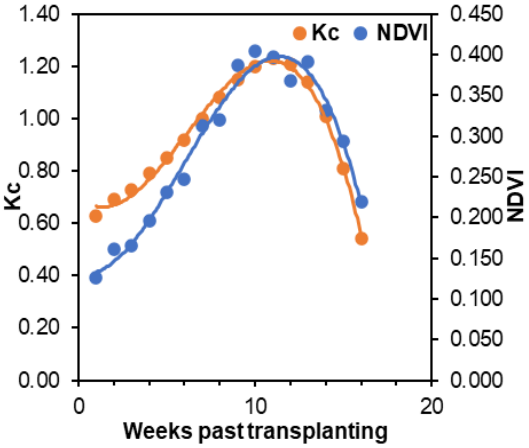

Fig. 45 NDVI and K_c profile of onion for 2020-21

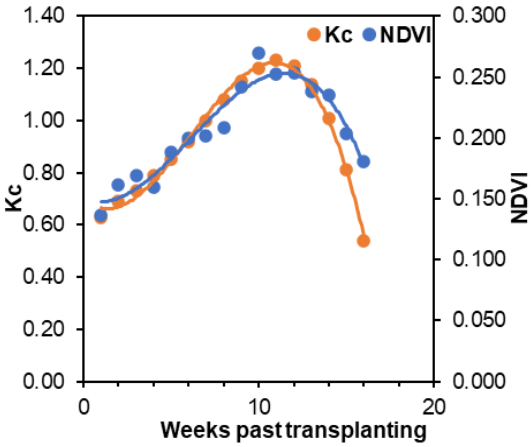

Fig. 46 NDVI and K_c profile of onion for 2021-22

Pooled NDVI trends were plotted along with K_c values over the weeks past transplanting shows same trend and shown in Fig. 47. The pattern of pooled NDVI and K_c values throughout the initial, crop development and mid-season stage of *rabi* onion exhibits similarity between pooled NDVI and K_c. Pooled NDVI curve crosses K_c curve at 13th week. The pattern of almost non fluctuating distance between pooled NDVI and K_c values throughout the growing season of *rabi* onion exhibits cohesivity between NDVI and crop coefficients.

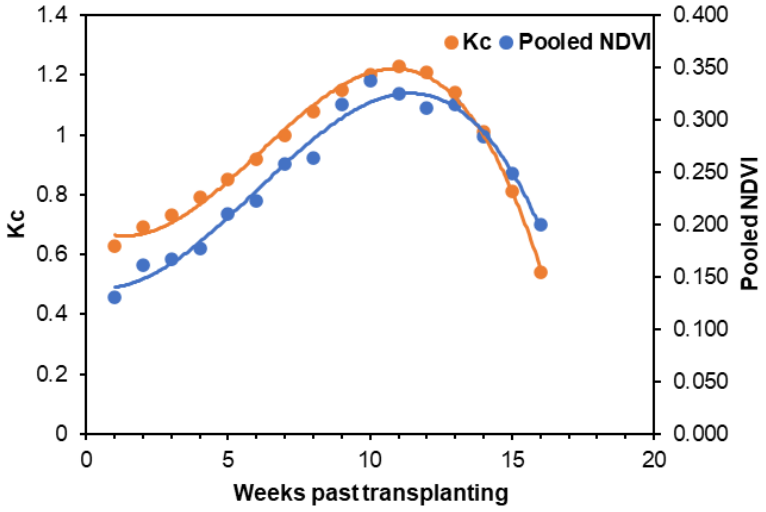

Fig. 47 Pooled NDVI and K_c profile of onion

4.4.2 NDWI profile of onion

For *rabi* season of 2020-21 and 2021-22, Analysis of weekly variation of NDWI throughout the growing season shows developing trend with the growth of *rabi* onion crop as shown in Fig 48. and Fig. 49. It confirms the third order polynomial equation as:

For year 2020-21,

$y = -0.0005x^3 + 0.0098x^2 - 0.0293x + 0.0389$ $R^2 = 0.938$ ----------20

For year 2021-22,

$y = -0.0003x^3 + 0.005x^2 - 0.0121x + 0.0238$ $R^2 = 0.964$ ----------21

where, y = NDWI and x = Weeks past transplanting

It is observed that during initial stage the crop shows lower NDWI value of 0.017 and 0.011 and increases till 10th week past transplanting achieving highest NDWI of 0.227 and 0.157 for year 2020-21 and 2021-22 respectively. In 2020-21, values of NDWI increases gradually till 5th week and then increases rapidly till 10th week. After that NDWI values decreases sharply till 16th week. In 2021-22, values of NDWI increases and decreases gradually.

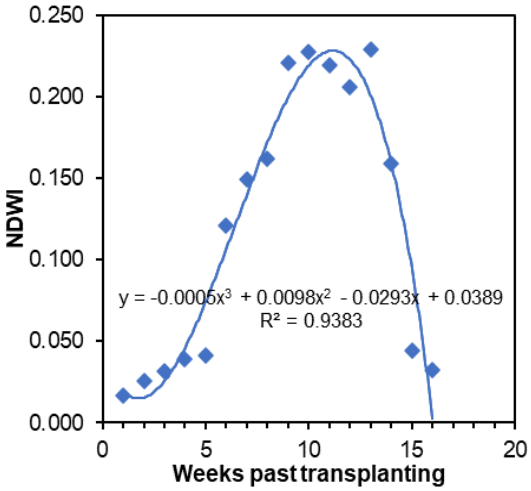

Fig. 48 NDWI profile of onion for 2020-21

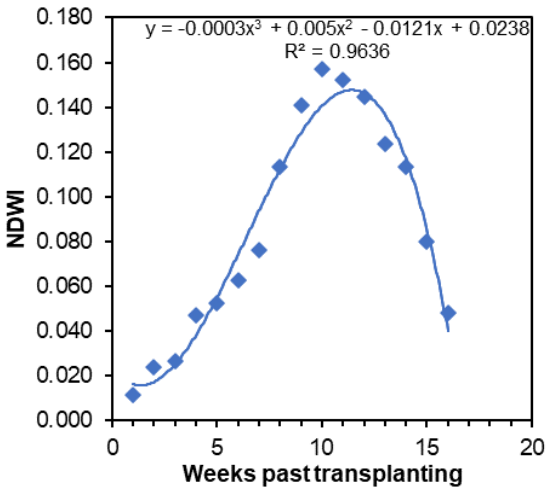

Fig. 49 NDWI profile of onion for 2021-22

When pooled NDWI and weeks past transplanting plotted together (Fig. 50), it indicates gradual increase of pooled NDWI started from 0.014 and increasing till 0.192 up to 10th week and then decreases gradually. Higher value pooled NDWI indicates maximum water content in vegetation.

The value of NDWI decreases as water content of vegetation decreases i.e. at maturity stage of crop. It follows third order polynomial equation as:

$y = -0.0004x^3 + 0.0074x^2 - 0.0207x + 0.0314$ $R^2 = 0.967$ ----------22

where, y = pooled NDWI and x = weeks past transplanting.

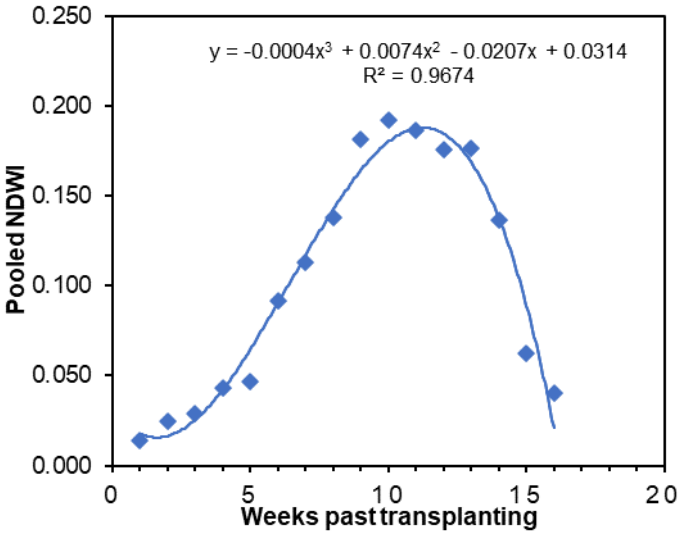

Fig. 50 Pooled NDWI profile for onion

When NDWI and K_c are together plotted against weeks past transplanting, it is observed that the trend of development of NDWI is similar to the trend of crop coefficient for both years 2020-21 (Fig. 51) and 2021-22 (Fig. 52) respectively. NDWI curve crosses K_c curve at two points i.e. 9th and 13th week in 2020-21 and the curves are collinear in 2021-22.

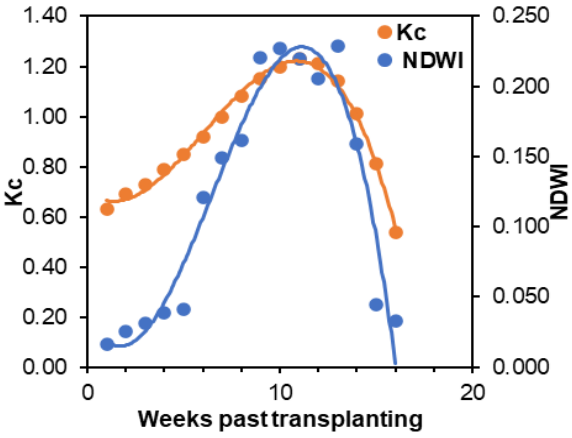

Fig. 51 NDWI and K_c profile of onion for 2020-21

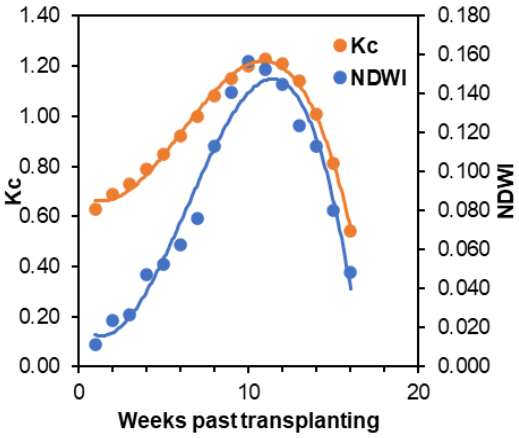

Fig. 52 NDWI and K_c profile of onion for 2021-22

Pooled NDWI and K_c plotted against weeks past transplanting as shown in Fig. 53, it is observed that both pooled NDWI and K_c show similar temporal pattern. Both curves are parallel to each other and attains highest values at 10th week. The pattern of almost non fluctuating distance between pooled NDWI and K_c values throughout the growing season of *rabi* onion exhibits cohesivity between NDWI and crop coefficients. This co-linearity observed may help in replacing difficult calculations involved in evaluating the K_c values.

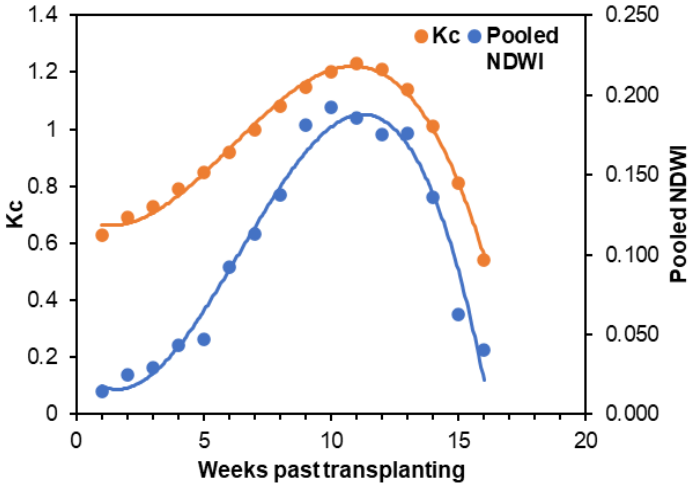

Fig. 53 Pooled NDWI and K_c profile of onion

4.4.3 SAVI profile of onion

The plot of weeks past transplanting against SAVI exhibits the temporal development of SAVI for *rabi* season of 2020-21 and 2021-22 as shown in Fig. 54 and Fig. 55. It is found that SAVI increases from 0.188 and 0.214 to 0.608 and 0.402 up to 10th week for year 2020-21 and 2021-22 respectively. They follow polynomial equation of third order:

For year 2020-21,

$y = -0.0006x^3 + 0.0097x^2 - 0.0009x + 0.1852$ $R^2 = 0.919$----------23

For year 2021-22,

$y = -0.0003x^3 + 0.0057x^2 - 0.0123x + 0.2257$ $R^2 = 0.920$----------24

where, y = SAVI and x = weeks past transplanting

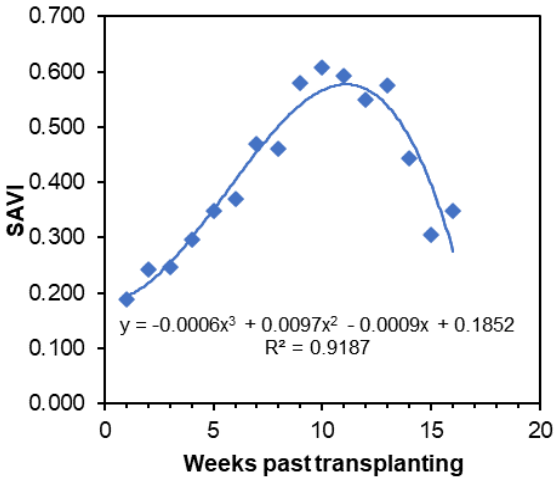

Fig. 54 SAVI profile of onion for 2020-21

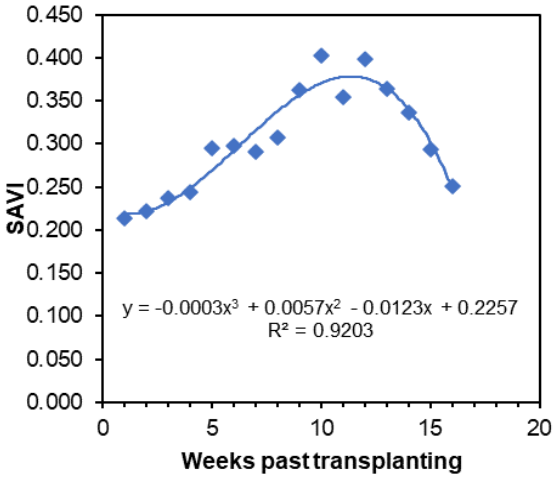

Fig. 55 SAVI profile of onion for 2021-22

The pooled SAVI and weeks past transplanting are plotted together, it shows that the values of pooled SAVI increased gradually and reached to peak at 10th week and then decreases gradually till 16th week as shown in Fig. 56. The highest value of pooled SAVI is 0.505 at 10th week. The trend of SAVI obeys third order polynomial equation:

$y = -0.0004x^3 + 0.0077x^2 - 0.0066x + 0.2055$ $R^2 = 0.943$ ----------25

where, y = pooled SAVI and x = weeks past transplanting

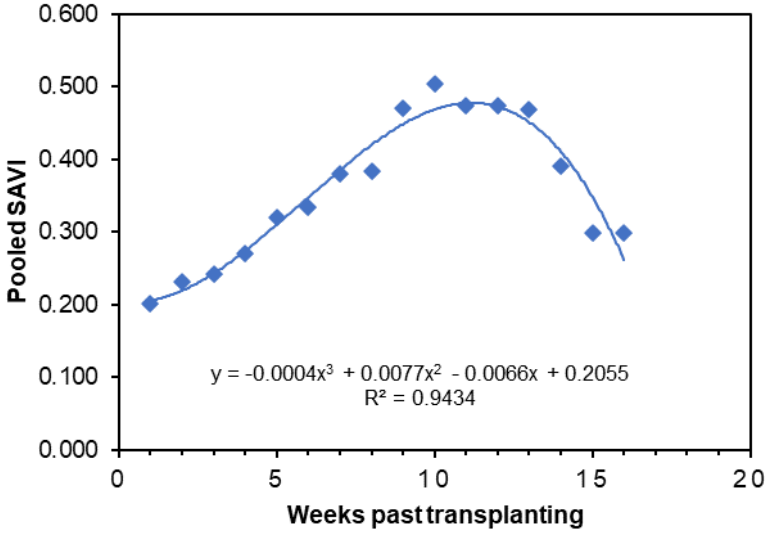

Fig. 56 Pooled SAVI profile for onion

For *rabi* season of 2020-21 and 2021-22, SAVI and K_c plotted against weeks past transplanting and indicates the similar trend between

them, as shown in Fig. 57 and Fig. 58. In both years SAVI curve overlaps K_c curve at some weeks.

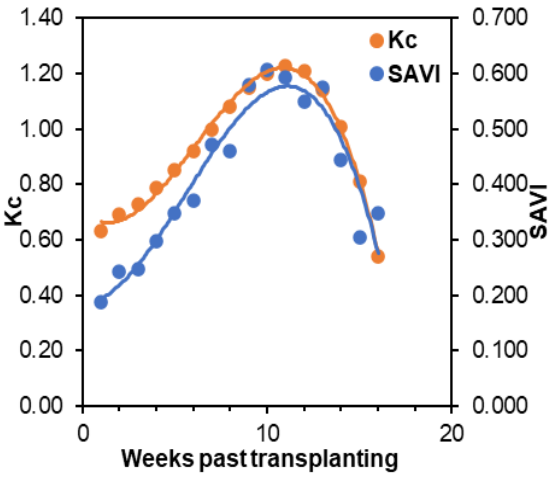

Fig. 57 SAVI and K_c profile of onion for 2020-21

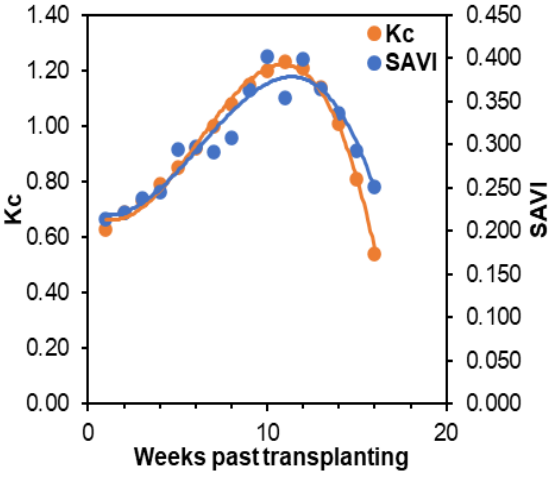

Fig. 58 SAVI and K_c profile of onion for 2021-22

When pooled SAVI and K_c values were plotted together versus weeks past transplanting it was seen that both the parameters SAVI and K_c had the same trend through different growth stages as shown in Fig. 59. Pooled SAVI curve and K_c curves are collinear and crosses at 14th week.

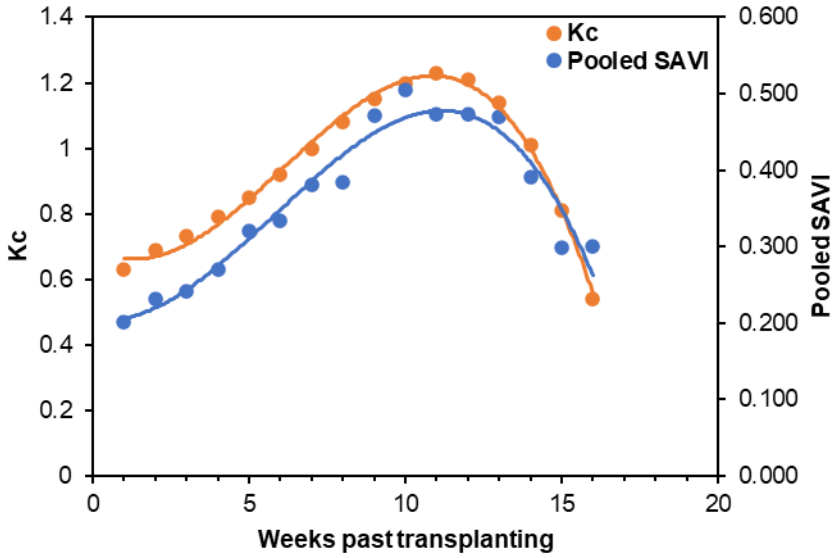

Fig. 59 Pooled SAVI and K_c profile of onion

4.4.4 MSAVI2 profile of onion

The plot of weeks after transplanting and MSAVI2 exhibits the temporal profile of MSAVI2 for *rabi* season of 2020-21 (Fig. 60) and 2021-22 (Fig. 61). It follows polynomial equation of third order as:

For year 2020-21,

$y = -0.0004x^3 + 0.0064x^2 + 0.0102x + 0.2087$ $R^2 = 0.942$ ----------26

For year 2021-22,

$y = -0.0002x^3 + 0.0045x^2 - 0.0054x + 0.2464$ $R^2 = 0.938$ ----------27

where, y = MSAVI2 and x = weeks past transplanting

Beginning of MSAVI2 is from 0.221 and 0.243 at 1st week to 0.575 and 0.422 at 10th week for 2020-21 and 2021-22 respectively. After that the values are decreasing slowly till 16th week i.e. up to maturity of onion crop.

Pooled MSAVI2 plotted against weeks past transplanting indicates gradual increasing of MSAVI2 and reached to peak at 10th week and then decreases gradually as shown in Fig. 62. The initial value of pooled MSAVI2 is 0.232 and highest MSAVI2 value is 0.498. The pooled value of MSAVI2 at 8th, 9th and 10th week are nearly same. It follows polynomial equation:

$y = -0.0003x^3 + 0.0055x^2 + 0.0024x + 0.2276$ $R^2 = 0.962$ ----------28

where, y = pooled MSAVI2 and x = weeks past transplanting

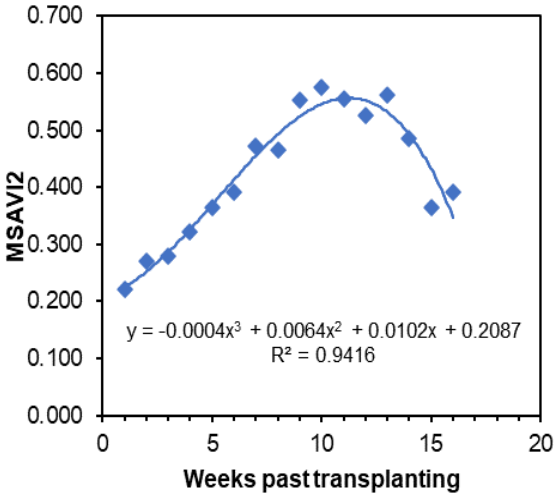

Fig. 60 MSAVI2 profile of onion for 2020-21

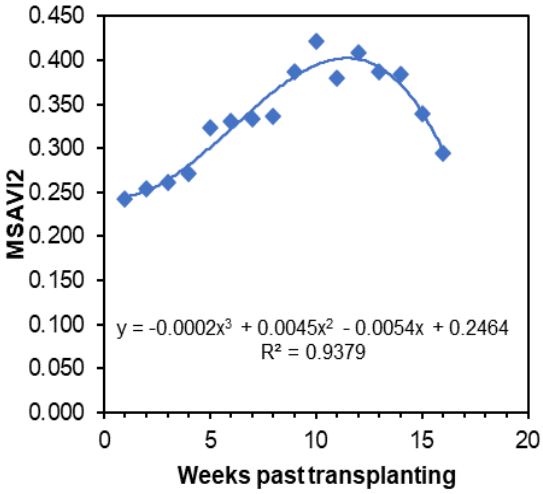

Fig. 61 MSAVI2 profile of onion for 2021-22

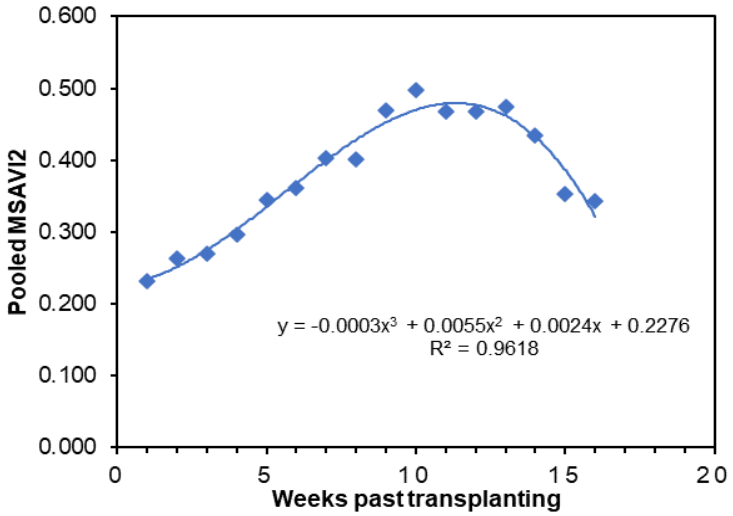

Fig. 62 Pooled MSAVI2 profile for onion

When MSAVI2 and K_c are compared, it was observed that MSAVI2 shows higher values till 10th week for both year 2020-21 and 2021-22. MSAVI2 and K_c curve shows similar trend as shown in Fig. 63 and Fig 64.

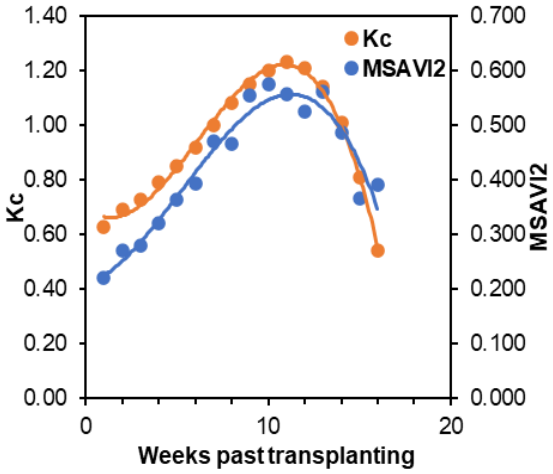

Fig. 63 MSAVI2 and K_c profile of onion for 2020-21

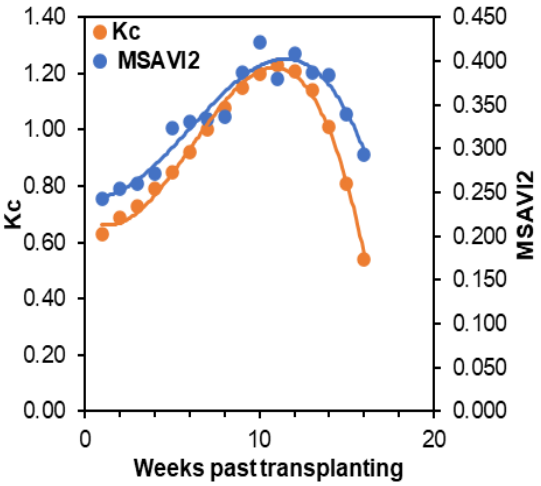

Fig. 64 MSAVI2 and K_c profile of onion for 2021-22

Pooled MSAVI2 and K_c was plotted together, it shows that both the curve shows similar trend as shown in Fig. 65 The pooled MSAVI2 curve crosses K_c curve at 14th week.

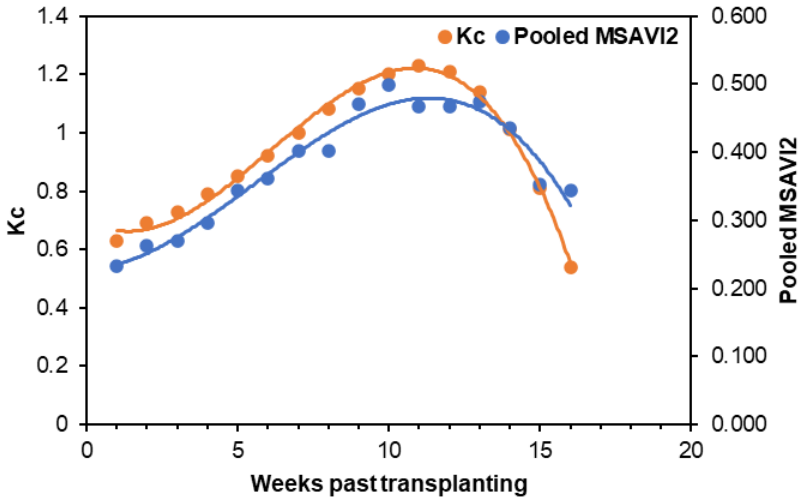

Fig. 65 Pooled MSAVI2 and K_c profile of onion

4.4.5 RVI profile of onion

Analysis of weekly variation of RVI throughout the growing season shows developing trend with the growth of *rabi* onion crop for year 2020-21 and 2021-22 as shown in Fig. 66 and Fig 67.

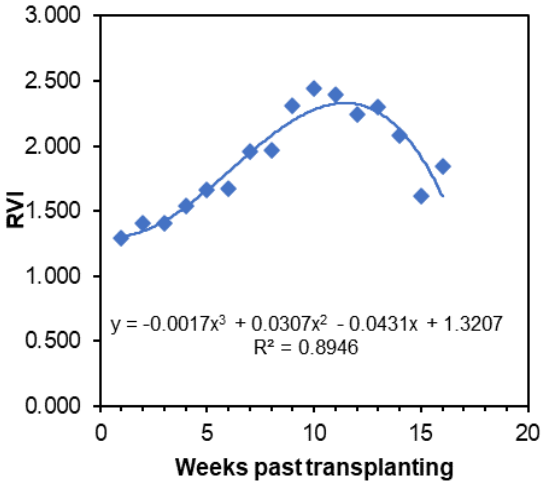

Fig. 66 RVI profile of onion for 2020-21

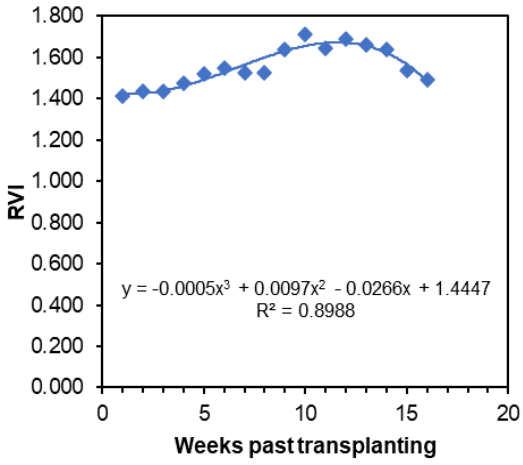

Fig. 67 RVI profile of onion for 2021-22

It follows the third order polynomial equation.

For year 2020-21,

$y = -0.0017x^3 + 0.0307x^2 - 0.0431x + 1.3207$ $R^2 = 0.895$ ----------29

For year 2021-22,

$y = -0.0005x^3 + 0.0097x^2 - 0.0266x + 1.4447$ $R^2 = 0.899$ ----------30

where, y = RVI and x = weeks past transplanting

The values of RVI started from 1.291 and 1.413 and go on up to 2.440 and 1.712 till 10th week for year 2020-21 and 2021-22. In 2021-22 the values of RVI is nearly same at 5th, 7th and 8th week.

When Pooled RVI was plotted against weeks past transplanting as shown in Fig. 68, it indicates that values increasing gradually till 10th week i.e. mid-season stage and then decreases gradually till 16th week at maturity.

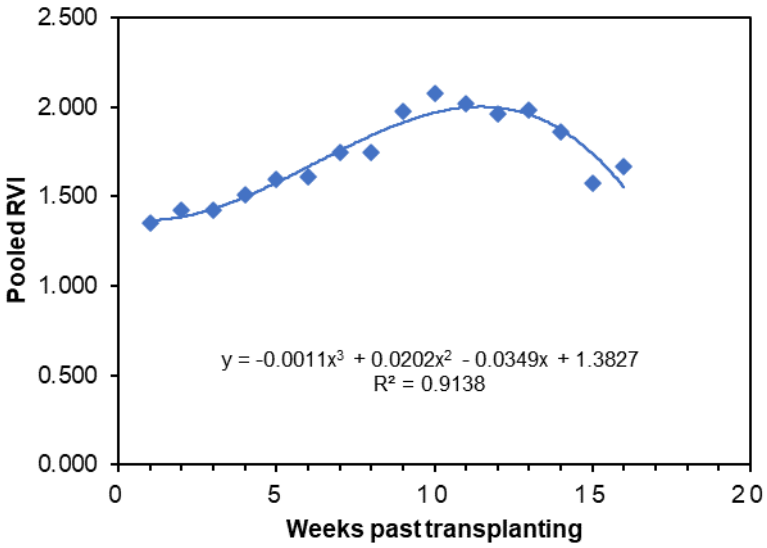

Fig. 68 Pooled RVI profile for onion

It obeys third order polynomial equation as:

$y = -0.0011x^3 + 0.0202x^2 - 0.0349x + 1.3827 \quad R^2 = 0.914$ ----------31

where, y = pooled RVI and x = weeks past transplanting

By comparing RVI and K_c curve, it shows higher values throughout growing period of year 2020-21 and 2021-22 as shown in Fig. 69 and Fig. 70. The temporal pattern of both curves is same. In 2020-21, RVI curve crosses K_c at 15th week, whereas in 2021-22 RVI curve is parallel to K_c curve.

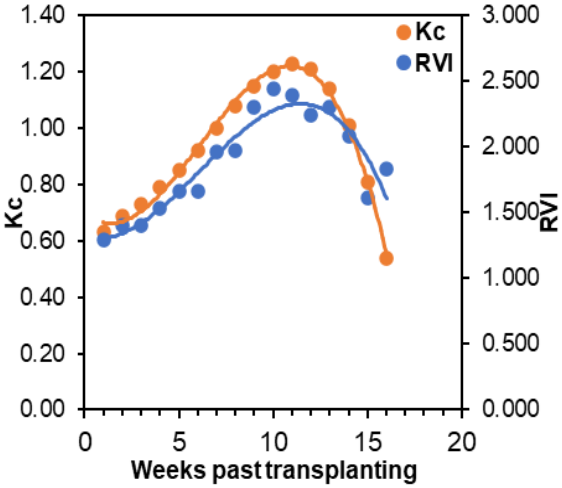

Fig. 69 RVI and K_c profile of onion for 2020-21

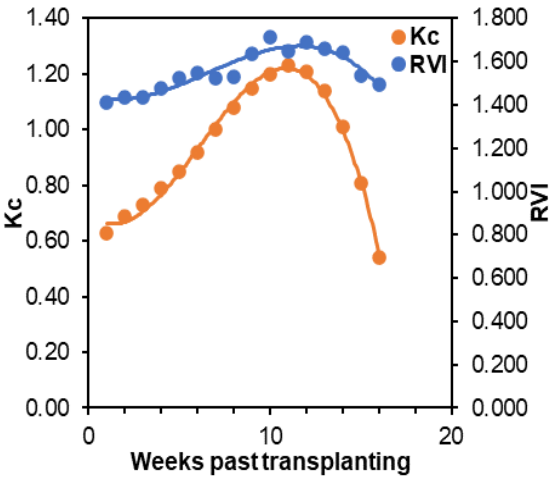

Fig. 70 RVI and K_c profile of onion for 2021-22

When Pooled RVI and K_c plotted against weeks past transplanting as shown in Fig. 71, It indicates that both curve follows similar trend. Pooled RVI curve crosses K_c curve at two points i.e 6th and 13th week.

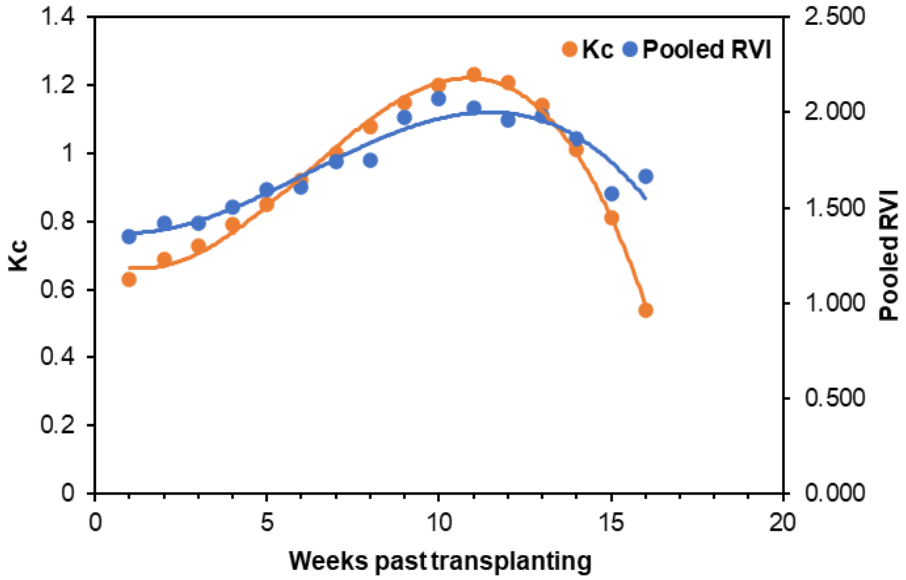

Fig. 71 Pooled RVI and K_c profile of onion

4.4.6 Overall trend of VIs for *rabi* onion

Average weekly values of VIs of *rabi* onion for year 2020-21 and 2021-22 are shown in Table 17 and Table 18, respectively and also pooled weekly VIs of *rabi* onion are presented in Table 19. All VI profiles discussed separately in preceding paragraphs indicate that almost all vegetation indices show lower values at initial stages of onion crop after transplanting.

The values of VIs increase as crop development stage, mid-season stage and reached to the peak at 10th week. After 11th or 12th week all the VIs show decreasing trend indicating yellowing and wilting of the onion crop. Values of VIs decrease up to maturity of crop i.e. 16th week. *Rabi* onion crop in study area have generally sparse to medium canopies and do not cover complete ground. Similar pattern of crop coefficients representing the growth of crops were observed by Hunsaker *et al.* (2003) for cotton, Suifan *et al.* (2007) for vegetable crops in Mafraq, Singh *et al.* (2013) for cotton. Pimpale *et al.* (2019) for sorghum. However, exactly similar studies related to *rabi* onion were not observed in the literature survey.

4.5 Identification and Acreage Estimation of Wheat and Onion Crop

A hybrid classification method based on K-means clustering and visual analysis is adopted for the identification and acreage estimation of *rabi* wheat and onion crop using multidate time series remote sensing data of Sentinel 2A satellite for year 2020-21.

NDVI layer stack was prepared using the NDVI images derived from subsets. The shape file was used to map the geographical locations of GT sites onto the image. For each day of the satellite overpass, the average NDVI values of the fields of wheat and onion which are grown in the similar period were obtained. Graphs representing NDVI values for various dates of satellite image acquisition were plotted for wheat and onion. These graphs display the Reference Temporal Spectral Profiles (RTSPs) of the corresponding class. RTSPs representing different sowing dates of the wheat and onion crop were prepared in addition to the general RTSP. In order to reduce data load, Non Crop Mask (NCM) was overlaid on the NDVI stack and output multilayer dataset representing cropped area was used for further processing.

K-means clustering method of unsupervised classification was carried out on this resultant multilayer dataset and a classified image with 100 classes of clusters was generated. The signatures of all of these classes were acquired from the attribute table and then exported to Microsoft Excel. Based on their signatures, temporal spectral profiles (TSPs) were created for each class. After a visual comparison with known

RTSPs with the assistance of an expert, the cluster classes were allocated to a certain crop or other with which it matched the most.

TSPs of 22 and 19 classes were found to matching with RTSPs of wheat and onion crop respectively. Fig. 72 shows the results of unsupervised classification and was then utilized for supervised classification using visual analysis and a signature editing tool. Crop recoding was performed on the output of supervised classification to create a real thematic map by combining similar clusters. The spatial distribution of wheat and onion and other crops is represented by choosing different colors for different classes. Final classified image is shown in Fig. 73. The district wise pixel count of wheat was obtained by applying zonal attributes/majority count function of ArcGIS. For this process, option of intersection/union and ignore zero values were selected. After running of process, the attribute of the vector layer show majority count i.e. number of pixels of wheat in each district. The area under wheat crop in each district was obtained by multiplying these number of pixels by resolution of the data i.e. 10x10 m and converted into hectares. Similar procedure was carried out for district-wise area estimation of onion crop.

Similar procedure was adopted for year 2021-22 to identification and estimation of acreage of *rabi* wheat and onion crop except in year 2021-22 there was TSPs of 21 and 17 classes found to matched with RTSPs of wheat and onion crop respectively. Fig. 74 shows image obtained after unsupervised classification and then this unsupervised classified image was utilized for supervised classification using visual analysis and signature editing tool. Final classified image is shown in Fig. 75

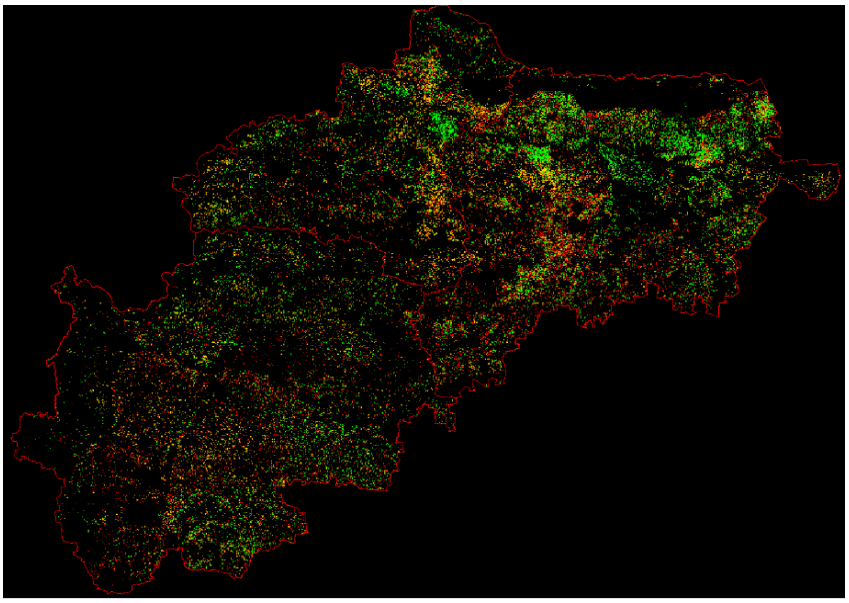

Fig. 72 Classified image obtained after unsupervised classification for 2020-21

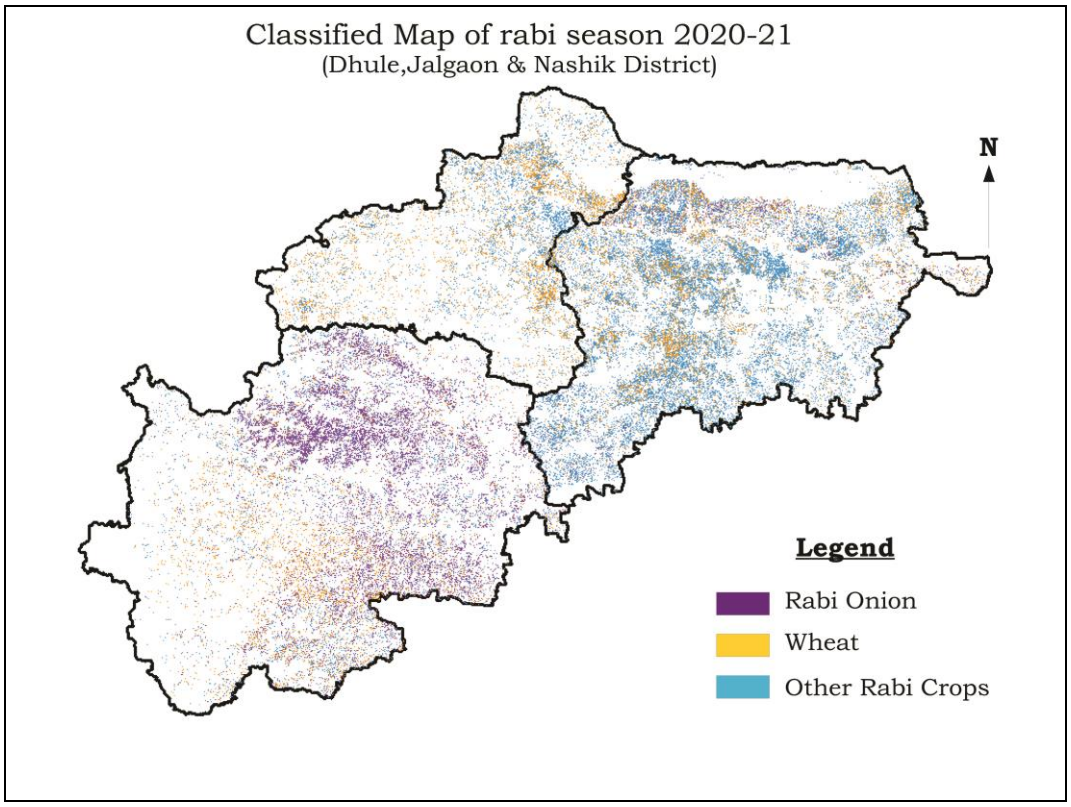

Fig. 73 Final Classified image for 2020-21

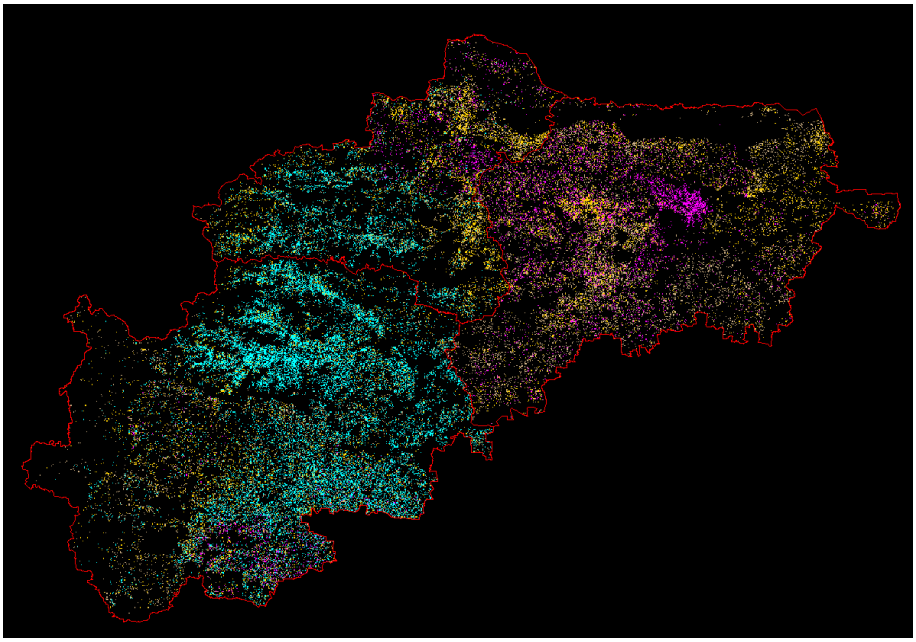

Fig. 74 Classified image obtained after unsupervised classification for 2021-22

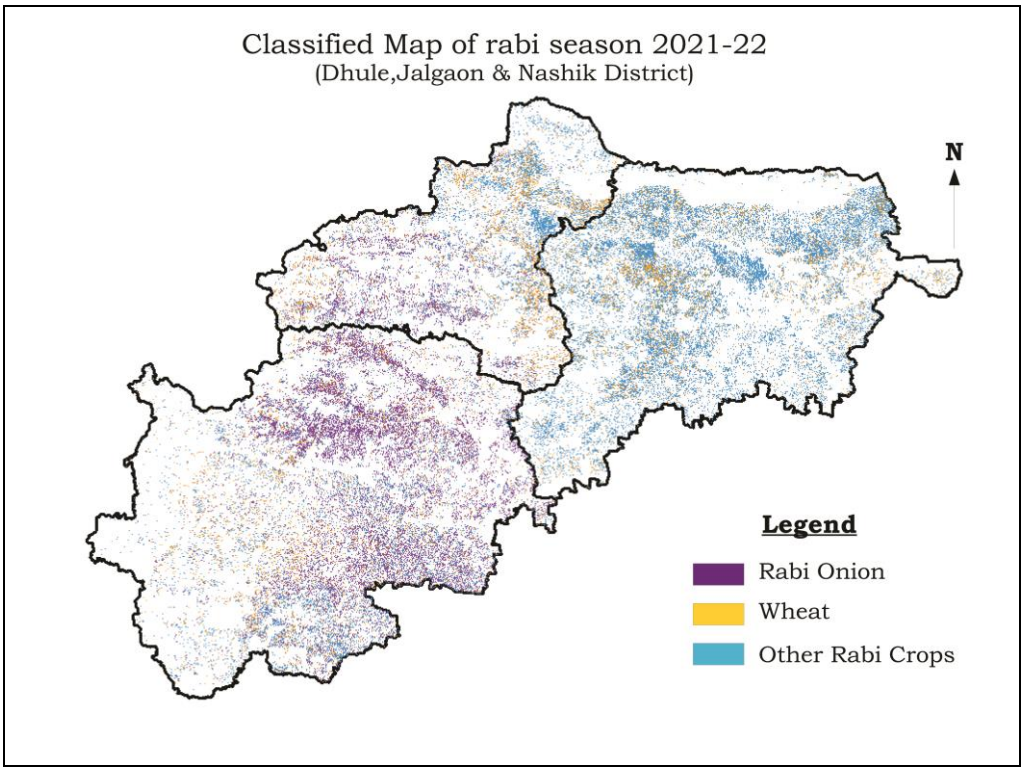

Fig. 75 Final Classified image for 2021-22

The results of acreage estimation of wheat and onion for year 2020-21 and 2021-22 and its comparison with reference figures received from crop statistics by Department of Agriculture, Government of Maharashtra are given in Table. 20

Table 20. Estimated district-wise acreage of *rabi* wheat and onion for year 2020-21 and 2021-22

Crop	District	2020-21			2021-22		
		RS estimates (ha)	DOA estimates (ha)	Deviation (%)	Rs estimates (ha)	DOA estimates (ha)	Deviation (%)
Wheat	Dhule	44386	41609	6.67	45384	41154	10.28
	Jalgaon	67927	61747	10.01	65294	57474	13.61
	Nashik	60590	63442	-4.50	60474	58794	2.86
	Total	172903	166798	3.66	171152	157422	8.72
Onion	Dhule	16529	14789	11.77	31776	29445	7.92
	Jalgaon	10359	9891	4.73	8771	7668	14.38
	Nashik	163516	149866	9.11	210917	190306	10.83
	Total	190404	174546	9.08	251464	227419	10.57

For year 2020-21, Remote sensing-based wheat crop acreage when compared with average data collected from Department of Agriculture showed an average deviation of 3.66 per cent on study area basis. When district-wise results are studied, lowest deviation of -4.50 per cent (under-estimation) was found in Nashik district while Jalgaon district showed higher deviation of 10.01 per cent. For year 2021-22, total wheat crop acreage of study area using remote sensing was found 171152 ha and compared with data collected from Department of agriculture as 157422 ha. The average deviation was found 8.72 per cent. Lowest deviation was found in Nashik district as 2.86 per cent while Jalgaon district showed higher deviation of 13.61 per cent.

Overall Remote sensing-based onion crop acreage was found 190404 ha for year 2020-21 and 251464 ha for 2021-22 while the data given by Department of Agriculture was 174546 ha (2020-21) and 227419 ha (2021-22) for study area. Overall deviation of 9.08 per cent for 2020-21 and 10.57 per cent for 2021-22 was found in onion acreage estimation for study area. When district-wise acreage calculated it was observed that Jalgaon district has lowest deviation of 4.73 per cent for year 2020-21 while in year 2021-22 the lowest deviation of 7.92 per cent was found in Dhule

district. For year 2020-21, highest deviation of 11.77 per cent in acreage estimation of onion was found in Dhule district. Highest deviation of 14.38 per cent was found in Jalgaon district for year 2021-22.

Over-estimation of acreage of wheat and onion may be due to similar spectral profiles of coexisting crops like sorghum, groundnut, maize etc. *Rabi* wheat and onion are irrigated crops, soil moisture also affects the reflectance of crop. Under-estimation of wheat crop acreage in year 2020-21 may be due to not counting area of small crop holding, mix cropping, etc.

The results obtained were in agreement with similar studies conducted by Pandit *et al.* (2006) used digital image processing of multidate, multi-sensor high resolution satellite data for identification of sugarcane and onion crops. Goswami *et al.* (2012) used remote sensing and GIS for wheat crop acreage estimation of Indore District. Pimpale *et al.* (2015) estimated wheat acreage of five district and was found 189481 ha, which is deviating by 9.78 % from the reference data as reported by Government of Maharashtra. Paul and Kumar (2019) compared Landsat-8 and Sentinel-2A datasets for *Rabi* crop classifications. They found average overall accuracy of 80.96 per cent and 88.16 per cent were achieved using the Landsat-8 and Sentinel-2A datasets respectively. Rawat *et al.* (2021) evaluated wheat acreage using remote sensing and GIS in Jabalpur (M.P., India). They found that the area of wheat crop corresponds to 83.07 per cent. The overall accuracy and Kappa Statistics of the classification using Sentinel-2 imagery are 85.71 per cent and 0.819 per cent, respectively.

4.6 Relationship between Crop Coefficients and VIs for Wheat

The relationship between crop coefficients and vegetation indices are derived for wheat for *rabi* season of 2020-21 and 2021-22. The average weekly values of vegetation indices i.e. NDVI, NDWI, SAVI, MSAVI2 and RVI for wheat as shown in Table 12 (2020-21) and Table 13 (2021-22) were plotted against weekly crop coefficients (K_c) recommended by MPKV Rahuri (discussed in 3.14, Table 9). Also pooled VIs values (Table 14) were plotted against crop coefficient recommended by MPKV Rahuri. Simple linear regression analysis was used to develop the

relationship between these crop coefficients and vegetation indices for both years. It was observed that a strong correlation exists between all the vegetation indices and crop coefficients of wheat for both years 2020-21 and 2021-22 respectively. Figures 76a, 76b, 76c, 76d and 76e show the relationships of the vegetation indices i.e. NDVI, NDWI, SAVI, MSAVI2 and RVI for *rabi* season of 2020-21. Figures 77a, 77b, 77c, 77d and 77e show the relationships of the vegetation indices for year 2021-22. Pooled weekly VIs also show the relationship between VIs and K_c as shown in Figures 78a, 78b, 78c, 78d and 78e.

From the regression analysis linear prediction models for wheat were obtained for year 2020-21 and 2021-22 and also for pooled weekly VI values. These prediction models are:

Prediction Model of wheat for year 2020-21:

$K_c = 3.493\ NDVI - 0.095$ $R^2 = 0.845$ ----------32

$K_c = 3.061\ NDWI + 0.493$ $R^2 = 0.954$ ----------33

$K_c = 2.051\ SAVI + 0.057$ $R^2 = 0.809$ ----------34

$K_c = 2.512\ MSAVI2 - 0.139$ $R^2 = 0.812$ ----------35

$K_c = 0.408\ RVI + 0.095$ $R^2 = 0.703$ ----------36

Prediction Model of wheat for year 2021-22:

$K_c = 2.881\ NDVI + 0.180$ $R^2 = 0.849$ ----------37

$K_c = 4.229\ NDWI + 0.372$ $R^2 = 0.937$ ----------38

$K_c = 1.860\ SAVI + 0.223$ $R^2 = 0.811$ ----------39

$K_c = 2.317\ MSAVI2 + 0.059$ $R^2 = 0.817$ ----------40

$K_c = 0.495\ RVI + 0.005$ $R^2 = 0.731$ ----------41

Prediction model of wheat for pooled VIs

$K_c = 3.224\ NDVI + 0.035$ $R^2 = 0.865$ ----------42

$K_c = 3.608\ NDWI + 0.433$ $R^2 = 0.962$ ----------43

$K_c = 1.999\ SAVI + 0.123$ $R^2 = 0.830$ ----------44

$K_c = 2.459\ MSAVI2 - 0.057$ $R^2 = 0.831$ ----------45

$K_c = 0.457\ RVI + 0.034$ $R^2 = 0.731$ ----------46

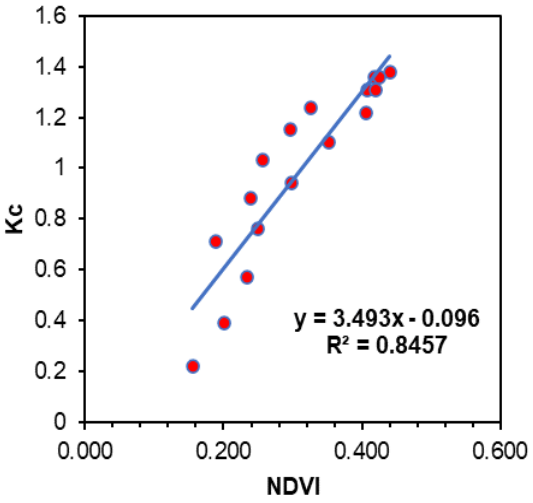

(a) NDVI vs K_c

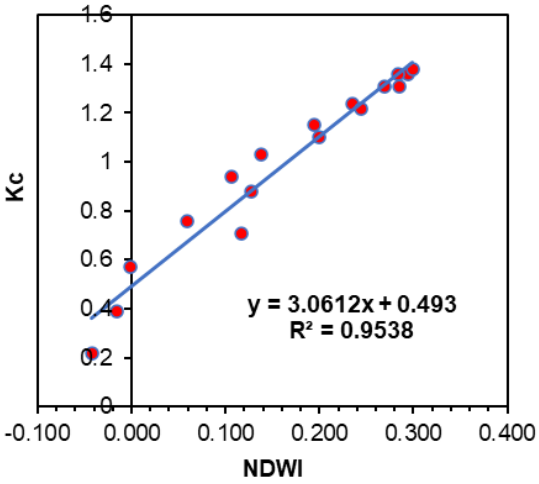

(b) NDWI vs K_c

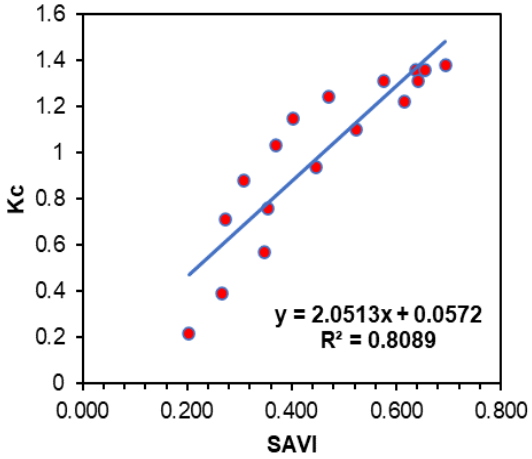

(c) SAVI vs K_c

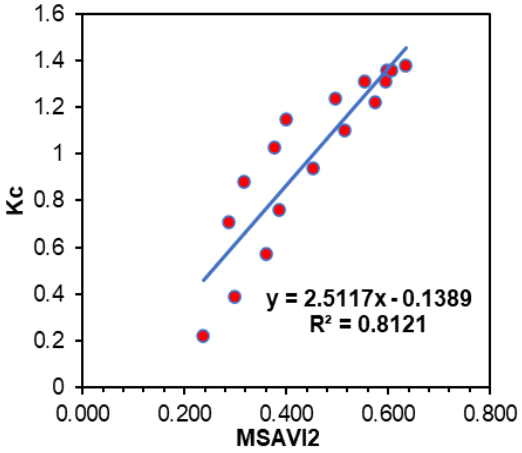

(d) MSAVI2 vs K_c

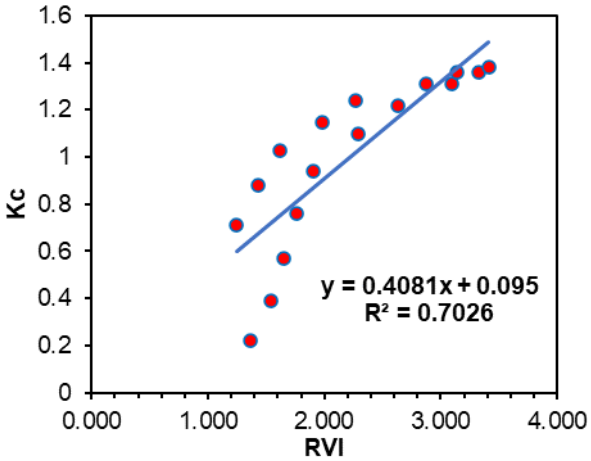

(e) RVI vs K_c

Fig. 76 (a, b, c, d and e) Relationship of crop coefficients with vegetation indices of wheat for year 2020-21

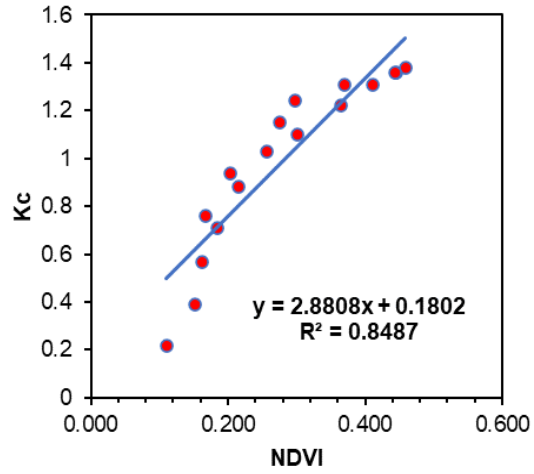

(a) NDVI vs K_c

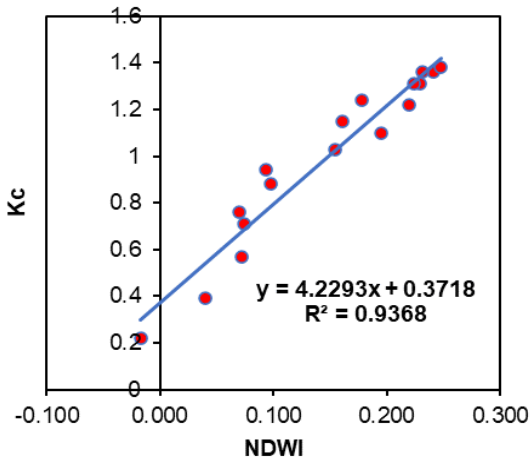

(b) NDWI vs K_c

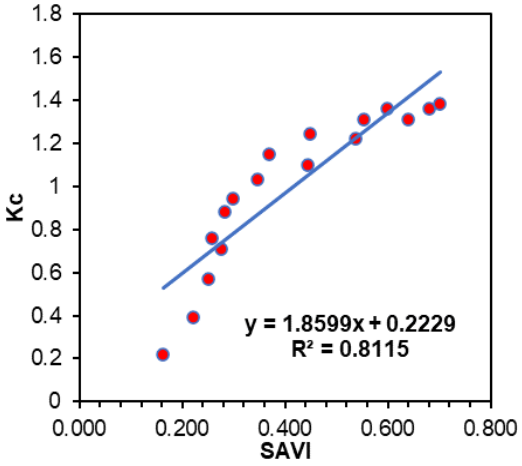

(c) SAVI vs K_c

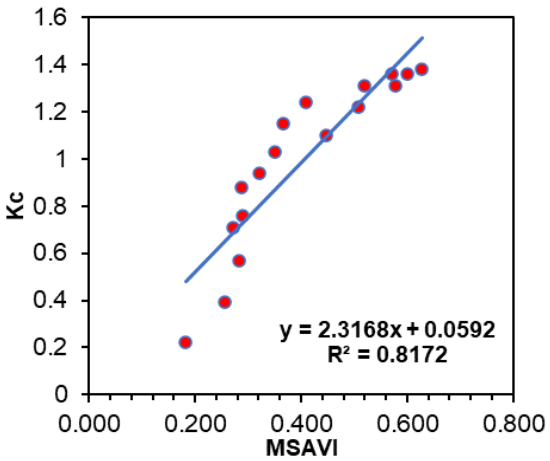

(d) MSAVI2 vs K_c

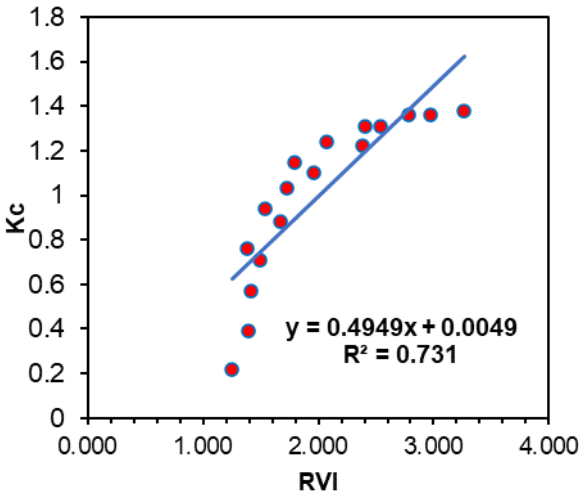

(e) RVI vs K_c

Fig. 77 (a, b, c, d and e) Relationship of crop coefficients with vegetation indices of wheat for year 2021-22

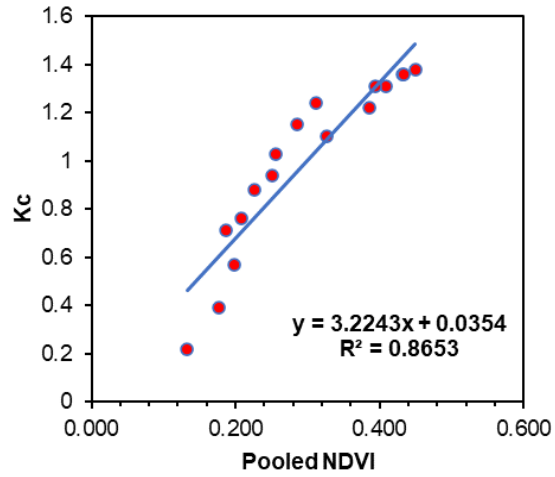

(a) Pooled NDVI vs K_c

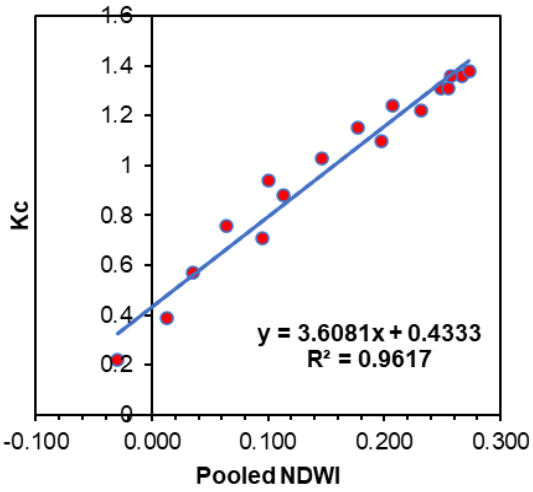

(b) Pooled NDWI vs K_c

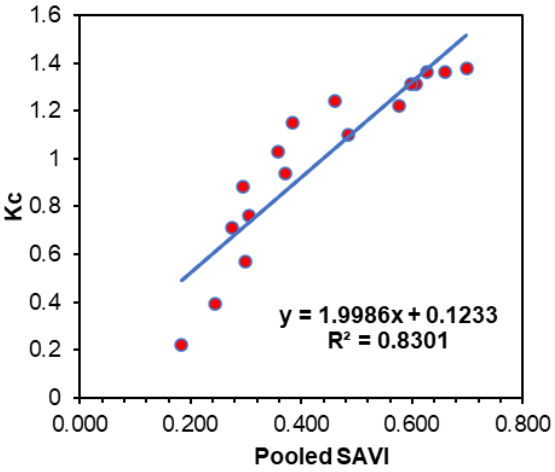

(c) Pooled SAVI vs K_c

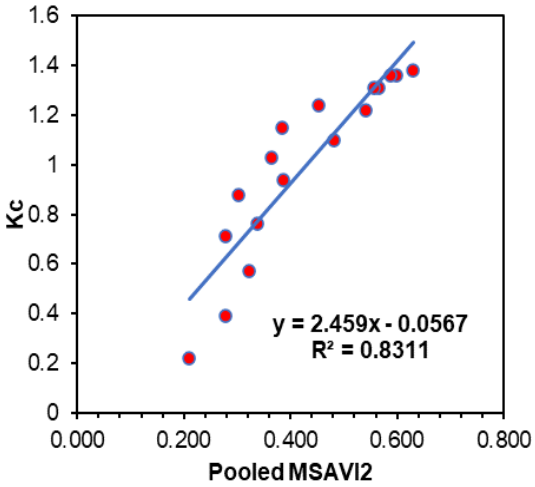

(d) Pooled MSAVI2 vs K_c

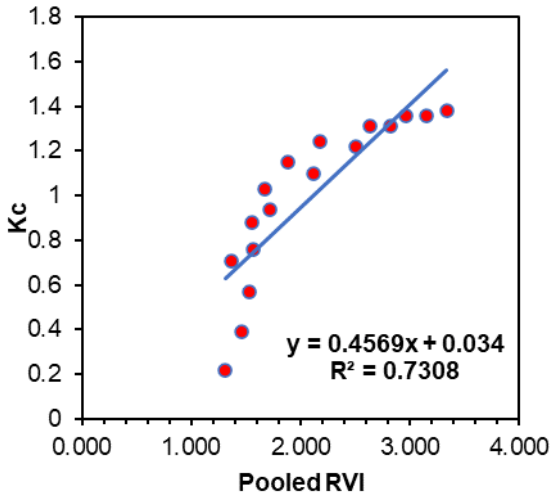

(e) Pooled RVI vs K_c

Fig. 78 (a, b, c, d and e) Relationship of crop coefficients with pooled vegetation indices of wheat.

All the models generated above were statistically evaluated by most frequently used statistical parameters such as R^2 (coefficient of determination), S.E (standard error), RMSE (root mean square error), PD (percent deviation) and Willmott index of agreement (D). The results of statistical analysis of wheat for year 2020-21 and 2021-22 are presented in Table 21 and Table 22. The statistical results of pooled VIs are presented in Table 23.

It is found that all the vegetation indices have reasonably good correlation with wheat crop coefficients with significantly high R^2 values. However, NDWI- K_c model show highest R^2 values 0.954 (2020-21), 0.937 (2021-22) and 0.962 (pooled VIs) followed by NDVI- K_c which have R^2 values 0.846 (2020-21), 0.849 (2021-22), 0.865 (pooled VIs). NDWI-Kc model showed lowest values of SE, RMSE and PD of 0.0796, 0.0748 and 3.14 for 2020-21, 0.0932, 0.0875 and 3.07 for 2021-22 and 0.0725, 0.0681 and 2.71 for pooled VIs respectively than the other models. NDWI- K_c model showed highest D value of 0.990 (2020-21), 0.986 (2021-22), 0.992 (pooled VIs).

SAVI-K_c model and MSAVI2-K_c model showed similar trends with higher R^2 and D value and lower values of SE, RMSE and PD for year 2020-21 and 2021-22. SAVI- K_c and MSAVI2-K_c model also showed similar trend for pooled VIs values which has higher R^2 and D values (R^2 =0.830, D = 0.960 for SAVI-K_c) (R^2 = 0.831, D = 0.960 for MSAVI2) and lower values of SE, RMSE and PD.

On the other hand, the RVI-$_c$ model showcased comparatively poor performance with an R^2 value of 0.703 for 2020-21, 0.731 for 2021-22 and 0.731 for pooled VIs, suggesting it is less accurate in forming linear relationships. This might be because RVI is just a simple ratio and doesn't entirely account for the greenness of vegetation.

The vegetation indices are the function of greenness and leaf area index. Wheat crop is mostly grown in irrigated conditions having dense population. As a result canopy always covers maximum surface of soil very fast after seed emergence. There soil background effect does not affect vegetation indices. NDWI measures water content of crop as well as soil.

Therefore, when crop is in development stage NDWI is maximum due to higher water content and decreases in maturity stage as water content of crop is reduced.

The findings were in agreement with similar studies by Pimpale *et al.* (2014) developed K_c and NDVI relationship for chickpea shows higher value of R^2 of 0.874, Gontia and Tiwari (2010) in TSMC command for comparison of NDVI and SAVI for wheat showed higher R^2 in case of SAVI., Farg *et al.* (2012) estimated relationship between crop coefficient with NDVI and SAVI for wheat and they found higher value of R^2 and lower values of RMSE, Ozcan *et al.* (2014) using NDVI and MSAVI for wheat, Pimpale *et al.* (2019) using RVI, SAVI, NDVI, TNDVI and MSAVI2 for sorghum. They found that NDVI-K_c model has the greatest R^2 and D values of 0.895 and 0.980. Most of the studies were observed to be utilizing NDVI to derive crop coefficients from remotely sensed data.

Table 21. Statistical analysis of VI-K_c prediction models of wheat crop for 2020-21

Regression	Intercept	Coefficient	S.E.	R^2	RMSE	PD	D
NDVI x K_c	-0.096	3.493	0.1456	0.846	0.1367	6.99	0.964
NDWI x K_c	0.493	3.061	0.0796	0.954	0.0748	3.14	0.990
SAVI x K_c	0.057	2.051	0.1620	0.809	0.1522	7.96	0.954
MSAVI2 x K_c	-0.139	2.512	0.1606	0.812	0.1522	7.66	0.955
RVI x K_c	0.095	0.408	0.2021	0.703	0.1522	12.83	0.923

Table 22. Statistical analysis of VI-K_c prediction models of wheat crop for 2021-22

Regression	Intercept	Coefficient	S.E.	R^2	RMSE	PD	D
NDVI x K_c	0.180	2.881	0.1441	0.849	0.1354	7.82	0.965
NDWI x K_c	0.372	4.229	0.0932	0.937	0.0875	3.07	0.986
SAVI x K_c	0.223	1.860	0.1609	0.811	0.1511	8.91	0.955
MSAVI2 x K_c	0.059	2.317	0.1611	0.817	0.1488	8.26	0.956
RVI x K_c	0.005	0.495	0.1922	0.731	0.1805	11.80	0.931

Table 23. Statistical analysis of VI-K_c prediction models of wheat crop for pooled VIs

Regression	Intercept	Coefficient	S.E.	R^2	RMSE	PD	D
NDVI x K_c	0.035	3.224	0.1360	0.865	0.1278	7.01	0.969
NDWI x K_c	0.433	3.608	0.0725	0.962	0.0681	2.71	0.992
SAVI x K_c	0.123	1.999	0.1528	0.830	0.1435	7.98	0.960
MSAVI2 x K_c	-0.057	2.459	0.1523	0.831	0.1430	7.57	0.960
RVI x K_c	0.034	0.457	0.1923	0.731	0.1806	12.03	0.932

4.7 Relationship between Crop Coefficients and VIs Onion

The relationship between crop coefficients and vegetation indices are derived for *rabi* onion for 2020-21 and 2021-22. The average weekly values of vegetation indices i.e. NDVI, NDWI, SAVI, MSAVI2 and RVI for *rabi* onion as shown in Table 15 (2020-21) and Table 16 (2021-22) were plotted against weekly crop coefficients (K_c) recommended by MPKV Rahuri (mentioned in 3.14, Table 9). Also pooled weekly VIs values (Table 17) were plotted against weekly crop coefficient recommended by MPKV Rahuri. The relationship between the vegetation indices and crop coefficients was investigated using simple linear regression analysis and a strong linear relation was identified. The correlation between the recommended weekly crop coefficients for the *rabi* onion crop and the vegetation indices namely, NDVI, NDWI, SAVI, MSAVI2 and RVI are depicted in Figures 79a-79e for year 2020-21, Figures 80a-80e for year 2021-22 and Figures 81a-81e for pooled VIs. From the regression analysis linear prediction models for *rabi* onion crop coefficients in terms of VI are obtained for year 2020-21 and 2021-22 and also for pooled weekly VI values. These prediction models are:

Prediction Model of onion for year 2020-21:

K_c = 2.201 NDVI + 0.319 R^2 = 0.876 ----------47

K_c = 2.500 NDWI + 0.635 R^2 = 0.909 ----------48

K_c = 1.474 SAVI + 0.326 R^2 = 0.850 ----------49

K_c = 1.737 MSAVI2 + 0.198 R^2 = 0.805 ----------50

K_c = 0.511 RVI - 0.025 R^2 = 0.769 ----------51

Prediction Model of onion for year 2021-22:

K_c = 5.166 NDVI - 0.130 R^2 = 0.849 ----------52

K_c = 4.221 NDWI + 0.574 R^2 = 0.937 ----------53

K_c = 3.377 SAVI - 0.092 R^2 = 0.811 ----------54

K_c = 3.486 MSAVI2 - 0.231 R^2 = 0.817 ----------55

K_c = 2.052 RVI - 2.257 R^2 = 0.731 ----------56

Prediction model of onion for pooled VIs

K_c = 3.141 NDVI + 0.172 R^2 = 0.873 ----------57

K_c = 3.231 NDWI + 0.603 R^2 = 0.920 ----------58

K_c = 2.111 SAVI + 0.178 R^2 = 0.873 ----------59

K_c = 2.376 MSAVI2 - 0.034 R^2 = 0.822 ----------60

K_c = 0.835 RVI - 0.500 R^2 = 0.788 ----------61

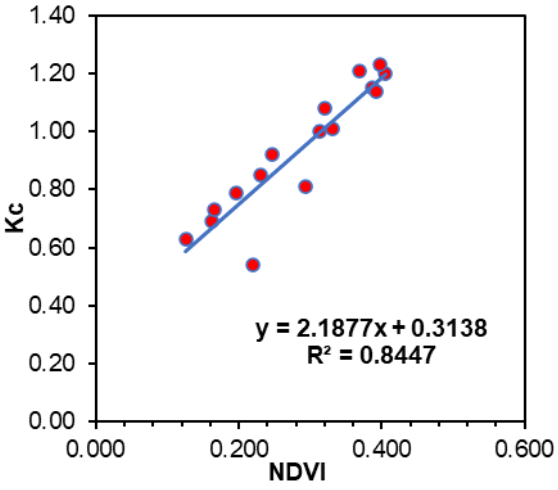

(a) NDVI vs K_c

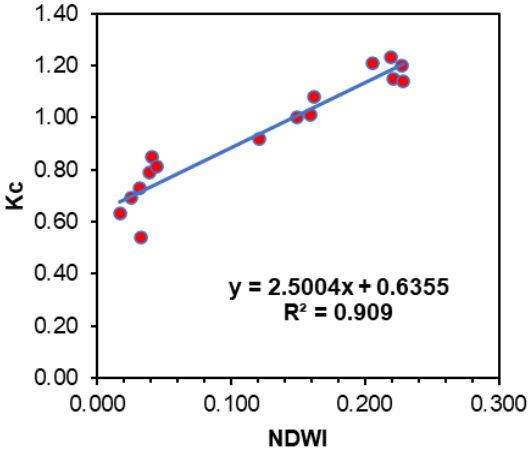

(b) NDWI vs K_c

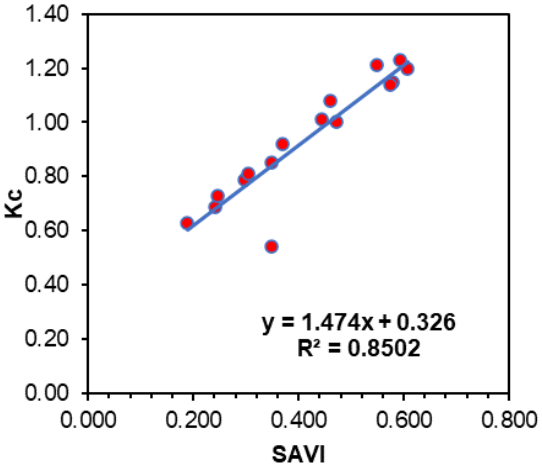

(c) SAVI vs K_c

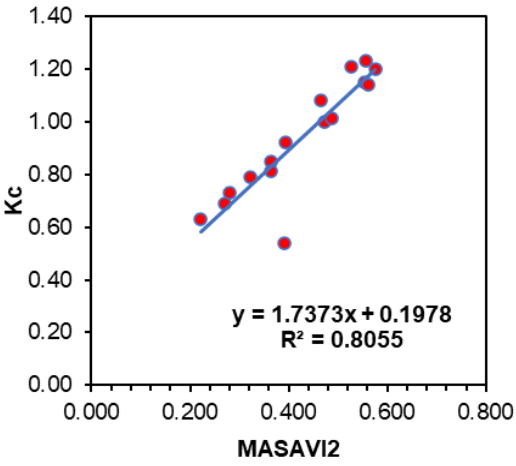

(d) MSAVI2 vs K_c

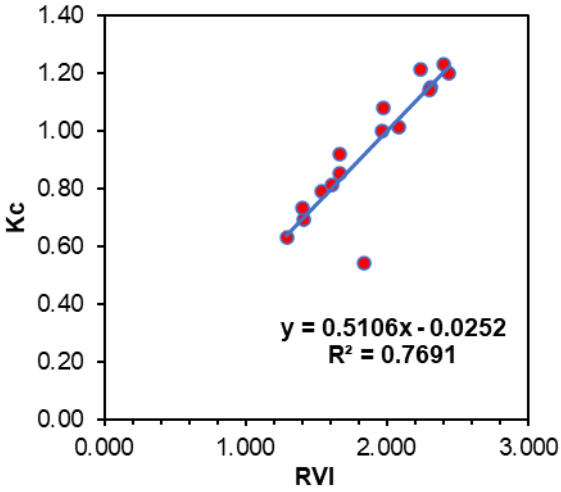

(e) RVI vs K_c

Fig. 79 (a-e) Relationship of crop coefficients with vegetation indices of onion for year 2020-21

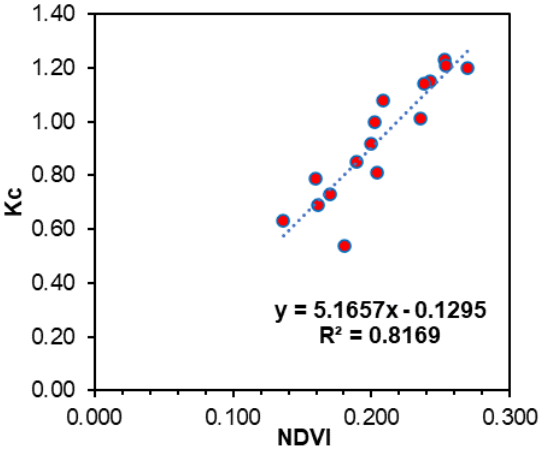

(a) NDVI vs K_c

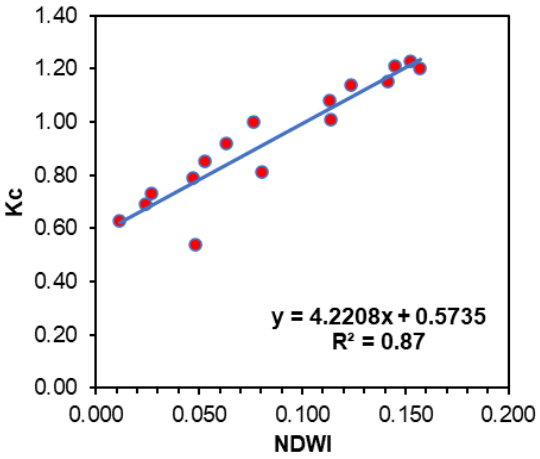

(b) NDWI vs K_c

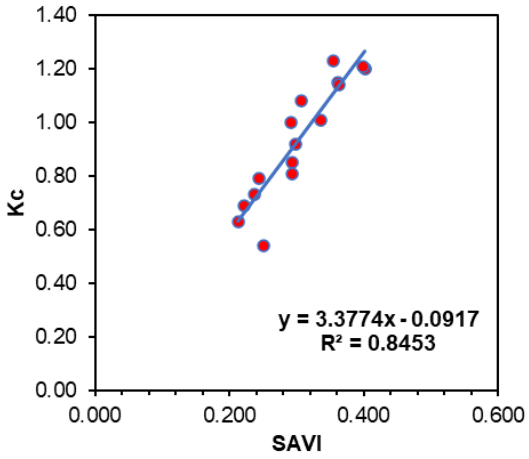

(c) SAVI vs K_c

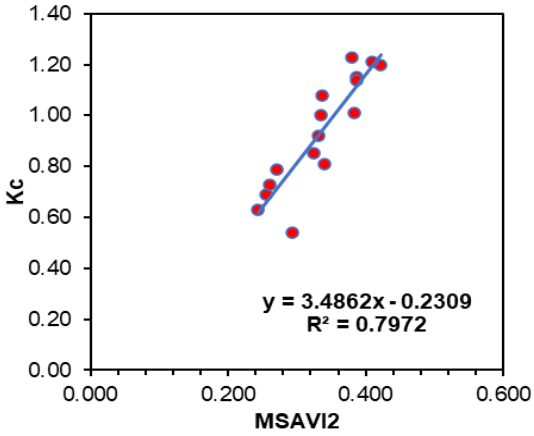

(d) MSAVI2 vs K_c

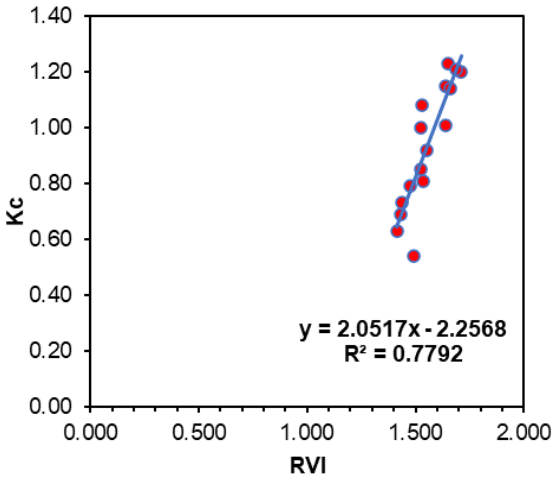

(e) RVI vs K_c

Fig. 80 (a-e) Relationship of crop coefficients with vegetation indices of onion for year 2021-22

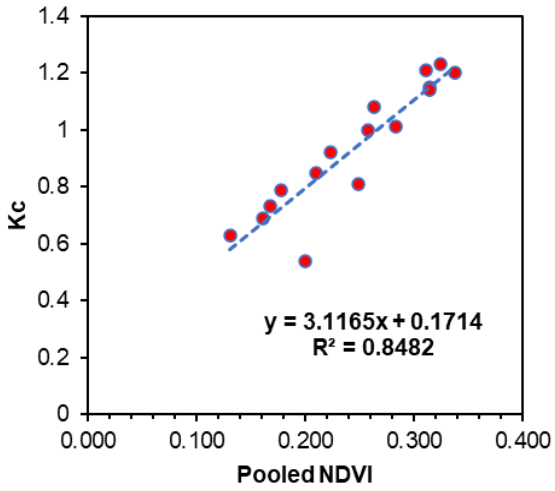

(a) Pooled NDVI vs K_c

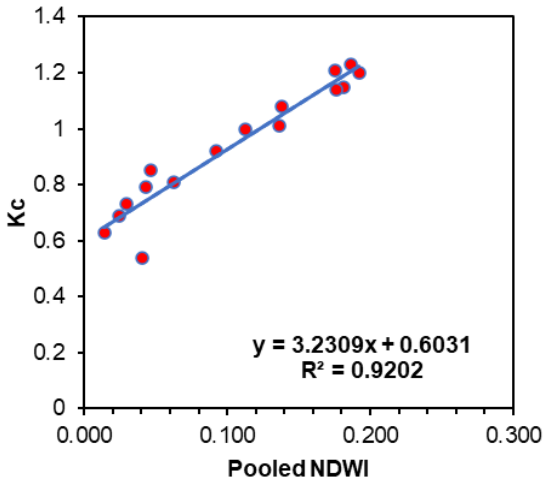

(b) Pooled NDWI vs K_c

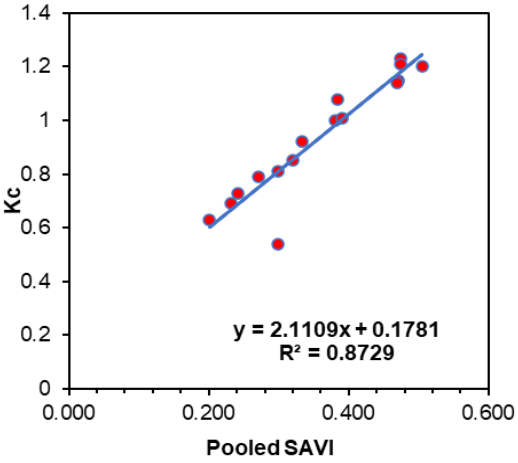

(c) Pooled SAVI vs K_c

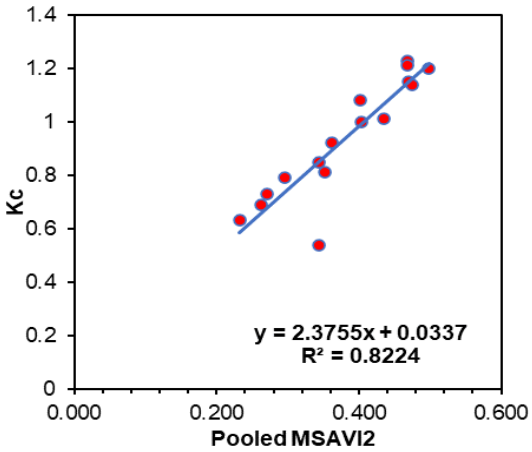

(d) Pooled MSAVI2 vs K_c

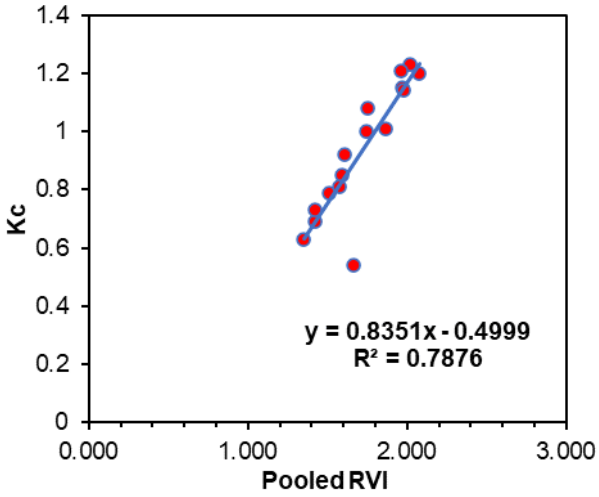

(e) Pooled RVI vs K_c

Fig. 81 (a-e) Relationship of crop coefficients with pooled vegetation indices of onion.

Models generated above are statistically analyzed by most frequently used statistical parameters such as coefficient of determination (R^2), standard error (SE), root mean square error (RMSE), percent deviation (PD) and Willmott index of agreement (D). The outcomes of statistical analysis are presented in Table 24 for year 2020-21, Table 25 for year 2021-22 and Table 26 for pooled VIs of *rabi* onion.

Each vegetation index have been found to have a strong correlation with recommended crop coefficients of *rabi* onion with high R^2 values. However, NDWI-K_c model showed highest R^2 and D values 0.909 and 0.979 for year 2020-21, 0.870 and 0.970 for year 2021-22 and 0.920 and 0.982 for pooled VIs followed by SAVI-K_c which have R^2 and D values 0.850 and 0.964 for 2020-21, 0.845 and 0.963 for 2021-22 and 0.873 and 0.970 for pooled VIs. NDWI-K_c model showed lower values of SE, RMSE and PD of 0.0697, 0.0652 and 0.85 (2020-21), 0.0833, 0.0779 and 1.14 (2021-22) and 0.0652, 0.0610 and 0.81 (pooled VIs) respectively than the other models. SAVI-K_c model also showed lowest values of SE, RMSE and PD of 0.0894, 0.0836 and 1.33 (2020-21), 0.0909, 0.0850 and 1.21 (2021-22) and 0.0823, 0.0770 and 1.15 (pooled VIs).

NDVI-K_c model and MSAVI2-K_c model showed similar trends with higher R^2 and D value and lower values of SE, RMSE and PD for year 2020-21 and 2021-22. NDVI-K_c and MSAVI2-K_c model also showed similar trend for pooled VIs values which has higher R^2 and D values (R^2 =0.848, D = 0.964 for pooled NDVI-K_c) (R^2 = 0.822, D = 0.957 for pooled MSAVI2) and lower values of SE, RMSE and PD.

On the other hand, the RVI-K_c model show comparatively poor performance with an R^2 and D value of 0.769 and 0.943 for 2020-21, 0.779 and 0.945 for 2021-22 and 0.788 and 0.948 for pooled VIs, suggesting it is less accurate in forming linear relationships. This might be because RVI is just a simple ratio and doesn't entirely account for the greenness of vegetation.

The results obtained were in agreement with similar studies conducted by Pimpale *et al.* (2014) found that there exists a good linear relationship between K_c and NDVI with a R^2 value of 0.874 for chickpea

crop. Pimpale *et al.* (2019) found that MSAVI2 has highly superior for its linear correlation with crop coefficient with highest R^2 and D values of 0.805 and 0.943 respectively for sorghum crop. However, exactly similar studies related to onion were not observed in the literature survey.

Table 24. Statistical analysis of VI-K_c prediction models of *rabi* onion crop for 2020-21

Regression	Intercept	Coefficient	S.E	R^2	RMSE	PD	D
NDVI x K_c	0.314	2.188	0.0910	0.845	0.0852	1.22	0.963
NDWI x K_c	0.635	2.500	0.0697	0.909	0.0652	0.85	0.979
SAVI x K_c	0.326	1.474	0.0894	0.850	0.0836	1.33	0.964
MSAVI2 x K_c	0.198	1.737	0.1019	0.806	0.0953	1.57	0.953
RVI x K_c	-0.025	0.511	0.1110	0.769	0.1038	1.93	0.943

Table 25. Statistical analysis of VI-K_c prediction models of *rabi* onion crop for 2021-22

Regression	Intercept	Coefficient	S.E	R^2	RMSE	PD	D
NDVI x K_c	-0.130	5.166	0.0989	0.817	0.0925	1.43	0.956
NDWI x K_c	0.574	4.221	0.0833	0.870	0.0779	1.14	0.970
SAVI x K_c	-0.092	3.377	0.0909	0.845	0.0850	1.21	0.963
MSAVI2 x K_c	-0.231	3.486	0.1040	0.797	0.0973	1.47	0.950
RVI x K_c	-2.257	2.052	0.1086	0.779	0.1015	1.66	0.945

Table 26. Statistical analysis of VI-K_c prediction models of *rabi* onion crop for pooled VIs

Regression	Intercept	Coefficient	S.E	R^2	RMSE	PD	D
NDVI x K_c	0.171	3.117	0.0900	0.848	0.0842	1.21	0.964
NDWI x K_c	0.603	3.231	0.0652	0.920	0.0610	0.81	0.982
SAVI x K_c	0.178	2.111	0.0823	0.873	0.0770	1.15	0.970
MSAVI2 x K_c	0.034	2.376	0.0974	0.822	0.0911	1.42	0.957
RVI x K_c	-0.500	0.835	0.1065	0.788	0.0996	1.78	0.948

4.8 Utilization of Developed Relationship for Near Real Time Irrigation Water Management.

The reference crop evapotranspiration (ET_o) of Dhule, Jalgaon and Nashik district were calculated for two consecutive years 2020-21 and 2021-22 by using FAO Penman Monteith method by using meteorological data collected from NASA power website and are presented in Table 27 (2020-21) and Table 28 (2021-22). As discussed in 4.6 and 4.7, NDWI and crop coefficient recommended by MPKV Rahuri has strong correlation for *rabi* wheat and as well as onion for both year 2020-21 and 2021-22. Weekly crop coefficients (K_c) were obtained by utilizing these best fit linear regression equations.

The crop evapotranspiration (ET_c) of wheat was estimated by multiplying the reference evapotranspiration (ET_o) by K_{cs} obtained by NDWI-K_c model and shown in Table 29 for 2020-21 and Table 30 for 2021-22 respectively. Estimated total crop evapotranspiration of wheat for Dhule was 449.65 mm (2020-21) and 431.62 mm (2021-22). For Jalgaon total wheat crop evapotranspiration was 440.92 mm for 2020-21 and 398.43 mm for 2021-22. Total crop evapotranspiration of wheat for Nashik was 429.16 mm (2020-21) and 395.97 mm (2021-22) respectively.

The crop evapotranspiration of *rabi* onion was estimated by multiplication of ET_o and by K_{cs} obtained by NDWI-K_c model as shown in Table 31 (2020-21) and Table 32 (2021-22) respectively. The total crop evapotranspiration of onion for Dhule, Jalgaon and Nashik for year 2020-21 was found as 486.52 mm, 482.77 mm and 488.79 mm respectively. For year 2021-22, Total crop evapotranspiration of Dhule, Jalgaon and Nashik was found as 493.74 mm, 473.91 mm and 477.29 mm respectively. The difference in ET_c of wheat and onion crop for both year at different places is because of variation in reference evapotranspiration which depends on condition of weather and physiology of the area.

Finally water demand for wheat and onion in each week for each district for year 2020-21 and 2021-22 was estimated by multiplying crop coverage obtained as per section 4.5 by corresponding crop evapotranspiration (ET_c) of the week. (Calculations are given in Annexure IV for wheat and Annexure V for onion). The resulted water demand for

wheat is shown in Table 33 (2020-21) and Table 34 (2021-22). Also, the resulted water demand for *rabi* onion is shown in Table 35 for year 2020-21 and Table 36 for year 2021-22 respectively.

For year 2020-21, water demand of wheat for Dhule, Jalgaon and Nashik district was observed as 177.60 Mm^3, 266.59 Mm^3 and 230.30 Mm^3 respectively. Water demand of wheat for year 2021-22 for Dhule, Jalgaon and Nashik was found as 170.91 Mm^3, 224.45 Mm^3 and 204.48 Mm^3 respectively.

Water demand of *rabi* onion for Dhule, Jalgaon and Nashik for year 2020-21 was estimated as 70.54 Mm^3, 43.80 Mm^3 and 693.23 Mm^3 respectively and for year 2021-22, water demand was found as 128.16 Mm^3, 33.94 Mm^3 and 825.76 Mm^3 respectively. Highest water demand for *rabi* onion was found in Nashik district due to highest acreage of onion cultivation.

The similar findings were found using remote sensing technique for calculating water requirement of crops given by Pimpale *et al.* (2015) estimated water requirement of wheat using multispectral vegetation indices for five wheat-growing districts in central Maharashtra. They observed that ET_c of wheat was found varying from 378.34 mm to 439.10 mm in the study area. Kivrak *et al.* (2019) quantified water uses by Onion crop in the Mesilla Valley, New Mexico by using plant phenology and Landsat-8 satellite data. Water demand estimated a maximum ET of 973 mm in 2015 and 975 mm in 2016.

Table 27. Reference evapotranspiration (ET_o, mm) of various districts of study area in *rabi* season of 2020-21

Met. Week	Reference evapotranspiration (ET_o) (mm)		
	Dhule	Jalgaon	Nashik
45	3.56	3.29	3.51
46	3.47	3.25	3.16
47	3.31	3.16	3.07
48	3.48	3.31	3.22
49	3.86	3.64	3.65
50	2.49	2.42	2.27
51	3.46	3.31	3.42
52	3.59	3.44	3.37
1	3.21	3.25	2.57
2	3.64	3.49	3.21
3	4.08	4.30	3.90
4	4.21	4.33	4.54
5	4.91	5.12	4.76
6	4.95	5.00	5.42
7	4.82	4.77	4.72
8	5.34	5.24	5.44
9	6.45	6.22	6.28
10	5.72	5.49	6.32
11	5.87	5.82	6.46
12	5.82	5.92	6.23

Table 28. Reference evapotranspiration (ET_o, mm) of various districts of study area in *rabi* season of 2021-22

Met Weeks	Reference evapotranspiration (ET_o) (mm)		
	Dhule	Jalgaon	Nashik
45	3.53	3.17	3.11
46	3.31	2.92	2.95
47	3.08	2.84	2.75
48	3.00	2.73	2.71
49	2.74	2.53	2.49
50	3.04	2.85	2.61
51	3.18	2.95	2.97
52	3.17	2.82	3.06
1	3.37	3.06	2.90
2	3.55	3.07	2.81
3	4.13	3.67	3.61
4	4.20	3.84	3.77
5	4.77	4.50	4.44
6	4.73	4.67	4.81
7	4.79	4.82	4.94
8	5.51	5.35	5.75
9	5.50	5.55	6.08
10	5.39	5.64	5.46
11	7.39	7.27	7.44
12	7.94	7.45	7.03

Table 29. Crop evapotranspiration (ET_c, mm) for wheat of 2020-21

Weeks Past Sowing	Crop evapotranspiration (ET_c) (mm)		
	Dhule	Jalgaon	Nashik
1	21.20	19.61	20.89
2	21.50	20.11	19.59
3	21.17	20.23	19.64
4	26.58	25.23	24.55
5	32.79	30.89	31.02
6	22.97	22.28	20.91
7	33.69	32.23	33.31
8	35.44	33.89	33.26
9	30.53	30.96	24.44
10	34.87	33.35	30.75
11	35.46	37.31	33.89
12	32.47	33.43	35.05
13	28.14	29.36	27.27
14	23.31	23.58	25.52
15	16.53	16.36	16.19
16	16.64	16.32	16.95
17	16.36	15.77	15.93
Total	**449.65**	**440.92**	**429.16**

Table 30. Crop evapotranspiration (ET_c, mm) for wheat of 2021-22

Weeks past Sowing	Crop evapotranspiration (ET_c) (mm)		
	Dhule	Jalgaon	Nashik
1	16.89	15.18	14.88
2	18.18	16.08	16.24
3	22.15	20.37	19.75
4	22.01	20.06	19.93
5	21.57	19.92	19.62
6	28.50	26.74	24.45
7	30.93	28.67	28.89
8	31.42	27.99	30.35
9	31.89	28.88	27.38
10	32.72	28.37	25.89
11	37.50	33.37	32.85
12	35.12	32.18	31.57
13	25.66	24.20	23.89
14	22.02	21.75	22.42
15	22.60	22.74	23.29
16	20.89	20.30	21.79
17	11.55	11.64	12.76
Total	**431.62**	**398.43**	**395.97**

Table 31. Crop evapotranspiration (ET_c, mm) for *rabi* onion of 2020-21

Weeks past Transplanting	Crop evapotranspiration (ET_c), mm		
	Dhule	Jalgaon	Nashik
1	18.24	17.18	17.25
2	12.16	11.80	11.07
3	17.24	16.50	17.05
4	18.38	17.57	17.25
5	16.53	16.76	13.23
6	23.87	22.83	21.05
7	28.79	30.30	27.52
8	30.58	31.48	33.00
9	40.74	42.52	39.49
10	41.63	42.11	45.58
11	39.93	39.51	39.09
12	42.95	42.12	43.75
13	54.44	52.47	53.01
14	41.30	39.67	45.60
15	30.58	30.33	33.65
16	29.16	29.63	31.19
Total	**486.52**	**482.77**	**488.79**

Table 32. Crop evapotranspiration (ET_c, mm) for *rabi* onion of 2021-22

Weeks past Transplanting	Crop evapotranspiration (ET_c) (mm)		
	Dhule	Jalgaon	Nashik
1	11.91	11.00	10.84
2	14.36	13.47	12.31
3	15.29	14.17	14.28
4	17.11	15.24	16.53
5	18.78	17.00	16.13
6	20.82	18.05	16.47
7	25.86	23.00	22.65
8	30.89	28.31	27.77
9	39.03	36.81	36.35
10	40.89	40.39	41.63
11	40.78	41.03	42.04
12	45.68	44.38	47.64
13	42.19	42.52	46.61
14	39.75	41.55	40.26
15	47.18	46.44	47.51
16	43.22	40.54	38.27
Total	**493.74**	**473.91**	**477.29**

Table 33. Crop Water demand (m^3) in various districts of study area for *wheat* of 2020-21

Weeks past Sowing	Water Demand of wheat (m^3) (2020-21)		
	Dhule	**Jalgaon**	**Nashik**
1	9411349.6	13323597.1	12658945.4
2	9545162.4	13662904.1	11868176.3
3	9398179.7	13738860.2	11902481.3
4	11796309.7	17139792.7	14876106.2
5	14554936.7	20981856.8	18793371.5
6	10194788.3	15136088.6	12672263.9
7	14954701.5	21894586.3	20181842.6
8	15729183.6	23020173.2	20150619.4
9	13549232.3	21027119.5	14806544.0
10	15475613.6	22651880.0	18633383.5
11	15738619.0	25345285.6	20534374.3
12	14412040.5	22706591.6	21234902.1
13	12489094.0	19944398.3	16522960.6
14	10348247.0	16016712.8	15464932.7
15	-	-	-
16	-	-	-
17	-	-	-
Total (m^3)	**177597458**	**266589847**	**230300904**
Mm^3	**177.60**	**266.59**	**230.30**

***Mm^3 –** Million Cubic Meters

*Since water is needed only up to physiological maturity, water demand calculations are done only up to 14^{th} week

Table 34. Crop Water demand (m^3) in various districts of study area for *wheat* of 2021-22

Weeks Past Sowing	Water demand of wheat (m^3) (2021-22)		
	Dhule	**Jalgaon**	**Nashik**
1	7666535.2	9909359.2	8999503.6
2	8251719.5	10502455.1	9818622.2
3	10053511.9	13301248.4	11943699.5
4	9990232.1	13098545.6	12051220.8
5	9790055.8	13005553.1	11865263.0
6	12936361.2	17462706.8	14787134.3
7	14038800.8	18720916.1	17473051.2
8	14261815.7	18274920.9	18356758.4
9	14472112.0	18854989.3	16559361.1
10	14849799.1	18523792.4	15658996.5
11	17019644.0	21786091.4	19864714.2
12	15939582.0	21014927.6	19092445.8
13	11643550.4	15798333.1	14446857.0
14	9994750.1	14200705.1	13558755.4
15	-	-	-
16	-	-	-
17	-	-	-
Total (m^3)	170908470	224454544	204476383
Mm^3	**170.91**	**224.45**	**204.48**

***Mm^3-** Million Cubic Meters

*Since water is needed only up to physiological maturity, water demand calculations are done only up to 14^{th} week

Table 35. Crop Water demand (m^3) in various districts of study area for *rabi* onion of 2020-21

Weeks past Transplanting	Water demand of onion (m^3) (2020-21)		
	Dhule	**Jalgaon**	**Nashik**
1	3014882.4	1779829.9	28211358
2	2010196.2	1222217.3	18108133
3	2849983.5	1708739.5	27873060
4	3037614.7	1820579.4	28201625
5	2732098	1736344.5	21636874
6	3945120.3	2364782.2	34424159
7	4758918.3	3138436.4	44996873
8	5053924.3	3260841.9	53965072
9	6734525.6	4404245.7	64568869
10	6881813.7	4361983.7	74532106
11	6599444	4092883	63912959
12	7098548.6	4363206.1	71544267
13	8998751.4	5435520.3	86682316
14	6826123.8	4109664.7	74570387
15	-	-	-
16	-	-	-
Total (m^3)	70541945	43799275	693228061
Mm^3	**70.54**	**43.80**	**693.23**

***Mm^3-** Million Cubic Meters

Since water is needed only up to physiological maturity, water demand calculations are done only up to 14^{th} week

Table 36. Crop Water demand (m^3) in various districts of study area for *rabi* onion of 2021-22

Weeks past Transplanting	Water demand of onion (m^3) (2021-22)		
	Dhule	**Jalgaon**	**Nashik**
1	3786014.0	964960.5	22857521.7
2	4561503.9	1181384.1	25973750.3
3	4857527.0	1242784.9	30116790.8
4	5438260.1	1336978.1	34868709.1
5	5966885.5	1491508.5	34010584.4
6	6614590.9	1583054.9	34745700.0
7	8215855.2	2017740.3	47768252.4
8	9816610.2	2483111.2	58573464.0
9	12403539.1	3228903.8	76663438.0
10	12994190.2	3542181.7	87811588.3
11	12958838.5	3598855.9	88662033.9
12	14515027.5	3892437.4	100485721.7
13	13405884.7	3729532.7	98312514.9
14	12629369.6	3644173.1	84912390.9
15	-	-	-
16	-	-	-
Total (m^3)	128164096.5	33937607.16	825762460.3
Mm^3	**128.16**	**33.94**	**825.76**

***Mm^3-** Million Cubic Meters

*Since water is needed only up to physiological maturity, water demand calculations are done only up to 14^{th} week

CHAPTER V

SUMMARY AND CONCLUSIONS

In the current scenario of climate change leading to water shortage, precision irrigation water management is critical for obtaining improved water use efficiency. This necessitates an upgrade in current irrigation scheduling systems based on crop irrigation water requirements. FAO-56 guidelines for calculating crop water requirements have been accepted worldwide. In this method crop water requirements are calculated using reference evapotranspiration and crop coefficients. The tabular crop coefficients utilized in this technique are time-based and lack spatial variability. Remote sensing-based multispectral vegetation indices (VIs) exhibit the same pattern as crop coefficients (K_c) and can thus be utilized as proxy crop coefficients, resulting in spatial values that can lead to accurate irrigation water management. Therefore, present investigation entitled “Irrigation water management using multispectral vegetation indices” was undertaken in order to study spectral behavior of *rabi* wheat and onion crops, calculating acreages, establishing the relationship between crop coefficients recommended by MPKV, Rahuri and vegetation indices and identifying best performing VI-K_c relation and utilization of the best model for water demand calculations.

The study was conducted in *rabi* wheat and onion growing three districts situated in region of North Maharashtra viz. Dhule, Jalgaon and Nashik for two consecutive year 2020-21 and 2021-22. The suitability of five most important vegetative indices (VIs) i.e. NDVI, NDWI, SAVI, MSAVI2 and RVI, to develop a relationship with crop coefficients of the crops under investigation was evaluated. These VIs were generated by digital processing on multidate Sentinel 2A images and values were arranged according to the age of the crops in weeks. A hybrid classification method based on K-means clustering and visual analysis was used for the identification and acreage estimation of *rabi* wheat and onion crop for year 2020-21 and 2021-22. Reference evapotranspiration (ET_o) for *rabi* reason of 2020-21 and 2021-22 was estimated by FAO Penman Monteith method.

Real-time crop water requirements were calculated using the FAO-recommended equation $ET_c = ET_o \times K_c$ and crop water demands were computed.

The following paragraphs outline the principal outcomes and conclusions of the current investigation.

According to the analysis of spectral profiles of wheat (NDVI, NDWI, SAVI, MSAVI2 and RVI) for *rabi* season of 2020-21 and 2021-22, almost all vegetation indices follow the same pattern with lower values at the beginning of germination and tillering and peak values at the 7^{th} and 8^{th} week which coincides with the pollination to milk development stage. The VIs fluctuated within a constrained range throughout the era of maximum growth. After the 10^{th} or 11^{th} week, when leaf yellowing and senescence begin, the VIs begin to drop and at the end of the season they were comparatively lower than they had been at the beginning of the season. The trend of development of all the VIs is almost same to that of crop coefficients, according to the comparison of VIs with K_c during the growth period. VIs and K_c both follow the similar growth curve pattern for year 2020-21 and also for 2021-22 and these curves satisfies third order polynomial.

The observations of spectral profiles of *rabi* onion i.e NDVI, NDWI, SAVI, MSAVI2 and RVI exhibited similar trend of low values at the initial stages for both years 2020-21 and 2021-22. All of the VIs peaked between the 8^{th} and 10^{th} weeks of the midseason stage and then began to decline as the crop matured in the late-season stage. Additionally, it was discovered that all VIs exhibits a pattern that is very similar to that of crop coefficients and the stages of onion crop growth for both the years 2020-21 and 2021-22.

According to general observations for both crop wheat and onion for year 2020-21 and 2021-22, all VIs peak when the crop reaches full effective green cover and coincides with the highest K_c and then they all begin to decline as the crops mature and reach low values.

A hybrid technique based on K-means clustering and visual analysis was used for identifying wheat and onion crops and estimating their acreages revealed that the resulting acreages were quite similar to the real data provided by the Department of Agriculture, Government of Maharashtra with a per cent difference of 3.36 for year 2020-21 and 8.72 for year 2021-22 in case of wheat and 9.08 (2020-21) and 10.57 (2021-22) for onion crop. When findings are examined district-by-district, this variance for wheat varied from -4.50 to 10.01 per cent for year 2020-21 and 2.86 to 13.61 per cent for year 2021-22 whereas this variance for onion varied from 4.73 to 11.77 per cent and 10.57 to 14.38 per cent for year 2020-21 and 2021-22 respectively. These remote sensing estimates were acquired far earlier than those that the Department of Agriculture provided.

For wheat crop, among the five vegetation indices NDVI, NDWI, SAVI, MSAVI2 and RVI under study, NDWI was found highly superior for its linear correlation with crop coefficient with highest R^2 and D values of 0.954 and 0.990 (2020-21) and 0.937 and 0.986 (2021-22) with lowest values of SE, RMSE and PD of 0.0796, 0.0748 and 3.14 for year 2020-21 and 0.0932, 0.0875 and 3.07 for 2021-22. NDWI was also found highly superior for correlation with crop coefficient for pooled VIs with highest R^2 and D values of 0.962 and 0.992 with lowest values of SE, RMSE and PD values of 0.0725, 0.0681 and 2.71 respectively. Thus, the developed NDWI-K_c model for year 2020-21, K_c = 3.061 NDWI + 0.493 for year 2021-22, K_c = 4.229 NDWI + 0.372 was found superior among all the tested VIs. If we consider pooled week wise VI values pooled NDWI shows superiority and is given by K_c = 3.608 NDWI + 0.433. This NDWI-K_c model can be suggested (recommended) prediction of spatial crop coefficient for wheat.

For onion crop, among the five vegetation indices NDVI, NDWI, SAVI, MSAVI2 and RVI under study, NDWI was found superior for its correlation with crop coefficient with highest R^2 and D values of 0.909 and 0.979 for year 2020-21, 0.870 and 0.970 for year 2021-22 and 0.920 and 0.982 for pooled VIs. NDWI showed lower values of SE, RMSE and PD of 0.0697, 0.0652 and 0.85 (2020-21), 0.0833, 0.0779 and 1.14 (2021-22) and 0.0652, 0.0610 and 0.81 (pooled VIs) respectively. Thus the developed

NDWI-K_c model for year 2020-21, K_c = 2.500 NDWI + 0.635, for year 2021-22, K_c = 4.221 NDWI + 0.574 and for pooled VIs, K_c = 3.231 NDWI + 0.603 can be used for prediction of spatial crop coefficient of onion.

For both the years 2020-21 and 2021-22, week-wise crop coefficients (K_c) of wheat and onion were obtained by best performing prediction model i.e NDWI. Reference evapotranspiration (ET_o) of the stations was estimated by FAO Penman Monteith method for both years 2020-21 and 2021-22. The crop evapotranspiration (ET_c) was calculated by the product of ET_o and K_c estimated by NDWI-K_c model. The total crop evapotranspiration i.e water requirement of wheat for Dhule was 449.65 mm (2020-21) and 431.62 mm (2021-22). For Jalgaon total wheat crop evapotranspiration was 440.92 mm for 2020-21 and 398.43 mm for 2021-22. Total crop evapotranspiration of wheat for Nashik was 429.16 mm (2020-21) and 395.97 mm (2021-22) respectively. For the year 2020–21, the total crop evapotranspiration for onion in Dhule, Jalgaon and Nashik was determined to be 486.52 mm, 482.77 mm and 488.79 mm respectively. Total crop evapotranspiration for Dhule, Jalgaon and Nashik was determined to be 493.74 mm, 473.91 mm and 477.29 mm respectively, for the year 2021–2022.

The water demand for wheat and onion per week for each district in 2020-2021 and 2021-2022 was calculated by multiplying crop coverage. The water demand for wheat in the Dhule, Jalgaon and Nashik districts were 177.60 Mm^3, 266.59 Mm^3 and 230.30 Mm^3 correspondingly during the 2020–21 crop year. For the year 2021-2022, the water demands for wheat in Dhule, Jalgaon and Nashik were calculated to be 170.91 Mm^3, 224.45 Mm^3 and 204.48 Mm^3 respectively. Water demand of *rabi* onion for Dhule, Jalgaon and Nashik for year 2020-21 was estimated as 70.54 Mm^3, 43.80 Mm^3 and 693.23 Mm^3 respectively and for year 2021-22, water demand was found as 128.16 Mm^3, 33.94 Mm^3 and 825.76 Mm^3 respectively.

Conclusions:

The following conclusions are reached based on the findings of the investigation:

1) All of the vegetative indices (VIs) followed a similar trend to crop coefficients. On the other hand, temporal variations in VIs can be used to track phenological information. The defined VI patterns can be used to determine the likely date of planting. The pattern of VIs and K_c are similar, indicating that K_c may be calculated using vegetative indices for wheat and onion crops.
2) Acreage estimation of wheat and onion for *rabi* season of 2020-21 and 2021-22 was carried out by hybrid classification technique based on K-means clustering and compared with actual measurements done by Department of Agriculture, Government of Maharashtra. It was found per cent difference of 3.36 for year 2020-21 and 8.72 for year 2021-22 in case of wheat and 9.08 (2020-21) and 10.57 (2021-22) for onion crop. Hence, timely and precise estimates of crop acreages can be obtained by using Remote Sensing and GIS techniques.
3) The vegetation index, NDWI of wheat and onion crops was found to be highly superior to other VIs under study, for its linear correlation with crop coefficient for both years 2020-21 and 2021-22. Therefore, these developed VI-K_c relationships can be incorporated in the FAO-56 procedures in place of conventional tabulated K_c.
4) An integrated strategy utilising remote sensing and GIS may be used to provide the precise amount of irrigation water at various places in accordance with the actual crop water demand resulting in effective irrigation water management. This technique may also be applied in cases of water shortage to provide the ideal irrigation water as a lifesaving irrigation to avoid crop failure.
5) An expert system for precise irrigation scheduling may be created using real-time, high-resolution data from distant sensors and automated weather stations.

CHAPTER VI

LITERATURE CITED

Ahmad, F. 2012a. Spectral vegetation indices performance evaluated for Cholistan Desert. *J. Geog. and Reg. Planning*. 5(6): 165-172.

Ahmad, F. 2012b. A review of remote sensing data change detection: Comparison of Faisalabad and Multan Districts, Punjab Province. Pakistan *J. Geog. and Reg. Planning*. 5(9): 236-251

Ahmed, R. and H. Sajjad 2015. Crop acreage estimation of Boro Paddy using Remote Sensing and GIS Techniques: A Case from Nagaon district, Assam, India. *Advances in Appl. Agric. Sci.,* 3(3): 16-25

Ahmed, R. H. and C. M. U. Neale. 1997. A district irrigation management using airborne multi spectral video imagery. *Proc. 16th Biennial Workshop on Color Photo,* ASPRS, Bethesda. Maryland, USA: 167-178

Aich, S., S. K. Singh, S. Kanga and Sudhanshu. 2017. Wheat Acreage Area of Jalandhar District in Punjab and Health monitoring of crop growing stage. *Inter. J. of Advanced and Innov. Res*., 60(9)

Akkara, M. S. 2022. Estimation of evapotranspiration of chickpea using vegetation indices based crop coefficients. Department of Irrigation and Drainage Engineering, Dr. Panjabrao Deshmukh Krishi Vidyapeeth, Akola. M. Tech. 2022. Print. xiv, 113p. (Unpublished).

Allen, R. G., L. S. Pereira, O. Raes and M. Smith. 1998. Crop evapotranspiration Guidelines for computing crop water requirements. FAO Irrigation and Drainage paper 56. Food and Agriculture Organization of the United Nations: Rome, Italy.

Allen, R. G., M. E. Jensen, J. L. Wright and R. D. Burman. 1989. Operational estimates of evapotranspiration. *J. Agron.* 81:650-662.

Allen, R. G., M. Smith, L. S. Pereira and A. Perrier. 1994. An update for the calculation of reference evapotranspiration.

Allen, R. G., M. Smith, L. S. Pereira, D. Raes and J. L. Wright. 2000. Revised FAO Procedures for Calculating Evapotranspiration: Irrigation and Drainage Paper No. 56 for testing in Idaho. In *Proc. Watershed Management and Operations Management.* June 20-24, Fort Coll ins, CO.

Alvino, C. G. F., C. C. Aleman, R. Filgueiras, A. Daniel and F. C. Fernando. 2020. Vegetation Indices for Irrigated Corn Monitoring. *Engenharia Agrícola, Jaboticabal*, 40(3):322-333

Anonymous 2022. Agricultural land and Water statistics of India. India Water Portal, *https://www.indiawaterportal.org*

Anonymous. 2021. Crop statistics. Department of Agriculture, Maharashtra. Website- www.krishi.maharshtra.gov.in

Anonymous. 2022. Crop statistics. Department of Agriculture, Maharashtra. Website- www.krishi.maharshtra.gov.in

Anonymous. 2022. Meteorological data. NASA Power Data. Website- www.power.larc.nasa.gov.in

Arshad, A., A. Bakhsh, A. Azzam, S. Ali and M. Awais. 2018. Computing Spatio - Temporal Water Demand of Wheat Crop Using GIS and Remote Sensing - A Case Study of Faisalabad Irrigation District, Pakistan., *J. Agric. Res*., 3(6): 000178.

Ayyangar, R., P. P. N. Rao and K. R. Rao. 1980. Crop covers and crop phenological information from red and infrared spectral responses. *J. Indian Soc. of Remote Sens.,* 8: 23-29

Bandyopadhyay, P. K. and S. Mallick. 1993. Actual evapotranspiration and crop coefficients of wheat (*Triticum aestivum*) under varying moisture levels of humid tropical canal command area. *Agric. Water Manage.,* 59(1): 33-47

Barnes, E. M., K. A. Sudduth, J. W. Hummel, S. M. Lesch and D. L. Corwin. 2003. Remote and ground-based sensor techniques to map soil properties. *Photogramm. Eng. Remote Sens.*, 69: 619-630

Bausch, W. C. 1993. Soil background effects on reflectance-based crop coefficients for corn. *Remote Sens. Environ*., 46: 1-10

Bausch, W. C. and C. M. U. Neale. 1987. Crop coefficients derived from reflected canopy radiation: A concept. *Trans. ASAE*., 30(3): 703-709

Bhatt, C. K. and A. S. Nain. 2018. Rice Acreage estimation using Sentinel-1A dual Polarised SAR Data in Udham Singh Nagar (Uttarakhand). *Inter. J. of Current Microb. and Applied Sci.*, 7(4), 2319-7706

Blaney, H. F. and W. D. Criddle. 1950. Determining water requirements of irrigated areas from climatological and irrigation data. *USDA(SCS)TP*- 96: 48

Calera, B. A. and P. J. Gonzalez. 2007. Biophysical parameters of vegetation cover. Operational relations to obtain maps of these parameters of the satellite images. Albacete Spain: Remote Sensing and GIS Group, lOR, UCLM. PLEIADES Paper.

Chai, K. 2018. Detecting Rice Cropping Patterns with Sentinel-1 Multitemporal Imagery. Enschede, Netherland.

Choudhury, B. J., N. U. Amhed, R. J. Reginato and C. S. Daughtry. 1994. Relations between evaporation coefficients and vegetation indices studied by model simulations. *Remote Sens. Environ*., 50: 1-17

Csillik, O. and M. Belgiu. 2017. Cropland mapping from Sentinel-2 time series data using object-based image analysis. The 20th AGILE International Conference on Geographic Information Science: Societal Geo-innovation Celebrating 20 years of GIS research, 9-12.

Dadhwal, V. K. and J. S. Parihar. 1985. Estimation of 1983-84 wheat acreage of Karnal district (Haryana) using Landsat MSS digital data. Technical Note, IRS-UP/SAC/CPF/TN/09/85. Space Applications Centre, Ahmedabad, India.

Desai, K., U. K. Shanwad, N. L. Rajesh, B. G. Koppalkar and N. Ananda. 2018. Paddy (*Oryza sativa* L.) Crop Acreage estimation using Geo-spatial Technologies in Shorapur Taluk of Yadgir District. *Research Frontiers in Precision Agric*., 113-115.

Dimitrov, P., L. Filchev, E. Roumenina, G. Jelev. 2021. Crop Type Mapping in Bulgaria using Sentinel-1/2 Data. *Bulgarian Acad. of Sci.* Space Research and Technology Institute. Aerospace Research in Bulgaria., 40-50.

Dingre, S. K. and S. D. Gorantiwar. 2020. Determination of the water requirement and crop coefficient values of sugarcane by field water balance method in semiarid region. *Agric. Water Manage.,* 1-8

Doorenbos, J. and W. O. Pruitt. 1977. Crop water requirements. Irrigation and Drainage Paper No. 24, (rev.) FAO, Rome, Italy., pp. 144.

Dua, V. K., Sushma Panigrahy, R. L. Mehta, S. S. Lal, P. M. Govindakrishnan, J. P. Singh, R. K. Arora, M. Kumar, P. Kumar, S. Rawat, N. Bhatt and I. Ahmad. 2007. Estimation of potato acreage in the Indo-Gangetic region using IRS AWiFS data. *J. Potato*., 34 (1-2): 123-124.

Duchemin, B., R. Hadria, S. Er-Raki, G. Boulet, P. Maisongrande, A. Chehbouni, R. Escadafal, J. Ezzahar, J. C. B. Hoedjes, M. H. Kharrou, S. Khabba, B. Mougenot, A. Olioso, J. C. Rodriguez and V. Simmoneaux. 2006. Monitoring wheat phenology and irrigation in central Morocco: On the use of relationships between evapotranspiration, crop coefficients, leaf area index and remotely-sensed vegetation indices. *Agric. Water Manage*., 79: 1-27.

Er-Raki, S., A. Chehbouni and B. Duchemin. 2010. Combining satellite remote sensing data with the FAO-56 Dual approach for water use mapping in irrigated wheat fields of a semi-arid region. *Remote Sens*., 2(1): 375-387

Er-Raki, S., A. Chehbouni, N. Guemouria, B. Duchemin, J. Ezzahar and R. Hadria. 2007. Combining FAO-56 and ground-based remote sensing to estimate water consumptions of wheat crops in a semi-arid region. *Agric. Water Manage*., 87: 41-54

Farg, E., S. M. Arafat, M. S. Abd EI-Wahed and A. M. EL-Gindy. 2012. Estimation of evapotranspiration ET_c and crop coefficient K_c of

wheat, in south Nile delta of Egypt using integrated FAO-56 approach and remote sensing data. *The Egyptian J. of Remote Sens. and Space Sci.*, 15(1): 83-89

Fathizad, H., B. Azad, A. Yousefi and A. Jafarian. 2016. Using Remote sensing technique for estimation of real evapotranspiration. *Inter. J. of Engg. and Advanced Res. Tech. (IJEART),* 3(2): 51-57

Gandharum, L., M. E. Mulyani, D. M. Hartono, A. Karsidi and M. Ahmad 2020. Remote sensing versus the area sampling frame method in paddy rice acreage estimation in Indramayu regency, West Java province, Indonesia. *Inter. J. of Remote Sens..,* 42(5): 1738–1767

Gao, B. C. 1996. NDWI- A normalized difference water index for remote sensing of vegetation liquid water from space. *Remote Sens. of Environ*. 58(3): 257–266.

Gitelson, A. A., Y. J. Kaufman and M. N. Merzlyak. 1996. Use of a green channel in remote sensing of global vegetation from EOSMODIS. *Remote Sens. of Environ.*, 58: 289-298

Glenn, E. P, A. R. Huete, P. L. Nagler and S. G. Nelson. 2008. Relationship between remotely-sensed vegetation indices, canopy attributes and plant physiological processes: What vegetation indices can and cannot tell us about the landscape. *Sensors*, 8: 2136-2160

Gontia, N. K. and K. N. Tiwari. 2010. Estimation of crop coefficient and evapotranspiration of wheat (*Triticuum aerstivum*) in a irrigation command using remote sensing and GIS. *Water Res. Manag.* 24:1399- 1414

Goswami, S. B., Aruna Saxena and G. O. Bairagi. 2012. Remote sensing and GIS based wheat crop acreage estimation of Indore district of M.P. *Inter. J. of emerging Tech. and Advance Engg.* 2(3):200-203

Goswami, S. B., G.D. Bairagi, C. K. Sarat and S.K. Sharma. 2016. Evaluation of LISS-III And AWiFS Sensor data for Wheat Acreage estimation., *Proc. of SPIE* Vol. 9880: 1-10

Guruge, P. A. P. 1996. The use of remote sensing data for identifying development of sugarcane in Buttala area. *Proc. of XVII Asia Conference on Remote Sensing*, November 4-8, 1996, Sri Lanka <http:/ www.gisdevelopment.neUacrs/dated 04.08.2013>

Hassan, D. F., A. J. Abdalkadhum, R. J. Mohammed and A. Shaban. 2022. Integration remote sensing and meteorological data to monitoring plant phenology and estimation crop coefficient and evapotranspiration. *J. of Eco. Engg.*, 23(4).

Howell, T. A., S. R. Evett, J. A. Tolk, K. S. Copeland, D. A. Dusek and P. D. Colaizzi. 2006. Crop coefficients developed at Bushland, Texas for corn, wheat, sorghum, soybean, cotton and alfalfa. *In Proc. World Water and Environmental Resources Congress. Examining the*

Confluence of Environmental and Water Concerns, May 21-25, Omaha, Nebraska

Hudait, M. and P. P. Patel. 2022. Crop-type mapping and acreage estimation in smallholding plots using Sentinel-2 images and machine learning algorithms: Some comparisons. *The Egyptian J. of Remote Sens. and Space Sci.*, 25(1): 147-156.

Huete, A. R. 1988. A soil adjusted vegetation index (SAVI). *J. Remote Sens. Environ*., 25: 295-309

Hunsaker, D. J., P. J. Pinter and B. A. Kimball. 2005. Wheat basal crop coefficients determined by normalized difference vegetation index *J. Irrig. Sci*., 24: 1-14

Hunsaker, D. J., P. J. Pinter, E. M. Barnes and B. A. Kimball. 2003. Estimating cotton evapotranspiration crop coefficients with a multispectral vegetation index. *J. lrrig. Sci*., 22: 95-104

Jackson, R. D., S. B. ldso, R. J. Reginato and P. J. Pinter. 1980. Remotely sensed crop temperatures and reflectances as inputs to irrigation scheduling. In: Irrigation and drainage special conference proceedings, 23-25 July, Boise, Idaho. ASCE, New York, 390-397

Jagtap, S. S. and J. W. Jones. 1989 Stability of crop coeffic1ents under d1fferent climatic and irrigation management practices. *J. lrrig. Sci*., 10: 231-244.

Jensen, M. E. 1998. Coefficients for vegetative evapotranspiration and open water evaporation for the Lower Colorado River Accounting System. United States Bureau of Reclamation, Boulder Canyon Operations Office: Boulder City, Nevada

Jha, A., A. S. Nain and R. Ranjan. 2013. Wheat Acreage Estimation Using Remote Sensing in *Tarai* Region of Uttarakhand. *Soc. for Plant Res.*, Vol. 26 (2): 105-111

Jordan, C. F. 1969. Derivation of leaf area index from quality of light on the forest floor. *Ecology*, 50: 663-666

Kadam, S. A., S. D. Gorantiwar, S. D. Dahiwalkar and M. G. Shinde. 2019. Crop Evapotranspiration and Normalized Difference Vegetation Index relationship for Wheat crop. *Agric. Res. J.,* 56 (2):336-339

Kamble, B., A. lrmak and K. Hubbard. 2013. Estimating Crop Coefficients Using Remote Sensing-Based Vegetation Index. *Remote Sens*., 5: 1588-1602

Kimothi, M. M., M. H. Kalubarm, S. Dutta, R. Thapa and R. K. Sood. 1997. Remote sensing of horticultural plantations in Kumarsain tehsil in Shimla district, Himachal Pradesh. *J. Indian Soc. of Remote Sens.*, 25: 19-26

Kivrak, C., A. S. Bawazir, Z. Samani, C. Steele and B. Sonmez. 2019. Using Plant Phenology and Landsat-8 Satellite Data to Quantify Water Use by Onion Crop in the Mesilla Valley, New Mexico. *Inter. J. of Crop Sci. and Tech.,* 5(1): 1-13

Koc, D. L., M. Unlu, A. Nur and R. Kanber. 2021. Determination of Crop Evapotranspiration and Single Crop Coefficients of Maize using by a Weighing Lysimeter in Mediterranean Region in Turkey. *J. Agric. Nat*., 25 (4): 890-900

Kosle A. 2021. Vegetation indices-based crop coefficients to estimate evapotranspiration of wheat. M. Tech thesis (unpub.), Department of Irrigation and Drainage Engineering, Dr. PDKV, Akola.

Lei, H. and D. Yang. 2014. Combining crop coefficient of winter wheat and summer maize with remotely-sensed vegetation index for estimating evapotranspiration in the North China Plain *J. Hydrol. Eng*., 19(1): 243-251

Leprieur, C. E. 1989. Red edge measurements and canopy structure: a first look with AVIRIS data. In: Proc. Int. Geosci. & Remote Sens.

Lu, H. Q. and A. R. Huete. 1995. A feedback-based modification of the NDVI to minimize canopy background and atmospheric noise, IEEE Transeosci. *Remote Sens*., 33: 457-465

Mamta, K., N. R. Patel and P. Y. Khayruloevich. 2013. Estimation of crop water requirement in rice-wheat system from multi-temporal AWIFS satellite data. *Inter. J. of Geomatics and Geosci.*, 4(1): 61-74

Mamta, K., V. Srilatha, K. P. C. Reddy, T.L. Neelima, C.S. Murthy B. Laxman and M. U. Devi. 2019. Soybean Acreage Estimation using Temporal Microwave and Optical Remote Sensing Data: A Case study in Nizamabad District, Telangana. *J. of Agric. Physics*., 19(2): 158-167

Mandal, U. K., U. S. Victor, N. N. Srivastava, K. L. Sharma, V. Ramesh, M. Vanaja, G. R. Karwar and Y. S. Ramakrishna. 2007. Estimating yield of sorghum using root zone water balance model and spectral characteristics of crop in a dryland Alfisol. *Agric. Water Manage*., 87: 315-327

Mariana de, J. M., E. O. Ronald, I. J. Sergio and O. B. Waldo. 2021. Maize Crop Coefficient Estimation Based on Spectral Vegetation Indices and Vegetation Cover Fraction derived from UAV-Based Multispectral Images. *Agronomy.*, 11: 1-19

Mishra, S., V. Mahammood and D. K. H. V. Rao. 2022. Assessment of Irrigation Performance by Using Remote Sensing Techniques in Naryanpur Command Area, India. *Environ. and Eco. Res.* 10(3): 370-384

Mohite, J. D., S. A. Sawant, A. Kumar, M. Prajapati, S. V. Pusapati, D. Singh and S. Pappula. 2018. Operational near real time rice area mapping using multi-temporal sentinel-1 SAR observations. *The Inter. Archives of the Photogram., Remote Sens. and Spatial Infor. Sci.*, 42(4):1-5.

Monteith, J. L. 1965. Evaporation and environment. p. 205-234. In G.E. Fogg (ed.) The state and movement of water in living organisms. *In Proc. Symp. Soc. Exp. Bioi*. Vol. 19. Academic Press, New York

Moran, M. S., S. J. Mass and P. J. Pinter. 1995. Combining remote sensing and modelling for estimating surface evaporation and biomass production. *Remote Sens. Review,* 12: 335-353

Moran, M. S., T. R. Clarke, Y. Inoue and A. Vidal. 1994. Estimating crop water deficit using the relation between the surface-air temperature and spectral vegetation index. *Remote Sens. Environ*., 49: 246-263

MPKV. 2021. Krishi Darshani-2021. Directorate of Extension Education, Rahuri, Maharashtra.

Mukherjee, J., G. Gebru, A. Sood, R. K. Mahey, S. K. Bal, H. Singh and P. K. Sidhu. 2010. Wheat yield and acreage prediction using LISS-III and AWiFS sensors data of Indian remote sensing satellite of Rupnager district of Punjab, India. *Italian J. of Remote Sens*. 42 (3): 115-127

Munshi, M. K. 1982. A Study of the Determination of Wheat Crop Statistics in India through the Utilisation of Landsat Data. Ph.D. Thesis. IIT Delhi.

Narciso, G. and E. Schmidt. 1999. Identification and classification of sugarcane based on satellite remote sensing. Agricultural Research Council, Institute for Soil, Climate and Water. Private Bag X79, Pretoria, 0001

Neale, C. M. U., H. Jayanthi and J. L. Wright. 2005. Irrigation water management using high resolution airborne remote sensing. *Irrigation and Drainage Systems*, 19(3-4): 321-336

Ozcan, O., N. Musaoglu and B. Ustundag 2014. Crop water requirement estimation of wheat cultivated fields by remote sensing and GIS. *J. Food, Agri. and Environ*., 12(1): 289-293

Pakhale, G., P. Gupta and J. Nale. 2010. Crop and irrigation water requirement estimation by remote sensing and GIS: A case study of Karnal district. Haryana, India. *Int. J. Engg and Tech.*, 2(4): 207-211

Palacios, E. V., L. S. Palacios, E. S. Mejia Models of Crop Growth and Remote Sensing for Estimating Crop Yield in Irrigated Agriculture. <http:II cigr. ageng2012.org/documentos/orales/O-SW.pdf dated 20.04.2013> pp. 1-6

Pandit, D. S., V. N. Yelisetti, K. Murthy, V. Jayaraman. 2006. Identification of sugarcane and onion crops using digital image processing of multidate, multisensor high resolution satellite data. *Agriculture and Hydrology Applications of Remote Sensing, Proc. of SPIE.* 6411: 1-10

Parmar, M., H. Solanki and M. H. Kalubarme. 2020. Wheat Crop Growth Monitoring using Multi-Spectral Vegetation Indices in Bhal Region, Gujarat State. *International Journal of Advances in Agricultural Science and Technology*, 7(9): 47-66.

Paul, S. and D. N. Kumar. 2019. Comparison of Landsat-8 and Sentinel-2 data for Classification of Rabi crops over Karnataka, India. The International Archives of the Photogrammetry, Remote Sensing and Spatial Information Sciences, Volume XLII-3/W6, ISPRS-GEOGLAM-ISRS *Joint Int. Workshop on "Earth Observations for Agricultural Monitoring*", 18–20 February 2019, New Delhi, India

Pearson, R. L. and L. D. Miller. 1972 Remote mapping of standing crop biomass for estimation of the productivity of the shortgrass prairie, Pawnee National Grasslands, Colorado. *Proceedings of the 8th International Symposium on Remote Sensing of the Environment II*: 1355-1379.

Penman, H. L. 1948. Natural evaporation from open water, bare soil and grass. Proc. Roy. Soc. London 193: 120-146

Pimpale, A. R., P. B. Rajankar, S. B. Wadatkar and I. K. Ramteke. 2015. Determination of Spatial crop coefficient of Chickpea using Remote Sensing and GIS. *American Inter. J. of Res. in Formal, Appl. & Natural Sci.,* 7(1): 59-64

Pimpale, A. R., P. B. Rajankar, S. B. Wadatkar and I. K. Ramteke. 2015. Application of remote sensing and GIS for acreage estimation of wheat. *Inter. J. of Engg, Business and Enterprise App. (IJEBEA).,* 12(2): 167-171

Pimpale, A. R., P. B. Rajankar, S. B. Wadatkar, S. S. Wanjari and I. K. Ramteke 2015. Estimation of water requirement of wheat using multispectral vegetation indices. *J. of Agromet.,* 17 (2): 208-212

Pimpale, A. R., S. B. Wadatkar, P. B. Rajankar and I. K. Ramteke. 2019. Comparative Performance of different Multispectral Vegetation Indices for Determination of Crop Coefficients of *Rabi* Sorghum. *Inter. J. of Agricu. Sci.,* 11(6):8164-8167

Prajapati, G. V., R. Subbaiah, A. N. Kunapara, N. S. Vithlani and J. J. Makwana (2016). Crop Coefficient for Mulched Cotton under variable Irrigation Regimes. *Current World Environment.,* 11(2), 648-653

Prananda, I. R. A., M. Kamal and W. K. Denny. 2020. The effect of using different vegetation indices for mangrove leaf area index modelling.

The Fifth International Conferences of Indonesian Society for Remote Sensing. *IOP Conf. Series: Earth and Environmental Science.* pp. 1-12

Qadir, A., I. A. Abir, S. Nawaz, N. Khan, M. A. Aman, R. K. Olukunle, N. Akhtar, M. T. Anees, K. Hossain and A. Ahmad. 2019. Crop Acreage and Crop Yield Estimation using Remote Sensing and GIS Techniques, Bulandshahr District. *Indian J. of Eco.,* 46(3): 470-474

Qi, J., A. Chehbouni, A. R. Huete, Y. H. Kerr and S. Sorooshian. 1994a. A modified soil adjusted vegetation index (MSAVI). *Remote Sens. Environ*, 48:119-126

Rafn, E. B., C. Bryce and P. A. Daniel. 2008. Evaluation of a Method for Estimating Irrigated Crop-Evapotranspiration Coefficients from Remotely Sensed Data in Idaho. *J. Irrig. and Drain. Eng*., 134(6): 722-729

Rahimian, M. H., S. Poormohammadi and M. H. Mokhtari. 2011. Determination of winter wheat crop coefficient using MODIS-derived vegetation indices: a case study of the Azadegan plain, Iran. *ICID 21st International Congress on Irrigation and Drainage*, 15-23 October 2011. Tehran. Iran pp. 297-304

Rawat, K. S. and A. K. Mishra. 2020. Retrieval of K_c from Sebal and Comparison among NDVI and LAI based K_c. *Inter. J. of Advanced Res. in Engg. and Tech.,* 11(9): 1108-1111

Rawat, U., A. Yadav, P.S. Pawar, A. Rajput, D. Vasht and S. Nema, 2021. Wheat Crop Acreage Estimation Based on Remote Sensing and GIS in Jabalpur (Madhya Pradesh, India*). Asian J. of Agricu. Ext., Eco. & Socio.,* 39(2): 88-94

Ray, S. S. and V. K. Dadhwal. 2001. Estimation of crop evapotranspiration of irrigation command area using remote sensing and GIS. *Agric. Water Manage*., 49: 239-249

Reddy, K. C., S. Arunajyothy, P. Mallikarjuna. 2015. Crop Coefficients of Some Selected Crops of Andhra Pradesh. *J. Inst. Eng.* India Ser. A 96(2):123-130

Robertson, A. N., A. Gitelson, Y. Peng, W. S. Elizabeth, B. Leavitt and A. Timothy. 2013. Continuous Monitoring of Crop Reflectance, Vegetation Fraction and Identification of Developmental Stages Using a Four Band Radiometer. *J. Agronomy* 105(6): 1769-1779

Rouse, J. W., R. H. Haas, J. A. Schell and O. W. Deering. 1973. Monitoring vegetation systems in the Great Plains with ERTS, Third ERTS Symposium, NASA SP-351, pp:309-317

Russo, A. L., T. Simoniello, M. Greco, G. Squicciarrino, M. Lanfredi and M. Macchiato. 2010. Correlation between satellite vegetation indices and crop coefficients. *Geophysical Research Abstracts.* Vol. 12

Sandholt, I., K. Rasmussen and J. Andersen. 2002. A simple interpretation of the surface temperature/vegetation index space for assessment of surface moisture status. *Remote Sens. Environ*., 79(2-3): 213-224

Sawasawa, H. L. A. 2003. Crop yield estimation: Integrating RS, GIS and Land factors. M. S. Thesis. International institute for Geo-information and earth observation Enschede, The Netherlands

Sharma, R., L. Pradhan, M. Kumari and P. Bhattacharya. 2021. Comparative Analysis of Different Vegetation Indices of Noida City using Landsat Data. *Advances in Energy and Environment*, Lecture Notes in Civil Engineering. pp: 209-221.

Singh, S. K., Dutta S. and Dharaiya N. 2016. Remote Sensing Indices for Crop Water Management. *Inter. J. of Engg. Sci. & Res. Tech.*, ISSN: 2277-9655: 326-334

Singh, S. K., S. Dutta and N. Dharaiya. 2013. Estimation of Crop Evapotranspiration of Cotton using Remote Sensing Technique. *Inter. J. of Enviro. Engg. and Manage*., 4(5): 523-528

Siyal, A. A., A. G. Siyal and R. B. Mahar. 2014. Remote sensing and GIS based Wheat crop Acreage and Yield estimation of District Hyderabad, Pakistan. *Mehran University Res. J. of Engg. & Tech.*, 34(1): 33-39

Spiliotopoulos, M, A. Loukas. 2019. Hybrid Methodology for the Estimation of Crop Coefficients Based on Satellite Imagery and Ground Based Measurements. *Water*. 11-1364.

Subbarao, N. V., J. K. Mani, A. Shrivastava, K. Srinivas and A. O. Varghese. 2021. Acreage estimation of kharif rice crop using Sentinel-1 temporal SAR data. *Spatial Information Res*, 29(4): 495-505.

Suifan, M. S., M. R. Shatanawi, J. T. Al-Bakri, K. M. Bali and A. A. Suleiman. 2007. Modeling evapotranspiration for Irrigated crops in Jordan using remotely sensed data. WWDL SCADA and related technologies for irrigation district modernization, II USCID June 2007 proceedings, Denver USCID Water Management Conference. pp: 185-197.

Suleiman, A. A., S. C. M. Tojo and G. Hoogenboom. 2007. Evaluation of FAO-56 crop coefficient procedures for deficit irrigation management of cotton in a humid- climate. *Agric. Water Manage*., 91 (1-3): 33-42

Sun, C., Y. Bian, T. Zhou and J. Pan. 2019. Using of Multi-Source and Multi-Temporal Remote Sensing Data Improves Crop-Type Mapping in the Subtropical Agriculture Region. *Sensors*, 19: 1-23

Tasumi, M., R. Allen R. Trezza and J. Wright. 2005. Satellite-Based energy balance to assess within-population variance of crop coefficient curves. *J. Irrig. Drain Engg*., 131 94-109

Thornthwaite, C. W. 1948. "An approach toward a rational classification of climate." The Geographical Review., 38(1): 55-94

Torbick, N., D. Chowdhury, W. Salas and J. Qi. 2017. Monitoring Rice Agriculture across Myanmar Using Time Series Sentinel-1 Assisted by Landsat-8 and PALSAR-2. *Remote sens*, 9: 119.

Tsiligirides, T. A. 1998. Remote sensing as a tool for agricultural statistics: a case study of area frame sampling methodology in Hellas. *Comput. Electron. Agr.*, 20(1): 45-77

Tucker, C. J. 1979. Red and photographic infrared linear combinations for monitoring vegetation. *Remote Sens. Environ*., 8:127-150

Tyagi, N. K., D. K. Sharma and S. K. Luthra. 2000. Determination of evapotranspiration and crop coefficients of rice and sunflower with lysimeter. *Agril. Water Manag.*, 45: 41-54

Tyagi, N. K., D. K. Sharma and S. K. Luthra. 2000. Evapotranspiration and crop coefficients of wheat and sorghum. *J. Irrig. Drain Eng.*, 126:215-222.

Wang, P., X. Li, J. Gong and C. Song. 2001. “Vegetation temperature condition index and its application for drought monitoring.” *Inter. Geoscience and Remote Sens. Symposium*, Sydney, Australia, 9·14 July, pp:141-143

Wardlow, B. D., S. L Egbert and J. H Kastens. 2007. Analysis of time-series MODIS 250 m vegetation index data for crop classification in the U.S. Central Great Plains. *Remote Sens. Environ*., 108: 290-310

Wright, J. L. 1982. New evapotranspiration crop coefficients. *J. Irrig. Drain.* Div. ASCE, 108: 57-74.

Yoshioka, H., A. R. Huete and T. Miura. 2000. Derivation of vegetation isoline equations in red -NIR reflectance space. *IEEE Trans. Geosci. Remote. Sens*., 38: 838-848

Zhang, H., Y. Lan, R. Lacey, W. C. Hoffmann and Y. Huang. 2009. Analysis of vegetation indices derived from aerial multispectral and ground hyperspectral data. *Int. J. Agric. and Biol. Engg*., 2(3):33-40

Zolfagharnejad, H., B. Kamkar and O. Abdi. 2017. Vegetation index-deduced crop coefficient of wheat (triticum aestivum) using remote sensing: case study on four basins of Golestan Province, Iran. *Inter. J. of Agricu. and Bios. Engg*, 11(7): 498-501.

ANNEXURE I

Meteorological Data of Study Area

I) For *rabi* season of 2020-21

A) Weekly meteorological data of Dhule (2020-21)

Met Week	Tmax (^oC)	Tmin (^oC)	Tmean	Rs $MJ/m^2/day$	U_2(m/s)	RHmean (%)
45	28.94	13.83	21.38	18.59	1.51	64.88
46	31.29	18.06	24.67	17.43	1.43	73.56
47	30.99	16.26	23.63	15.41	1.48	66.14
48	30.95	15.91	23.43	16.29	1.79	66.89
49	31.86	14.01	22.94	17.28	1.69	53.97
50	29.89	17.82	23.86	9.73	1.39	69.05
51	28.95	12.17	20.56	15.90	1.72	54.42
52	30.47	12.62	21.55	14.97	1.78	53.02
1	30.54	18.39	24.46	11.55	1.76	60.12
2	32.10	18.58	25.34	14.81	1.61	57.56
3	33.89	17.23	25.56	15.72	1.39	38.35
4	33.00	14.22	23.61	17.50	1.30	28.36
5	32.59	13.19	22.89	17.63	1.68	21.04
6	32.86	13.61	23.24	19.45	1.55	20.67
7	33.91	17.95	25.93	17.83	1.49	29.94
8	34.64	18.25	26.44	20.01	1.63	30.70
9	38.34	19.56	28.95	23.06	1.75	19.42
10	38.65	20.62	29.64	22.46	1.28	20.19
11	38.84	22.40	30.62	20.67	1.40	21.65
12	38.62	22.97	30.79	19.54	1.43	25.27

B) Weekly Meteorological data of Jalgaon (2020-21)

Met Week	Tmax (ºC)	Tmin (ºC)	Tmean	Rs MJ/m^2/day	U_2(m/s)	RHmean (%)
45	27.57	13.33	20.45	17.46	1.54	67.18
46	30.15	17.74	23.94	16.67	1.58	77.38
47	29.40	15.97	22.69	15.63	1.55	69.88
48	29.75	15.45	22.60	16.29	1.85	70.29
49	30.71	13.39	22.05	16.94	1.69	57.28
50	29.16	17.12	23.14	8.33	1.71	70.18
51	27.97	11.74	19.86	15.81	1.73	56.63
52	29.43	11.91	20.67	14.89	1.87	56.81
1	29.83	17.35	23.59	11.50	2.11	62.60
2	31.85	17.52	24.68	13.23	1.68	57.42
3	33.24	16.58	24.91	15.73	1.66	39.96
4	32.55	13.65	23.10	17.69	1.44	30.44
5	32.22	12.96	22.59	18.76	1.82	20.87
6	32.54	13.59	23.07	19.90	1.60	21.33
7	33.72	17.72	25.72	17.09	1.53	30.48
8	34.22	17.86	26.04	20.24	1.57	30.35
9	37.94	18.88	28.41	22.86	1.65	19.62
10	38.42	20.16	29.29	22.77	1.16	18.88
11	38.70	22.09	30.40	19.89	1.43	22.24
12	38.03	22.95	30.49	21.40	1.44	30.50

C) Weekly Meteorological data of Nashik (2020-21)

Met Week	Tmax (°C)	Tmin (°C)	Tmean	Rs MJ/m^2/day	U_2(m/s)	RHmean (%)
45	26.50	13.73	20.12	18.98	2.11	71.16
46	27.92	16.60	22.26	17.46	1.57	79.29
47	28.31	16.83	22.57	16.17	1.40	74.68
48	27.96	16.38	22.17	16.31	2.24	75.28
49	28.65	13.45	21.05	17.80	1.91	59.99
50	27.39	17.05	22.22	10.59	1.33	77.34
51	27.11	12.60	19.86	16.92	1.95	60.41
52	28.62	13.16	20.89	16.26	1.76	61.23
1	27.79	17.23	22.51	12.14	1.45	74.89
2	29.99	18.01	24.00	15.01	1.52	69.10
3	31.41	16.08	23.75	17.79	1.43	51.29
4	31.54	14.07	22.80	19.36	1.64	36.04
5	31.07	13.74	22.40	18.47	1.79	31.17
6	31.79	13.63	22.71	20.67	1.97	24.99
7	32.32	16.95	24.63	18.50	1.59	37.39
8	32.26	17.31	24.79	19.95	2.25	42.03
9	36.14	19.12	27.63	23.45	1.82	24.53
10	36.58	19.54	28.06	23.64	1.75	26.08
11	36.73	20.65	28.69	21.85	1.88	24.81
12	36.54	21.33	28.93	22.16	1.68	26.51

II) For *rabi* season of 2021-22

A) Weekly Meteorological data of Dhule (2021-22)

Met Week	Tmax (°C)	Tmin (°C)	Tmean	Rs MJ/m^2/day	U_2(m/s)	RHmean (%)
45	30.41	16.34	23.37	16.21	1.80	68.03
46	31.26	17.09	24.18	14.29	2.12	73.25
47	32.27	21.38	26.83	13.29	1.68	76.63
48	28.11	15.86	21.98	12.22	2.13	68.08
49	28.39	15.86	22.13	12.78	1.70	72.54
50	29.48	14.81	22.15	13.39	1.80	66.71
51	29.26	12.57	20.92	15.08	1.46	56.97
52	29.12	14.29	21.70	13.87	1.60	58.51
1	30.76	15.81	23.29	13.50	1.83	60.88
2	27.78	13.07	20.43	14.72	2.04	54.58
3	30.88	13.89	22.38	16.96	1.92	49.37
4	26.94	9.42	18.18	17.42	2.12	39.77
5	32.09	13.07	22.58	19.80	1.66	31.46
6	31.67	13.13	22.40	19.66	1.59	30.88
7	33.18	15.10	24.14	18.73	1.53	32.96
8	36.42	17.58	27.00	21.33	1.48	23.61
9	36.31	18.03	27.17	20.83	1.45	23.53
10	35.76	21.59	28.68	18.95	1.55	33.53
11	40.54	21.15	30.85	23.52	2.00	18.85
12	40.96	22.76	31.86	21.92	2.32	18.32

B) Weekly Meteorological data of Jalgaon (2021-22)

Met Week	Tmax (^oC)	Tmin (^oC)	Tmean	Rs $MJ/m^2/day$	U_2(m/s)	RHmean (%)
45	27.97	15.60	21.79	16.52	1.66	73.77
46	29.24	16.91	23.08	14.34	2.06	79.71
47	30.22	20.66	25.44	13.37	1.73	81.18
48	26.24	14.89	20.57	13.15	1.98	72.82
49	27.14	15.39	21.26	12.48	1.66	75.57
50	27.99	14.11	21.05	12.79	1.94	69.11
51	27.43	11.50	19.46	15.06	1.53	62.33
52	27.55	13.66	20.61	13.70	1.58	66.55
1	29.22	14.92	22.07	13.08	1.91	66.86
2	26.47	12.61	19.54	14.33	1.99	64.13
3	29.53	13.05	21.29	16.55	1.79	56.13
4	26.12	8.73	17.42	16.67	2.08	45.33
5	31.12	12.46	21.79	19.20	1.60	33.98
6	31.02	12.33	21.68	20.13	1.63	33.79
7	32.70	14.65	23.67	19.15	1.61	34.93
8	35.90	17.13	26.52	21.05	1.44	24.50
9	36.10	18.24	27.17	20.86	1.51	25.71
10	35.88	21.63	28.76	17.79	1.80	31.60
11	40.36	21.00	30.68	23.07	1.98	18.80
12	41.00	22.38	31.69	21.54	2.05	17.61

C) Weekly Meteorological data of Nashik (2021-22)

Met Week	Tmax (°C)	Tmin (°C)	Tmean	Rs MJ/m²/day	U_2(m/s)	RHmean (%)
45	26.89	16.78	21.84	15.41	2.16	76.31
46	28.22	18.21	23.22	14.56	2.31	81.40
47	29.03	20.40	24.72	13.72	1.62	84.13
48	25.50	15.26	20.38	12.76	2.63	76.76
49	25.60	15.08	20.34	13.65	1.95	81.38
50	26.01	14.53	20.27	13.99	1.66	76.32
51	26.55	12.75	19.65	15.79	1.60	66.55
52	26.73	13.16	19.95	16.08	1.75	67.59
1	27.53	14.68	21.11	14.42	1.74	71.81
2	25.14	11.39	18.26	15.65	1.72	71.36
3	28.26	13.57	20.92	17.54	1.97	62.99
4	24.78	8.75	16.77	17.44	2.34	51.44
5	29.99	11.97	20.98	20.41	1.76	44.47
6	30.43	12.32	21.38	20.97	1.94	42.54
7	31.37	13.73	22.55	20.94	1.89	43.55
8	34.86	16.77	25.82	22.38	1.76	30.60
9	34.62	17.79	26.21	21.85	1.92	25.20
10	34.07	20.85	27.46	20.39	1.69	37.90
11	38.21	20.06	29.14	23.79	2.27	21.71
12	38.23	20.75	29.49	21.57	2.19	27.25

ANNEXURE II

WHEAT 2020-21

A) Week-wise distribution of wheat mean NDVI for 2020-21

Weeks past sowing	Wheat Polygon ID 2020-21														
	1	2	3	4	5	6	7	8	9	10	11	12	13	14	15
1															
2															
3						0.208									
4						0.311					0.381		0.358		
5	0.349	0.481	0.314	0.288	0.306		0.346	0.288			0.531	0.288	0.424		
6	0.597	0.526	0.584	0.548	0.606		0.626	0.330	0.099	0.036		0.429		0.454	0.367
7									0.202	0.114				0.463	0.528
8						0.193									
9						0.155					0.350		0.338		
10	0.510	0.484	0.429	0.441	0.460		0.436	0.146			0.441		0.417		
11	0.425	0.480	0.433	0.425	0.506	0.163	0.408	0.143	0.428	0.426		0.412		0.419	0.318
12									0.514	0.489	0.266	0.553	0.276	0.344	0.226
13	0.239	0.234	0.274	0.291	0.347	0.116	0.316	0.213							
14									0.570	0.372	0.140	0.419	0.109	0.191	0.176
15	0.195	0.172	0.232	0.224	0.223	0.123	0.206	0.543							
16						0.127			0.659	0.329	0.126	0.203	0.096	0.163	0.153
17	0.175	0.094	0.182	0.189	0.165		0.110	0.391			0.122		0.092		

Table continued…

Weeks past sowing	Wheat Polygon ID 2020-21													NDVI Average
	16	17	18	19	20	21	22	23	24	25	26	27	28	
1												0.189		0.189
2												0.239		0.239
3	0.263												0.298	0.256
4	0.271			0.273	0.157	0.302		0.270					0.346	0.297
5		0.249		0.380	0.091	0.593	0.245	0.433	0.114		0.160			0.327
6		0.330	0.244				0.516		0.593	0.039	0.287	0.535		0.408
7			0.461							0.536		0.622		0.418
8	0.625												0.503	0.440
9	0.509			0.524	0.158	0.639		0.562				0.483	0.531	0.425
10		0.404		0.507	0.166	0.507	0.505	0.545	0.424		0.316			0.420
11	0.431	0.501	0.428				0.515		0.346	0.308	0.483	0.428	0.513	0.406
12			0.469	0.295	0.135	0.424		0.356		0.225				0.352
13	0.387	0.322					0.393		0.243		0.356	0.220	0.520	0.298
14			0.321	0.226	0.173	0.221		0.202		0.147		0.228		0.250
15	0.187	0.228					0.200		0.171		0.215		0.356	0.234
16	0.133		0.302	0.162	0.136	0.072		0.162		0.159		0.180	0.248	0.201
17		0.194		0.156	0.109	0.137	0.116	0.133	0.163		0.159	0.113		0.156

B) Week-wise distribution of wheat mean NDWI for 2020-21

Weeks past sowing	Wheat Polygon ID 2020-21														
	1	**2**	**3**	**4**	**5**	**6**	**7**	**8**	**9**	**10**	**11**	**12**	**13**	**14**	**15**
1															
2															
3						0.084									
4						0.016					0.383		0.277		
5	0.275	0.322	0.211	0.166	0.233		0.227	0.315			0.371		0.373		
6	0.442	0.403	0.304	0.291	0.411		0.342	0.209	0.164	0.069		0.264		0.318	0.303
7									0.086	0.038		0.349		0.424	0.437
8						0.123									
9						-0.084					0.285		0.274		
10	0.309	0.253	0.242	0.299	0.407		0.379	0.113			0.292		0.242		
11	0.215	0.173	0.207	0.290	0.347	-0.092	0.333	0.064	0.298	0.256		0.357		0.354	0.258
12									0.356	0.294	0.128	0.390	0.113	0.222	0.107
13	-0.060	-0.047	0.062	0.145	0.159	-0.093	0.152	0.100							
14									0.363	0.212	-0.049	0.294	-0.105	0.038	-0.008
15	-0.120	-0.109	-0.051	0.005	-0.074	-0.118	-0.079	0.315							
16						-0.095			0.365	0.118	-0.118	0.030	-0.124	-0.098	-0.112
17	-0.094	-0.060	-0.122	-0.012	-0.095		-0.074	0.304			-0.097		-0.089		

Table continued…

Weeks past sowing	Wheat Polygon ID 2020-21													NDWI Average
	16	17	18	19	20	21	22	23	24	25	26	27	28	
1												0.117		0.117
2												0.128		0.128
3	0.189												0.140	0.138
4	0.167			0.239	0.183	0.186		0.147					0.156	0.195
5		0.179		0.317	0.050	0.332	0.231	0.268	0.067		0.066			0.235
6		0.265	0.191				0.357		0.355	0.053	0.090	0.284		0.269
7			0.317							0.327		0.373		0.294
8	0.381												0.393	0.299
9	0.309			0.310	0.117	0.478		0.340				0.348	0.454	0.283
10		0.313		0.277	0.091	0.469	0.442	0.309	0.167		0.249			0.285
11	0.287	0.335	0.265				0.366		0.089	0.105	0.214	0.221	0.430	0.244
12			0.245	0.128	0.093	0.309		0.192		0.013				0.199
13	0.170	0.168					0.190		0.010		0.147	0.060	0.434	0.106
14			0.085	0.003	0.062	-0.002		-0.020		-0.056		0.007		0.059
15	0.019	-0.010					0.071		-0.099		0.010		0.225	-0.001
16	-0.050		-0.030	-0.083	0.061	0.083		-0.064		-0.099		-0.048	-0.004	-0.016
17		-0.102		-0.052	0.104	0.032	-0.112	-0.086	-0.109		-0.047	-0.057		-0.043

C) Week-wise distribution of wheat mean SAVI for 2020-21

Weeks past sowing	Wheat Polygon ID 2020-21														
	1	2	3	4	5	6	7	8	9	10	11	12	13	14	15
1															
2															
3						0.397									
4						0.476					0.371		0.537		
5	0.523	0.713	0.471	0.458	0.459		0.518	0.433			0.647		0.736		
6	0.845	0.858	0.775	0.834	1.028		0.740	0.495	0.149	0.053		0.432		0.681	0.551
7									0.304	0.171		0.743		0.895	0.902
8						0.490									
9						0.233					0.524		0.507		
10	0.704	0.613	0.643	0.618	0.784		0.654	0.219			0.662		0.625		
11	0.638	0.612	0.649	0.736	0.759	0.244	0.717	0.215	0.746	0.638		0.678		0.629	0.477
12									0.721	0.733	0.399	0.829	0.414	0.516	0.339
13	0.359	0.314	0.411	0.446	0.520	0.174	0.473	0.320							
14									0.755	0.558	0.210	0.528	0.163	0.287	0.264
15	0.292	0.257	0.348	0.317	0.334	0.184	0.309	0.564							
16						0.191			0.688	0.493	0.189	0.305	0.144	0.244	0.230
17	0.212	0.142	0.272	0.279	0.248		0.165	0.337			0.102		0.128		

Table continued…

Weeks past sowing	Wheat Polygon ID 2020-21													SAVI Average
	16	17	18	19	20	21	22	23	24	25	26	27	28	
1												0.273		0.273
2												0.308		0.308
3	0.314												0.396	0.369
4	0.357			0.409	0.285	0.303		0.355					0.519	0.401
5		0.374		0.569	0.136	0.589	0.367	0.609	0.171		0.240			0.471
6		0.694	0.366				0.624		0.620	0.058	0.430	0.703		0.576
7			0.741							0.504		0.832		0.637
8	0.688												0.905	0.694
9	0.763			0.787	0.238	0.959		0.843				0.725	0.960	0.654
10		0.601		0.760	0.249	0.985	0.808	0.817	0.551		0.630			0.643
11	0.647	0.751	0.706				0.722		0.519	0.462	0.725	0.531	0.719	0.615
12			0.704	0.443	0.202	0.636		0.534		0.338				0.524
13	0.581	0.484					0.590		0.365		0.534	0.331	0.780	0.445
14			0.411	0.319	0.260	0.332		0.303		0.220		0.341		0.354
15	0.280	0.343					0.450		0.256		0.422		0.504	0.347
16	0.200		0.253	0.243	0.203	0.108		0.242		0.239		0.180	0.372	0.266
17		0.250		0.234	0.103	0.206	0.224	0.199	0.204		0.238	0.110		0.203

D) Week-wise distribution of wheat mean MSAVI2 for 2020-21

Weeks past sowing	Wheat Polygon ID 2020-21														
	1	2	3	4	5	6	7	8	9	10	11	12	13	14	15
1															
2															
3						0.371									
4						0.401					0.386		0.527		
5	0.517	0.644	0.478	0.468	0.469		0.514	0.448			0.704		0.728		
6	0.721	0.837	0.737	0.715	0.813		0.77	0.496	0.181	0.069		0.447		0.624	0.537
7									0.337	0.205		0.732		0.718	0.671
8						0.384									
9						0.268					0.588		0.565		
10	0.575	0.600	0.600	0.616	0.718		0.607	0.255			0.612		0.588		
11	0.597	0.58	0.604	0.658	0.602	0.280	0.647	0.25	0.614	0.597		0.622		0.591	0.483
12									0.761	0.657	0.420	0.712	0.433	0.512	0.369
13	0.386	0.346	0.430	0.458	0.515	0.208	0.480	0.351							
14									0.726	0.542	0.245	0.591	0.196	0.321	0.300
15	0.326	0.292	0.327	0.349	0.364	0.219	0.342	0.582							
16						0.225			0.694	0.495	0.224	0.338	0.175	0.280	0.266
17	0.247	0.173	0.207	0.214	0.283		0.198	0.459			0.117		0.168		

Table continued…

Weeks past sowing	Wheat Polygon ID 2020-21													MSAVI2 Average
	16	17	18	19	20	21	22	23	24	25	26	27	28	
1												0.286		0.286
2												0.316		0.316
3	0.278												0.484	0.378
4	0.393			0.429	0.227	0.336		0.391					0.514	0.400
5		0.399		0.734	0.166	0.645	0.393	0.635	0.205		0.275			0.495
6		0.692	0.392				0.612		0.745	0.075	0.446	0.597		0.553
7			0.718							0.628		0.767		0.597
8	0.735												0.783	0.634
9	0.674			0.688	0.273	0.780		0.720				0.652	0.844	0.605
10		0.625		0.672	0.285	0.793	0.614	0.705	0.605		0.630			0.594
11	0.603	0.667	0.604				0.761		0.514	0.471	0.651	0.456	0.760	0.573
12			0.639	0.456	0.237	0.595		0.525		0.367				0.514
13	0.558	0.488					0.564		0.391		0.525	0.361	0.737	0.453
14			0.486	0.369	0.295	0.362		0.336		0.256		0.371		0.385
15	0.305	0.372					0.372		0.292		0.379		0.526	0.361
16	0.235		0.364	0.249	0.239	0.135		0.278		0.275		0.305	0.298	0.299
17		0.224		0.209	0.198	0.241	0.328	0.234	0.280		0.274	0.215		0.237

E) Week-wise distribution of wheat mean RVI for 2020-21

Weeks past sowing	Wheat Polygon ID 2020-21														
	1	2	3	4	5	6	7	8	9	10	11	12	13	14	15
1															
2															
3						1.595									
4						1.670					2.442		2.116		
5	2.071	2.810	1.915	1.879	1.883		2.057	1.811			3.426		3.317		
6	5.602	6.136	3.803	3.505	5.362		4.355	1.985	1.221	1.074		1.809		2.662	2.161
7									1.508	1.258		4.390		4.939	4.373
8						2.479									
9						1.367					2.075		2.020		
10	3.078	2.501	2.502	2.607	3.546		2.546	1.343			2.580		2.429		
11	2.481	2.379	2.526	2.927	3.050	1.389	2.832	1.334	2.981	2.482		2.649		2.445	1.933
12									4.184	2.914	1.724	3.474	1.763	2.049	1.585
13	1.630	1.529	1.755	1.845	2.063	1.263	1.922	1.542							
14									3.651	2.184	1.325	2.443	1.244	1.473	1.428
15	1.483	1.413	1.605	1.537	1.574	1.280	1.520	3.098							
16						1.291			4.066	1.981	1.289	1.511	1.213	1.389	1.363
17	1.423	1.209	1.444	1.458	1.096		1.247	2.133			1.277		1.203		

Table continued…

Weeks past sowing	Wheat Polygon ID 2020-21													RVI Average
	16	17	18	19	20	21	22	23	24	25	26	27	28	
1												1.244		1.244
2												1.428		1.428
3	1.334												1.923	1.617
4	2.914			1.750	1.180	1.807		1.910					2.057	1.983
5		1.664		3.059	1.200	3.915	1.647	3.280	1.258		1.380			2.269
6		3.252	1.644				4.207		3.920	1.081	1.805	3.302		3.099
7			3.551							3.311		3.287		3.327
8	3.139												4.608	3.409
9	3.071			3.206	1.876	4.542		3.967				2.871	6.428	3.142
10		2.663		3.054	1.398	4.823	4.639	3.394	2.535		3.128			2.869
11	2.516	3.007	2.981				4.192		2.058	1.890	2.869	2.904	4.168	2.636
12			2.769	1.838	1.311	2.471		2.105		1.581				2.290
13	2.265	1.952					2.296		1.643		2.104	1.565	3.152	1.902
14			1.945	1.584	1.419	1.568		1.506		1.344		1.589		1.765
15	1.460	1.492					1.034		1.412		1.520		2.675	1.650
16	1.307		1.466	1.386	1.314	1.156		1.385		1.379		1.439	1.160	1.535
17		1.380		1.369	1.662	1.318	1.188	1.306	1.389		1.078	1.419		1.367

WHEAT 2021-22

A) Week-wise distribution of wheat mean NDVI for 2021-22

Weeks past sowing	Wheat Polygon ID 2021-22														
	1	2	3	4	5	6	7	8	9	10	11	12	13	14	15
1		0.101									0.216				0.126
2			0.193	0.189		0.103	0.197	0.287	0.278						
3	0.120	0.172									0.198				0.397
4			0.384	0.203			0.343		0.404					0.282	
5	0.177				0.272					0.392		0.287	0.299		
6						0.505		0.410						0.402	
7		0.664			0.076	0.429		0.350		0.543	0.691	0.412	0.544		0.606
8		0.454	0.639	0.576			0.604		0.457		0.527				0.449
9	0.587		0.534	0.506			0.536		0.306						
10	0.301					0.267		0.299						0.562	
11		0.297			0.404	0.237		0.356		0.599	0.415	0.514	0.703	0.364	0.216
12		0.317	0.338	0.234	0.402		0.268		0.140	0.416	0.433	0.352	0.481		0.222
13	0.166		0.385	0.189		0.101	0.233	0.372	0.134						
14	0.138	0.155									0.313			0.224	0.186
15			0.205	0.097	0.207	0.087	0.164	0.343	0.123	0.216		0.151	0.240	0.233	
16	0.138	0.136			0.386	0.081		0.239		0.171	0.142	0.162	0.214		0.088
17		0.131	0.137	0.101		0.098	0.161	0.237	0.122		0.143			0.164	0.083

Table continued…

Weeks past sowing	Wheat Polygon ID 2021-22													NDVI Average
	16	17	18	19	20	21	22	23	24	25	26	27	28	
1					0.099	0.399		0.138		0.245			0.151	0.184
2			0.195	0.202					0.289					0.215
3					0.273	0.447				0.291			0.153	0.256
4							0.272				0.071	0.241		0.275
5	0.319	0.162						0.471						0.297
6			0.528	0.513			0.354	0.301	0.504		0.189	0.403		0.411
7	0.591	0.074	0.435	0.483	0.520	0.432			0.382	0.653			0.118	0.445
8					0.540	0.258				0.461			0.079	0.459
9								0.192						0.444
10			0.315	0.296			0.599	0.210	0.113		0.549	0.552		0.369
11	0.708	0.523	0.337	0.324	0.333	0.119	0.370		0.171	0.273	0.344	0.348	0.068	0.365
12	0.479	0.453			0.293	0.131		0.125		0.266			0.074	0.301
13			0.179	0.194					0.072					0.203
14					0.195	0.109	0.168	0.120		0.110	0.204	0.177	0.072	0.167
15	0.201	0.215	0.118	0.108			0.101	0.103	0.087		0.108	0.120		0.161
16	0.206	0.328	0.086	0.095	0.111	0.075		0.108	0.071	0.121			0.077	0.152
17			0.051	0.036	0.111	0.069	0.105		0.069	0.113	0.089	0.093	0.073	0.109

B) Week-wise distribution of wheat mean NDWI for 2021-22

Weeks past sowing	Wheat Polygon ID 2021-22														
	1	**2**	**3**	**4**	**5**	**6**	**7**	**8**	**9**	**10**	**11**	**12**	**13**	**14**	**15**
1		0.087									-0.035				0.177
2			0.128	0.076		0.071	0.107	0.174	0.141						
3	0.081	0.139									0.121				0.230
4			0.181	0.168			0.187		0.199					0.177	
5	0.074				0.129					0.299		0.191	0.199		
6						0.302		0.185						0.197	
7		0.329			-0.001	0.255		0.211		0.321	0.343	0.260	0.296		0.396
8		0.272	0.337	0.206			0.260		0.294		0.309				0.315
9	0.040		0.301	0.325			0.207		0.251						
10	0.095					0.219		0.235						0.269	
11		0.219			0.220	0.157		0.230		0.366	0.274	0.340	0.404	0.203	0.223
12		0.206	0.264	0.110	0.225		0.195		0.088	0.276	0.307	0.216	0.321		0.119
13	0.031		0.266	0.055		0.040	0.141	0.226	0.061						
14	0.013	0.044									0.165			0.174	0.024
15			0.081	-0.037	0.209	0.012	0.024	0.086	0.008	0.158		0.084	0.178	0.141	
16	-0.041	-0.034			0.275	0.000		0.095		0.114	0.044	0.044	0.099		0.029
17		-0.035	-0.034	-0.032		-0.061	-0.001	0.083	-0.046		-0.044			0.061	-0.019

Table continued…

Weeks past sowing	Wheat Polygon ID 2021-22													NDWI Average
	16	17	18	19	20	21	22	23	24	25	26	27	28	
1					0.026	0.181		0.041		0.038				0.074
2			0.109	0.055					0.100				0.018	0.098
3					0.165	0.160				0.187				0.155
4							0.192				0.081	0.097		0.160
5	0.279	0.048						0.206						0.178
6			0.351	0.365			0.139	0.166	0.330		0.056	0.198		0.229
7	0.346	0.068	0.277	0.302	0.314	0.078			0.262	0.272			0.000	0.241
8					0.338	0.068				0.298			0.024	0.247
9								0.264						0.231
10			0.259	0.242			0.322	0.125	0.100		0.306	0.290		0.224
11	0.402	0.306	0.133	0.115	0.295	-0.046	0.209		0.110	0.224	0.220	0.183	0.034	0.219
12	0.354	0.285			0.210	-0.055		0.152		0.188			0.046	0.195
13			0.079	0.055					-0.016					0.094
14					0.029	-0.095	0.144	0.092		-0.001	0.193	0.094	0.027	0.069
15	0.116	0.179	0.000	-0.022			0.109	0.020	-0.068		0.093	0.059		0.072
16	0.108	0.241	0.023	-0.033	-0.073	-0.038		0.027	-0.077	-0.030			0.031	0.040
17			0.026	-0.004	-0.072	-0.039	0.014		-0.076	-0.037	-0.009	-0.048	0.032	-0.017

C) Week-wise distribution of wheat mean SAVI for 2021-22

Weeks past sowing	Wheat Polygon ID 2021-22														
	1	**2**	**3**	**4**	**5**	**6**	**7**	**8**	**9**	**10**	**11**	**12**	**13**	**14**	**15**
1		0.151									0.324				0.189
2			0.245	0.293		0.250	0.276	0.230	0.386						
3	0.179	0.259									0.297				0.595
4			0.576	0.304			0.515		0.606					0.423	
5	0.365				0.375					0.484		0.395	0.498		
6						0.777		0.615						0.663	
7		0.797			0.227	0.640		0.525		0.814	0.937	0.617	0.815		0.809
8		0.680	0.908	0.863			0.966		0.836		0.790				0.673
9	0.680		0.801	0.609			0.653		0.459						
10	0.452					0.393		0.449						0.843	
11		0.445			0.532	0.340		0.534		0.848	0.623	0.731	1.054	0.546	0.398
12		0.476	0.507	0.351	0.451		0.402		0.210	0.623	0.650	0.528	0.722		0.332
13	0.250		0.578	0.283		0.155	0.350	0.558	0.202						
14	0.207	0.232									0.469			0.336	0.259
15			0.308	0.146	0.346	0.139	0.247	0.415	0.184	0.325		0.227	0.309	0.250	
16	0.207	0.204			0.418	0.131		0.358		0.257	0.213	0.243	0.321		0.132
17		0.196	0.206	0.151		0.125	0.241	0.355	0.183		0.215			0.246	0.125

Table continued…

Weeks past sowing	Wheat Polygon ID 2021-22													SAVI Average
	16	17	18	19	20	21	22	23	24	25	26	27	28	
1					0.149	0.598		0.207		0.367			0.226	0.276
2			0.282	0.192					0.383					0.282
3					0.259	0.670				0.287			0.230	0.347
4							0.208				0.107	0.211		0.369
5	0.378	0.382						0.706						0.448
6			0.742	0.844			0.531	0.451	0.876		0.283	0.605		0.639
7	0.826	0.111	0.652	0.725	1.080	0.618			0.573	0.910			0.570	0.680
8					0.810	0.387				0.692			0.118	0.702
9								0.387						0.598
10			0.472	0.444			0.898	0.315	0.170		0.823	0.828		0.553
11	0.910	0.835	0.506	0.486	0.499	0.179	0.555		0.257	0.410	0.516	0.522	0.103	0.538
12	0.718	0.679			0.440	0.196		0.188		0.399			0.110	0.443
13			0.269	0.230					0.107					0.298
14					0.272	0.164	0.281	0.180		0.265	0.306	0.266	0.108	0.257
15	0.391	0.473	0.177	0.162			0.170	0.154	0.130		0.253	0.205		0.251
16	0.309	0.493	0.129	0.142	0.167	0.113		0.162	0.106	0.182			0.116	0.220
17			0.077	0.055	0.167	0.103	0.158		0.104	0.169	0.133	0.140	0.110	0.163

D) Week-wise distribution of wheat mean MSAVI2 for 2021-22

Weeks past sowing	Wheat Polygon ID 2021-22														
	1	**2**	**3**	**4**	**5**	**6**	**7**	**8**	**9**	**10**	**11**	**12**	**13**	**14**	**15**
1		0.183									0.305				0.224
2			0.281	0.163		0.382	0.209	0.266	0.384						
3	0.214	0.294									0.331				0.568
4			0.555	0.337			0.511		0.576					0.440	
5	0.271				0.393					0.488		0.396	0.481		
6						0.638		0.509						0.613	
7		0.798			0.141	0.598		0.532		0.703	0.817	0.583	0.704		0.785
8		0.624	0.850	0.731			0.783		0.716		0.690				0.620
9	0.658		0.696	0.577			0.607		0.469						
10	0.463					0.415		0.468						0.720	
11		0.458			0.615	0.370		0.527		0.823	0.587	0.713	0.826	0.534	0.420
12		0.482	0.505	0.379	0.574		0.422		0.246	0.587	0.605	0.521	0.650		0.363
13	0.285		0.556	0.318		0.188	0.378	0.545	0.237						
14	0.242	0.268									0.476			0.466	0.292
15			0.341	0.177	0.446	0.170	0.282	0.408	0.218	0.316		0.263	0.386	0.308	
16	0.242	0.239			0.557	0.160		0.389		0.293	0.248	0.279	0.352		0.162
17		0.201	0.241	0.183		0.135	0.277	0.285	0.218		0.230			0.282	0.133

Table continued…

Weeks past sowing	Wheat Polygon ID 2021-22													MSAVI2 Average
	16	17	18	19	20	21	22	23	24	25	26	27	28	
1					0.181	0.470		0.242		0.303			0.262	0.271
2			0.298	0.284					0.318					0.287
3					0.295	0.517				0.321			0.266	0.351
4							0.134				0.133	0.245		0.366
5	0.292	0.278						0.680						0.410
6			0.711	0.703			0.523	0.463	0.737		0.317	0.571		0.579
7	0.743	0.137	0.606	0.652	0.837	0.603			0.553	0.790			0.211	0.600
8					0.701	0.410				0.631			0.146	0.627
9								0.422						0.572
10			0.479	0.457			0.749	0.347	0.204		0.709	0.706		0.520
11	0.742	0.568	0.504	0.389	0.499	0.213	0.540		0.292	0.429	0.512	0.496	0.128	0.508
12	0.647	0.623			0.454	0.231		0.222		0.420			0.137	0.448
13			0.304	0.266					0.134					0.321
14					0.296	0.197	0.287	0.214		0.298	0.339	0.269	0.134	0.291
15	0.414	0.380	0.211	0.195			0.305	0.186	0.160		0.288	0.227		0.284
16	0.342	0.494	0.158	0.173	0.200	0.140		0.195	0.132	0.216			0.143	0.256
17			0.098	0.070	0.186	0.128	0.191		0.130	0.203	0.163	0.160	0.137	0.183

E) Week-wise distribution of wheat mean RVI for 2021-22

Weeks past sowing	Wheat Polygon ID 2021-22														
	1	**2**	**3**	**4**	**5**	**6**	**7**	**8**	**9**	**10**	**11**	**12**	**13**	**14**	**15**
1		1.224									1.551				1.289
2			1.390	1.195		1.222	1.565	1.199	1.923						
3	1.272	1.417									1.494				2.814
4			2.247	1.609			2.046		2.357					1.786	
5	1.572				1.614					1.972		1.893	1.796		
6						2.014		2.432						2.586	
7		4.961			1.165	2.489		2.137		3.372	4.475	2.400	3.382		4.651
8		2.660	6.665	3.713			4.615		3.517		3.224				2.629
9	2.662		3.294	2.366			2.543		2.882						
10	1.862					1.710		1.881						3.567	
11		1.845			2.595	1.586		2.114		4.641	2.420	3.482	4.734	2.146	1.724
12		1.930	2.021	1.612	2.347		1.732		1.326	2.423	2.530	2.086	2.855		1.569
13	1.399		2.254	1.466		1.231	1.608	2.197	1.311						
14	1.320	1.366									1.910			1.577	1.237
15			1.517	1.215	1.806	1.204	1.394	1.034	1.279	1.552		1.357	1.630	1.608	
16	1.319	1.315			2.255	1.191		1.636		1.414	1.330	1.387	1.544		1.193
17		1.301	1.318	1.225		1.182	1.383	1.626	1.278		1.335			1.392	1.181

Table continued…

Weeks past sowing	Wheat Polygon ID 2021-22													RVI Average
	16	17	18	19	20	21	22	23	24	25	26	27	28	
1					1.221	2.326		1.319		1.648			1.335	1.489
2			1.712	2.996					1.866					1.674
3					1.418	2.614				1.473			1.331	1.729
4							1.755				1.187	1.328		1.789
5	2.894	1.885						2.979						2.076
6			3.377	4.399			2.097	1.861	2.807		1.463	2.351		2.539
7	3.968	1.159	2.539	2.870	4.154	2.521			2.237	3.772			1.269	2.973
8					3.347	1.696				2.713			1.162	3.267
9								2.974						2.787
10			1.918	1.842			3.984	1.532	1.256		3.434	3.466		2.405
11	3.056	4.311	2.018	1.957	1.997	1.271	2.173		1.413	1.752	2.060	2.067	1.127	2.386
12	2.835	2.656			1.830	1.300		1.286		1.724			1.153	1.956
13			1.436	1.363					1.154					1.542
14					1.259	1.245	1.403	1.272		1.248	1.505	1.431	1.153	1.379
15	1.636	1.922	1.267	1.242			1.439	1.229	1.190		1.310	1.410		1.412
16	1.526	1.978	1.188	1.210	1.251	1.163		1.242	1.152	1.276			1.168	1.387
17			1.108	1.075	1.251	1.147	1.236		1.149	1.254	1.193	1.206	1.149	1.249

ANNEXURE III

ONION 2020-21

A) Week-wise distribution of *rabi* onion mean NDVI for 2020-21

Weeks Past Trans.	*Rabi* Onion Polygon ID 2020-21													
	1	**2**	**3**	**4**	**5**	**6**	**7**	**8**	**9**	**10**	**11**	**12**	**13**	**14**
1					0.052	0.129	0.123	0.154			0.170		0.122	0.130
2					0.088	0.209			0.084		0.354		0.154	0.139
3	0.093								0.224					
4	0.170			0.053						0.207		0.182		
5				0.109			0.164	0.169		0.265		0.231		
6		0.279	0.107		0.223	0.279	0.268	0.221			0.350		0.227	0.257
7		0.407	0.124		0.217	0.398			0.258	0.233	0.445	0.247	0.324	0.350
8	0.262						0.278	0.285	0.314					
9	0.280			0.293	0.301	0.383				0.378	0.316	0.473	0.342	0.365
10				0.344			0.436	0.460	0.352					
11	0.244	0.141	0.194		0.552	0.431				0.348	0.429	0.398	0.498	0.516
12		0.141	0.260	0.348			0.349	0.348	0.520	0.398		0.458		
13	0.386				0.398	0.277	0.418	0.371			0.360		0.394	0.439
14		0.196	0.313	0.462	0.412	0.271			0.416	0.172	0.441	0.319	0.449	0.432
15	0.302						0.333	0.282	0.386	0.283		0.297		
16	0.275	0.332	0.302	0.300	0.344	0.134	0.139	0.161			0.216		0.236	0.209

Table continued…

Weeks Past Trans.	*Rabi* Onion Polygon ID 2020-21												NDVI Average
	15	**16**	**17**	**18**	**19**	**20**	**21**	**22**	**23**	**24**	**25**	**26**	
1				0.148	0.126	0.156	0.145					0.052	0.126
2						0.151	0.162					0.112	0.161
3										0.178			0.165
4	0.174	0.161	0.136					0.212	0.462	0.231	0.162		0.195
5	0.245	0.232	0.197	0.159	0.131			0.294	0.580		0.223		0.231
6				0.299	0.180	0.205	0.304			0.270		0.231	0.247
7	0.317	0.311	0.257			0.332	0.396	0.304	0.481		0.248	0.299	0.313
8				0.357	0.288					0.453			0.320
9	0.523	0.471	0.486			0.382	0.368	0.407	0.493		0.390	0.320	0.387
10				0.469	0.381					0.393			0.405
11	0.452	0.398	0.419			0.542	0.537	0.376	0.203	0.441	0.344	0.488	0.398
12	0.486	0.433	0.457	0.404	0.382			0.421	0.127		0.365		0.369
13				0.442	0.424	0.434	0.434			0.347		0.355	0.391
14	0.413	0.273	0.392			0.217	0.505	0.404	0.096	0.172	0.193	0.421	0.332
15	0.396	0.268	0.372	0.282	0.294			0.321	0.119		0.183		0.294
16				0.187	0.183	0.122	0.202					0.171	0.220

B) Week-wise distribution of *rabi* onion mean NDWI for 2020-21

Weeks Past Trans.	*Rabi* Onion Polygon ID 2020-21													
	1	**2**	**3**	**4**	**5**	**6**	**7**	**8**	**9**	**10**	**11**	**12**	**13**	**14**
1					0.056	-0.032	-0.080	0.013			0.176		0.009	0.053
2					-0.028	0.049			0.075		0.097		0.030	-0.069
3	0.043								0.030					
4	0.036			0.036						0.041		0.082		
5				-0.034			-0.015	-0.041		0.060		0.059		
6		0.319	0.192		0.045	0.129	0.087	0.043			0.123		0.068	0.183
7		0.297	0.097		0.090	0.261			0.033	0.100	0.209	0.199	0.158	0.123
8	0.053						0.158	0.198	0.091					
9	0.069			0.170	0.171	0.287				0.152	0.209	0.289	0.263	0.211
10				0.189			0.224	0.239	0.245					
11	0.009	0.100	0.143		0.226	0.193				0.175	0.183	0.311	0.318	0.249
12		0.057	0.186	0.276			0.253	0.189	0.273	0.171		0.307		
13	0.074				0.312	0.104	0.250	0.170			0.232		0.268	0.270
14		0.089	0.271	0.309	0.246	0.076			0.345	-0.031	0.265	0.145	0.240	0.238
15	0.054						0.136	0.021	0.059	0.073		0.003		
16	-0.005	0.199	0.229	0.212	0.141	-0.079	-0.083	-0.014			-0.048		0.016	0.017

Table continued…

Weeks Past Trans.	*Rabi* Onion Polygon ID 2020-21												NDWI Average
	15	16	17	18	19	20	21	22	23	24	25	26	
1				0.006	-0.046	-0.031	0.053					0.023	0.017
2						-0.016	0.019					0.073	0.026
3										0.022			0.032
4	0.051	0.011	0.020					-0.004	0.117	0.044	-0.008		0.039
5	0.029	-0.004	0.082	0.106	0.019			0.056	0.164		0.053		0.041
6				0.151	0.048	0.042	0.136			0.084		0.163	0.121
7	0.076	0.164	0.186			0.119	0.197	0.128	0.130		0.069	0.204	0.149
8				0.154	0.194					0.286			0.162
9	0.299	0.261	0.340			0.242	0.255	0.185	0.133		0.120	0.320	0.221
10				0.198	0.229					0.268			0.227
11	0.223	0.233	0.350			0.373	0.341	0.205	0.038	0.268	0.112	0.342	0.220
12	0.226	0.250	0.334	0.225	0.275			0.259	-0.114		0.126		0.206
13				0.183	0.286	0.235	0.328			0.191		0.301	0.229
14	0.185	0.043	0.191			0.064	0.295	0.204	-0.128	0.028	-0.001	0.268	0.159
15	0.004	-0.075	0.187	-0.033	0.016			0.045	0.136		-0.007		0.044
16				-0.053	0.001	-0.047	-0.012					0.048	0.033

C) Week-wise distribution of *rabi* onion mean SAVI for 2020-21

Weeks Past Trans.	*Rabi* Onion Polygon ID 2020-21													
	1	**2**	**3**	**4**	**5**	**6**	**7**	**8**	**9**	**10**	**11**	**12**	**13**	**14**
1					0.078	0.193	0.185	0.231			0.254		0.183	0.195
2					0.131	0.313			0.126		0.531		0.231	0.208
3	0.139								0.335					
4	0.255			0.079						0.311		0.272		
5				0.163			0.246	0.253		0.397		0.346		
6		0.418	0.161		0.334	0.419	0.402	0.331			0.525		0.340	0.385
7		0.610	0.187		0.325	0.597			0.387	0.350	0.667	0.371	0.485	0.524
8	0.392						0.417	0.428	0.470					
9	0.420			0.439	0.451	0.574				0.567	0.474	0.710	0.513	0.548
10				0.516			0.654	0.690	0.528					
11	0.366	0.211	0.291		0.828	0.647				0.522	0.644	0.597	0.747	0.774
12		0.212	0.390	0.521			0.523	0.522	0.780	0.597		0.687		
13	0.579				0.598	0.416	0.627	0.557			0.539		0.591	0.659
14		0.293	0.469	0.693	0.617	0.406			0.624	0.172	0.662	0.319	0.673	0.648
15	0.453						0.333	0.242	0.428	0.275		0.235		
16	0.412	0.948	0.753	0.601	0.344		0.209	0.241			0.216		0.236	0.209

Table continued…

Weeks Past Trans.	*Rabi* Onion Polygon ID 2020-21												SAVI Average
	15	16	17	18	19	20	21	22	23	24	25	26	
1				0.222	0.188	0.233	0.217					0.079	0.188
2						0.227	0.242					0.168	0.242
3										0.267			0.247
4	0.261	0.242	0.204					0.318	0.692	0.346	0.284		0.297
5	0.368	0.348	0.296	0.239	0.196			0.441	0.870		0.356		0.348
6				0.448	0.271	0.307	0.455			0.405		0.347	0.370
7	0.476	0.466	0.386			0.498	0.594	0.455	0.721		0.396	0.449	0.471
8				0.461	0.372					0.680			0.460
9	0.785	0.706	0.729			0.574	0.552	0.611	0.740		0.559	0.480	0.580
10				0.704	0.571					0.590			0.608
11	0.678	0.597	0.628			0.813	0.805	0.564	0.304	0.661	0.465	0.732	0.594
12	0.728	0.649	0.686	0.607	0.573			0.631	0.190		0.493		0.549
13				0.662	0.636	0.650	0.651			0.347		0.532	0.575
14	0.413	0.273	0.392			0.326	0.758	0.404	0.096	0.259	0.201	0.631	0.444
15	0.339	0.176	0.543	0.222	0.214			0.332	0.178		0.300		0.305
16				0.281	0.274	0.122	0.202					0.171	0.348

D) Week-wise distribution of *rabi* onion mean MSAVI2 for 2020-21

Weeks Past Trans.	*Rabi* Onion Polygon ID 2020-21													
	1	**2**	**3**	**4**	**5**	**6**	**7**	**8**	**9**	**10**	**11**	**12**	**13**	**14**
1					0.098	0.228	0.220	0.267			0.290		0.218	0.230
2					0.161	0.345			0.155		0.523		0.267	0.243
3	0.170								0.365					
4	0.290			0.100						0.343		0.307		
5				0.196			0.281	0.289		0.419		0.375		
6		0.436	0.194		0.364	0.437	0.423	0.362			0.519		0.370	0.409
7		0.578	0.221		0.356	0.569			0.411	0.378	0.616	0.396	0.489	0.518
8	0.415						0.435	0.444	0.477					
9	0.438			0.453	0.463	0.554				0.549	0.480	0.642	0.510	0.535
10				0.512			0.607	0.630	0.521					
11	0.392	0.247	0.325		0.712	0.602				0.516	0.601	0.570	0.665	0.681
12		0.248	0.413	0.516			0.517	0.516	0.684	0.569		0.628		
13	0.557				0.570	0.434	0.589	0.541			0.529		0.565	0.610
14		0.327	0.476	0.632	0.583	0.426			0.588	0.294	0.612	0.484	0.620	0.603
15	0.464						0.500	0.390	0.444	0.310		0.271		
16	0.431	0.775	0.669	0.572	0.512	0.237	0.244	0.277			0.356		0.381	0.346

Table continued…

Weeks Past Trans.	*Rabi* Onion Polygon ID 2020-21												MSAVI2 Average
	15	16	17	18	19	20	21	22	23	24	25	26	
1				0.257	0.223	0.269	0.253					0.100	0.221
2						0.262	0.278					0.201	0.271
3										0.303			0.279
4	0.297	0.278	0.239					0.350	0.632	0.375	0.318		0.321
5	0.394	0.377	0.329	0.275	0.231			0.454	0.734		0.383		0.364
6				0.460	0.306	0.340	0.466			0.425		0.376	0.392
7	0.482	0.474	0.409			0.499	0.567	0.466	0.649		0.418	0.460	0.471
8				0.470	0.397					0.624			0.466
9	0.687	0.640	0.654			0.553	0.538	0.579	0.661		0.543	0.485	0.554
10				0.639	0.551					0.565			0.575
11	0.623	0.569	0.590			0.703	0.698	0.547	0.337	0.612	0.473	0.656	0.556
12	0.654	0.604	0.628	0.576	0.553			0.592	0.225		0.494		0.526
13				0.613	0.595	0.605	0.606			0.515		0.524	0.561
14	0.585	0.429	0.563			0.357	0.671	0.575	0.175	0.294	0.334	0.592	0.487
15	0.368	0.210	0.531	0.364	0.352			0.362	0.212		0.333		0.365
16				0.315	0.309	0.217	0.337					0.293	0.392

E) Week-wise distribution of *rabi* onion mean RVI for 2020-21

Weeks Past Trans.	*Rabi* Onion Polygon ID 2020-21													
	1	**2**	**3**	**4**	**5**	**6**	**7**	**8**	**9**	**10**	**11**	**12**	**13**	**14**
1					1.109	1.296	1.282	1.364			1.409		1.279	1.299
2					1.192	1.527			1.184		2.097		1.365	1.322
3	1.205								1.576					
4	1.409			1.111						1.523		1.444		
5				1.244			1.392	1.406		1.721		1.601		
6		1.772	1.241		1.574	1.776	1.732	1.567			2.078		1.587	1.692
7		2.373	1.284		1.554	2.321			1.697	1.608	2.602	1.657	1.957	2.075
8	1.708						1.870	1.798	1.914					
9	1.778			1.827	1.861	2.241				2.215	1.925	2.796	2.039	2.150
10				2.048			2.545	2.705	2.086					
11	1.645	1.328	1.481		3.467	2.516				2.067	2.505	2.324	2.983	3.131
12		1.329	1.704	2.065			2.072	2.067	3.167	2.321		2.688		
13	2.257				2.325	1.768	2.436	2.181			2.123		2.301	2.566
14		1.486	1.910	2.716	2.400	1.743			2.427	1.417	2.578	1.937	2.630	2.521
15	1.866						1.998	1.639	1.800	1.449		1.372		
16	1.757	2.437	2.019	2.336	2.049	1.310	1.323	1.384			1.552		1.616	1.529

Table continued…

Weeks Past Trans.	*Rabi* Onion Polygon ID 2020-21												RVI Average
	15	16	17	18	19	20	21	22	23	24	25	26	
1				1.347	1.287	1.368	1.339					1.111	1.291
2						1.356	1.386					1.252	1.409
3										1.434			1.405
4	1.422	1.385	1.314					1.539	2.715	1.601	1.467		1.539
5	1.550	1.605	1.491	1.379	1.301			1.633	3.766		1.522		1.662
6				1.851	1.440	1.515	1.872			1.740		1.602	1.669
7	1.929	1.902	1.692			1.994	2.310	1.872	2.851		1.717	1.854	1.960
8				1.887	1.760					2.858			1.971
9	3.195	2.780	2.890			2.238	2.166	2.373	2.948		2.189	1.942	2.309
10				2.768	2.429					2.497			2.440
11	2.650	2.321	2.440			3.065	3.316	2.207	1.509	2.577	1.899	2.509	2.397
12	2.889	2.527	2.686	2.358	2.238			2.453	1.291		1.978		2.240
13				2.581	2.471	2.531	2.536			2.063		2.100	2.303
14	2.409	1.751	2.287			1.555	3.042	2.354	1.212	1.417	1.502	2.453	2.083
15	1.583	1.267	2.134	1.572	1.543			1.568	1.270		1.500		1.612
16				1.460	1.448	1.277	1.507					1.414	1.651

ONION 2021-22

A) Week-wise distribution of *rabi* onion mean NDVI for 2021-22

Weeks Past Trans.	*Rabi* Onion Polygon ID 2021-22														
	1	**2**	**3**	**4**	**5**	**6**	**7**	**8**	**9**	**10**	**11**	**12**	**13**	**14**	**15**
1	0.117			0.085				0.115			0.164			0.217	
2			0.162				0.214		0.200				0.112		
3	0.132			0.112	0.297	0.185		0.244		0.126		0.243	0.106		
4		0.160			0.203	0.113				0.109		0.135			0.239
5		0.118									0.191			0.272	0.182
6			0.324				0.175		0.220		0.139		0.194	0.203	
7	0.114		0.259	0.174	0.176	0.170	0.122	0.171	0.158	0.172		0.202	0.356		
8	0.091	0.179		0.150	0.239	0.228		0.143		0.215		0.248			0.200
9		0.241									0.180		0.272	0.305	0.238
10			0.219		0.256	0.249	0.145		0.219	0.234	0.258	0.297		0.360	
11	0.146	0.271	0.268	0.156			0.190	0.194	0.301				0.314		0.275
12	0.205			0.242	0.243	0.234		0.246		0.250	0.226	0.269	0.276	0.274	
13		0.252	0.190		0.195	0.202	0.225		0.328	0.244		0.120	0.310		0.247
14	0.269	0.198		0.290	0.143	0.153		0.235		0.179	0.262	0.084		0.259	0.203
15		0.178	0.087				0.238		0.317		0.285			0.293	0.146
16	0.204		0.076	0.198			0.117	0.144	0.247		0.163			0.136	

Table continued…

Weeks Past Trans.	*Rabi* Onion Polygon ID 2021-22													NDVI Average
	16	**17**	**18**	**19**	**20**	**21**	**22**	**23**	**24**	**25**	**26**	**27**	**28**	
1		0.155		0.085	0.129		0.089		0.154			0.191		0.136
2	0.193					0.163				0.088				0.162
3	0.102		0.149											0.170
4			0.098				0.114	0.228	0.160		0.081		0.279	0.160
5		0.194		0.218	0.177			0.183		0.115		0.298	0.128	0.189
6	0.125	0.178		0.141	0.155	0.204					0.185	0.350		0.199
7	0.185		0.193			0.155	0.340		0.286					0.202
8			0.269			0.223	0.232	0.252	0.198	0.281			0.180	0.208
9	0.216	0.236		0.212	0.216	0.254		0.289		0.224		0.285	0.224	0.242
10		0.379	0.235	0.281	0.266						0.332	0.313		0.270
11	0.278					0.375	0.376	0.258	0.200		0.201		0.234	0.252
12	0.198	0.301	0.259	0.300	0.293		0.305		0.278	0.205		0.209		0.253
13	0.210		0.237			0.299		0.254		0.263			0.232	0.238
14		0.231	0.288	0.338	0.324	0.265	0.284	0.222	0.327		0.196	0.262	0.166	0.235
15		0.156		0.231	0.291	0.090		0.158		0.198	0.254	0.202	0.134	0.204
16		0.134		0.188	0.248		0.216		0.258			0.201		0.181

B) Week-wise distribution of *rabi* onion mean NDWI for 2021-22

Weeks Past Trans.	*Rabi* Onion Polygon ID 2021-22														
	1	**2**	**3**	**4**	**5**	**6**	**7**	**8**	**9**	**10**	**11**	**12**	**13**	**14**	**15**
1	-0.058			-0.008				0.002			0.017			0.070	
2			0.042				0.071		0.007				0.029		
3	-0.074			0.081	0.125	0.000		0.016		-0.042		0.107	0.004		
4		0.070			0.120	0.013				0.008		0.052			0.074
5		0.031									0.044			0.120	0.064
6			0.144				0.009		-0.004		0.027		0.113	0.119	
7	-0.075		0.147	-0.005	0.117	0.119	0.042	-0.027	0.010	0.084		0.126	0.208		
8	-0.037	0.137		0.068	0.152	0.152		0.030		0.121		0.156			0.108
9		0.160									0.102		0.169	0.284	0.132
10			0.192		0.154	0.178	0.048		0.157	0.135	0.144	0.192		0.306	
11	0.029	0.174	0.182	0.101			0.083	0.087	0.192				0.195		0.148
12	0.030			0.147	0.130	0.138		0.147		0.136	0.180	0.146	0.170	0.228	
13		0.158	0.053		0.099	0.096	0.105		0.213	0.114		-0.005	0.181		0.123
14	0.126	0.090		0.163	0.026	0.018		0.119		0.025	0.224	-0.037		0.212	0.099
15		0.053	-0.038				0.126		0.184		0.172			0.196	0.017
16	0.101		-0.044	0.105			0.054	-0.051	0.083		0.098			0.114	

Table continued…

Weeks Past Trans.	*Rabi* Onion Polygon ID 2021-22													NDWI Average
	16	17	18	19	20	21	22	23	24	25	26	27	28	
1		-0.102		-0.116	-0.044		0.039		0.039			0.286		0.011
2	-0.036					-0.028				0.083				0.024
3	0.012		0.027				0.028		0.037					0.027
4			0.009					0.038		0.005	0.145		-0.016	0.047
5		-0.143		0.022	0.014			0.076				0.278	0.019	0.053
6	0.045	0.006		0.018	0.036	-0.023					0.124	0.203		0.063
7	0.069		0.100			0.019	0.188		0.098					0.076
8			0.163				0.150	0.177	0.114	0.125			0.084	0.113
9	0.096	0.098		0.091	0.114			0.202		0.117		0.168	0.102	0.141
10		0.120	0.132	0.131	0.151	0.089					0.213	0.169		0.157
11	0.173					0.190	0.241	0.147	0.253		0.153		0.090	0.152
12	0.090	0.145	0.132	0.121	0.157		0.158		0.194	0.176		0.126		0.145
13	0.084		0.105			0.147		0.185		0.224			0.095	0.124
14		0.139	0.128	0.161	0.173		0.114	0.053	0.222		0.179	0.091	0.058	0.113
15		-0.007		0.072	0.130	0.113		-0.002		0.087	0.106	0.049	0.025	0.080
16		-0.008		-0.007	0.046	-0.020	0.073		0.139			0.043		0.048

C) Week-wise distribution of *rabi* onion mean SAVI for 2021-22

Weeks Past Trans.	*Rabi* Onion Polygon ID 2021-22														
	1	**2**	**3**	**4**	**5**	**6**	**7**	**8**	**9**	**10**	**11**	**12**	**13**	**14**	**15**
1	0.176			0.127				0.172			0.246			0.325	
2			0.243				0.222		0.200				0.317		
3	0.198			0.168	0.445	0.232		0.306		0.189		0.365	0.159		
4		0.240			0.304	0.170				0.163		0.203			0.358
5		0.177									0.287			0.409	0.273
6			0.486				0.262		0.330		0.209		0.291	0.304	
7	0.171		0.388	0.261	0.264	0.255	0.183	0.257	0.237	0.257		0.303	0.473		
8	0.137	0.268		0.225	0.359	0.341		0.215		0.322		0.372			0.299
9		0.362									0.271		0.408	0.457	0.358
10			0.328		0.383	0.374	0.267		0.329	0.351	0.388	0.445		0.540	
11	0.220	0.406	0.403	0.234			0.285	0.292	0.452				0.471		0.412
12	0.308			0.363	0.364	0.352		0.369		0.375	0.489	0.403	0.413	0.460	
13		0.377	0.285		0.293	0.303	0.338		0.493	0.366		0.179	0.465		0.371
14	0.403	0.297		0.435	0.215	0.230		0.353		0.269	0.543	0.126		0.383	0.304
15		0.266	0.131				0.356		0.475		0.427			0.240	0.219
16	0.356		0.115	0.346			0.326	0.216	0.371		0.395			0.154	

Table continued…

Weeks Past Trans.	*Rabi* Onion Polygon ID 2021-22													SAVI Average
	16	**17**	**18**	**19**	**20**	**21**	**22**	**23**	**24**	**25**	**26**	**27**	**28**	
1		0.232		0.128	0.193		0.134		0.230			0.386		0.214
2	0.190					0.245				0.132				0.221
3	0.154		0.223				0.171		0.239					0.237
4			0.147					0.342		0.273	0.221		0.268	0.244
5		0.291		0.327	0.265			0.275				0.446	0.192	0.294
6	0.187	0.266		0.212	0.233	0.307					0.277	0.508		0.298
7	0.277		0.260			0.233	0.510		0.328					0.291
8			0.404				0.349	0.379	0.296	0.422			0.226	0.308
9	0.324	0.355		0.318	0.325			0.434		0.336		0.427	0.337	0.362
10		0.488	0.382	0.421	0.399	0.375					0.498	0.469		0.402
11	0.358					0.380	0.414	0.387	0.300		0.302		0.351	0.354
12	0.298	0.451	0.388	0.450	0.440		0.458		0.416	0.307		0.463		0.398
13	0.316		0.355			0.412		0.531		0.395			0.348	0.364
14		0.396	0.232	0.307	0.386		0.426	0.333	0.491		0.295	0.393	0.249	0.336
15		0.234		0.346	0.236	0.348		0.237		0.296	0.381	0.303	0.200	0.293
16		0.201		0.177	0.222	0.197	0.255		0.237			0.201		0.251

D) Week-wise distribution of *rabi* onion mean MSAVI2 for 2021-22

Weeks Past Trans.	*Rabi* Onion Polygon ID 2021-22														
	1	**2**	**3**	**4**	**5**	**6**	**7**	**8**	**9**	**10**	**11**	**12**	**13**	**14**	**15**
1	0.210			0.156				0.206			0.282			0.356	
2			0.279				0.353		0.334				0.149		
3	0.233			0.201	0.358	0.268		0.339		0.223		0.391	0.191		
4		0.276			0.387	0.293				0.196		0.238			0.385
5		0.211									0.321			0.428	0.308
6			0.489				0.298		0.361		0.245		0.325	0.337	
7	0.205		0.411	0.296	0.299	0.291	0.317	0.292	0.373	0.293		0.336	0.480		
8	0.167	0.303		0.261	0.386	0.371		0.251		0.353		0.397			0.333
9		0.389									0.306		0.428	0.467	0.385
10			0.359		0.407	0.399	0.253		0.460	0.479	0.411	0.457		0.530	
11	0.255	0.426	0.423	0.270			0.319	0.325	0.463				0.478		0.431
12	0.341			0.390	0.390	0.380		0.395		0.400	0.492	0.424	0.432	0.444	
13		0.402	0.319		0.327	0.336	0.368		0.494	0.392		0.214	0.473		0.396
14	0.424	0.330		0.450	0.250	0.266		0.381		0.304	0.432	0.155		0.460	0.337
15		0.302	0.161				0.384		0.481		0.343			0.353	0.254
16	0.466		0.142	0.459			0.357	0.252	0.296		0.217			0.282	

Table continued…

Weeks Past Trans.	*Rabi* Onion Polygon ID 2021-22													MSAVI2 Average
	16	**17**	**18**	**19**	**20**	**21**	**22**	**23**	**24**	**25**	**26**	**27**	**28**	
1		0.208		0.157	0.228		0.164		0.266			0.443		0.243
2	0.224					0.281				0.161				0.254
3	0.186		0.259				0.205		0.275					0.261
4			0.179					0.372		0.207	0.149		0.303	0.271
5		0.331		0.358	0.300			0.310				0.448	0.227	0.324
6	0.222	0.287		0.247	0.269	0.339					0.312	0.570		0.331
7	0.312		0.295			0.298	0.507		0.341					0.334
8			0.424				0.377	0.403	0.330	0.439			0.261	0.337
9	0.355	0.365		0.350	0.356			0.449		0.366		0.443	0.367	0.387
10		0.417	0.380	0.438	0.420	0.365					0.498	0.476		0.422
11	0.385					0.404	0.432	0.410	0.333		0.335		0.379	0.379
12	0.331	0.463	0.311	0.462	0.453		0.408		0.434	0.340		0.472		0.409
13	0.348		0.383			0.431		0.523		0.417			0.377	0.388
14		0.504	0.447	0.505	0.489		0.442	0.363	0.493		0.328	0.415	0.284	0.384
15		0.287		0.375	0.450	0.460		0.273		0.330	0.405	0.336	0.236	0.339
16		0.208		0.211	0.258	0.319	0.481		0.227			0.234		0.294

E) Week-wise distribution of *rabi* onion mean RVI for 2021-22

Weeks Past Trans.	*Rabi* Onion Polygon ID 2021-22														
	1	**2**	**3**	**4**	**5**	**6**	**7**	**8**	**9**	**10**	**11**	**12**	**13**	**14**	**15**
1	1.266			1.185				1.259			1.392			1.553	
2			1.387				1.546		1.501				1.537		
3	1.305			1.252	1.844	1.366		1.513		1.388		1.643	1.237		
4		1.380			1.609	1.455				1.244		1.613			1.627
5		1.268									1.473			1.749	1.444
6			1.959				1.424		1.565		1.324		1.482	1.509	
7	1.257		1.698	1.421	1.426	1.410	1.278	1.413	1.375	1.414		1.507	1.922		
8	1.201	1.435		1.353	1.629	1.590		1.334		1.547		1.659			1.499
9		1.637									1.440		1.748	1.876	1.626
10			1.560		1.686	1.664	1.339		1.561	1.611	1.697	1.843		2.126	
11	1.343	1.743	1.734	1.369			1.469	1.483	1.863				1.916		1.757
12	1.517			1.638	1.640	1.613		1.652		1.666	1.968	1.735	1.761	1.193	
13		1.672	1.468		1.485	1.506	1.582		1.978	1.645		1.272	1.898		1.657
14	1.735	1.494		1.817	1.334	1.362		1.616		1.437	1.836	1.184		1.273	1.509
15		1.432	1.192				1.623		1.527		1.596			1.830	1.341
16	1.472		1.166	1.648			1.255	1.236	1.457		1.514			1.617	

Table continued…

Weeks Past Trans.	*Rabi* Onion Polygon ID 2021-22													RVI Average
	16	**17**	**18**	**19**	**20**	**21**	**22**	**23**	**24**	**25**	**26**	**27**	**28**	
1		1.263		1.187	1.296		1.196		1.363			2.584		1.413
2	1.479					1.390				1.193				1.433
3	1.228		1.431				1.457		1.580					1.437
4			1.535					1.692		1.361	1.275		1.435	1.475
5		1.496		1.559	1.429			1.448				2.072	1.294	1.523
6	1.286	1.403		1.328	1.367	1.514					1.653	2.325		1.549
7	1.554		1.719			1.467	2.030		1.518					1.526
8			1.760				1.606	1.675	1.492	1.782			1.354	1.528
9	1.551	1.574		1.538	1.552			1.815		1.576		1.795	1.579	1.639
10		1.717	1.609	1.780	1.725	1.574					1.994	1.909		1.712
11	1.626					1.679	1.762	1.696	1.499		1.504		1.911	1.647
12	1.495	1.862	1.705	1.857	1.830		1.878		1.768	1.515		1.793		1.689
13	1.533		1.677			1.758		2.098		1.714			1.604	1.659
14		2.016	1.926	2.021	1.958		1.794	1.571	1.972		1.489	1.710	1.398	1.641
15		1.402		1.600	1.820	1.853		1.375		1.493	1.681	1.506	1.309	1.536
16		1.262		1.468	1.548	1.721	1.926		1.614			1.502		1.494

ANNEXURE IV

WATER DEMAND CALCULATIONS (WHEAT)

I. Water demand of wheat for year 2020-21

a) Water demand calculations for wheat in Dhule district.

Met. Week	Month	Dates	Weeks Past Sowing	ETo (mm/day)	ETo Week (mm)	VI (NDWI)	Kc by NDWI	ETc = (ETo x Kc) (mm)	Crop Acreage (ha)	Water Demand (m^3)	Water Demand (Mm^3)
45	Nov.	05-11	1	3.56	24.91	0.117	0.85	21.20	44386	9411350	9.41
46		12-18	2	3.47	24.30	0.128	0.88	21.50	44386	9545162	9.55
47		19-25	3	3.31	23.16	0.138	0.91	21.17	44386	9398180	9.40
48		26-02	4	3.48	24.39	0.195	1.09	26.58	44386	11796310	11.80
49	Dec.	03-09	5	3.86	27.02	0.235	1.21	32.79	44386	14554937	14.55
50		10-16	6	2.49	17.44	0.269	1.32	22.97	44386	10194788	10.19
51		17-23	7	3.46	24.19	0.294	1.39	33.69	44386	14954701	14.95
52		24-31	8	3.59	25.16	0.299	1.41	35.44	44386	15729184	15.73
1	Jan.	01-07	9	3.21	22.45	0.283	1.36	30.53	44386	13549232	13.55
2		08-14	10	3.64	25.51	0.285	1.37	34.87	44386	15475614	15.48
3		15-21	11	4.08	28.58	0.244	1.24	35.46	44386	15738619	15.74
4		22-28	12	4.21	29.44	0.199	1.10	32.47	44386	14412041	14.41
5		29-04	13	4.91	34.36	0.106	0.82	28.14	44386	12489094	12.49
6	Feb.	05-11	14	4.95	34.63	0.059	0.67	23.31	44386	10348247	10.35
7		12-18	15	4.82	33.76	-0.001	0.49	16.53	44386	-	-
8		19-25	16	5.34	37.41	-0.016	0.44	16.64	44386	-	-
9		26-04	17	6.45	45.15	-0.043	0.36	16.36	44386	-	-
							Total	**449.65**	**44386**	**177597458.06**	**177.60**

***Mm^3-** Million Cubic Meters

*Since water is needed only up to physiological maturity, water demand calculations are done only up to 14th week

b) Water demand calculations for wheat in Jalgaon district.

Met. Week	Month	Dates	Weeks Past Sowing	ETo (mm/day)	ETo Week (mm)	VI (NDWI)	Kc by NDWI	ETc = (ETo x Kc) (mm)	Crop Acreage (ha)	Water Demand (m^3)	Water Demand (Mm^3)
45	Nov.	05-11	1	3.29	23.04	0.117	0.85	19.61	67927	13323597	13.32
46		12-18	2	3.25	22.73	0.128	0.88	20.11	67927	13662904	13.66
47		19-25	3	3.16	22.12	0.138	0.91	20.23	67927	13738860	13.74
48		26-02	4	3.31	23.16	0.195	1.09	25.23	67927	17139793	17.14
49	Dec.	03-09	5	3.64	25.45	0.235	1.21	30.89	67927	20981857	20.98
50		10-16	6	2.42	16.92	0.269	1.32	22.28	67927	15136089	15.14
51		17-23	7	3.31	23.15	0.294	1.39	32.23	67927	21894586	21.89
52		24-31	8	3.44	24.06	0.299	1.41	33.89	67927	23020173	23.02
1	Jan.	01-07	9	3.25	22.77	0.283	1.36	30.96	67927	21027119	21.03
2		08-14	10	3.49	24.40	0.285	1.37	33.35	67927	22651880	22.65
3		15-21	11	4.30	30.08	0.244	1.24	37.31	67927	25345286	25.35
4		22-28	12	4.33	30.31	0.199	1.10	33.43	67927	22706592	22.71
5		29-04	13	5.12	35.85	0.106	0.82	29.36	67927	19944398	19.94
6	Feb.	05-11	14	5.00	35.03	0.059	0.67	23.58	67927	16016713	16.02
7		12-18	15	4.77	33.41	-0.001	0.49	16.36	67927	-	-
8		19-25	16	5.24	36.69	-0.016	0.44	16.32	67927	-	-
9		26-04	17	6.22	43.52	-0.043	0.36	15.77	67927	-	-
							Total	**440.92**	**67927**	**266589846.86**	**266.59**

Mm^3- Million Cubic Meters

*Since water is needed only up to physiological maturity, water demand calculations are done only up to 14^{th} week

c) Water demand calculations for wheat in Nashik district.

Met. Week	Month	Dates	Weeks Past Sowing	ETo (mm/day)	ETo Week (mm)	VI (NDWI)	Kc by NDWI	ETc = (ETo x Kc) (mm)	Crop Acreage (ha)	Water Demand (m^3)	Water Demand (Mm^3)
45	Nov.	05-11	1	3.51	24.55	0.117	0.85	20.89	60590	12658945	12.66
46		12-18	2	3.16	22.14	0.128	0.88	19.59	60590	11868176	11.87
47		19-25	3	3.07	21.48	0.138	0.91	19.64	60590	11902481	11.90
48		26-02	4	3.22	22.53	0.195	1.09	24.55	60590	14876106	14.88
49	Dec.	03-09	5	3.65	25.55	0.235	1.21	31.02	60590	18793372	18.79
50		10-16	6	2.27	15.88	0.269	1.32	20.91	60590	12672264	12.67
51		17-23	7	3.42	23.92	0.294	1.39	33.31	60590	20181843	20.18
52		24-31	8	3.37	23.62	0.299	1.41	33.26	60590	20150619	20.15
1	Jan.	01-07	9	2.57	17.97	0.283	1.36	24.44	60590	14806544	14.81
2		08-14	10	3.21	22.50	0.285	1.37	30.75	60590	18633384	18.63
3		15-21	11	3.90	27.32	0.244	1.24	33.89	60590	20534374	20.53
4		22-28	12	4.54	31.78	0.199	1.10	35.05	60590	21234902	21.23
5		29-04	13	4.76	33.30	0.106	0.82	27.27	60590	16522961	16.52
6	Feb.	05-11	14	5.42	37.92	0.059	0.67	25.52	60590	15464933	15.46
7		12-18	15	4.72	33.05	-0.001	0.49	16.19	60590	-	-
8		19-25	16	5.44	38.11	-0.016	0.44	16.95	60590	-	-
9		26-04	17	6.28	43.97	-0.043	0.36	15.93	60590	-	-
							Total	**429.16**	**60590**	**230300903.86**	**230.30**

Mm^3- Million Cubic Meters

*Since water is needed only up to physiological maturity, water demand calculations are done only up to 14^{th} week

II. Water demand of wheat for year 2021-22

a) Water demand calculations for *rabi* wheat in Dhule district.

Met. Week	Month	Dates	Weeks Past Sowing	ETo (mm/day)	ETo Week (mm)	NDWI	Kc by NDWI	ETc = (ETo x Kc) (mm)	Crop Acreage (ha)	Water Demand (m^3)	Water Demand (Mm^3)
45	Nov.	05-11	1	3.53	24.73	0.074	0.68	16.89	45384	7666535	7.67
46		12-18	2	3.31	23.14	0.098	0.79	18.18	45384	8251720	8.25
47		19-25	3	3.08	21.59	0.155	1.03	22.15	45384	10053512	10.05
48		26-02	4	3.00	20.97	0.160	1.05	22.01	45384	9990232	9.99
49	Dec.	03-09	5	2.74	19.17	0.178	1.13	21.57	45384	9790056	9.79
50		10-16	6	3.04	21.27	0.229	1.34	28.50	45384	12936361	12.94
51		17-23	7	3.18	22.27	0.241	1.39	30.93	45384	14038801	14.04
52		24-31	8	3.17	22.16	0.247	1.42	31.42	45384	14261816	14.26
1	Jan.	01-07	9	3.37	23.62	0.231	1.35	31.89	45384	14472112	14.47
2		08-14	10	3.55	24.82	0.224	1.32	32.72	45384	14849799	14.85
3		15-21	11	4.13	28.88	0.219	1.30	37.50	45384	17019644	17.02
4		22-28	12	4.20	29.37	0.195	1.20	35.12	45384	15939582	15.94
5		29-04	13	4.77	33.38	0.094	0.77	25.66	45384	11643550	11.64
6	Feb.	05-11	14	4.73	33.09	0.069	0.67	22.02	45384	9994750	9.99
7		12-18	15	4.79	33.52	0.072	0.67	22.60	45384	-	-
8		19-25	16	5.51	38.56	0.040	0.54	20.89	45384	-	-
9		26-04	17	5.50	38.53	-0.017	0.30	11.55	45384	-	-
							Total	**431.62**	**45384**	**170908469.89**	**170.91**

Mm^3- Million Cubic Meters

*Since water is needed only up to physiological maturity, water demand calculations are done only up to 14^{th} week

b) Water demand calculations for wheat in Jalgaon district.

Met. Week	Month	Dates	Weeks Past Sowing	ETo (mm/day)	ETo Week (mm)	VI (NDWI)	Kc by NDWI	ETc = (ETo x Kc) (mm)	Crop Acreage (ha)	Water Demand (m^3)	Water Demand (Mm^3)
45	Nov.	05-11	1	3.17	22.22	0.074	0.68	15.18	65294	9909359	9.91
46		12-18	2	2.92	20.47	0.098	0.79	16.08	65294	10502455	10.50
47		19-25	3	2.84	19.85	0.155	1.03	20.37	65294	13301248	13.30
48		26-02	4	2.73	19.11	0.160	1.05	20.06	65294	13098546	13.10
49	Dec.	03-09	5	2.53	17.70	0.178	1.13	19.92	65294	13005553	13.01
50		10-16	6	2.85	19.96	0.229	1.34	26.74	65294	17462707	17.46
51		17-23	7	2.95	20.64	0.241	1.39	28.67	65294	18720916	18.72
52		24-31	8	2.82	19.74	0.247	1.42	27.99	65294	18274921	18.27
1	Jan.	01-07	9	3.06	21.39	0.231	1.35	28.88	65294	18854989	18.85
2		08-14	10	3.07	21.52	0.224	1.32	28.37	65294	18523792	18.52
3		15-21	11	3.67	25.69	0.219	1.30	33.37	65294	21786091	21.79
4		22-28	12	3.84	26.91	0.195	1.20	32.18	65294	21014928	21.01
5		29-04	13	4.50	31.48	0.094	0.77	24.20	65294	15798333	15.80
6	Feb.	05-11	14	4.67	32.68	0.069	0.67	21.75	65294	14200705	14.20
7		12-18	15	4.82	33.72	0.072	0.67	22.74	65294	-	-
8		19-25	16	5.35	37.46	0.040	0.54	20.30	65294	-	-
9		26-04	17	5.55	38.83	-0.017	0.30	11.64	65294	-	-
							Total	**398.43**	**65294**	**224454544.02**	**224.45**

Mm^3- Million Cubic Meters

*Since water is needed only up to physiological maturity, water demand calculations are done only up to 14^{th} week

c) Water demand calculations for wheat in Nashik district.

Met. Week	Month	Dates	Weeks Past Sowing	ETo (mm/day)	ETo Week (mm)	VI (NDWI)	Kc by NDWI	ETc = (ETo x Kc) (mm)	Crop Acreage (ha)	Water Demand (m^3)	Water Demand (Mm^3)
45	Nov.	05-11	1	3.11	21.79	0.074	0.68	14.88	60474	8999504	9.00
46		12-18	2	2.95	20.66	0.098	0.79	16.24	60474	9818622	9.82
47		19-25	3	2.75	19.25	0.155	1.03	19.75	60474	11943700	11.94
48		26-02	4	2.71	18.99	0.160	1.05	19.93	60474	12051221	12.05
49	Dec.	03-09	5	2.49	17.44	0.178	1.13	19.62	60474	11865263	11.87
50		10-16	6	2.61	18.25	0.229	1.34	24.45	60474	14787134	14.79
51		17-23	7	2.97	20.80	0.241	1.39	28.89	60474	17473051	17.47
52		24-31	8	3.06	21.41	0.247	1.42	30.35	60474	18356758	18.36
1	Jan.	01-07	9	2.90	20.28	0.231	1.35	27.38	60474	16559361	16.56
2		08-14	10	2.81	19.64	0.224	1.32	25.89	60474	15658996	15.66
3		15-21	11	3.61	25.30	0.219	1.30	32.85	60474	19864714	19.86
4		22-28	12	3.77	26.40	0.195	1.20	31.57	60474	19092446	19.09
5		29-04	13	4.44	31.09	0.094	0.77	23.89	60474	14446857	14.45
6	Feb.	05-11	14	4.81	33.69	0.069	0.67	22.42	60474	13558755	13.56
7		12-18	15	4.94	34.55	0.072	0.67	23.29	60474	-	-
8		19-25	16	5.75	40.22	0.040	0.54	21.79	60474	-	-
9		26-04	17	6.08	42.57	-0.017	0.30	12.76	60474	-	-
							Total	**395.97**	**60474**	**204476383.01**	**204.48**

Mm^3- Million Cubic Meters

*Since water is needed only up to physiological maturity, water demand calculations are done only up to 14^{th} week

ANNEXURE V

WATER DEMAND CALCULATIONS (ONION)

I. Water demand of *rabi* onion for year 2020-21

a) Water demand calculations for *rabi* onion in Dhule district.

Met. Week	Month	Dates	Weeks Past Transp.	ETo (mm/day)	ETo Week (mm)	VI (NDWI)	Kc by NDWI	ETc = (ETo x Kc) (mm)	Crop Acreage (ha)	Water Demand (m^3)	Water Demand (Mm^3)
49	Dec.	03-09	1	3.86	27.02	0.017	0.68	18.24	16529	3014882	3.01
50		10-16	2	2.49	17.44	0.026	0.70	12.16	16529	2010196	2.01
51		17-23	3	3.46	24.19	0.032	0.71	17.24	16529	2849983	2.85
52		34-31	4	3.59	25.16	0.039	0.73	18.38	16529	3037615	3.04
1	Jan.	01-07	5	3.21	22.45	0.041	0.74	16.53	16529	2732098	2.73
2		08-14	6	3.64	25.51	0.121	0.94	23.87	16529	3945120	3.95
3		15-21	7	4.08	28.58	0.149	1.01	28.79	16529	4758918	4.76
4		22-28	8	4.21	29.44	0.162	1.04	30.58	16529	5053924	5.05
5		29-04	9	4.91	34.36	0.221	1.19	40.74	16529	6734526	6.73
6	Feb.	5-11	10	4.95	34.63	0.227	1.20	41.63	16529	6881814	6.88
7		12-18	11	4.82	33.76	0.220	1.18	39.93	16529	6599444	6.60
8		19-25	12	5.34	37.41	0.206	1.15	42.95	16529	7098549	7.10
9		26-04	13	6.45	45.15	0.229	1.21	54.44	16529	8998751	9.00
10	Mar.	05-11	14	5.72	40.04	0.159	1.03	41.30	16529	6826124	6.83
11		12-18	15	5.87	41.10	0.044	0.74	30.58	16529	-	-
12		19-25	16	5.82	40.77	0.033	0.72	29.16	16529	-	-
							Total	**486.52**	**16529**	**70541944.75**	**70.54**

Mm^3- Million Cubic Meters

*Since water is needed only up to physiological maturity, water demand calculations are done only up to 14th week

b) Water demand calculations for *rabi* onion in Jalgaon district.

Met. Week	Month	Dates	Weeks Past Transp.	ETo (mm/day)	ETo Week (mm)	VI (NDWI)	Kc by NDWI	ETc = (ETo x Kc) (mm)	Crop Acreage (ha)	Water Demand (m^3)	Water Demand (Mm^3)
49	Dec.	03-09	1	3.64	25.45	0.017	0.68	17.18	10359	1779830	1.78
50		10-16	2	2.42	16.92	0.026	0.70	11.80	10359	1222217	1.22
51		17-23	3	3.31	23.15	0.032	0.71	16.50	10359	1708740	1.71
52		34-31	4	3.44	24.06	0.039	0.73	17.57	10359	1820579	1.82
1	Jan.	01-07	5	3.25	22.77	0.041	0.74	16.76	10359	1736344	1.74
2		08-14	6	3.49	24.40	0.121	0.94	22.83	10359	2364782	2.36
3		15-21	7	4.30	30.08	0.149	1.01	30.30	10359	3138436	3.14
4		22-28	8	4.33	30.31	0.162	1.04	31.48	10359	3260842	3.26
5		29-04	9	5.12	35.85	0.221	1.19	42.52	10359	4404246	4.40
6	Feb.	5-11	10	5.00	35.03	0.227	1.20	42.11	10359	4361984	4.36
7		12-18	11	4.77	33.41	0.220	1.18	39.51	10359	4092883	4.09
8		19-25	12	5.24	36.69	0.206	1.15	42.12	10359	4363206	4.36
9		26-04	13	6.22	43.52	0.229	1.21	52.47	10359	5435520	5.44
10	Mar.	05-11	14	5.49	38.46	0.159	1.03	39.67	10359	4109665	4.11
11		12-18	15	5.82	40.76	0.044	0.74	30.33	10359	-	-
12		19-25	16	5.92	41.44	0.033	0.72	29.63	10359	-	-
							Total	**482.77**	**10359**	**43799274.54**	**43.80**

Mm^3- Million Cubic Meters

*Since water is needed only up to physiological maturity, water demand calculations are done only up to 14th week

c) Water demand calculations for *rabi* onion in Nashik district.

Met. Week	Month	Dates	Weeks Past Transp.	ETo (mm/day)	ETo Week (mm)	VI (NDWI)	Kc by NDWI	ETc = (ETo x Kc) (mm)	Crop Acreage (ha)	Water Demand (m^3)	Water Demand (Mm^3)
49	Dec.	03-09	1	3.65	25.55	0.017	0.68	17.25	163516	28211358	28.21
50		10-16	2	2.27	15.88	0.026	0.70	11.07	163516	18108133	18.11
51		17-23	3	3.42	23.92	0.032	0.71	17.05	163516	27873060	27.87
52		34-31	4	3.37	23.62	0.039	0.73	17.25	163516	28201625	28.20
1	Jan.	01-07	5	2.57	17.97	0.041	0.74	13.23	163516	21636874	21.64
2		08-14	6	3.21	22.50	0.121	0.94	21.05	163516	34424159	34.42
3		15-21	7	3.90	27.32	0.149	1.01	27.52	163516	44996873	45.00
4		22-28	8	4.54	31.78	0.162	1.04	33.00	163516	53965072	53.97
5		29-04	9	4.76	33.30	0.221	1.19	39.49	163516	64568869	64.57
6	Feb.	5-11	10	5.42	37.92	0.227	1.20	45.58	163516	74532106	74.53
7		12-18	11	4.72	33.05	0.220	1.18	39.09	163516	63912959	63.91
8		19-25	12	5.44	38.11	0.206	1.15	43.75	163516	71544267	71.54
9		26-04	13	6.28	43.97	0.229	1.21	53.01	163516	86682316	86.68
10	Mar.	05-11	14	6.32	44.22	0.159	1.03	45.60	163516	74570387	74.57
11		12-18	15	6.46	45.23	0.044	0.74	33.65	163516	-	-
12		19-25	16	6.23	43.62	0.033	0.72	31.19	163516	-	-
							Total	**488.79**	**163516**	**693228060.51**	**693.23**

Mm^3- Million Cubic Meters

*Since water is needed only up to physiological maturity, water demand calculations are done only up to 14th week

II. Water demand of *rabi* onion for year 2021-22

a) Water demand calculations for *rabi* onion in Dhule district.

Met. Week	Month	Dates	Weeks Past Transp.	ETo (mm/day)	ETo Week (mm)	VI (NDWI)	Kc by NDWI	ETc = (ETo x Kc) (mm)	Crop Acreage (ha)	Water Demand (m^3)	Water Demand (Mm^3)
49	Dec.	03-09	1	2.74	19.17	0.011	0.62	11.91	31776	3786014	3.79
50		10-16	2	3.04	21.27	0.024	0.67	14.36	31776	4561504	4.56
51		17-23	3	3.18	22.27	0.027	0.69	15.29	31776	4857527	4.86
52		34-31	4	3.17	22.16	0.047	0.77	17.11	31776	5438260	5.44
1	Jan.	01-07	5	3.37	23.62	0.053	0.80	18.78	31776	5966886	5.97
2		08-14	6	3.55	24.82	0.063	0.84	20.82	31776	6614591	6.61
3		15-21	7	4.13	28.88	0.076	0.90	25.86	31776	8215855	8.22
4		22-28	8	4.20	29.37	0.113	1.05	30.89	31776	9816610	9.82
5		29-04	9	4.77	33.38	0.141	1.17	39.03	31776	12403539	12.40
6	Feb.	5-11	10	4.73	33.09	0.157	1.24	40.89	31776	12994190	12.99
7		12-18	11	4.79	33.52	0.152	1.22	40.78	31776	12958838	12.96
8		19-25	12	5.51	38.56	0.145	1.18	45.68	31776	14515027	14.52
9		26-04	13	5.50	38.53	0.124	1.10	42.19	31776	13405885	13.41
10	Mar.	05-11	14	5.39	37.76	0.113	1.05	39.75	31776	12629370	12.63
11		12-18	15	7.39	51.74	0.080	0.91	47.18	31776	-	-
12		19-25	16	7.94	55.57	0.048	0.78	43.22	31776	-	-
							Total	**493.74**	**31776**	**128164096.55**	**128.16**

Mm^3- Million Cubic Meters

*Since water is needed only up to physiological maturity, water demand calculations are done only up to 14th week

b) Water demand calculations for *rabi* onion in Jalgaon district.

Met. Week	Month	Dates	Weeks Past Transp.	ETo (mm/day)	ETo Week (mm)	VI (NDWI)	Kc by NDWI	ETc (ETo x Kc) (mm)	Crop Acreage (ha)	Water Demand (m3)	Water Demand (Mm3)
49	Dec.	03-09	1	2.53	17.70	0.011	0.62	11.00	8771	964960	0.96
50		10-16	2	2.85	19.96	0.024	0.67	13.47	8771	1181384	1.18
51		17-23	3	2.95	20.64	0.027	0.69	14.17	8771	1242785	1.24
52		34-31	4	2.82	19.74	0.047	0.77	15.24	8771	1336978	1.34
1	Jan.	01-07	5	3.06	21.39	0.053	0.80	17.00	8771	1491509	1.49
2		08-14	6	3.07	21.52	0.063	0.84	18.05	8771	1583055	1.58
3		15-21	7	3.67	25.69	0.076	0.90	23.00	8771	2017740	2.02
4		22-28	8	3.84	26.91	0.113	1.05	28.31	8771	2483111	2.48
5		29-04	9	4.50	31.48	0.141	1.17	36.81	8771	3228904	3.23
6	Feb.	5-11	10	4.67	32.68	0.157	1.24	40.39	8771	3542182	3.54
7		12-18	11	4.82	33.72	0.152	1.22	41.03	8771	3598856	3.60
8		19-25	12	5.35	37.46	0.145	1.18	44.38	8771	3892437	3.89
9		26-04	13	5.55	38.83	0.124	1.10	42.52	8771	3729533	3.73
10	Mar.	05-11	14	5.64	39.48	0.113	1.05	41.55	8771	3644173	3.64
11		12-18	15	7.27	50.92	0.080	0.91	46.44	8771	-	-
12		19-25	16	7.45	52.12	0.048	0.78	40.54	8771	-	-
							Total	**473.91**	**8771**	**33937607.16**	**33.94**

Mm^3- Million Cubic Meters

*Since water is needed only up to physiological maturity, water demand calculations are done only up to 14^{th} week

c) Water demand calculations for *rabi* onion in Nashik district.

Met. Week	Month	Dates	Weeks Past Transp.	ETo (mm/day)	ETo Week (mm)	VI (NDWI)	Kc by NDWI	ETc (ETo x Kc) (mm)	Crop Acreage (ha)	Water Demand (m^3)	Water Demand (Mm^3)
49	Dec.	03-09	1	2.49	17.44	0.011	0.62	10.84	210917	22857522	22.86
50		10-16	2	2.61	18.25	0.024	0.67	12.31	210917	25973750	25.97
51		17-23	3	2.97	20.80	0.027	0.69	14.28	210917	30116791	30.12
52		34-31	4	3.06	21.41	0.047	0.77	16.53	210917	34868709	34.87
1	Jan.	01-07	5	2.90	20.28	0.053	0.80	16.13	210917	34010584	34.01
2		08-14	6	2.81	19.64	0.063	0.84	16.47	210917	34745700	34.75
3		15-21	7	3.61	25.30	0.076	0.90	22.65	210917	47768252	47.77
4		22-28	8	3.77	26.40	0.113	1.05	27.77	210917	58573464	58.57
5		29-04	9	4.44	31.09	0.141	1.17	36.35	210917	76663438	76.66
6	Feb.	5-11	10	4.81	33.69	0.157	1.24	41.63	210917	87811588	87.81
7		12-18	11	4.94	34.55	0.152	1.22	42.04	210917	88662034	88.66
8		19-25	12	5.75	40.22	0.145	1.18	47.64	210917	100485722	100.49
9		26-04	13	6.08	42.57	0.124	1.10	46.61	210917	98312515	98.31
10	Mar.	05-11	14	5.46	38.25	0.113	1.05	40.26	210917	84912391	84.91
11		12-18	15	7.44	52.10	0.080	0.91	47.51	210917	-	-
12		19-25	16	7.03	49.20	0.048	0.78	38.27	210917	-	-
							Total	**477.29**	**210917**	**825762460.27**	**825.76**

Mm^3- Million Cubic Meters

*Since water is needed only up to physiological maturity, water demand calculations are done only up to 14th week

VITA

1. Name of Student : **Adawadkar Mayur Prakash**
2. Date of Birth : 30th October, 1994
3. Name of college : Department of Irrigation and Drainage Engineering, Post Graduate Institute, Dr. P. D. K. V., Akola
4. Residential Address : Pramod Nagar Sector no- 4, Nakane Road, Deopur, Dhule-424002
   Mobile – 9359451730, 9637159152
   email ID - mayur.adawadkar@gmail.com
5. Academic Qualification :

Name of Course	Subject	Name of University/Board	Marks obtained %/CGPA	Year of Passing
ASRB NET	Land and Water Management	ASRB, New Delhi	47.56/100	2019
M.Tech	Irrigation and Drainage Engineering	Dr. P. D. K. V., Akola	8.09/10.00	2018
B.Tech	Agril. Engg.	M. P. K. V., Rahuri	7.37/10.00	2016
MSCIT	Computer	MKCL	88/100	2010

6. Research paper published : 5
7. Field of interest : Remote sensing applications, Teaching, Research in the field of irrigation.

Place : Akola

Date : Signature of student